This is to certify that the
dissertation entitled

TOWARD THE DEVELOPMENT OF A CHEMO-ENZYMATIC PROCESS FOR THE PRODUCTION OF NEXT-GENERATION TAXOL ANALOGS

presented by

Mark Evans Ondari

has been accepted towards fulfillment
of the requirements for the

Doctoral degree in Chemistry

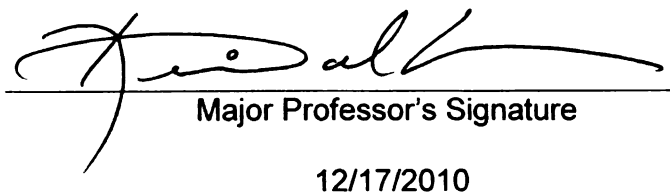

Major Professor's Signature

12/17/2010

Date

MSU is an Affirmative Action/Equal Opportunity Employer

TOWARD THE DEVELOPMENT OF A CHEMO-ENZYMATIC PROCESS FOR THE PRODUCTION OF NEXT-GENERATION TAXOL ANALOGS

By

Mark Evans Ondari

A DISSERTATION

Submitted to
Michigan State University
in partial fulfillment of the requirements
for the degree of

DOCTOR OF PHILOSOPHY

Chemistry

2010

ABSTRACT

TOWARD THE DEVELOPMENT OF A CHEMO-ENZYMATIC PROCESS FOR THE PRODUCTION OF NEXT-GENERATION TAXOL ANALOGS

By

Mark Evans Ondari

In the last two decades, phenomenal progress has been made in the development of methodologies to produce potent analogs of the anti-cancer drug Taxol® (Bristol-Myers Squibb). However, due to the structural complexity of Taxol, current semi-synthetic methodologies use necessary but often redundant protecting group manipulations to circumvent problems associated with differential reactivity of the various functional groups on the molecule. While biotechnological developments such as cell culture fermentation technology provide a steady supply of the drug, its derivatives cannot be similarly produced *in planta* without extensive engineering of the Taxol biosynthetic pathway.

Therefore, a process incorporating a combination of enzyme-mediated transformations and chemical synthesis will have distinct advantages over purely semi-synthetic or purely biosynthetic approaches. Enzymatic processes could potentially reduce the redundancy in protecting group chemistry, while chemical transformations could replace inherently low yielding enzymatic reactions or be applied in steps where biotransformations are not tenable. We developed a shorter semi-synthetic methodology incorporating one-pot protection of three hydroxyl groups of a Taxol intermediate baccatin III, and a one-pot process for selective reductive ester cleavage-selective reductive desilylation. This methodology could potentially reduce four synthetic steps from chemical transformations routinely used in the semi-synthesis of Taxol derivatives

such as BMS-275183. This study also demonstrated that an intramolecular hydrogen bond modulates the chemical reactivity of the hydroxyl groups of the Taxol intermediate baccatin III.

Additionally, we screened a library of *Taxus* enzymes for novel acyltransferase activity using semi-synthetically prepared surrogate substrates. This screen uncovered a promiscuous acetyltransferase enzyme, abbreviated DBAT, which catalyzes transfer of acetyl group from the CoA donor to the secondary as well as tertiary hydroxyl groups of advanced taxane substrates. Consequently, a study was initiated to assess whether DBAT could catalyze transfer of non-natural acyl groups, such as the methoxycarbonyl group found in a water soluble Taxol derivative BMS-275183. The catalytic mechanism of the DBAT reaction was probed by acetyl group exchange between two taxane substrates in the presence or absence of the co-substrate CoASH. Preliminary findings from this study seem to suggest a mechanism for DBAT that is different from the one proposed for the plant family of acyltransferases, referred to as the BAHD superfamily, in which DBAT is a member. Furthermore, site-directed mutagenesis of the *dbat* gene was performed to evaluate the role of an Asp residue of a conserved HXXXD motif. Even though this motif is presumed to constitute the active site of the BAHD acyltransferases, the role of the Asp residue is speculated to be only structural. However, when we performed site-specific substitution of the Asp residue with less nucleophilic or non-nucleophilic residues, the resulting mutants were >90% less active than wild-type DBAT, indicating that this Asp residue plays more than a perfunctory role during DBAT catalysis.

ACKNOWLEDGMENTS

It is with an overwhelming sense of gratitude that I come to the end of my five year journey through graduate school. There is no doubt in my mind that I would never have come this far without the elevation I got from "standing on the shoulders of giants."

First, I would like to sincerely thank my research advisor Prof Kevin D Walker for patiently guiding me through the program. There was a time in the spring of 2006 when I felt like I didn't possess what it takes to make it through the program. A pep talk later, my bruised confidence was completely reconfigured, and I have never looked back since then. I would also like to thank him for giving me an opportunity to pursue independent hypotheses in my research projects, notwithstanding the fact that he had tenure to worry about then. This not only helped me develop a sense of ownership over my research projects, it also helped me uncover the lid of curiosity that has stood me in good stead over the years.

I would also like to thank the members of my guidance: Professor Babak Borhan, for being an enthusiastic teacher and a great mentor; Professor Gregory Baker for always finding a way to make every difficult prospect look tenable; Professor Daniel Jones for being so resourceful and for always suggesting some alternative approaches and experiments. To you all I say thanks for the help that you accorded me individually and collectively.

Members of the Walker lab, with whom I have spent most of my five years, have been particularly instrumental in helping shape my viewpoints: Irosha, Danielle, and I literally survived happy times as well as disappointing moments together for the last five years. It's gratifying to see how far the three of us have come from 2005, and how we've

grown into resilient folks, patiently sitting through long hours of group meetings or seminar preparations. Danielle, I still remember that it wasn't trivial obtaining the C-terminal His-tagged *dbat* clone; thank you for letting me use it. Irosha, I recall how you helped me discover interesting chemistry by quenching a reaction for me while I was away teaching; thank you. I wish you two the very best in your personal and professional aspirations. I would also like to thank Udayanga for helping me develop and sustain an interest in volleyball; Dilini for being a great neighbor and friend, always making sure to bring an extra banana or cookie! Ruth, Chelsea, Getrude, Sean, Washington... you all helped knit a unique family. I will miss you all. Undergraduate students Becky, Chris, Christian, Thomas, Josh, Aws, Noelle, Ebony; I haven't forgotten that you helped me somewhere along the way.

I am greatly indebted to the Department of Chemistry for the graduate teaching assistantship and fellowships that enabled me get through the program. I am also grateful to the College of Natural Sciences and the Graduate School at Michigan State University for the travel funds to attend scientific conferences. Finally, my appreciation goes to the Michigan Agricultural Experiment Station (MAES) for research funds that helped me complete my projects in time.

And yet definitive as this moment is to me, it is difficult to think of it solely in terms of the way it has shaped my outlook in life through the lenses of science without acknowledging where it all began. This moment is for all those folks who helped start a transformative flame inside of this village boy as it is for those who helped tend the fire: My high school chemistry teacher Mr Otunga (RIP) for seeing a potential chemist in me;

my seven siblings for their unwavering support, especially my brother Jacob for always setting high standards for the rest of us. I truly appreciate.

My sincere appreciation goes to Mercy for helping me stay sane when things looked bleak after my second year oral examination. For all the sacrifices you made for me, I truly appreciate. I will always love you.

None of this would have come to be if it wasn't for the stalwart among all the giants in my life: my mom Milkah. Armed with singular determination and less of everything else, she raised eight kids the best way she knew how with absolute love and sacrifice. It's impossible for our family to appreciate enough the sacrifices she made for us, like walking for hours on end carrying heavy loads on her head to sell in Oyugis every Tuesday and Friday; to Marani every Monday and Wednesday; to Kegogi every Thursday and Saturday... so we could put something on the table. She is the epitome of absolute diligence and sacrifice. And this I say for lack of a better description. Thanks a million mom. We love you so much!

Finally, I thank God for answering every small and big prayer that I made since I was a little boy. I pray that His light may illuminate the path of every poor kid out there so that they too may find opportunities in life.

TABLE OF CONTENTS

LIST OF TABLES

LIST OF FIGURES

Images in this dissertation are presented in color

LIST OF SCHEMES

LIST OF ABBREVIATIONS

DNA, deoxyribonucleic acid

cDNA, complementary deoxyribonucleic acid

BMS, Bristol-Myers Squibb

CrEL, cremophor Emulsifying of Polyoxyethylenglyceroltriricinolate

MAPs, microtubule-associated proteins

GTP, guanosine-5'-triphosphate

SAR, structure activity relationships

NMR, nuclear magnetic resonance

DAB, deacetylbaccatin III

TS, taxadiene synthase

MEP, 2-C-methyl-d-erythritol 4-phosphate

GGPP, (*E*, *E*, *E*)-geranylgeranyl diphosphate

TBT, taxane 2α-*O*-benzoyltransferase

TAT, taxane5α-*O*-acetyltransferases (TAT)

CoA/CoASH, coenzyme A

BAHD, benzylalcohol-*O*-acetyltransferase; anthocyanin-*O* hydroxycinnamoyltransferase; anthranilate hydroxycinnamoyl/benzoyltransferase; deacetylvindoline 4-*O* acetyltransferase

SCPL, serine carboxy-peptidase-like

AATs, anthocyanin malonyl CoA acyltransferases

DFGWG, aspartate; phenylalanine; glycine; tryptophan; glycine motif

CATs, chloramphenicol acetyltransferases

Dm3MaT1, anthocyanin-3-*O*-glucoside-6"-*O*-malonyltransferase

Dm3MaT2, anthocyanin-3-*O*-glucoside-3",6"-*O*-dimalonyltransferase

DMSO, dimethylsulfoxide

Q-ToF, quadrupole time-of-flight

HPLC, high pressure liquid chromatography

PTLC, preparative thin-layer chromatography

UV, ultra-violet

BAPT, baccatin III-13-*O*-phenylpropanoyltransferase

NDTBT, *N*-debenzoyltaxol-3'*N*-benzoyltransferase

EtOAc, ethyl acetate

Na_2SO_4, sodium sulfate

DMF, *N,N*-dimethylformamide

DMS, dimethylsilane

MHz, megahertz

THF, tetrahydrofuran

Re-Al, sodium bis(2-methoxyethoxy)aluminum hydride

TES, triethylsilane

HF, hydrogen fluoride

DMAP, dimethylaminopyridine

TEA, triethylamine

IPTG, isopropyl-β-D-thiogalactopyranoside

MOPSO, 3-(*N*-morpholino)-2-hydroxypropanesulfonic acid

DTT, dithiothreitol

NaCl, sodium chloride

SDS-PAGE, sodium dodecyl sulfate-polyacrylamide gel electrophoresis

DBAT, 10-deacetylbaccatin III acetyltransferase

Ni-NTA, nickel-nitroloacetate

ESI-MS, electrospray ionization mass spectrometry

K_m, Michaelis constant

k_{cat}, catalytic efficiency

Boc, tert-butoxycarbonyl

LgtC, saccharide-polymerizing glycosyltransferase

CAT, choline/carnitine acyltransferase

His, histidine

VS, vinorine synthase

Cys, cystine

TPCK, *N*-tosyl-L-phenylalanine chloromethylketone

DEPC, diethyl pyrocarbonate

Ser, serine

Asp, aspartate

GCT, glutaconate CoA-transferase

LiHMDS, lithium hexamethyldisilazide

$Cu(OAc)_2$, copper (II) acetate

DCM, dichloromethane

H_2SO_4, sulfuric acid

$NaHCO_3$, sodium bicarbonate

SDS-PAGE, sodium dodecylsulfate polyacrylamide gel electrophoresis

MWCO, molecular weight cut-off

Tris, tris(hydroxymethyl)aminomethane

HCl, hydrochloric acid

PCR, polymerase chain reaction

dNTP, deoxyribonucleotide triphosphate

NZCYM, pancreatic enzyme caseine digest

LB, luria Bertani

DMDC, dimetheyl dicarbonate

TLC, thin layer chromatography

$MgCl_2$, magnesium chloride

TBDMS, tertiary butyldimethylsilane

Glu, glutamine

FPLC, fast performance liquid chromatography

CD, circular dichroism

DDS, drug delivery system

Mab, monoclonal antibody

RCM, ring closing metathesis

Ac_2O, acetic anhydride

MeOC(O)Cl, methylchloroformate

TMS, trimethylsilyl

TFA, trifluroacetic acid

1 Chapter One: Overview of Natural Products in Cancer Chemotherapy

1.1 Introduction

Spatiotemporal models estimate that in 2009 there were 1,500 cancer-related deaths per day in the United States, accounting for 23% of all deaths.[1] This makes cancer the second leading cause of death in all age groups with an estimated national economic burden of $200 billion annually.[1-3] Systemic antineoplastic chemotherapy remains one of the most important among conventional strategies employed to combat cancer. To improve existing chemotherapy, emphasis is placed on the development of new chemotherapeutic agents, refinement of existing treatment approaches, and use of combined modality therapy.[3,4]

Even though the first commercial isolation of a natural product (morphine) was in 1826, and the first natural product-based semi-synthetic drug to be marketed was in 1899,[5,6] the use of natural products in folk medicine predates the Middle Ages. Natural products have since emerged from the ethno-medical toolkit of antiquity to become the mainstay of and templates for contemporary drug discovery.[4] Not surprisingly, an estimated 80% of the world population still rely on folk medicine for their primary healthcare.[7] Additionally, approximately 30% of all pharmaceutical drugs are either natural products or contain active pharmaceutical excipients derived from higher plants. For example, in the cancer disease segment, over 60% of the drugs originate from natural sources[8,9] and only a few of the therapeutic entities currently in clinical use were discovered through rational structural design.

The Madagascar periwinkle plant (*Catharanthus roseus*) was traditionally used as a hypoglycemic agent in parts of Asia; however, it was not until 1958 when it was found to contain the cytotoxic constituents vinblastine and vincristine[4] (**Figure 1-1**). Clinically used in curative combination chemotherapy regimens, these drugs continue to make significant contributions to long-term remissions with non-small cell lung cancer, childhood leukemias, lymphoma, Hodgkin's disease, and breast cancer.[4,10]

Figure 1-1. Anti-tumor agents Topotecan **I-1** and vincristine **I-2**.

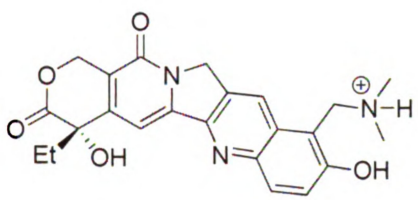

I-1

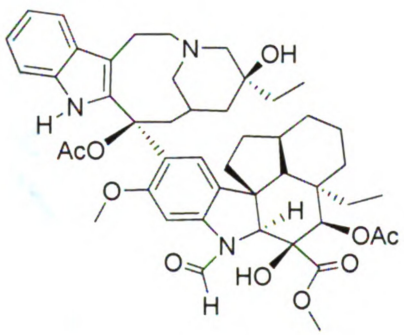

I-2

The role of the mitotic spindle in cell division has long been documented and identified as an important target in cancer chemotherapy,[11] as discussed in section **1.2.2**. Both vinblastine and vincristine are tubulin poisons and they inhibit microtubule assembly by inducing tubulin self-association into non-microtubular spiral aggregates.[10,12] Within a concentration range that blocks cell proliferation, these drugs bind tubulin and disrupt mitotic spindle formation stalling the cell cycle at mitosis[11] (**Figure 1-2**). At the lower end of this concentration range, they change the microtubule dynamics without altering the microtubule polymer levels, and at higher concentrations they induce microtubule depolymerization.[11]

Figure 1-2. The eukaryotic cell cycle[13]

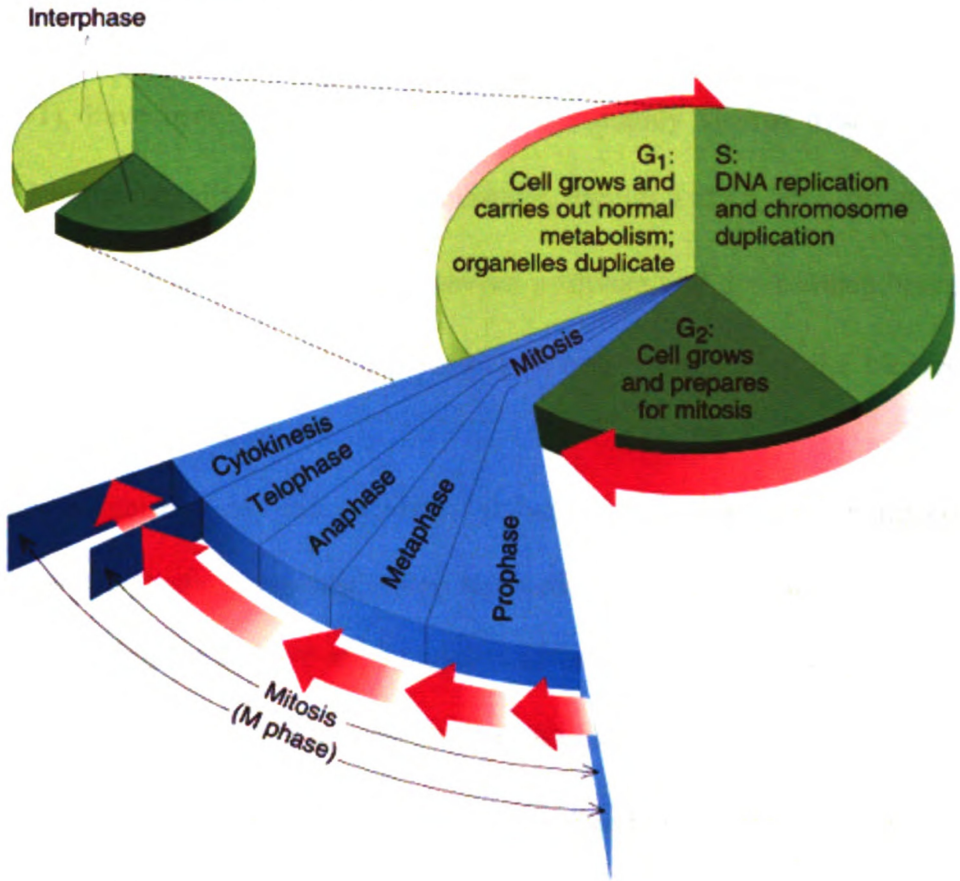

Another notable natural product is camptothecin, a monoterpene indole alkaloid initially isolated by Wall and Wani in 1966 from the stem bark of the Chinese native plant *Camptotheca acuminata*.[14] Even though camptothecin showed early promise in the 1970s, its low water solubility and associated dose-limiting toxicity hampered clinical development. Camptothecin was later found to uniquely stabilize the reversible formation of DNA-topoisomerase I complex.[4,14-16] Eukaryotic topoisomerase I (topo I) enzyme is implicated in the relaxation of DNA supercoils that are created during fundamental cell processes like transcription, DNA replication, and chromosomal segregation.[17] This makes topo I a good target in rapidly dividing tumor cells.

To overcome the insolubility of camptothecin and mitigate its toxicity, two analogs, topotecan (Hycamtin, GlaxoSmithKline) and irinotecan (Camptosar, Pfizer) (**Figure 1-1**), have been approved for clinical use mainly against ovarian and colon cancers.[17] Mechanistically, topotecan, for example, mimics a DNA base pair and binds at the DNA cleavage site by intercalating between upstream and downstream base pairs.[17] By displacing downstream DNA, topotecan prevents religation of the cleaved DNA strands and leads to cell death.

Microorganisms are the principle sources of antibacterial pharmaceuticals. However, cancer chemotherapeutics such as dactinomycin, doxorubicin (adriamycin), and bleomycins (**Figure 1-3**) are among notable natural products that have been extracted from microorganisms.[18,19] While most of the anti-cancer drugs from microorganisms exert their cytotoxicity through DNA damage using free-radical intermediates,[4] there is a growing body of evidence indicating that analogs could be synthesized that have more defined modes of action. For example, it has been demonstrated that the bleomycins likely target amino-acid transfer RNAs and DNA-independent protein synthesis inhibition.[18,19]

Figure 1-3. Chemical structures of bleomycins.

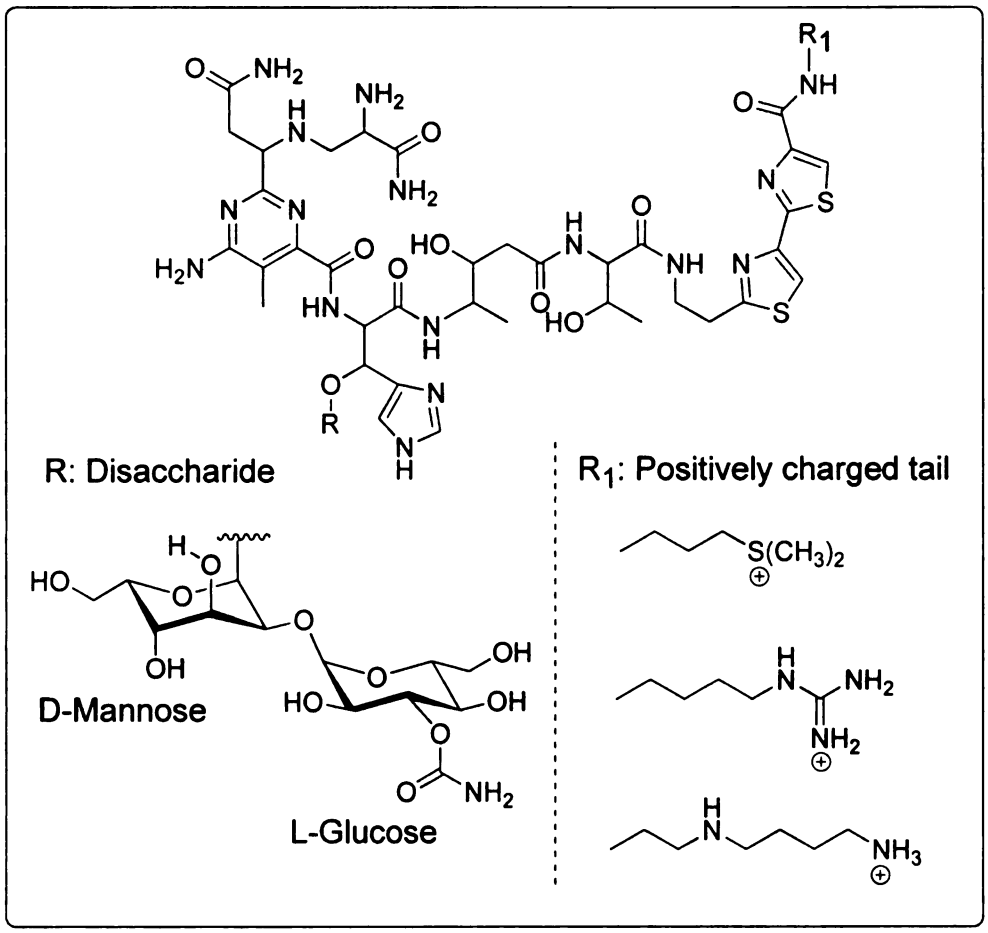

New classes of antitumor drugs have recently been discovered, including epothilones and the marine invertebrate metabolites discodermolide, eleutherobin, and sarcodictyins.[20] The mode of action of these novel natural products is by stabilization of the microtubules during cell divisions.[20]

Of all the antitumor natural products extracted so far, perhaps the most successful yet is Taxol (Bristol-Myers Squibb). The generic name for Taxol is paclitaxel, but due to associated familiarity the name "taxol" will used for the rest of the text. A more descriptive account of taxol and its analogs follows in the following sections and subsequent chapters.

1.2 Taxol

I.2.1 Discovery, Early Development and Clinical Uses

A bioassay-guided fractionation of *Taxus brevifolia* in 1961 by Mansukhal Wani and Monroe Wall at the National Cancer Institute led to the isolation of a bark extract that demonstrated cytotoxicity against L1210, P388 and P1534 leukemias, Walker 256 carcinosarcoma, sarcoma 180, and Lewis lung tumors.[21] In 1971, the active ingredient in the extract was subsequently characterized and identified as the complex diterpenoid taxol[21,22] (**Figure 1-4** compound **I-4**). In spite of its promising antineoplastic activity the development of taxol from discovery to clinical use took more than three decades.[23]

Figure 1-4. Structures of taxol **I-4** and its more water soluble analog docetaxel **I-5**.

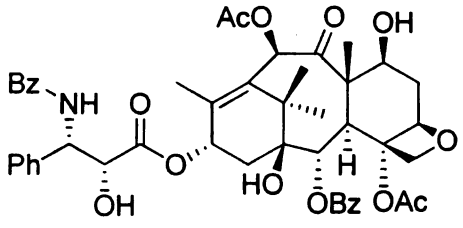

I-4

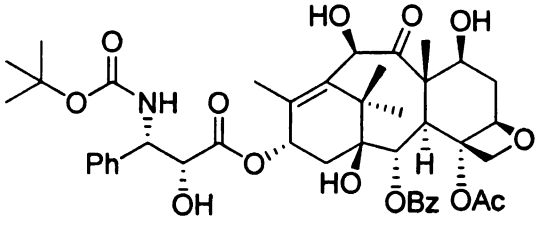

I-5

Development of taxol into a drug of suitable clinical formulation was initially hampered in part by its poor water solubility. However, problems associated with large-scale extraction presented a major bottleneck because taxol accumulates in limited quantities in the inner bark of *T. brevifolia*.[21,22] To mitigate solubility issues, a formulation of taxol in Cremophor EL (BASF) was developed.[24] Cremophor (CrEL) is a non-ionic excipient of polyoxyethylene glycerol used as an emulsifying and solubilizing agent for pharmaceuticals.[25] However, due to hypersensitivity associated with CrEL a

nanoparticle human-albumin bound taxol formulation Abraxane (Abraxis Biosciences) has recently been granted regulatory approval.[26,27]

Interest in taxol was later rekindled by discovery that it has a novel mechanism of action. Unlike the vinca alkaloids, taxol was found to induce tubulin polymerization through the formation of stable, nonfunctional microtubules.[28-32]

I.2.2 Microtubules and the Mechanism of Action of Taxol

Microtubules are ubiquitous linear polymers whose backbone is composed of microtubule-associated proteins (MAPs) that confer functional diversity.[11] Microtubules also have stoichiometric α-β tubulin heterodimeric peptides that form protofilaments, 13 of which bundle together to form hollow cylinders for strength and adaptability[11] (**Figure 1-5**). These cellular components are thought to be involved in many biological processes, such as axonemal motility, sensory transduction, or for the performance of interphase roles such as establishment and maintenance of cell shape.[11] More commonly, microtubules are known to orchestrate chromosome segregation during cell division.[33]

Figure 1-5. Structure of microtubules with their associated function and taxane binding site.[34]

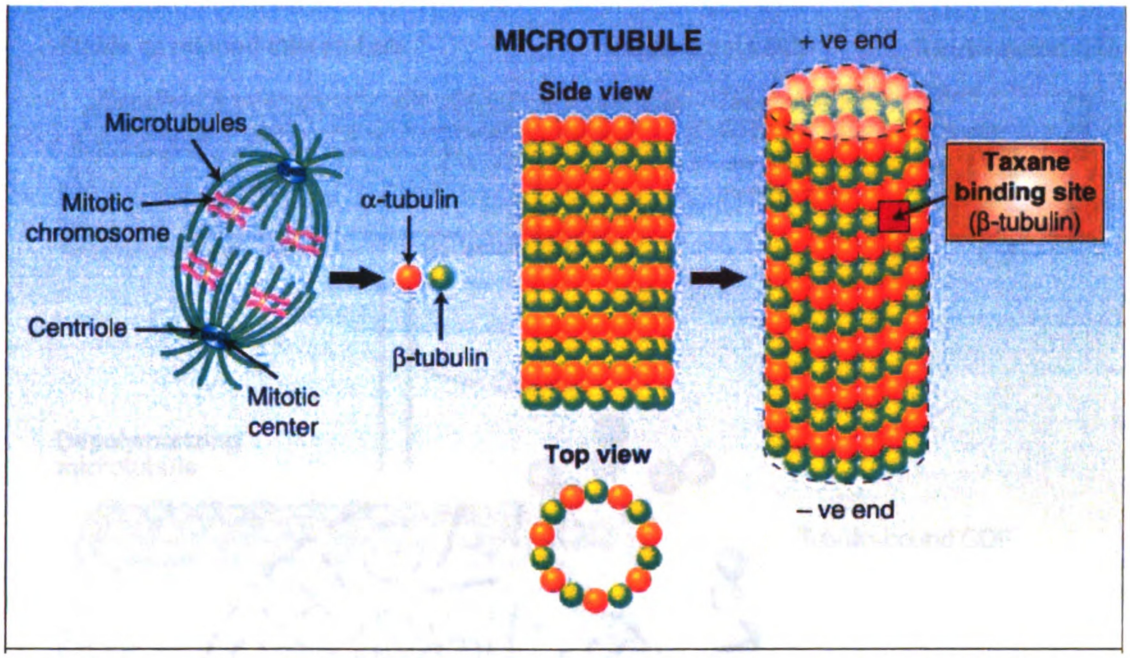

The microtubule subunits are arranged in a parallel orientation which creates heterogeneity in the dimers. This in turn creates structural polarity in microtubules wherein the α-tubulin is exposed at the slow-growing minus end, while the plus end terminates with β-tubulin.[35] Both α- and β-tubulin subunits bind guanosine-5'-triphosphate (GTP), but during elongation of the microtubule GTP hydrolysis lags behind subunit addition. Thus, a 'GTP cap' is formed at and stabilizes the plus end, which promotes further polymer extension.[35,36] However, when the rate of subunit addition decreases, GTP hydrolysis eventually "catches up" with subunit addition and the cap is lost, resulting in rapid depolymerization of the microtubule[11] (**Figure 1-6**).

Figure 1-6. A representation of microtubule dynamics.[36]

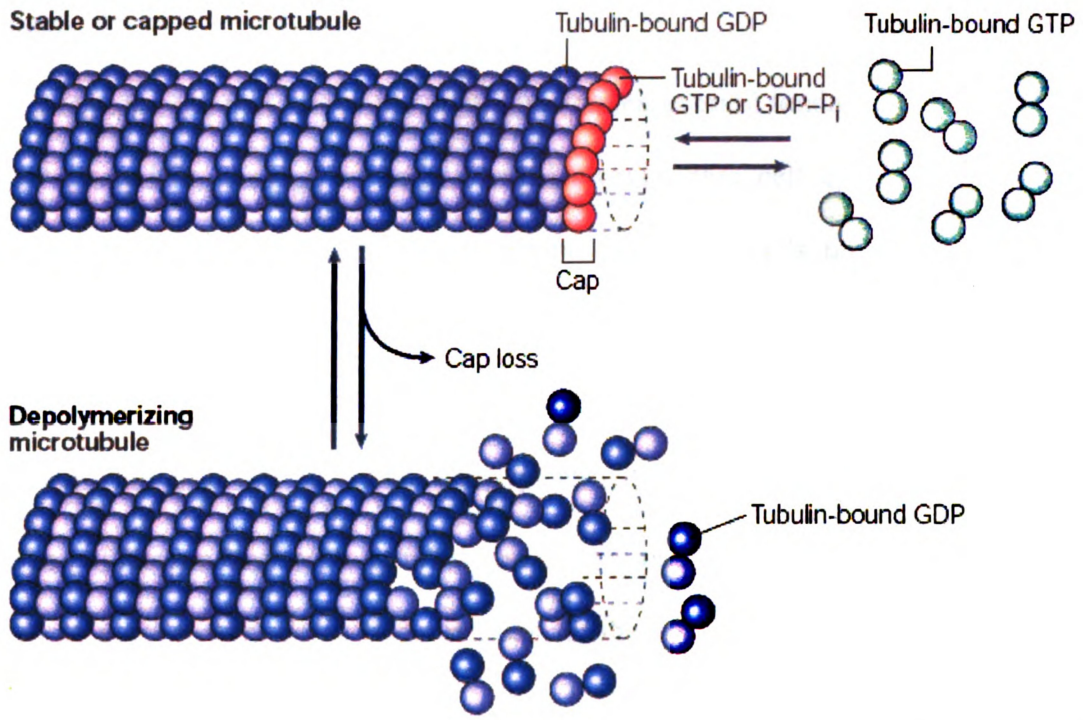

For normal functioning of the cell microtubules undergo dynamic incorporation of free heterodimers into the polymerized structures and release of dimers into the soluble tubulin pool.[35] The direction of this dynamic equilibrium is regulated by signals generated during specific cell-cycle phases.

Taxol acts on the β-tubulin; however, unlike vinblastine, vincristine and cholchicine which induce microtubule depolymerization at clinically relevant concentrations, taxol enhances polymerization even at higher doses.[10] By preferentially binding to the microtubules, rather than the tubulin subunits, taxol shifts the dynamic equilibrium toward microtubule assembly. This decreases the critical concentration of tubulin monomers required for the reorganization of the microtubule network thereby reducing depolymerization.[28-32] Even though chromosomes can still attach to taxol-stabilized microtubules during mitosis, the loss of microtubule dynamics due to

stabilization of the polymer means that mechanical tension is not produced across sister chromatids.[11]

It is presumed that anti-microtubule agents such as taxol fundamentally exert their cellular cytotoxicity through mitotic arrest. However, this cell cycle block is only transient, and after a period of time in mitotic arrest, the cells proceed into a state characteristic of the G1 phase of the cell cycle, and eventually undergo apoptosis. It is speculated that defects in the mitotic checkpoint machinery of cancerous cells could be the reason behind selective tumor cell cytotoxicity by anti-microtubule drugs.[10,37] Conversely, the abundant nature of tubulin in the neurons and the role of microtubules in axonal transport are considered likely reasons for the neurologic toxicity of anti-mitotic agents.[10]

Although the taxanes and vinca alkaloids differ in the specific nature of their local interactions with the cellular cytoskeleton, they share the overall mechanism of action, i.e., inhibition of microtubular dynamics.[12] Consequently, studies focused on elucidation and therapeutic modulation of microtubule dynamics are critical in order to improve the pharmacological properties and efficacy of microtubule binding drugs.[12]

I.2.3 Structure Activity Relationships (SAR) of Taxol

It has been demonstrated that taxol samples a large number of conformations in solution most of which are biologically inactive.[38] Consequently, the drug has a relatively weak association with tubulin *in vivo*. Thus, taxol-tubulin interactions are important in dissecting the pharmacophore of taxol, especially to rationalize why some structural modifications of taxol enhance biological activity while others are deleterious.

Additionally, such interactions provide the basis for design of simpler or hybrid constructs with similar or better tubulin-binding affinities.[39]

The core structure of taxol is made up of an oxetane, three free hydroxyl groups, two acetates, *O*-benzoyl, and *N*-benzoyl functional groups which define the pharmacophore of the drug (cf. **Figure 1-4**). Removal or modification of these functional groups has formed the basis of extensive structure-active relationship (SAR) studies[31,40-48] mainly by the Kingston, Ojima, and Holton research groups, among others.

Photoaffinity labeling, structural biology, solid-state NMR, and computational modeling studies are among the techniques that were used to determine the taxol binding site on the tubulin subunit.[49,50] Semi-synthetic analogs, notably 3'-(*p*-azidobenzamido)taxol, were the first to be used to identify the site of photoincorporation as being the N-terminal amino acids of β-tubulin.[49,50] This was later corroborated by a low-resolution crystal structure of zinc-induced, taxol-stabilized tubulin sheets.[51] While the electron crystallographic data was a milestone, it lacks the atomic resolution necessary to define precise intermolecular drug-protein contacts that would be helpful in structure-based analog design.[51]

1.2.3.1 SAR of the Taxol Side Chain

Structure-activity relationship studies have established that the C-13 side chain is necessary for the observed cytotoxicity as well as in promoting microtubule assembly in the absence of GTP.[22] Furthermore, baccatin III, a taxol analog lacking the C-13 side chain, does not possess the biological activity associated with taxol. However, other

studies indicate that the side chain can be eliminated with retention of biological activity with appropriate *meta* substitutions at the C-2 benzoyl group of baccatin III.[43]

Even though some structural variability is permissible within the side chain itself, a free C-2' hydroxyl is important for biological activity.[52] This hydroxyl group makes hydrogen bond contacts with an arginine residue of β-tubulin. However, the alcohol can be selectively modified into hydrolysable esters and unmasked *in vivo* like it has been demonstrated in taxol prodrugs.[53] Conversely, the C-3' phenyl of the side chain is not essential for microtubule activity; thus, C-3' alkyl or alkenoyl substituted analogs with superior pharmacological properties than taxol have been synthesized[54] (**Figure 1-7**).

Figure 1-7. Structure-activity relationships of taxol.

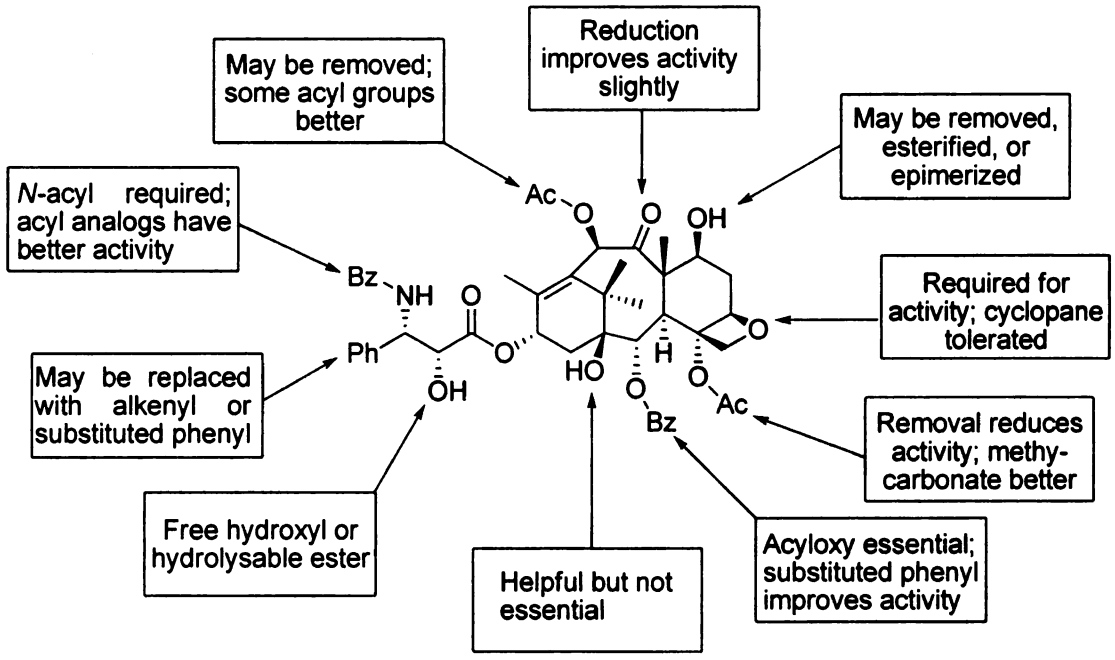

Some of the proposed solution conformations of taxol include the "polar" or "hydrophobic collapsed" in which the 3'-phenyl group is oriented towards the C-2 benzoyl group,[55] and a "non-polar" conformation in which the C-3'-*N*- and the C-2-*O*-

benzoyl groups are associated.[56] A "T-Taxol" conformation has also been proposed; in this conformation, the C-2 benzoyl group is juxtaposed between and equidistant from the two C-3' phenyl rings, which gives the conformer a "T-shaped" appearance.[52,55-58]

To reduce the number of inactive solution conformations of taxol, synthetic strategies have been devised that impose conformational rigidity to the molecule through tethering.[52,55-58] The assumption is that by constraining the drug in only the active conformation, purported to be the "T-Taxol", the pharmacological profile of the drug could be improved through enhanced binding[57]. Therefore, macrocyclic taxol analogs have been synthesized by tethering the side chain C-3' phenyl ring to the C-4 hydroxyl group to form structures have been semi-synthesized[59-61] (**Figure 1-8**); these analogs show enhanced cytotoxicity indices than the parent drug.

1.2.3.2 SAR of Acyl Groups on the Baccatin Core

Chemical modifications of the C-7 hydroxyl group and the C-10 acetate, such as Barton McCombie deoxygenation, have shown that these functional groups generally have little effect on the biological activity of taxol.[62,63] In contrast, 1-deoxytaxol, 4-deacetyltaxol, and 4-deacetoxytaxol analogs were found to be up to ten-fold less potent than taxol in tubulin assembly.[64,65] This indicates that they might form part of the molecular pharmacology of the drug. However, removal of the 2-benzoyl group and subsequent reacylation with *ortho*- and *meta*-substituted aroyl groups significantly improve the cytotoxicity of the analogs[66] (**Figure 1-8**).

Figure 1-8. Modified taxol analogs (**1-6, I-7,** and **I-8**) and a macrocyclic derivative (**I-9**).

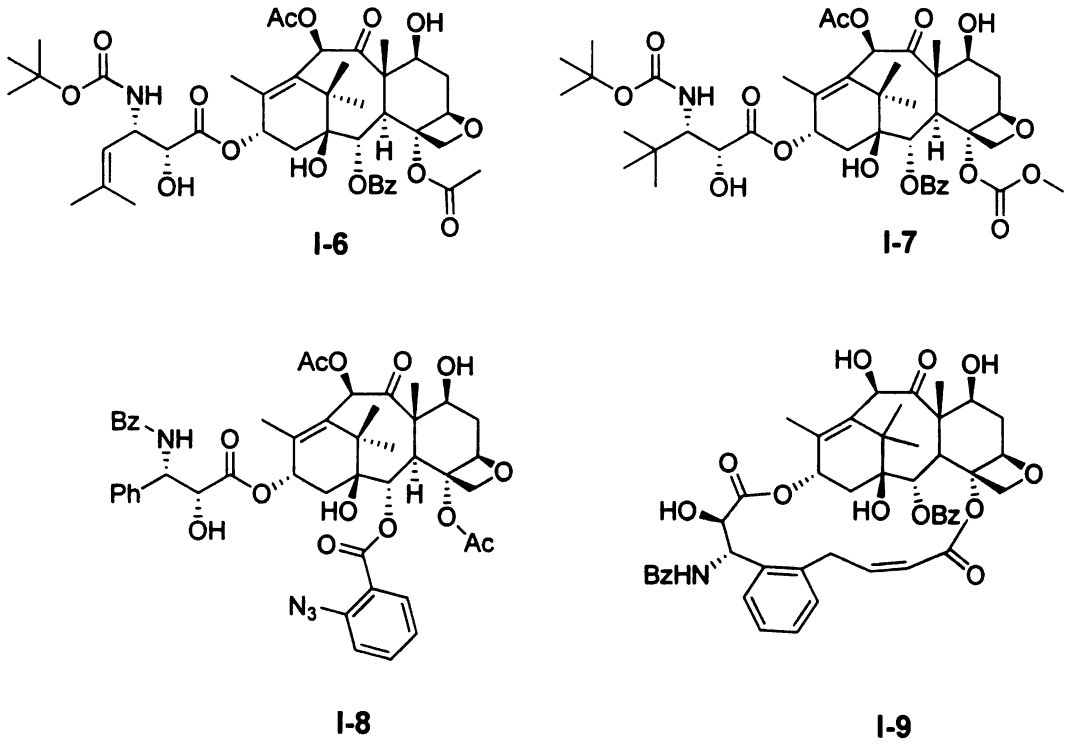

I.2.4 Chemical and Biotechnological Developments

I.2.4.1 Chemical Developments: Total Syntheses

The approval of taxol for clinical use attracted enormous interest in the early 1990s among synthetic organic chemists. The research groups of Holton, Nicolaou, Wender, Danishefsky, Mukaiyama, among others, have since synthesized taxol in over thirty linear steps by employing different synthetic strategies[67-71] (**Figure 1-9**). The Holton group was the first to accomplish the feat employing a linear synthesis approach starting from the natural product patchoulene oxide or borneol.[67,72] On the other hand, Wenders' group started from oxidation of pinene to verbenone,[73,74] while the Danishefsky group started from the Wieland-Miescher ketone.[75] The Nicolau group

employed a convergent approach using three different pre-assembled synthons[76] (**Figure 1-9**).

Figure 1-9. Summary of taxol total syntheses.

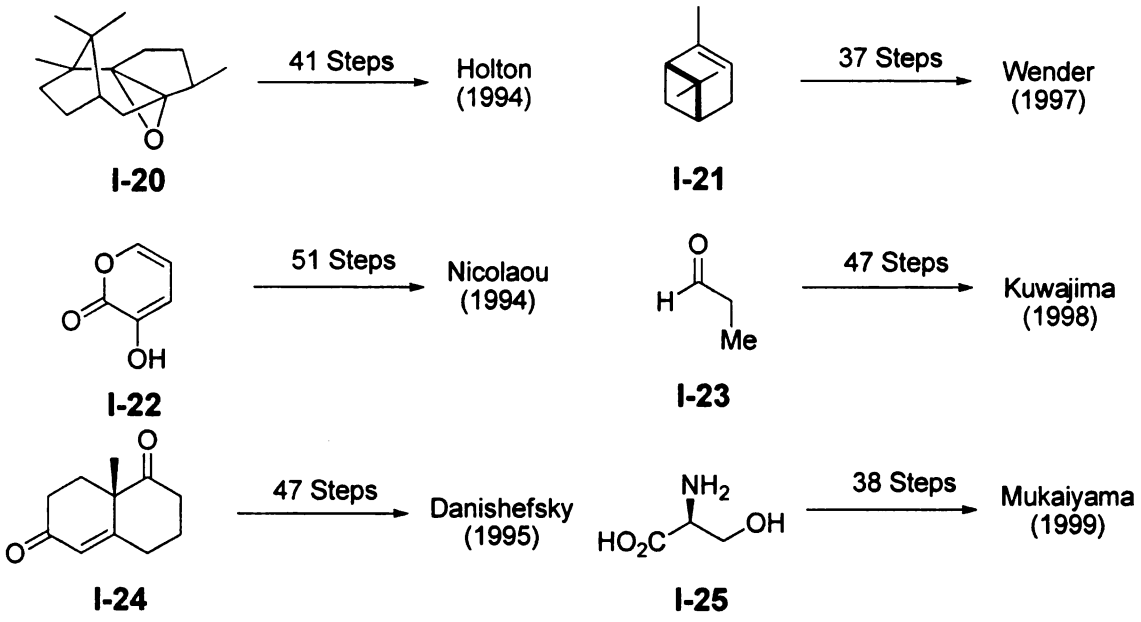

While the complexity of taxol precluded total synthesis as a viable means for commercial production, it has nonetheless presented opportunities for the development of novel methodologies for the semi-synthesis of more potent derivatives.

I.2.4.2 Chemical Developments: Synthesis of Taxol Side Chain

To meet the increasing demand for taxol a practical semi-synthetic method amenable to large-scale production was sought for the *N*-benzoyl-3-phenylisoserine side chain. This side chain could then be coupled to 10-deacetylbaccatin III (10-DAB), an abundant natural product intermediate from the needles of *Taxus baccata*.[77-79] Thus, enzymatic kinetic resolution of racemic esters, diastereoselective synthesis using chiral auxiliaries, and asymmetric catalysis were among the approaches towards the synthesis of enantiomerically enriched taxol side chain.[80-82]

In the enzymatic process, 2*S*-phenylglycine (compound **I-26**) was efficiently converted to its acyl chloride and subsequently converted to the corresponding nitrile[80] (**Scheme 1-1**). Methanolysis of the nitrile followed by Baker's yeast reduction furnishes methyl (2*R*,3*S*)-phenylisoserine analog (compound **I-30**) as a single diastereomer. Schotten-Baumann acylation of the ester gives the desired enantiomerically pure methyl-protected ester of *N*-benzoylphenylisoserine side chain.[80]

Scheme 1-1. Taxol side chain from enzymatic kinetic resolution of racemic esters.

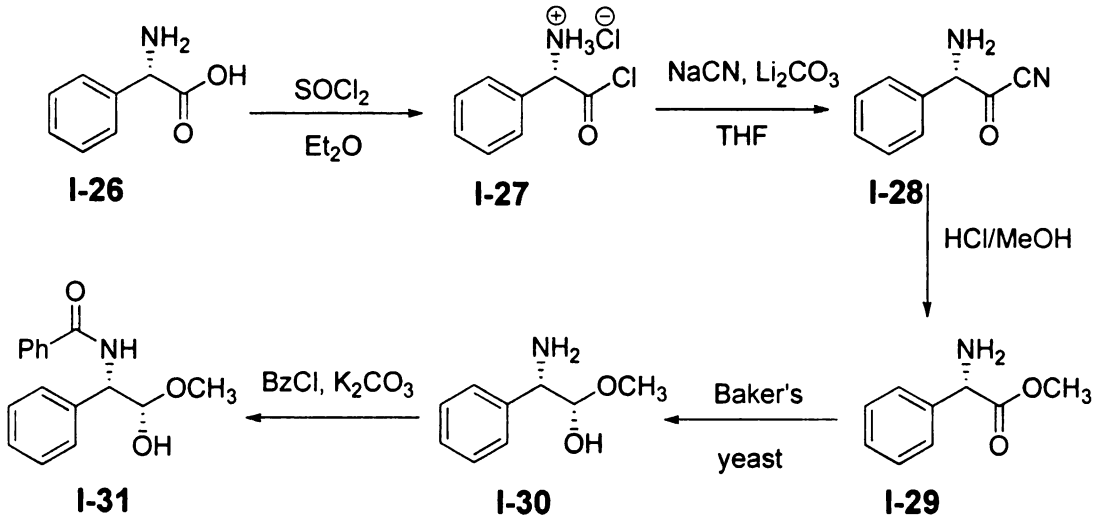

In the asymmetric catalysis approach, enantioselective epoxidation of *cis*-ethyl cinnamate using household bleach was employed with a (salen)Mn(III) complex as a catalyst[82] (**Scheme 1-2**). The diastereomeric epoxides were subjected to regioselective ring-opening using ammonia to generate 3-phenylisosereanamide. Amide hydrolysis and subsequent treatment of the 3-phenylisoserine intermediate with benzoyl chloride gives the desired taxol side chain, phenylisoserine.

Scheme 1-2. Jacobsen protocol for the synthesis of taxol side chain.

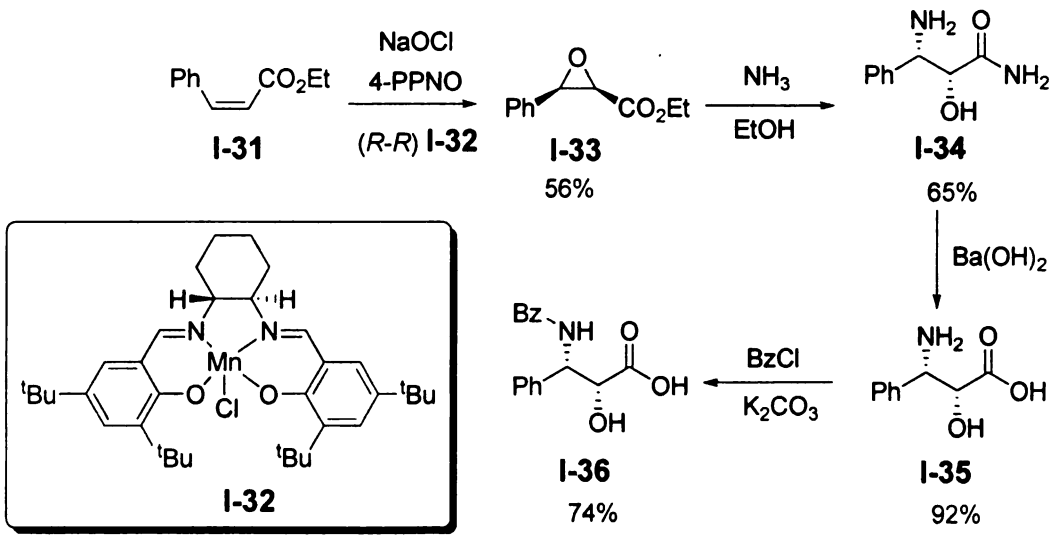

The Ojima-Holton β-lactam coupling method[77] was applied towards the initial commercial production of taxol. This methodology involves asymmetric synthesis of 3-hydroxy-4-aryl-β-lactams through regioselective cyclocondensation of lithium chiral ester enolate-imines followed by coupling of the *N*-acyl-β-lactams with baccatin III or 10-DAB to make the desired taxol analog[77,81] (**Scheme 1-3**).

Scheme 1-3. The Ojima β-lactam methodology for the *cis*-selective synthesis of the taxol side chain[77] (panel A). The origin of this selectivity is explained using the model proposed in panel (B).

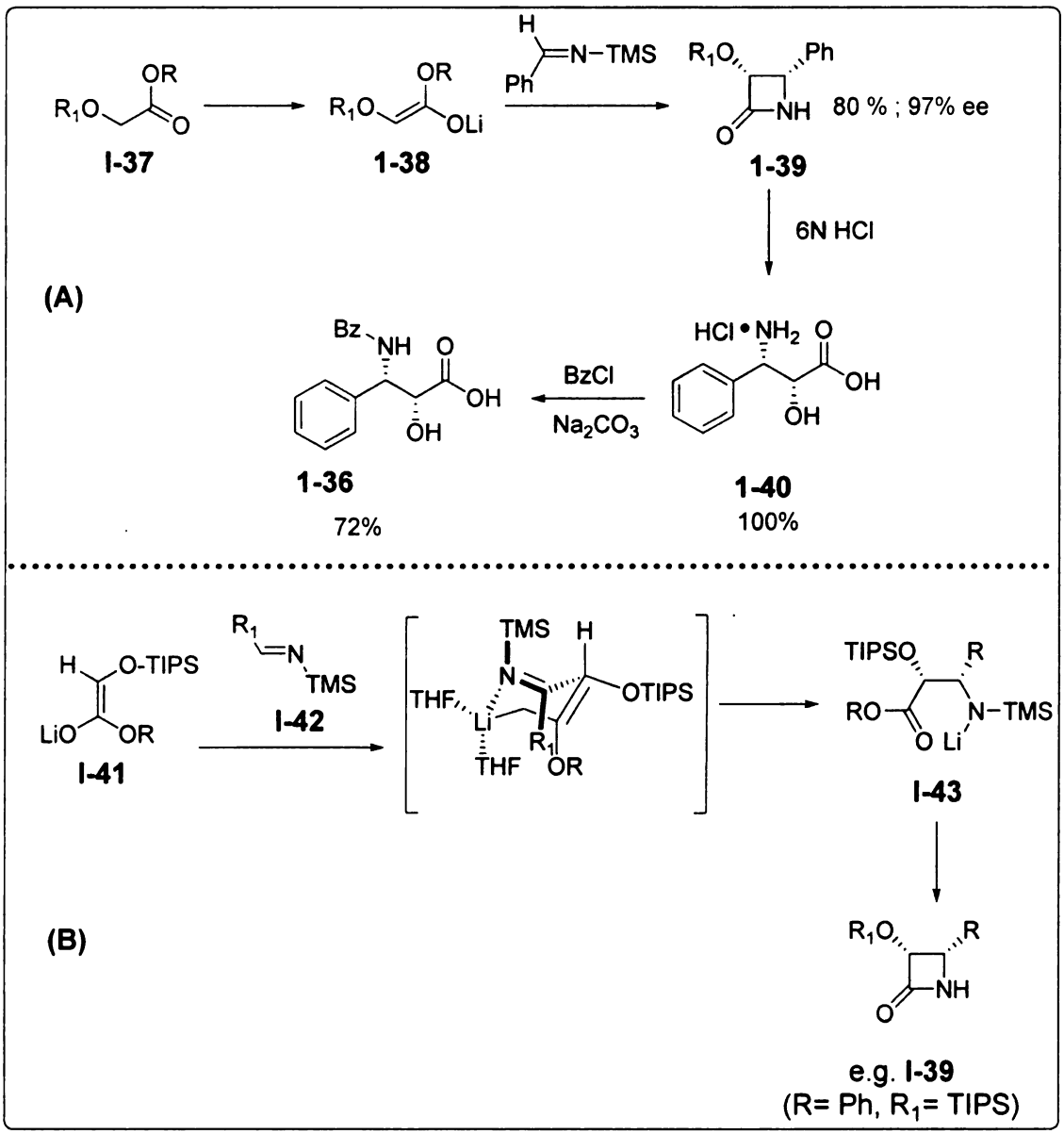

I.2.4.3 Biochemical Developments: Cell Culture Fermentation

The structural complexity of natural products such as taxol makes chemical synthesis untenable as a production option. Thus, biotechnological developments present an alternative approach to the production of taxol and its derivatives. However, viable exploitation of natural sources directly is difficult because bioactive natural products either exist in minute quantities or exhibit unpredictable accumulation.[83]

Plant cell suspension culture fermentation has become an increasingly attractive alternative to chemical synthesis because of sustainability and engineering advantages, such as reliable and renewable feedstocks, biotic and abiotic elicitation of enzyme systems, and scale-up.[84] However, due to the slow growing nature of plant cells, they are susceptible to microbial contamination. Therefore, to initiate plant tissue culture, seeds are sterilized and germinated under aseptic conditions, and a piece of the sterile plant tissue (explant) is then grown on solid culture containing agar[83] (**Figure 1-10**).

Figure 1-10. Plant cell culture fermentation from initiation to scale-up for industrial production.[83]

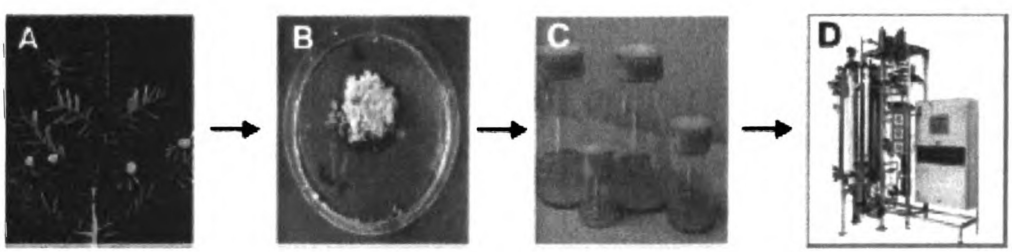

Due to an exponential increase in the medical demand for taxol, plant cell fermentation (PCF) has emerged as an environmentally benign alternative to semi-

synthesis.[85] An industrial collaborative effort between Bristol-Myers Squibb and Phyton (USA) resulted in the incorporation of PCF technology in the commercial production of taxol. This biotechnological breakthrough earned BMS the 2004 Presidential Green Chemistry Challenge Award in 2004 from EPA.[85,86] The PCF process allegedly eliminates an estimated 71,000 pounds of hazardous chemicals, 10 solvents and 6 drying steps.[87]

I.2.4.4 Biochemical Developments: Enzymology of Taxol

Bioengineering the biosynthetic pathway of taxol is an attractive alternative to semi-synthesis.[88,89] Significant progress has been made in the last decade with regard to identification and characterization of the genes encoding the relevant enzymes involved in the biosynthesis of taxol.[88,90-96] In total, there are nineteen enzymatic steps in the taxol biosynthetic pathway (**Scheme 1-4**).

The first committed step in the pathway involves the construction of the pentamethyl [9.3.1.0] tricyclopentadecane[3,8] skeleton from the universal diterpenoid precursor geranylgeranyl diphosphate by a terpene cyclase.[97,98] This is followed by several P450–mediated oxygenations and acyl CoA-dependent transacylations elaborate the skeleton[88,99].

Scheme 1-4. A schematic representation of the taxol biosynthetic pathway.

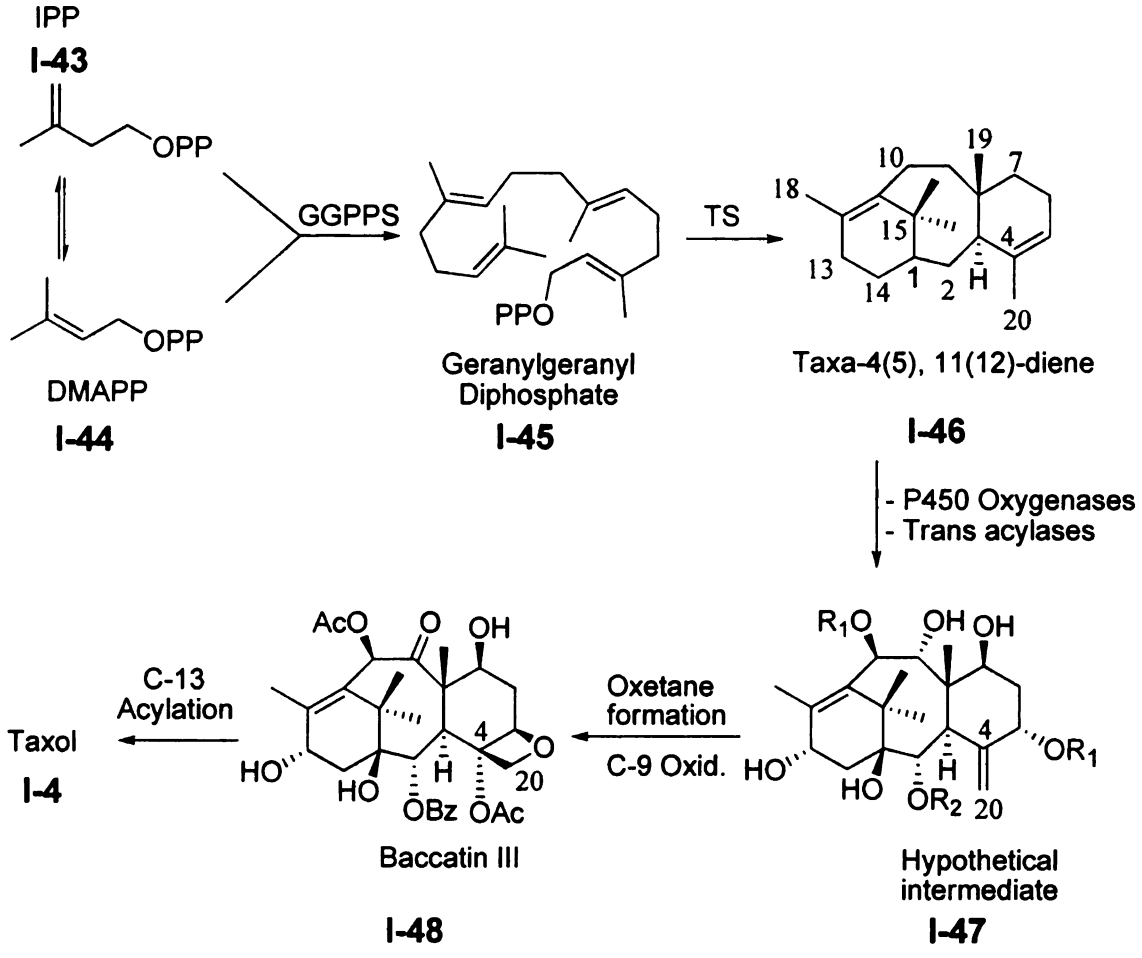

I.2.5 Skeleton Formation: Generanyl-geranyl Diphosphate Cyclization

The plastidial enzyme taxadiene synthase (TS) catalyzes the cyclization of the universal diterpenoid precursor (*E*, *E*, *E*)-geranylgeranyl diphosphate (GGPP) in a slow but non-rate limiting cyclization to form the taxol core.[100] Mechanistically, TS catalyzes a remarkable olefin cation cascade in a five-step overall stereochemical conversion of GGPP to taxa-4(5),11(12)-diene[98,100] (**Scheme 1-5**).

Scheme 1-5. The first committed step of the biosynthetic pathway of Taxol[98,100]

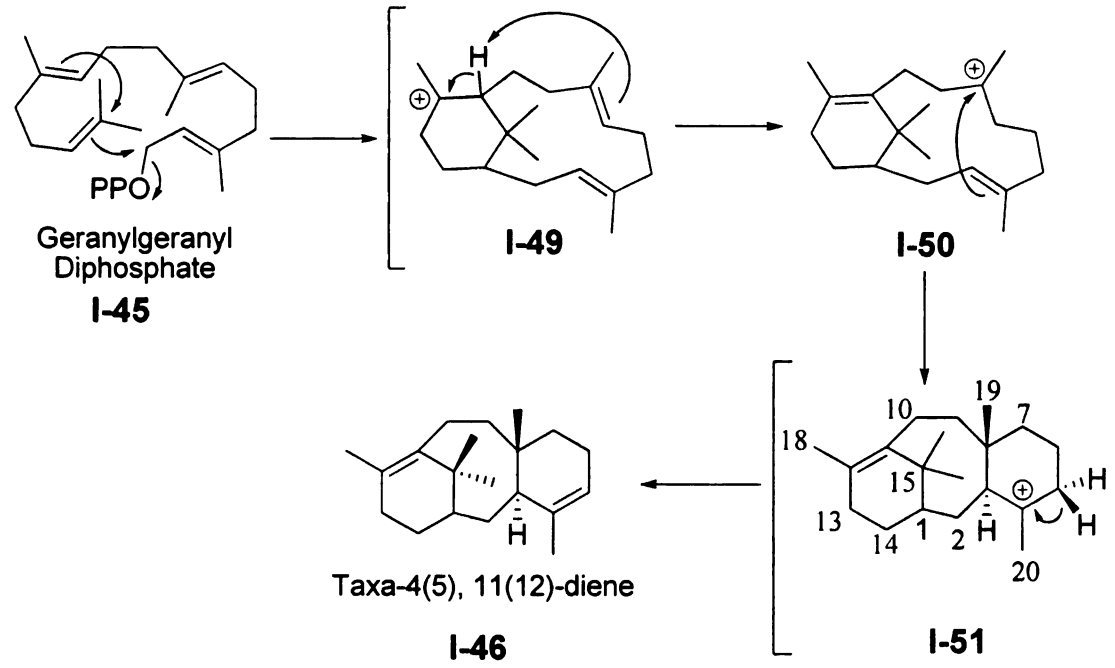

Thus, TS mediates an enantio- and face-selective polyolefin cation cascade that results in an overall formation of three carbon-carbon bonds, three stereogenic centers, and loss of a proton with absolute control of stereochemical fidelity, making it a strikingly unusual enzyme.[100]

I.2.5.1 Functionalization: Cytochrome P450-mediated Oxygenations

NMR studies and ^{18}O-feeding experiments with taxayunnanine C, a taxadiene tetraol derivative isolated from *Taxus yunnanesis*, indicate that cytochrome P450 monooxygenases are responsible for oxygenation of the taxane core.[93,101] These oxygenations constitute nearly half of the transformations of the taxol biosynthetic pathway.[102] The first oxidative modification on the progenitor diene by a *Taxus* microsomal cytochrome P450 monooxygenase constitutes the second specific step of taxol biosynthesis [88,103,104] (**Scheme 1-6**).

Scheme 1-6. Acetylation and subsequent hydroxylation of taxadien-5α-ol; the broken arrows indicate hydroxylation steps in the biosynthetic pathway that are not yet defined.

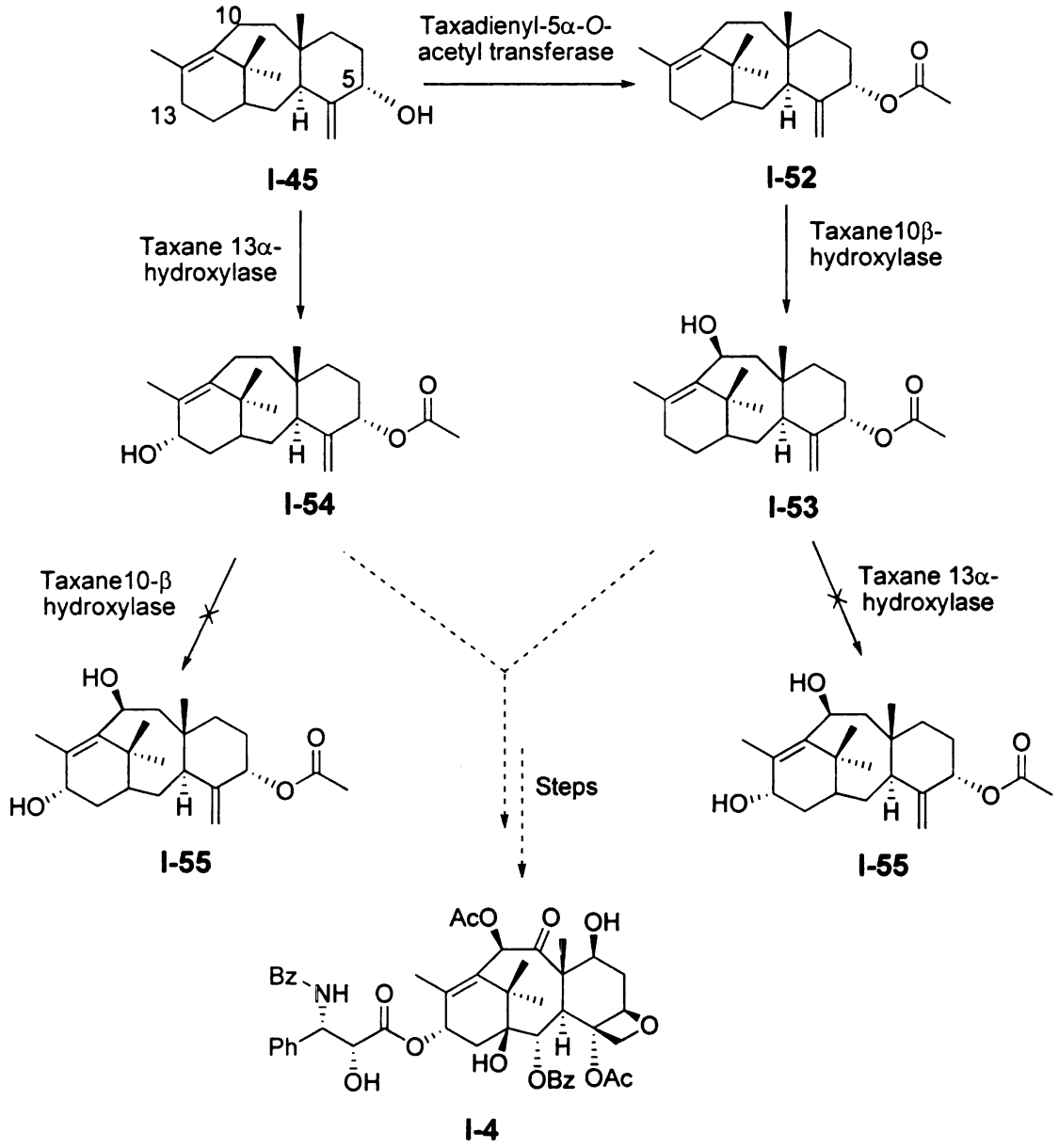

The C-5α hydroxylase is not only regio- and stereospecific but it is also responsible for the isomerization of the C4/C5 olefin to the exocyclic C4/C20 position.[98]

The order of subsequent hydroxylations of the taxane core is undefined. Thus, P450-mediated oxygenations beyond C-5α are formulated primarily on the relative abundance of oxygenated taxoids. The C-10 is thought to be oxygenated after C-5,

followed either by C-2 or C-9, then C-13; the C-1 and C-7 hydroxylases are considered late-stage enzymes.[88,102] Efforts to determine the order of hydroxylation is compounded by the observation that acylations of extant hydroxyl functional groups may precede new oxygenations of the skeleton.[105]

I.2.5.2 Elaboration of the Skeleton by Acyltransferases

Taxadienyl acetate is turned over more efficiently by cytochrome P450 enzymes than taxadienol[88] in subsequent hydroxylation steps (cf. **Scheme 1-6**). Thus, taxadienyl acetate likely represents the third specific intermediate in the taxol pathway. Two enzymes with comparable catalytic and kinetic properties against taxadienol substrates have been characterized as taxadien-5α-ol-*O*- acetyltransferases (TAT).[106] These two enzymes have moderate sequence similarity (77%) and identity (61%), and yet they utilize several common substrates with comparable kinetic efficiencies.[106] This makes it difficult to correlate primary structure to substrate utilization.

The first aroyltransferase on the taxol pathway is thought to be the taxane 2α-*O*-benzoyltransferase (TBT), which is specific for the C-2 hydroxyl group.[95] This proposition is based on biogenetic considerations using the relative abundances of naturally occurring taxoids of differing functionalization levels.[95] Unlike the 5α-*O*-acetyltransferases (TAT), TBT utilizes advanced and fully functionalized taxoids and is regioselective for the C-2α position of 7,13-diacetyl-2-debenzoylbaccatin III.[95,107] The fact that TBT does not utilize 10-deacetyl-2-debenzoylbaccatin III or simpler

substrates such as taxa-4(5),11(12)-dien-2α,5α-diol indicates that a higher level of substitution might be necessary for productive catalysis.[95]

Random sequencing and other homology-based cloning of transcripts isolated from *Taxus* cell culture have yielded a family of 16 acyltransferase clones, six of which have been functionally characterized.[108] Three of these clones encode for acetyltransferases, two encode for benzoyltransferases, and one encodes for a phenylisoserinyl transferase. The rest of the clones encode for proteins that are either functionally undefined as yet or are implicated in off-pathway transformations.[95,99,109]

I.2.5.3 Increasing Structural Complexity: Attachment of the Side Chain

The structural pharmacophore of taxol responsible for binding to β tubulin comprises, in part, the 13-*O*-(*N*-benzoyl-3-phenylisoseryinoyl) side chain.[22] The first committed step in the biosynthesis of the taxol phenylisoserinyl side chain involves phenylalanine amino mutase (PAM) which converts 2*S*-α-phenylalanine to 3*R*-β-phenylalanine.[110-112] β-phenylalanine is then ligated to CoA and ultimately incorporated into the C-13 hydroxyl group of baccatin III by an acyl-CoA-dependent transferase (**Scheme 1-7**). The relative abundance of late-stage taxoids such as baccatin III and 10-DAB indicate that either the β-phenylalanine CoA ligase or β-phenylalanoyltransferase may be rate limiting in the assembly of the side chain.[112]

In vivo feeding studies with deuterated amino acids indicate that *N*--benzoylphenylisoserine is not incorporated into baccatin III, while β-phenylalanine and β-phenylisoserine are productive substrates.[113,114] These results suggest that β-

phenylalanine as the free amine is first attached to baccatin III followed by either *N*-benzoylation or C-2' hydroxylation to complete the biosynthetic pathway.

Scheme 1-7. Biosynthesis of the taxol side chain. Isolation of taxane metabolites such as Taxine-B (inset), a metabolite with a C-5 substitution that is structurally analogous to the C-13 side chain of taxol, has led to speculation that the C-5 hydroxyl is the initial acylation site followed by an intramolecular esterification to transfer it to the C-13 position.

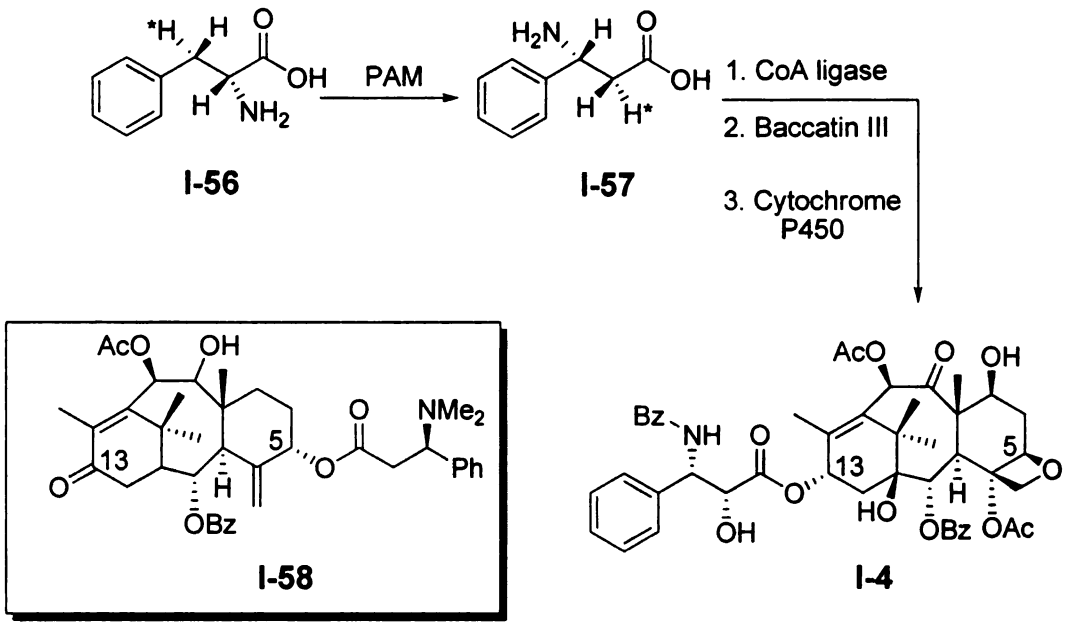

Interestingly, taxanes with C-5 side chains structurally analogous to the taxol C-13 side chain, such as taxine B (**Scheme 1-7**), have been isolated. This led to speculation that perhaps the side chain is first attached to the C-5 or C-4 position and then transferred to the C-13 position through intramolecular transesterification.[114,115]

I.2.6 Conclusion and Significance

Natural products have had storied success in clinical applications and many others reported in the literature have potential medicinal properties.[8] In spite of this success, the last decade has seen a precipitous decline in natural product screening efforts for drug discovery by big pharmaceutical companies.[9] Some reasons for this decline include the screening cost and incompatibility between established screening paradigm of natural product extract library and modern screening techniques such as high-throughput.[116] Additionally, the advent of novel techniques for identification of aberrant gene targets for new drugs, unprecedented development in computational chemistry, and combinatorial chemistry have enhanced identification of lead bioactive compounds without the need for the tedious traditional discovery approach.[4,117,118]

Due to advances in synthetic organic chemistry, even complex natural products continue to succumb to chemical modifications through parallel synthesis and semi-synthesis.[119] Moreover, recent advances in combinatorial biosynthesis have made it possible to efficiently and iteratively introduce structural diversity into natural product scaffolds that cannot otherwise be modified through conventional synthetic methodologies.[120,121]

The clinical demand for the antitumor natural product taxol has grown exponentially over the years. Currently, the drug is being tested for combination therapy against various forms of cancer and is also being tested for applications in new disease segments.[122] While biotechnological developments such as cell culture

fermentation technology provide a steady supply of taxol, its derivatives cannot be similarly produced *in planta* without engineering the taxol metabolic pathway. Thus, a full understanding of the enzymology of taxol is an important undertaking for a sustainable production of more efficacious taxol analogs.[123,124]

The next three chapters will highlight research projects aimed at developing a chemo-enzymatic process for the production of next generation taxol analogs. In Chapter 2, the critical role of plant acyltransferases in creating structural diversity in natural products will be evaluated. Specifically, an overview of plant acyltransferases that belong to the BAHD superfamily will be presented. The *Taxus* acyltransferases used to make taxol presented herein belong to BAHD superfamily. This chapter will present the findings of the initial screening of a library of *Taxus* acyltransferases in search of promiscuous enzyme activity.

In Chapter 3, some of the observations and insights arising from the screening study will be presented. In particular, an assessment of the potential application of promiscuous enzyme activity in the biocatalysis of unnatural acyl groups will be presented. Based on preliminary findings, the proposed mechanism for the BAHD acyltransferases will be reviewed and contrasted with an alternative mechanism proposed for a *Taxus* acyltransferase.

Chapter 4 will highlight the state-of-the-art in the semi-synthesis of taxol analogs, especially those involving modification of the C-4 and C-13 positions of baccatin III or its analogs. A methodology was developed that incorporates one-pot transformations to reduce the number of chemical transformations from current semi-synthetic methodologies. This strategy and its potential application will be evaluated.

1.3 References

(1) Jemal, A.; Siegel, R.; Ward, E.; Hao, Y.; Xu, J.; Thun, M. J. *CA: A Cancer Journal for Clinicians* **2009**, *59*, 225-249.

(2) Jemal, A.; Siegel, R.; Ward, E.; Hao, Y.; Xu, J.; Murray, T.; Thun, M. J. *CA: A Cancer Journal for Clinicians* **2008**, *58*, 71-96.

(3) Fazlul, H. S.; Yiwei, L. *Cancer Treatment Reviews* **2009**, *35*, 597-607.

(4) Mann, J. *Nature Reviews Cancer* **2002**, *2*, 143-148.

(5) Newman, D. J.; Cragg, G. M.; Snader, K. M. *Natural Product Reports* **2000**, *17*, 215-234.

(6) Newman, D. J.; Cragg, G. M.; Snader, K. M. *Journal of Natural Products* **2003**, *66*, 1022-1037.

(7) Alves, R.; Rosa, I. *Journal of Ethnobiology and Ethnomedicine* **2005**, *1*, 5.

(8) Gullo, V.; McAlpine, J.; Lam, K.; Baker, D.; Petersen, F. *Journal of Industrial Microbiology and Biotechnology* **2006**, *33*, 523-531.

(9) Lam, K. S. *Trends in Microbiology* **2007**, *15*, 279-289.

(10) Wood, K. W.; Cornwell, W. D.; Jackson, J. R. *Current Opinion in Pharmacology* **2001**, *1*, 370-377.

(11) Gascoigne, K. E.; Taylor, S. S. *Journal of Cell Science* **2009**, *122*, 2579-2585.

(12) Dumontet, C.; Sikic, B. I. *Journal of Clinical Oncolology* **1999**, *17*, 1061-.

(13) Access Date: 7/07/2010.

(14) Wall, M. E.; Wani, M. C. *Cancer Research* **1995**, *55*, 753-60.

(15) Huang, M.; Gao, H.; Chen, Y.; Zhu, H.; Cai, Y.; Zhang, X.; Miao, Z.; Jiang, H.; Zhang, J.; Shen, H.; Lin, L.; Lu, W.; Ding, J. *Clinical Cancer Research* **2007**, *13*, 1298-1307.

(16) Pommier, Y.; Cherfils, J. *Trends in Pharmacological Sciences* **2005**, *26*, 138-145.

(17) Staker, B. L.; Hjerrild, K.; Feese, M. D.; Behnke, C. A.; Burgin, A. B.; Stewart, L. *Proceedings of the National Academy of Sciences of the United States of America* **2002**, *99*, 15387-15392.

(18) Abraham, A. T.; Lin, J.-J.; Newton, D. L.; Rybak, S.; Hecht, S. M. *Chemistry & Biology* **2003**, *10*, 45-52.

(19) Tao, Z.-F.; Konishi, K.; Keith, G. r.; Hecht, S. M. *Journal of the American Chemical Society* **2006**, *128*, 14806-14807.

(20) Cragg, G.; Newman, D. *Journal of ethnopharmacology* **2005**, *100*, 72-79.

(21) Wani, M. C.; Taylor, H. L.; Wall, M. E.; Coggon, P.; McPhail, A. T. *Journal of the American Chemical Society* **1971**, *93*, 2325-7.

(22) Rowinsky, E. K.; Cazenave, L. A.; Donehower, R. C. *Journal of the National Cancer Institute* **1990**, *82*, 1247.

(23) Wall, M. E.; Wani, M. C. *Journal of Ethnopharmacol.* **1996**, *51*, 239-54.

(24) Sparreboom, A.; vanTellingen, O.; Nooijen, W. J.; Beijnen, J. H. *Cancer Research* **1996**, *56*, 2112-2115.

(25) Sparreboom, A.; van Tellingen, O.; Huizing, M. T.; Nooijen, W. J.; Beijnen, J. H. *Journal of Chromatography B: Biomedical Sciences and Applications* **1996**, *681*, 355-362.

(26) Lee, K.; Chung, H.; Im, S.; Park, Y.; Kim, C.; Kim, S.-B.; Rha, S.; Lee, M.; Ro, J. *Breast Cancer Research and Treatment* **2008**, *108*, 241-250.

(27) Green, M. R.; Manikhas, G. M.; Orlov, S.; Afanasyev, B.; Makhson, A. M.; Bhar, P.; Hawkins, M. J. *Annals of Oncology* **2006**, *17*, 1263-1268.

(28) Kumar, N. *Journal of Biological Chemistry* **1981**, *256*, 435-441.

(29) Manfredi, J. J.; Horwitz, S. B. *Pharmacology & Therapeutics* **1984**, *25*, 83-125.

(30) Schiff, P. B.; Horwitz, S. B. *Proceedings of the National Academy of Sciences of the United States of America* **1980**, *77*, 1561-1565.

(31) Ojima, I.; Chakravarty, S.; Inoue, T.; Lin, S. N.; He, L. F.; Horwitz, S. B.; Kuduk, S. D.; Danishefsky, S. J. *Proceedings of the National Academy of Sciences of the United States of America* **1999**, *96*, 4256-4261.

(32) Schiff, P. B.; Fant, J.; Horwitz, S. B. *Nature* **1979**, *277*, 665-667.

(33) Olmsted, J. B.; Borisy, G. G. *Annual Review of Biochemistry* **1973**, *42*, 507-540.

(34) Morris, P. G.; Fornier, M. N. *Clinical Cancer Research* **2008**, *14*, 7167-7172.

(35) Mitchison, T.; Kirschner, M. *Nature* **1984**, *312*, 237-242.

(36) Jordan, M.; Wilson, L. *Nature Reviews Cancer* **2004**, *4*, 253-265.

(37) Wassmann, K.; Benezra, R. *Current Opinion in Genetics & Development* **2001**, *11*, 83-90.

(38) Paik, Y.; Yang, C.; Metaferia, B.; Tang, S.; Bane, S.; Ravindra, R.; Shanker, N.; Alcaraz, A. A.; Johnson, S. A.; Schaefer, J.; O'Connor, R. D.; Cegelski, L.; Snyder, J. P.; Kingston, D. G. I. *Journal of the American Chemical Society* **2006**, *129*, 361-370.

(39) Kingston, D. *Pure & Applied Chemistry* **1998**, *70*, 331-334.

(40) Fang, W. S.; Liang, X. T. *Mini-Reviews in Medicinal Chemistry* **2005**, *5*, 1-12.

(41) Filizola, M.; Villar, H. O.; Loew, G. H. *Journal of Computer-Aided Molecular Design* **2001**, *15*, 297-307.

(42) Giannakakou, P.; Gussio, R.; Nogales, E.; Downing, K. H.; Zaharevitz, D.; Bollbuck, B.; Poy, G.; Sackett, D.; Nicolaou, K. C.; Fojo, T. *Proceedings of the National Academy of Sciences of the United States of America* **2000**, *97*, 2904-2909.

(43) He, L. F.; Jagtap, P. G. F.; Kingston, D. G. I.; Shen, H. J.; Orr, G. A.; Horwitz, S. B. *Biochemistry* **2000**, *39*, 3972-3978.

(44) Martello, L. A.; LaMarche, M. J.; He, L. F.; Beauchamp, T. J.; Smith, A. B.; Horwitz, S. B. *Chemistry & Biology* **2001**, *8*, 843-855.

(45) Winkler, J. D.; Axelsen, P. H. *Bioorganic & Medicinal Chemistry Letters* **1996**, *6*, 2963-2966.

(46) Kingston, D. G. I. *Phytochemistry* **2007**, *68*, 1844-1854.

(47) Guénard, D.; Guéritte-Voegelein, F.; Potier, P. *Accounts of Chemical Research* **1993**, *26*, 160-167.

(48) Kingston, D. G. I. *Pharmacology & Therapeutics* **1991**, *52*, 1-34.

(49) Rao, S.; Krauss, N. E.; Heerding, J. M.; Swindell, C. S.; Ringel, I.; Orr, G. A.; Horwitz, S. B. *Journal of Biological Chemistry* **1994**, *269*, 3132-3134.

(50) Rao, S.; He, L.; Chakravarty, S.; Ojima, I.; Orr, G. A.; Horwitz, S. B. *Journal of Biological Chemistry* **1999**, *274*, 37990-37994.

(51) Nogales, E.; Wolf, S. G.; Downing, K. H. *Nature* **1998**, *391*, 199-203.

(52) Snyder, J. P.; Nettles, J. H.; Cornett, B.; Downing, K. H.; Nogales, E. *Proceedings of the National Academy of Sciences of the United States of America* **2001**, *98*, 5312-5316.

(53) Skwarczynski, M.; Hayashi, Y.; Kiso, Y. *Journal of Medicinal Chemistry* **2006**, *49*, 7253-7269.

(54) Ojima, I.; Duclos, O.; Kuduk, S. D.; Sun, C.-M.; Slater, J. C.; Lavelle, F.; Veith, J. M.; Bernacki, R. J. *Bioorganic & Medicinal Chemistry Letters* **1994**, *4*, 2631-2634.

(55) Vandervelde, D. G.; Georg, G. I.; Grunewald, G. L.; Gunn, G. W.; Mitscher, L. A. *Journal of the American Chemical Society* **1993**, *115*, 11650-11651.

(56) Dubois, J.; Guenard, D.; Guerittevoegelein, F.; Guedira, N.; Potier, P.; Gillet, B.; Beloeil, J. C. *Tetrahedron* **1993**, *49*, 6533-6544.

(57) Ganesh, T.; Guza, R. C.; Bane, S.; Ravindra, R.; Shanker, N.; Lakdawala, A. S.; Snyder, J. P.; Kingston, D. G. I. *Proceedings of the National Academy of Sciences* **2004**, *101*, 10006-10011.

(58) Williams, H. J.; Scott, A. I.; Dieden, R. A.; Swindell, C. S.; Chirlian, L. E.; Francl, M. M.; Heerding, J. M.; Krauss, N. E. *Canadian Journal of Chemistry-Revue Canadienne De Chimie* **1994**, *72*, 252-260.

(59) Ganesh, T.; Norris, A.; Sharma, S.; Bane, S.; Alcaraz, A. A.; Snyder, J. P.; Kingston, D. G. I. *Bioorganic & Medicinal Chemistry* **2006**, *14*, 3447-3454.

(60) Kingston, D. G. I.; Bane, S.; Snyder, J. P. *Cell Cycle* **2005**, *4*, 279-289.

(61) Ojima, I.; Lin, S.; Inoue, T.; Miller, M. L.; Borella, C. P.; Geng, X.; Walsh, J. J. *Journal of the American Chemical Society* **2000**, *122*, 5343-5353.

(62) Chaudhary, A. G.; Kingston, D. G. I. *Tetrahedron Letters* **1993**, *34*, 4921-4924.

(63) Georg, G. I.; Cheruvallath, Z. S. *Journal of Organic Chemistry* **1994**, *59*, 4015-4018.

(64) Kingston, D. G. I.; Chordia, M. D.; Jagtap, P. G.; Liang, J.; Shen, Y.-C.; Long, B. H.; Fairchild, C. R.; Johnston, K. A. *Journal of Organic Chemistry* **1999**, *64*, 1814-1822.

(65) Neidigh, K. A.; Gharpure, M. M.; Rimoldi, J. M.; Kingston, D. G. I.; Jiang, Y. Q.; Hamel, E. *Tetrahedron Letters* **1994**, *35*, 6839-6842.

(66) Kingston, D.; Chaudhary, A.; Chordia, M.; Gharpure, M.; Gunatilaka, A.; Higgs, P.; Rimoldi, J.; Samala, L.; Jagtap, P.; Giannakakou, P. *Journal of Medicinal Chemistry* **1998**, *41*, 3715-3726.

(67) Holton, R. A.; Kim, H. B.; Somoza, C.; Liang, F.; Biediger, R. J.; Boatman, P. D.; Shindo, M.; Smith, C. C.; Kim, S.; et al. *Journal of the American Chemical Society* **1994**, *116*, 1599-1600.

(68) Masters, J. J.; Link, J. T.; Snyder, L. B.; Young, W. B.; Danishefsky, S. J. *Angewandte Chemie, International Edition in English* **1995**, *34*, 1723-1726.

(69) Nicolaou, K. C.; Yang, Z.; Liu, J. J.; Ueno, H.; Nantermet, P. G.; Guy, R. K.; Claiborne, C. F.; Renaud, J.; Couladouros, E. A.; Paulvannan, K.; Sorensen, E. J. *Nature* **1994**, *367*, 630-634.

(70) Wender, P. A.; Natchus, M. G.; Shuker, A. J. In *Taxol: Science and Applications*; Suffness, M., Ed.; CRC Press: New York, 1995.

(71) Walji, A. M.; MacMillan, D. W. C. *ChemInform* **2007**, *38*.

(72) Holton, R. A.; Somoza, C.; Kim, H. B.; Liang, F.; Biediger, R. J.; Boatman, P. D.; Shindo, M.; Smith, C. C.; Kim, S.; et al. *Journal of the American Chemical Society* **1994**, *116*, 1597-8.

(73) Wender, P. A.; Badham, N. F.; Conway, S., P. ; Floreancig, P. E.; Glass, T. E.; Granicher, C.; Houze, J. B.; Janichen, J.; Lee, D. S.; Marquess, D. G.; McGrane, P. L.; Meng, W.; Mucciaro, T. P.; Muhlebach, M.; Natchus, M. G.; Paulsen, H.; Rawlins, D. B.; Satkofsky, J.; Shuker, A. J.; Sutton, J. C.; Taylor, R. E.; Tomooka, K. *Journal of the American Chemical Society* **1997**, *119*, 2755-2756.

(74) Wender, P. A.; Badham, N. F.; Conway, S. P.; Floreancig, P. E.; Glass, T. E.; Houze, J. B.; Krauss, N. E.; Lee, D. S.; Marquess, D. G.; McGrane, P. L.; Meng, W.; Natchus, M. G.; Shuker, A. J.; Sutton, J. C.; Taylor, R. E. *Journal of the American Chemical Society* **1997**, *119*, 2757-2758.

(75) Danishefsky, S. J.; Masters, J. J.; Young, W. B.; Link, J. T.; Snyder, L. B.; Magee, T. V.; Jung, D. K.; Isaacs, R. C. A.; Bornmann, W. G.; Alaimo, C. A.; Coburn, C. A.; Di Grandi, M. J. *Journal of the American Chemical Society* **1996**, *118*, 2843-2859.

(76) Nicolaou, K. C.; Yang, Z.; Liu, J. J.; Ueno, H.; Nantermet, P. G.; Guy, R. K.; Claiborne, C. F.; Renaud, J.; Couladouros, E. A.; Paulvannan, K.; Sorensen, E. J. *Nature* **1994**, *367*, 630-634.

(77) Ojima, I.; Habus, I.; Zhao, M.; Zucco, M.; Park, Y. H.; Sun, C. M.; Brigaud, T. *Tetrahedron* **1992**, *48*, 6985.

(78) Denis, J. N.; Correa, A.; Greene, A. E. *The Journal of Organic Chemistry* **1990**, *55*, 1957-1959.

(79) Holton, R. A.; Biediger, R. J.; Boatman, P. D. In *Taxol: Science and Applications*; Suffness, M., Ed.; CRC Press: Boca Raton, FL, 1995.

(80) Kearns, J.; Kayser, M. M. *Tetrahedron Letters* **1994**, *35*, 2845-8.

(81) Ojima, I.; Habus, I.; Zhao, M.; Georg, G. I.; Jayasinghe, L. R. *Journal of Organic Chemistry* **1991**, *56*, 1681.

(82) Deng, L.; Jacobsen, E. N. *Journal of Organic Chemistry* **1992**, *57*, 4320-4323.

(83) McCoy, E.; O'Connor, S. E. In *Natural Compounds as Drugs Volume I*, 2008.

(84) Kolewe, M. E.; Gaurav, V.; Roberts, S. C. *Molecular Pharmaceutics* **2008**, *5*, 243-256.

(85) Tabata, H. *Biomanufacturing* **2004**, 1-23.

(86) Dunn, P. a. W., A. and Williams, M.T. *Green Chemistry in the Pharmaceutical Industry*; Wiley-VCH: Weinheim, 2010.

(87) EPA, 2004, Access date 07/05/2010; Vol. 2010.

(88) Walker, K.; Croteau, R. *Phytochemistry* **2001**, *58*, 1-7.

(89) Engels, B.; Dahm, P.; Jennewein, S. *Metabolic engineering* **2008**, *10*, 201-206.

(90) Walker, K.; Croteau, R. *Proceedings of the National Academy of Sciences of the United States of America* **2000**, *97*, 583-587.

(91) Walker, K.; Schoendorf, A.; Croteau, R. *Archives of Biochemistry and Biophysics* **2000**, *374*, 371-380.

(92) Walker, K.; Ketchum, R. E. B.; Hezari, M.; Gatfield, D.; Goleniowski, M.; Barthol, A.; Croteau, R. *Archives of Biochemistry and Biophysics* **1999**, *364*, 273-279.

(93) Chau, M.; Jennewein, S.; Walker, K.; Croteau, R. *Chemistry & Biology* **2004**, *11*, 663-672.

(94) Walker, K.; Croteau, R. *Recent Advances in Phytochemistry* **1999**, *33*, 31-50.

(95) Walker, K.; Croteau, R. *Proceedings of the National Academy of Sciences of the United States of America* **2000**, *97*, 13591-13596.

(96) Croteau, R. B.; Walker, K. D.; Schoendorf, A.; Wildung, M. R.; Washington State University Research Foundation: USA, 2006.

(97) Wildung, M. R.; Croteau, R. *Journal of Biological Chemistry* **1996**, *271*, 9201-9204.

(98) Lin, X.; Hezari, M.; Koepp, A. E.; Floss, H. G.; Croteau, R. *Biochemistry* **1996**, *35*, 2968-2977.

(99) Hampel, D.; Mau, C. J. D.; Croteau, R. B. *Archives of Biochemistry and Biophysics* **2009**, *487*, 91-97.

(100) Williams, D. C.; Carroll, B. J.; Jin, Q.; Rithner, C. D.; Lenger, S. R.; Floss, H. G.; Coates, R. M.; Williams, R. M.; Croteau, R. *Chemistry & Biology* **2000**, *7*, 969-977.

(101) Hezari, M.; Croteau, R. *Planta Medica* **1997**, *63*, 291-295.

(102) Jennewein, S.; Rithner, C. D.; Williams, R. M.; Croteau, R. B. *Proceedings of the National Academy of Sciences of the United States of America* **2001**, *98*, 13595-13600.

(103) Hefner, J.; Croteau, R. *Methods in Enzymology* **1996**, *272*, 243-250.

(104) Jennewein, S.; Long, R. M.; Williams, R. M.; Croteau, R. *Chemistry & Biology* **2004**, *11*, 379-387.

(105) Walker, K.; Croteau, R. *Phytochemicals in human health protection, nutrition and plant defense* **1999**, 31.

(106) Chau, M.; Croteau, R. *Archives of Biochemistry and Biophysics* **2004**, *427*, 48-57.

(107) Nawarathne, I.; Walker, K. *Journal Natural Product*, *73*, 151-159.

(108) Jennewein, S.; Wildung, M. R.; Chau, M.; Walker, K.; Croteau, R. *Proceedings of the National Academy of Sciences of the United States of America* **2004**, *101*, 9149-9154.

(109) Chau, M.; Walker, K.; Long, R.; Croteau, R. *Archives of Biochemistry and Biophysics* **2004**, *430*, 237-246.

(110) Walker, K. D.; Floss, H. G. *Journal of the American Chemical Society* **1998**, *120*, 5333-5334.

(111) Walker, K. D.; Klettke, K.; Akiyama, T.; Croteau, R. *Journal of Biological Chemistry* **2004**, *279*, 53947-53954.

(112) Steele, C. L.; Chen, Y.; Dougherty, B. A.; Li, W.; Hofstead, S.; Lam, K. S.; Xing, Z.; Chiang, S.-J. *Archives of Biochemistry and Biophysics* **2005**, *438*, 1-10.

(113) Floss, H. G.; Mocek, U. In *Taxol: Science and Applications*; Suffness, M., Ed.; CRC Press: Boca Raton, FL, 1995.

(114) Fleming, P. E.; Knaggs, A. R.; He, X.-G.; Mocek, U.; Floss, H. G. *Journal of the American Chemical Society* **1994**, *116*, 4137.

(115) Gueritte-Voegelein, F.; Guenard, D.; Potier, P. *Journal of Natural Products* **1987**, *50*, 9-18.

(116) Koehn, F. E.; Carter, G. T. *Nature Reviews Drug Discovery* **2005**, *4*, 206-220.

(117) Dobson, C. M. *Nature* **2004**, *432*, 824-828.

(118) Lipinski, C.; Hopkins, A. *Nature* **2004**, *432*, 855-861.

(119) Paterson, I.; Anderson, E. A. *Science* **2005**, *310*, 451-453.

(120) Sanchez, C.; Zhu, L.; Alfredo, B.; Salas, P.; Rohr, J.; Mendez, C.; Salas, J. *Proceedings of the National Academy of Sciences of the United States of America* **2005**, *102*, 461-466.

(121) Bode, H. B.; Müller, R. *Angewandte Chemie International Edition* **2005**, *44*, 6828-6846.

(122) Dangas, G.; Ellis, S. G.; Shlofmitz, R.; Katz, S.; Fish, D.; Martin, S.; Mehran, R.; Russell, M. E.; Stone, G. W. *Journal of the American College of Cardiology* **2005**, *45*, 1186-1192.

(123) Jennewein, S.; Croteau, R. *Applied Microbiology and Biotechnology* **2001**, *57*, 13-19.

(124) Croteau, R.; Ketchum, R.; Long, R.; Kaspera, R.; Wildung, M. *Phytochemistry Reviews* **2006**, *5*, 75-97.

2 Chapter Two: Enzyme Promiscuity as a Biocatalytic Tool

2.1 Specific Aims

The broad objective of this research project is to probe *Taxus* acyltransferases for non-native transacylase activity by first seeking to understand their substrate scope. Such knowledge is important because it provides the basis for evolving better biocatalysts through genetic engineering. For initial screening of novel activity, the acyltransferases on the taxol pathway will be central to the biochemical studies presented herein. More specifically, the goal will be to identify recombinant *Taxus* enzymes that transfer short alkyl chains from alkyl CoA thioesters to surrogate taxane substrates. From this pool of transacylases it is expected that an enzyme could be identified that catalyzes transfer of non-natural acyl donors such as the methylcarbonate group found in a water-soluble Taxol analog BMS-275183 (**Figure 2-1**).

In the last two decades, phenomenal progress has been made in the development of methodologies to semi-synthesize potent taxol analogs.[1,2] However, due to exponential increase in demand for this antineoplastic drug, in part due to new applications in other disease segments such as neurodegenerative diseases,[3,4] there is need for an integrated semi-synthetic approach that is not only expedient and cost effective, but tractable and environmentally benign as well.

Given the structural complexity of taxol, semi-synthesis of modified taxanes is lengthy and laborious. Current semi-synthetic methodologies use necessary but often redundant protecting group manipulations to circumvent problems associated with differential reactivity of the various functional groups on the taxol molecule.[1,5] For

example, in order to modify the C-4 acetate with acyl groups that confer better efficacy, sequential silyl protection of C-1, C-7, and C-13 hydroxyl groups is necessary before hydrolysis of the C-4 acetate.[1] Cleavage of the ester is followed by acylation with the desired acyl moiety, deprotection of the silyl groups, and a new round of selective silyl protection of the C-7 alcohol before attachment of the C-13 side chain.[6] A similar protocol has been used to install a methylcarbonate moiety at the C-4 position, a *tert*-butyl group, and an *N*-boc at the C-3' position of the taxol analog BMS-275183[1] (**Figure 2-1**). Unlike taxol, this analog is water-soluble and has a better bioavailability profile.[1]

Figure 2-1. Water-soluble taxol analog BMS-275183.

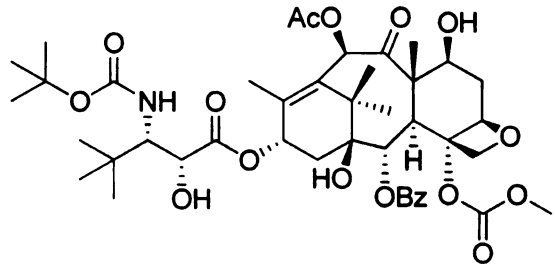

II-1

The differential reactivity of baccatin III hydroxyl groups necessitates multiple protection-deprotection cycles. This makes the synthetic protocol for production of potent analogs inherently redundant. Therefore, a process incorporating a combination of enzyme-mediated transformations and chemical synthesis will have distinct advantages over a purely semi-synthetic approach. Enzymatic processes could potentially reduce the redundancy of the protecting group chemistry commonly found in semi-synthetic approaches to next generation taxol compounds, while chemical transformations could replace inherently low yielding enzymatic reactions or be applied where biotransformations are not tenable.

This research project seeks to *establish the foundation for a chemo-enzymatic process for the production of more efficacious C-4-modified taxol analogs*. Development of such an enzymatic process is expected to be challenging because none of the functionally characterized *Taxus* acyltransferases possess transacylase activity at the tertiary C-4 acetate of advanced taxanes. Thus, the initial screen of the *Taxus* library of enzymes for novel C-4 activity is largely empirical. Although a total of six alkyl and aroyl transferases from this library are potential candidates, short-chain alkyl transferases are considered the best candidates for the preliminary screening efforts. These short chain alkyl transferases include the 10-deacetylbaccatin III acetyltransferase (DBAT)[7] and the early-pathway taxadienol acetyltransferases (TATs, designated TAT01 and TAT19).[8]

Prior to the discussion of the findings obtained from this study, an overview of plant acyltransferases referred to as the BAHD superfamily is presented in the following sections. The *Taxus* enzymes used in these biochemical studies belong to this family of enzymes. The implicit origin of the acyl-acceptor and acyl-donor specificities for these enzymes will be discussed using x-ray structural data of two BAHD enzymes. A brief discussion of enzymatic "side-reactions" that divert taxol biosynthesis to seemingly dead-end metabolites will also be presented. Conceivably, the apparent plasticity of the diversionary *Taxus* acyltransferases could find application in the biocatalysis of modified taxanes. The discovery of an acyltransferase with promiscuous C-4 transacylase activity will be discussed in detail for the remainder of the chapter. This finding and other observations made during the course of this study ultimately paved the way for preliminary studies into the mechanistic aspects of this enzyme (Chapter 3).

2.2 Introduction

2.2.1 Plant Acyltransferases: The BAHD Superfamily

Plant secondary metabolism produces a vast and increasing reservoir of structurally diverse natural products. A conservative estimate indicate that ~200,000 plant secondary metabolites have been identified and characterized,[9] a fraction of which has found pharmaceutical as well as agricultural applications. Acylation is a common and biochemically significant way through which modifying enzymes elaborate basic skeletons of natural products. Through these modifications the acyltransferase enzymes create structural variability in natural products, alter functional properties such as solubility, or protect the metabolites against enzymatic degradation.[10-12] Additionally, the acyl moieties may serve as transmembrane signal transducers,[13] and in some cases cellular remediation of self-produced toxic metabolites can be achieved by glycosylation to produce non-toxic metabolites for storage.[14] The activated donors in these enzymatic acyl transfer reactions come from diverse sources, including *O*-acyl-β-glucosides, activated acyl carrier proteins, or acyl-activated coenzyme A thioesters.[12] In most cases, alcohols or primary amines serve as acyl acceptors.

Plant-specific CoA-dependent acyltransferases sharing phylogenetic relationships belong to a large family of recently discovered proteins referred to as the BAHD superfamily. The BAHD acronym derives from the first letter of the first four enzymes to be characterized,[11] namely the benzylalcohol-*O*-acetyltransferase (BEAT) from *Clarkia breweri*; anthocyanin-*O*-hydroxycinnamoyltransferase (AHCT) from *Gentiana triflora*; anthranilate hydroxycinnamoyl/benzoyltransferase (HCBT) from *Dianthus caryophyllus*,

and deacetylvindoline 4-*O*-acetyltransferase (DAT) from *Catharanthus roseus*[11]. However, it should be noted that transfer of acyl groups *from* glucose esters in plant secondary metabolism is catalyzed by the serine carboxy peptidase-like (SCPL) acyltransferases.[15] SCPL is a class of ancestrally hydrolytic enzymes that have acquired transacylase function through CoA-independent activation mechanisms.[16]

Members of the BAHD family of acyltransferases have low primary sequence identity (10-30%), indicating high functional divergence.[11] This also implies that enzymes with remarkably close substrate specificity profiles may have evolved independently. For example, two phylogenetically distant anthocyanin malonyl CoA acyltransferases (AATs) from *Salvia splendens* utilize the same substrate (cyanidin 5-*O*-glucoside) but with different regiospecificities.[17] This substrate versatility and acquisition of new catalytic function often complicate the conventional prediction of gene function and sequence annotation in new species based on sequence homology or structural information.[16,18] Alternative approaches are being explored where, for example, genes co-induced at high metabolite production are associated with specificity for that particular metabolite.[18]

Notwithstanding their low overall consensus sequence, the putative enzymes of the BAHD superfamily share a conserved HXXXD motif found near the center of each enzyme and a DFGWG motif located near the carboxyl terminus.[12] The HXXXD motif is shared with several other acyltransferases that utilize coenzyme A thioesters, including chloramphenicol acetyltransferases (CATs) and carnitine-*O*-acyltransferases.[12,19] The HXXXD motif is speculated to constitute the active site of these enzymes for a general-

base acyl transfer mechanism. While the DFGWG motif has been shown to be catalytically indispensable, its actual catalytic function is speculated to be structural stabilization of the enzyme active site.[20]

2.2.2 Structural and Mutation Studies

To dissect the catalytic mechanism and understand the molecular basis for acyl-donor and acceptor specificities of the BAHD enzymes, structural and mutagenesis studies of representative members have been conducted.[9,20,21] From the BAHD superfamily, x-ray crystallographic data are available only for vinorine synthase and malonyl anthocyanin acyltransferase (AAT) enzymes. Vinorine synthase is an acetyltransferase on the biosynthetic pathway of the antiarrhythmic indole alkaloid drug ajmaline in *Rauvolfia serpentine*,[20] while anthocyanin acyltransferase is a malonyltransferase from red chrysanthemum petals.[9]

Vinorine synthase catalyzes acetyl CoA-dependent reversible acetylation of vinorine from 16-epi-villosimine. This reaction also triggers the last ring-closure in the biosynthesis of the six-membered ajmaline ring system[20] **(Scheme 2-1)**.

Scheme 2-1. Biosynthesis of ajmaline (top panel) and the proposed mechanism for the vinorine synthase-catalyzed acetylation and ring-closure (bottom panel).[20]

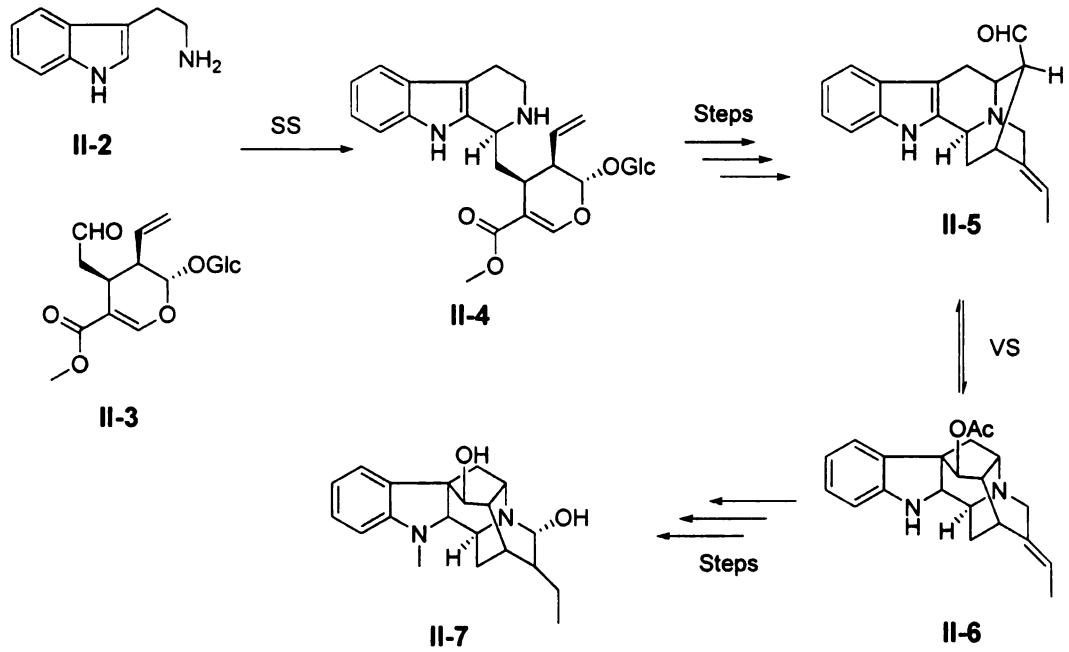

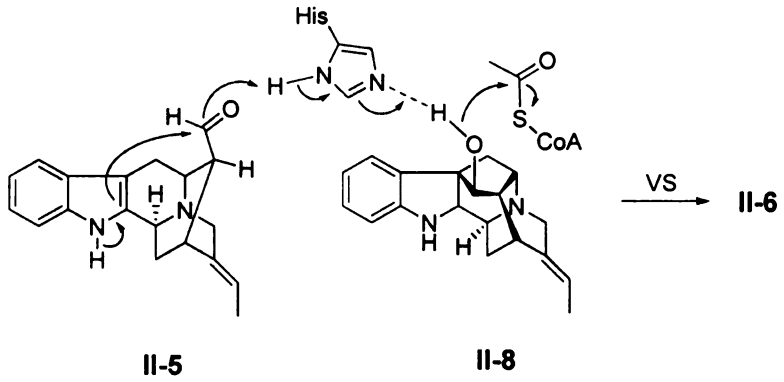

From the x-ray structure, vinorine synthase has two domains consisting of 14 β-strands and 13 α-helices.[20] The conserved amino acid residues characteristic of the BAHD family are located in domain 1. The proposed active site of vinorine synthase lies in a solvent accessible channel that runs between the two domains and is accessible from both sides of the channel.[20] Notably, the conserved and catalytically indispensable DFGWG

motif is located away from the active site (**Figure 2-2**). Thus, it is speculated that the motif indirectly participates in the catalytic mechanism of vinorine synthase by maintaining the structural integrity of the active site.[20]

Figure 2-2. Ribbon diagram of domain 1 of vinorine synthase generated using PyMOL. The proposed active site motif HXXXD are shown as sticks; His and Asp are shown as red sticks

Anthocyanins are a conspicuous class of natural colorants that are responsible for the orange to blue range of colors observed in flowers and fruits.[17] Biochemical studies suggest that multiple acylations of anthocyanins take place in an obligatorily sequential manner during anthocyanin biosynthesis and is catalyzed by anthocyanin acyltransferases (AATs) from the BAHD superfamily.[17] However, multiple malonylation of the anthocyanins in some plant species could be a consequence of promiscuous AATs catalyzing consecutive malonyl transfer reactions.[17] Although these AATs catalyze regiospecific transfer of acyl groups from acyl CoA to the glycosyl moiety of the anthocyanin, their acyl-acceptor specificities vary.[17,22]

Mutational and x-ray crystallographic studies of three similar anthocyanin malonyltransferases indicate that few amino acid residues dictate substrate specificity. Studies involving anthocyanin-3-*O*-glucoside-6"-*O*-malonyltransferase (Dm3MaT1), anthocyanin-3-*O*-glucoside-3",6"-*O*-dimalonyltransferase (Dm3MaT2), and a homolog, Dm3MaT3, revealed that seven amino acids in the N- and C-terminal regions are responsible for acyl-acceptor specificity differences.[9]

Multiple sequence alignment of Dm3MaT3 with other BAHD acyltransferases reveals that the amino acid residues involved in the binding of both the CoA and acyl portions of malonyl CoA are not strictly conserved.[9] This implies that acyl-donor specificity might arise from conservation of specific spatial arrangement of polar functional groups due to specific folding of the polypeptide chain rather than from the conservation of specific amino acid residues.[9]

The crystal structure of Dm3MaT3 in complex with malonyl CoA shows 20% identity with vinorine synthase.[9] Superposition of the Dm3MaT3 and vinorine synthase crystal structures reveals that the secondary structures of their "front" faces (acyl-donor binding sites) are similar. However, the spatial arrangement of secondary structures on their "back" faces (acyl-acceptor binding pockets) are substantially different.[9] Consequently, the acyl CoA-dependence of the BAHD acyltransferases is speculated to arise from structural conservation of the front face of the enzymes while the acyl-acceptor promiscuity might be due to the differential back-face spatial arrangement of amino acid residues.[9]

Due to their acyl acceptor plasticity, the BAHD enzymes are rapidly evolving catalytic function.[23] However, these acyltransferases still play specific roles in plant secondary metabolism, the most common of which is to confer odor and flavor to fruits and flowers through formation of volatile esters.[24] These enzymes also play prominent roles in the biosynthesis of bioactive natural products such as the analgesic drug morphine and anti-cancer drugs vinblastine, vincristine, and taxol.[25-27]

For example, in the biosynthetic pathway of taxol, six acyltransferases have been functionally characterized.[28] These include two benzoyl transferases, an *O*-phenylisoserinyl transferase, and three *O*-acetyl transferases. The natural acyl groups on the taxol skeleton, particularly the C-2 benzoyl, the C-4 acetyl, and the phenylisoserinyl side chain are critical for the efficacy of the parent drug. However, for example, chemical substitution of propionyl or butyryl for the C-10 acetyl with concomitant *N*-furanoyl substitution for the C-3' *N*-benzoyl results in a synergistic enhancement of efficacy to the modified taxol analogs[29] (**Figure 2-3**). These semi-synthetic studies have provided an impetus for biochemical studies with the aim of assessing the potential use of the *Taxus* acyltransferases in the production of more efficacious taxol analogs. Initial findings from these studies indicate that some of the *Taxus* acyltransferases are remarkably versatile with regard to acyl CoA specificity.[30-32]

Figure 2-3. Representative taxol analogs with non-natural alkyl and aroyl modifications.

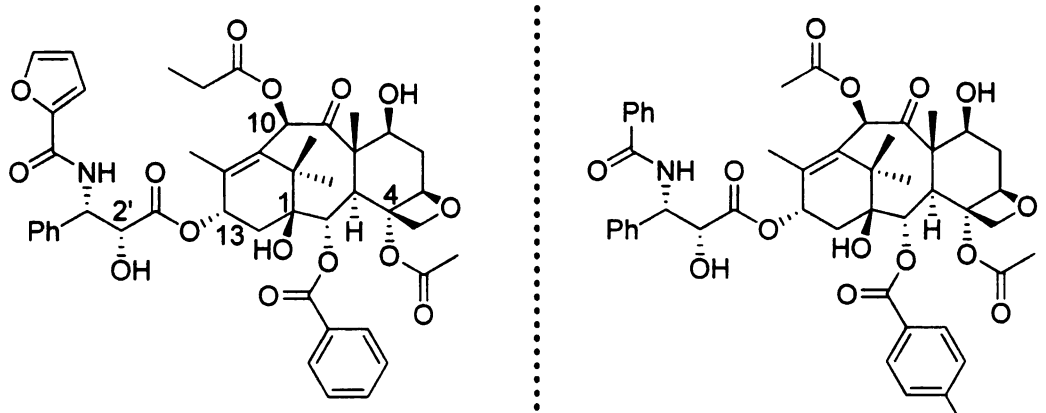

II-9 **II-10**

These biochemical studies and structural studies from anthocyanin acyltransferases[9] indicate that the broad acyl donor specificity might be a common feature of the BAHD superfamily of acyltransferases.[33]

2.2.3 "Diversionary" Pathways in Taxol Biosynthesis

The BAHD acyltransferases from *Taxus* plant species also manifest broad substrate specificity. For example, over 350 variously acylated taxoids have already been isolated from *Taxus* plants.[34] Some of the acyl groups found in these taxoids include acetyl, propionyl, butyryl, tigloyl, benzoyl, cinnamoyl, phenylisoserinyl esters, and glycosyl groups.[35-37] For example, taxoids bearing acetate at C-1, C-2, C-4, C-7, C-9, and C-13 are by far more abundant than taxol and its congeners.[36] These metabolites implicate the taxol pathway acyltransferases and other enzymes not yet characterized in the diversion of intermediate metabolites to other pathways. It has been proposed that these diversionary enzymes could be critical in flux regulation or organellar targeting of the taxoids.[7] Additionally, some of the metabolites may also form part of the plant defense in *Taxus* species.[8] While the physiological function of this vast array of

seemingly dead-end metabolites remains largely unknown, they are a manifestation of promiscuous enzymes not entirely committed to taxol biosynthesis.[36]

Through heterologous functional expression and characterization of recombinant enzymes in *E. coli*, the taxol biosynthetic pathway is almost fully defined. Thus, the focus has now shifted to enzymes that divert intermediate metabolites away from taxol production.[8,36] The apparent promiscuity also implies that some enzymes on the taxol pathway might demonstrate novel regio- or stereochemical preferences if incubated with non-cognate substrates. This has already been demonstrated for a few of the acyltransferases.[30-32] Therefore, a good understanding of the regulatory mechanisms responsible for the off-pathway carbon flux is critical for bioengineering of *Taxus* enzymes to produce novel biocatalysts with exquisite or amenable substrate selectivity.

2.3 In Search of a C-4 Acyltransferase

Taxol has poor bioavailability and water solubility; these problems have been addressed in part through development of elaborate formulations, such as the nanoparticle albumin-bound taxol (Abraxane®).[38] However, simpler modifications of the acyl groups on taxol have also been found to enhance the pharmacodynamic profile of taxol analogs.[1,39,40] This has been demonstrated for BMS-275183 (compound **II-1**), an oral derivative of taxol bearing a C-4 methylcarbonate and C-3' *N*-boc group. Currently, this taxol derivative is semi-synthesized from baccatin III through a series of protection-acylation-deprotection cycles[1] (**Scheme 2-2**).

Scheme 2-2. A truncated scheme for the semi-synthesis of BMS-275183.

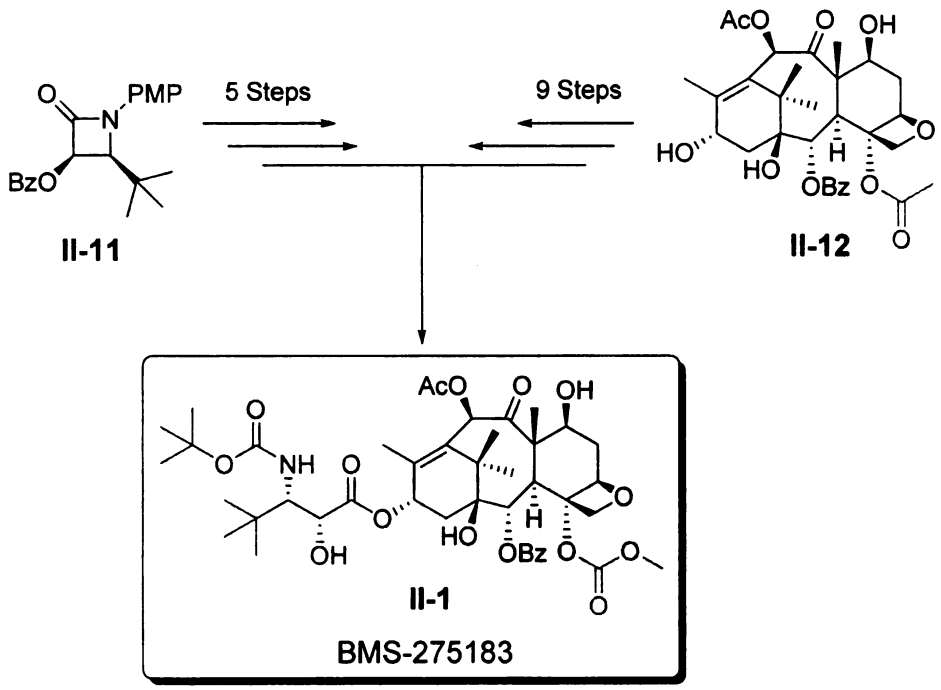

Conceivably, a biocatalytic process incorporating *Taxus* acyltransferases could replace repetitive chemical acylation-deacylation for the production of efficacious taxol derivatives such as BMS-275183. Unfortunately, however, none of the functionally characterized acyltransferases on the taxol pathway had been tested for acylation at the C-4 hydroxyl group of advanced taxanes. On the taxol biosynthetic pathway, the C-4 acetate is speculated to arise from an intramolecular rearrangement of C-4/C-20 epoxide with simultaneous migration of the C-5 acetate to the C-4 hydroxyl[41,42] (**Scheme 2-3**).

Scheme 2-3. Proposed biosynthesis of the oxetane ring and the C-4α acetyl group.

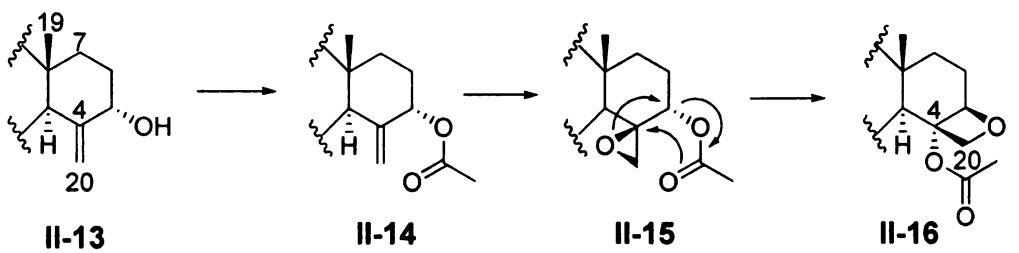

Therefore, to bridge this knowledge gap, studies towards understanding the substrate specificity of the remaining acyltransferases on the taxol biosynthetic pathway are necessary before these enzymes can be applied in the biocatalysis of taxol analogs.

The methoxycarbonyl group at the C-4 of BMS-275183 (compound **II-1**) is isosteric to a propionyl group, which is a productive substrate of one of the functionally characterized short-chain *Taxus* acyltransferases.[7] Therefore, acyltransferases that transfer short chain alkyl groups are good candidates to screen for novel methoxycarbonyl activity for potential application in the production of BMS-275181.

Three *Taxus* acetyl CoA-dependent transferases on the taxol biosynthetic pathway have been functionally characterized.[7,8] Even though the two previously characterized taxadienol acetyltransferases (TATs), designated TAT01 and TAT02, were both initially assigned 5α-*O*-acetyltransferase activity,[43] these two enzymes displayed remarkably distinct acylation preferences when separately incubated with a surrogate polyhdroxylated acceptor substrate and acetyl CoA thioester.[8] The tetraol substrate was preferentially acetylated at the C-9 and/or C-10 positions by TAT01, while TAT02 primarily acetylated the C-5 and/or C-13 with favorable kinetics[8] (**Scheme 2-4**).

Scheme 2-4. Distinct regiochemical preferences of TAT01 and TAT19, which were initially characterized as 5α-*O*- acetyltransferases.

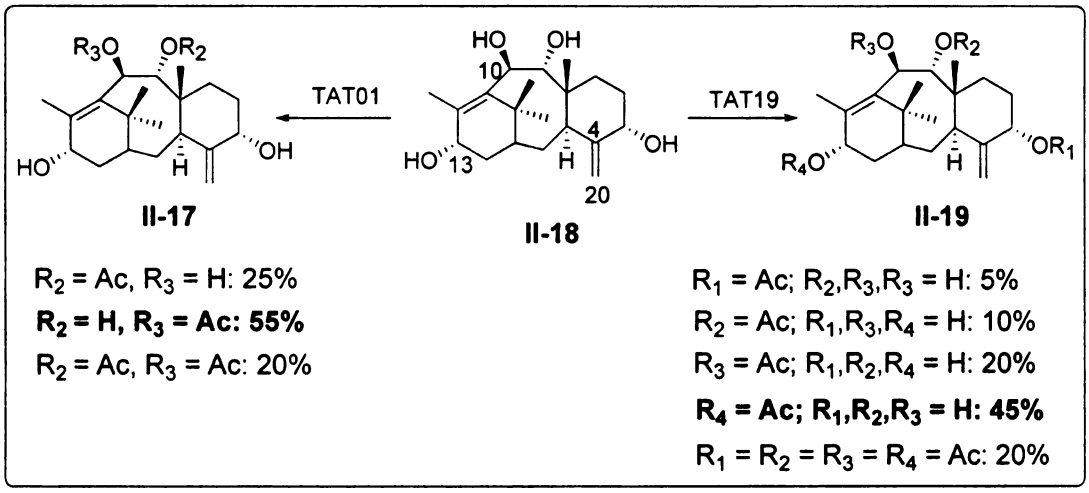

This finding indicates that other *Taxus* acyltransferases might also display novel regiospecificities if incubated with other taxoid substrates having varying acyl substitution.

The penultimate intermediate baccatin III on the taxol biosynthetic pathway is presumed to arise from regiospecific acetylation of the advanced intermediate 10-deacetylbaccatin III (10-DAB) by 10-deacetylbaccatin III:10β-*O*- acetyltransferase (DBAT).[7,32,35] DBAT, an acetyl coenzyme A-dependent enzyme from *Taxus cuspidata*, is a monomeric enzyme with a molecular weight of ~50 kDa.[7] Recombinant DBAT has a broad specificity with respect to both the acyl CoA donor substrates and taxane acceptor substrates.[32,44] Other than the natural acetyl CoA co-substrate, DBAT also catalyzes the transfer of propionyl and butyryl groups from their corresponding CoA thioesters to the C-10 position of 10-DAB both *in vivo* and *in vtro*[32,45] (**Scheme 2-5**). The study discussed herein also demonstrates that DBAT can utilize sterically encumbered taxane substrates.[44]

Scheme 2-5. DBAT-catalyzed acylation of 10-DAB.

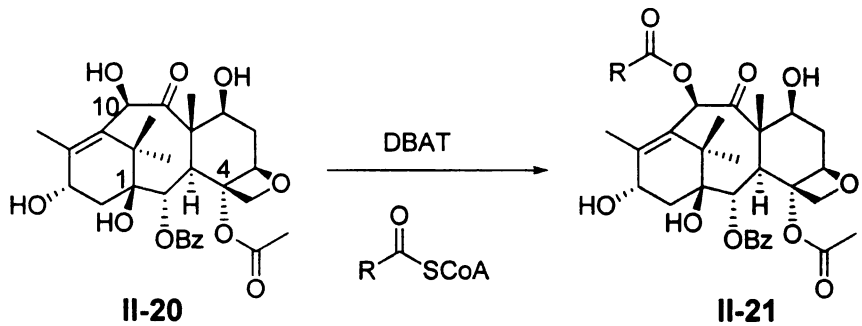

II-20 **II-21**

R = CH_3, CH_2CH_3,

or $CH_2CH_2CH_3$

Since no structural data for *Taxus* acyltransferases, the molecular basis of the substrate specificity of DBAT remains currently untenable. Therefore, engineering of the *dbat* gene in order to evolve a better biocatalyst will continue to rely on homology modeling using vinorine synthase or malonyl acyltransferases as guides.[9,20]

In the study described in this chapter, a library of *Taxus* acyltransferases was screened for novel or promiscuous activity using surrogate 4-deacetylbaccatin III substrates. Once a suitable enzyme candidate for novel activity is identified, the aim is to optimize it for regiospecific transfer of unnatural functional groups to advanced taxane substrates. This study provides the foundation on which to develop better biocatalysts through mutagenesis. The findings from this investigation and their biosynthetic and biocatalytic implications are discussed in the following sections.

2.4 Experimental: General

A Varian Inova-300 or a Varian UnityPlus500 instrument was used to acquire nuclear magnetic resonance (NMR) spectra. Chemical shifts are reported in δ units (ppm) using the residual ^{1}H- and ^{13}C signals of deuterated forms of water, chloroform, acetone,

methanol, or dimethylsulfoxide (DMSO). A Q-ToF Ultima API electrospray ionization tandem mass spectrometer (Waters, Milford, MA) was used for mass spectral analysis. An Agilent 1100 HPLC system (Agilent Technologies, Wilmington, DE) was employed for chromatographic separations and analyses. For radioactive analyses, the HPLC was connected in series with a Packard Radiomatic Flow-One Beta 150TR radioactivity detector (PerkinElmer, Shelton, CT), which mixed the effluent with 3a70B Complete Counting Cocktail (Research Products International, Mount Prospect, IL). Reaction products were purified by Kieselgel-60 F254 fluorescent preparative thin-layer chromatography (PTLC), and were visualized by absorbance of UV light at 254 nm. The purity of the synthetic compounds was determined by HPLC and/or ^{1}H-NMR. Taxol (paclitaxel), baccatin III, and 10-DAB were purchased from Natland Corporation (Research Triangle Park, NC). Unlabeled and tritium-labeled acetyl coenzyme A thioesters were obtained from Sigma-Aldrich, as were all other reagents, which were used without purification unless otherwise indicated. Docetaxel (Taxotere; Sanofi Aventis) was acquired from OChem Inc. (Des Plaines, IL).

The *Taxus cuspidata* cDNA clones encoding for the acyltransferases used in this study were donated by the Washington State University Research Foundation (Pullman, WA). The clones were either used in their original recombinant expression systems as described,[46] or appropriately subcloned into new expression systems followed by transformation of suitable bacteria expression system with the plasmid of interest. The 2α-*O*-benzoyltransferase (TBT or TAX02; accession number AF297618) was expressed from pCWori^{+} in JM109 *E. coli* cell line;[47] the 5α-*O*-acetyltransferases (TAT, designated TAX01 and TAX19; accession numbers AF190130 and AY628434, respectively) were

expressed from pSBET vectors in BL21(DE3) *E. coli* cells as previously described.[43,48] DBAT (accession number AF193765) was subcloned from pCWori$^+$ into pET28, while the 13-*O*-phenylpropanoyltransferase (BAPT; accession number AY082804) and 3'*N*-benzoyltransferase (NDTBT; accession number AF466397) were subcloned from pSBET into pET14 and pET28, respectively, and each vector was separately expressed in *E. coli* BL21(DE3) cell line.[34,46] A *Taxus* cDNA clone of unknown function, designated TAX05, was expressed from pSBET in *E. coli* BL21(DE3).[46]

2.4.1 Synthesis of Substrates

Figure 2-4. Synthesis of 4-Deacetylbaccatin III (4-DAB).

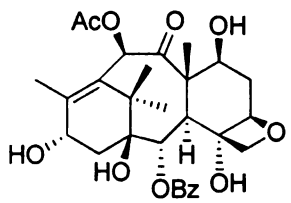

II-22

4-DAB (compound **II-22**) was synthesized via an established procedure[49] as follows. To a solution of baccatin III (338 mg, 0.41 mmol) in dry *N,N*-dimethylformamide (6 mL) was added imidazole (330 mg, 4.9 mmol), and the solution was stirred for 5 min, after which chlorotriethylsilane (1.36 mL, 8.2 mmol) was added dropwise at 23°C. The reaction was heated at 50°C for 6 h, cooled to room temperature, quenched by adding brine (10 mL), and then diluted with ethyl acetate (EtOAc) (10 mL). The organic layer was decanted, the remaining aqueous layer was extracted with EtOAc (3 × 20 mL), the organic fractions were combined, dried with sodium sulfate (Na_2SO_4), and the solvent was removed under vacuum. The crude product was crystallized from

EtOAc and hexanes (1:9) to obtain 7,13-bis(triethylsilyl)baccatin III at >95% yield, and judged to be >99% pure by ^{1}H-NMR.

To a solution of 7,13-bis(triethylsilyl)baccatin III (287 mg, 0.35 mmol) in dry *N,N*-dimethylformamide (DMF) (2 mL) at 0°C was added imidazole (72 mg, 1.1 mmol). The solution was stirred for 2 min and chlorodimethylsilane (0.11 mL, 1.1 mmol) was added dropwise. The reaction was stirred at 0°C for 45 min, then diluted with EtOAc (30 mL) and washed with water (4 × 20 mL). The organic phase was dried with Na_2SO_4 and concentrated under vacuum. The product was purified from the crude mixture by PTLC (15:85 (v/v) EtOAc:hexanes) to give 1-dimethylsilyl-7,13-bis(triethylsilyl)baccatin III product in 95% yield and 99% purity by ^{1}H-NMR. ^{1}H NMR (300 MHz, $CDCl_3$) δ: −0.3 (d, *J* = 3 Hz, $C\underline{H}_3Si(H)CH_3$), 0.00 (d, *J* = 3 Hz, $CH_3Si(H)C\underline{H}_3$), 0.60 (m, $CH_3C\underline{H}_2Si$−O), 0.98 (m, $C\underline{H}_3CH_2Si$−O), 1.01 (s, CH_3−16), 1.1 (s, CH_3−17), 1.60 (s, CH_3−19), 2.00 (s, CH_3−18), 2.10 (s, $OC(O)CH_3$ at 10β), 2.20 (s, $OC(O)CH_3$ at 4α), 2.30 (m, 6α, β), 2.40 (m, 14α, β), 3.80 (d, *J* = 6 Hz, 3α), 4.20 (dd, *J* = 9 Hz, *J* = 9 Hz, 20α, 20β), 4.40 (dd, *J* = 6 Hz, *J* = 6 Hz, 5α), 4.50 (m, $\underline{H}$-$Si(CH_3)_2$), 4.9 (m, 7α, 13α), 5.70 (d, *J* = 6 Hz, 2β), 6.40 (s, 10α), 7.4 (t, *J* = 6 Hz), 7.50 (t, *J* = 6 Hz), 8.00 (d, *J* = 6 Hz) [*m*-H, *p*-H, *o*-H of OBz, respectively].

To a solution of 1-dimethylsilyl-7,13-bis(triethylsilyl)baccatin III (120 mg, 0.14 mmol) in dry tetrahydrofuran (THF) (3 mL) at 0°C was added sodium bis(2-methoxyethoxy)aluminum hydride (Red-Al) (100 μL, 65% by weight in toluene) dropwise. The reaction was stirred for 40 min, and was then quenched with 1 mL of saturated sodium tartrate solution and the mixture was stirred for a further 10 min. The solution containing crude product was diluted with EtOAc (40 mL), washed with an

equal amount of water, and dried with Na_2SO_4. The organic layer was removed under vacuum and the crude product was purified by PTLC (20:80 (v/v) EtOAc in hexanes) to yield 1-dimethylsilyl-7,13-bis(triethylsilyl)-4-deacetylbaccatin III in 70% yield and >99% purity by ^{1}H-NMR. ^{1}H-NMR (300 MHz, $CDCl_3$) δ: −0.30 (d, J = 3 Hz, $C\underline{H}_3Si(H)CH_3$), 0.00 (d, J = 3 Hz, $CH_3Si(H)C\underline{H}_3$), 0.50 (m, $CH_3C\underline{H}_2Si$−O), 0.80 (m, $C\underline{H}_3CH_2Si$−O), 1.10 (s, CH_3−16), 1.20 (s, CH_3−17), 1.50 (s, CH_3−19), 2.00 (m, 6β), 2.1 (s, CH_3−18), 2.20 (s, $OC(O)CH_3$ at 10β), 2.30 (m, 6α), 2.4−2.8 (m, 14α, β), 3.50 (d, J = 6 Hz, 3α), 3.60 (bs, OH-4α), 4.1 (m, 7α), 4.20 (dd, J = 9 Hz, J = 9 Hz, 20α, 20β), 4.60 (m, $\underline{H}$-Si$(CH_3)_2$), 4.60−4.70 (m, 5α, 13α), 5.60 (d, J = 6 Hz, 2β), 6.40 (s, 10α), 7.40 (t, J = 6 Hz), 7.50 (t, J = 6 Hz), 8.00 (d, J = 6 Hz) [*m*-H, *p*-H, *o*-H of OBz, respectively].

To a solution of 1-dimethylsilyl-7,13-bis(triethylsilyl)-4-deacetylbaccatin III (56.6 mg, 0.068 mmol) in THF (2 mL) was added pyridine (400 μL). The solution was cooled to 0°C and a 60% HF-pyridine solution (400 μL) was added dropwise over 10 min. The reaction was allowed to room temperature and was stirred for 6 h. The reaction mixture was diluted with EtOAc (20 mL) and the organic fraction was washed with sodium bicarbonate (0.4 M), water and brine (2 × 20 mL each), dried over Na_2SO_4, and concentrated under vacuum. The product was purified by PTLC (80:20 (v/v) EtOAc in hexanes) to yield 4-deacetylbaccatin III (**Figure 2-4**) in 60% yield and 99% purity by ^{1}H-NMR. ^{1}H-NMR (300 MHz, $CDCl_3$) δ: 1.10 (s, CH_3-16), 1.15 (s, CH_3-17), 1.61 (s, CH_3-19), 2.14 (s, CH_3-18), 2.29 (s, $OC(O)CH_3$ at 10β), 2.50 (m, 6α, β), 2.58 (m, 14α, β), 3.50 (bs, 4α-OH), 3.63 (d, J=6 Hz, 3α), 4.09 (dd, J=6 Hz, J=6 Hz, 7α), 4.18 (d, J=8 Hz, 20α), 4.43 (d, J=8 Hz, 20β), 4.67 (bt, 13β), 4.85 (dd, J=4 Hz, J=4 Hz, 5α), 5.64 (d, J=6 Hz, 2β), 6.34 (s, 10α), 7.50 (m), 7.64 (m), 8.09 (m) [*m*-H , *p*-H, *o*-H of OBz, respectively].

Figure 2-5. Synthesis of 7-acetyl-4-DAB.

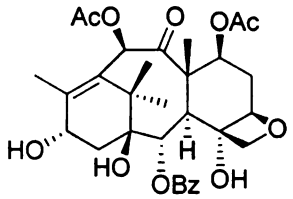

II-23

To a solution of 4-DAB (compound **II-22**) (20 mg, 0.037 mmol) in DMF (2 ml) were added imidazole (25 mg, 0.37 mmol) and chlorotriethylsilane (12.4 μL, 0.074 mmol). The reaction was stirred at 45°C for 3 h under nitrogen to obtain a 1:1 mixture of starting material and 13-triethylsilyl-4-DAB (55% yield) and was purified by PTLC (80:20 (v/v) EtOAc/hexanes). To a solution of 13-triethylsilyl-4-DAB (6 mg, 0.01 mmol) in tetrahydrofuran (2 mL) was added dimethylaminopyridine (DMAP) (5.6 mg, 0.05 mmol), triethylamine (TEA) (1.3 μL, 0.01 mmol), and acetic anhydride (172 μL, 0.2 mmol). The solution was stirred for 3 h at 23°C, and concentrated under vacuum; the sample was then loaded onto a PTLC plate and eluted with 80:20 (v/v) EtOAc in hexanes to give 7-acetyl-13-triethylsilyl-4-DAB in 99% yield and 99% purity by NMR. To a solution of 13-triethylsilyl-4-DAB (7 mg, 0.01 mmol) in THF (2 mL) and pyridine (60 μL) at 0°C under nitrogen was added a 60% HF-pyridine solution of HF (60 μL) dropwise over 5 min and the reaction was allowed to warm to room temperature. After 2 h, the solution was diluted with EtOAc (10 mL), quenched with water (5 mL), and extracted with EtOAc (2 × 5 mL). The organic extracts were dried with Na_2SO_4 and evaporated under vacuum. The 7-acetyl-4-DAB product (**Figure 2-5**) was purified by PTLC using 80% (v/v) EtOAc in hexanes and isolated in 95% yield and 98% purity by ^{1}H-NMR. ESI-MS (positive ion mode), *m/z*: 587 $[M+H]^+$, 604 $[M+NH_4]^+$, 609 $[M+Na]^+$. ^{1}H-NMR (300 MHz, $CDCl_3$) δ: 1.02 (s, CH_3-16), 1.13 (s, CH_3-17), 1.66 (s, CH_3-19), 2.04

(s, $OC(O)CH_3$ at 7β), 2.12 (s, CH_3-18), 2.18 (s, $OC(O)CH_3$ at 10β), 2.44 (m, 6α), 2.49 (m, 14α, β), 2.64 (m, 6β), 3.68 (d, *J*=6 Hz, 3α), 4.2 (d, *J*=8 Hz, 20β), 4.30 (d, *J*=8 Hz, 20α), 4.62 (bd, 13β), 4.84 (dd, *J*=3 Hz, *J*=4 Hz, 5α), 5.21 (dd, *J*=7 Hz, *J*=7 Hz, 7α), 5.57 (d, *J*=5 Hz, 2β), 6.22 (s, 10α), 7.46 (m), 7.57 (m), 8.06 (m) [*m*-H , *p*-H, *o*-H of OBz, respectively].

Figure 2-6. Synthesis of 13-Acetyl-4-DAB.

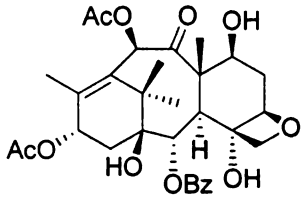

II-24

To a solution of 4-DAB (compound **II-23**) (20 mg, 0.04 mmol) in THF (2 mL) were added DMAP (23 mg, 0.18 mmol), TEA (5 μL, 0.04 mmol), and acetic anhydride (4 μL, 0.04 mmol). The solution was stirred for 15 min at 0°C and then the reaction was concentrated under vacuum, and the product was purified by PTLC using 80% (v/v) EtOAc in hexanes to give 13-acetyl-4-DAB (**Figure 2-6**) in 65% yield and 98% purity by ^{1}H-NMR. ESI-MS (positive ion mode), *m/z*: 587 $[M+H]^+$, 604 $[M+NH_4]^+$, 609 $[M+Na]^+$. ^{1}H-NMR (300 MHz, $CDCl_3$) δ: 1.15 (s, CH_3-16), 1.18 (s, CH_3-17), 1.38 (s, CH_3-19), 1.94 (s, CH_3-18), 2.19 (s, $OC(O)CH_3$ at 10β), 2.23 (s, $OC(O)CH_3$ at 13α), 2.39 (m, 6α), 2.49 (m, 14α, β), 2.59 (m, 6β), 2.69 (bs, 4α-OH), 3.28 (d, *J*=6 Hz, 3α), 3.98 (dd, *J*=6 Hz, *J*=6 Hz, 7α), 4.08 (d, *J*=9 Hz, 20β), 4.32 (d, *J*=9 Hz, 20α), 4.81 (dd, *J*=4 Hz, *J*=4 Hz, 5α), 5.62 (d, *J*=6 Hz, 2β), 5.94 (m, 13β), 6.29 (s, 10α), 7.46 (t, *J*=6 Hz, *J*=6Hz), 7.57 (m), 7.80 (m) [*m*-H , *p*-H, *o*-H of OBz, respectively].

Figure 2-7. Synthesis of 7,13-Diacetyl-4-DAB.

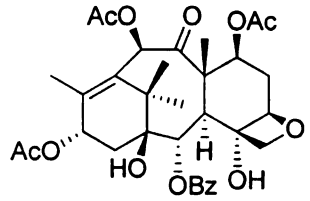

II-25

7,13-diacetyl-4-DAB was prepared analogous to the procedures described for the synthesis of 13-acetyl-4-DAB (compound **II-25**). Briefly, to a solution of 4-DAB (18 mg, 0.033 mmol) in THF (3 mL) was added DMAP (19 mg, 0.16 mmol), TEA (8.8 μL, 0.06 mmol), and acetic anhydride (9 μL, 0.09 mmol). The reaction mixture was stirred at 23°C for 20 min, diluted with 10 mL EtOAc, and washed with water (pH 1.0). The organic layer was concentrated, and the 7,13-diacetyl-4-DAB (**Figure 2-7**) was purified by PTLC using 60% EtOAc in hexanes, and isolated in 75% yield and >99% purity ^{1}H-NMR. ESI-MS (positive ion mode), *m/z*: 630 $[M+H]^+$, 647 $[M+NH_4]^+$, 652 $[M+Na]^+$. ^{1}H-NMR (300 MHz, $CDCl_3$) δ: 1.12 (s, CH_3-16), 1.15 (s, CH_3-17), 1.7 (s, CH_3-19), 2.00 (s, CH_3-18), 2.04 (s, $OC(O)CH_3$ at 10β), 2.17 (s, $OC(O)CH_3$ at 7β), 2.21 (s, $OC(O)CH_3$ at 13α), 2.45 (m, 6α, β), 2.48 (m, 14α, β), 2.68 (bs, 4α-OH), 3.42 (d, *J*=7 Hz, 3α), 4.14 (d, *J*=8 Hz, 20β), 4.29 (d, *J*=8 Hz, 20α), 4.82 (dd, *J*=3 Hz, *J*=3 Hz, 5α), 5.19 (dd, *J*=7 Hz, *J*=7 Hz, 7α), 5.62 (d, *J*=6 Hz, 2β), 5.92 (m, 13β), 6.20 (s, 10α), 7.46 (t, *J*=9 Hz), 7.59 (m), δ 8.00 (m) [*m*-H , *p*-H, *o*-H of OBz, respectively].

Figure 2-8. Synthesis of 13-Acetylbaccatin III.

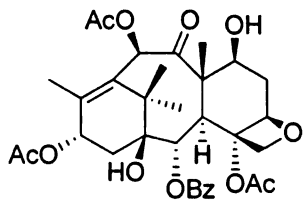

II-26

13-acetylbaccatin III was synthesized analogous to the procedure previously described for the synthesis of 13-butyrylbaccatin III.[45] Briefly, to a solution of 7-triethylsilylbaccatin III (48mg, 0.07 mmol) in THF (3 mL) at 40°C were added TEA (45 μL, 0.34 mmol), DMAP (42 mg, 0.34 mmol), and acetic anhydride (32 μL, 0.34 mmol). The reaction was stirred for 5 h, diluted with 10 mL EtOAc, quenched with water (10 mL), and washed with brine (2 x 10 mL). The product was purified by PTLC using 40% EtOAc in hexanes to give 45 mg 7-triethylsilyl-13-acetylbaccatin III. To a solution of 7-triethylsilyl-13-acetylbaccatin III (43 mg, 0.06 mmol) in THF (3 mL) at 0°C was added 340 μL pyridine, stirred for 5 minutes, and then a 60% solution of HF-Pyridine (340 μL) was added. The reaction mixture was stirred at 0°C and allowed to warm to temperature overnight, after which it was quenched with water, diluted with EtOAc and the organic fraction was washed with brine and sodium bicarbonate (2 × 3 mL each). The final product, 13-acetylbaccatin III (**Figure 2-8**), was purified by PTLC using 60% EtOAc in hexanes, dried and verified by ESI-MS. ESI-MS (positive ion mode), *m/z*: 629 $[M+H]^+$, 646 $[M+NH_4]^+$, 651 $[M+Na]^+$. ^{1}H-NMR (300 MHz, $CDCl_3$) δ: 1.13 (s, CH_3-16), 1.21 (s, CH_3-17), 1.65 (s, CH_3-19), 1.89 (d, *J*=2 Hz, CH_3-18), 2.19 (s, $OC(O)CH_3$ at 10β), 2.22 (s, $OC(O)CH_3$ at 4α), 2.23 (m, 6α, β), 2.31 (s, $OC(O)CH_3$ at 13α), 2.54 (m, 14α, β), 3.81 (d, *J*=7 Hz, 3α), 4.14 (d, *J*=9 Hz, 20α), 4.29(d, *J*=9 Hz, 20β), 4.42 (dd, *J*=7 Hz, *J*=7 Hz,

7α), 4.95 (dd, *J*= 2 Hz, *J*=2 Hz, 7α), 5.64 (d, *J*=7 Hz, 2β), 6.16 (m, 13β), 6.28 (s, 10α), 7.46 (m), 7.59 (m), 8.05 (m) [*o*-H, *p*-H, *m*-H of OBz, respectively].

2.4.2 Biochemical Methods

Each *E. coli* transformant was grown overnight at 37 °C in 5 mL Luria-Bertani (LB) media supplemented with appropriate antibiotic for selection (ampicilin at 100 μg · mL^{-1} for JM109 cell line and kanamycin at 50 μg · mL^{-1} for BL21(DE3) cell lines). The inoculum was then added to and grown in 4 L flasks containing 1 L LB medium that had been supplemented with appropriate antibiotic for selection at 37 °C. At OD_{600} of ~ 1.0, the cultures were induced with isopropyl-β-D-thiogalactopyranoside (IPTG) (1 mM final concentration), and the cultures were grown at 16-18°C for 14-18 h. The subsequent steps were performed on ice or in a cold room maintained at 4°C, unless otherwise indicated. For each protein, the cultures were separately harvested and centrifuged at 6,000*g* for 20 min, and the pellet was resuspended in 3-(*N*-morpholino)-2-hydroxypropanesulfonic acid (MOPSO) lysis buffer (pH 7.2) containing 3 mM dithiothreitol (DTT) and glycerol (5% v/v). The cells were lysed at 4°C using a Misonix sonicator (Farmingdale, NY) with 3 × 30-s bursts at 50-75% power (depending on the volume of the lysis buffer) with 2-min intervals between each burst. The cell-lysate was centrifuged at 10,000*g* for 20 min to remove cell debris and clarified by ultracentrifugation at 100, 000*g* for 2 h. Empty vectors of each type were similarly expressed in the corresponding *E. coli* for control assays, and the cell-free extracts were obtained by procedures identical to those described for the cells transformed with plasmids.

2.4.3 Activity Assays

To verify functional expression of the acyltransferases, each crude extract was assayed with its natural co-substrates,[46] except for the TAT05 enzyme whose function and natural substrate are unknown. A 1-mL aliquot of each extract containing active taxol pathway acyltransferases, the TAT05 enzyme, and enzymes isolated from hosts engineered for empty vector expression was incubated at 31°C with surrogate substrate 4-deacetylbaccatin III (4-DAB) at 1 mM concentration and [^{3}H]-acetyl coenzyme A (100 μM, 1 μCi/μmol) under similar assay conditions. After 3 h, the reactions were stopped by extraction with ethyl acetate (3 × 2 mL), the organic fractions were combined, the solvent was evaporated, and the residue was redissolved in 50 μL of acetonitrile. A 25-μL aliquot was loaded onto a reverse-phase column (Zorbax 5 μm XDB-C18, 4.6 × 250 mm, Agilent), eluted at 1 mL/min with 20:80 CH_3CN: H_2O (v/v) for 5 min, then with a linear gradient of CH_3CN in H_2O over 20 min to 100% CH_3CN, and finally returned to initial conditions with a 5 min hold. The HPLC analysis was done under continuous UV-absorbance detection (diode array detector) and radioactivity monitoring of effluent mixed with counting cocktail.

2.4.4 Mass Spectrometry and ^{1}H-NMR Analysis of Enzymatic Products

For the assay in which 4-DAB was incubated with [^{3}H]-acetyl CoA (1 μCi/μmol, 100 μM) and recombinantly-expressed DBAT, radio-HPLC analysis of the assay revealed a *de novo* radioactive signal whose retention time was identical to that of authentic baccatin III. To verify the identity of this product, *E. coli* cultures expressing the *dbat* clone were grown in a larger scale (6 L) in LB by IPTG induction for 18 h at 20°C. To remove small molecules and cell debris, the soluble enzyme extract (80 mL)

was loaded onto a Whatman DE-52 anion exchange column (2.5 × 6 cm, 20 g resin). The protein fractions containing desired acyltransferases were eluted at between 100-120 mM NaCl concentration, pooled (150 mL) and concentrated 20-fold by ultrafiltration using 10,000 kDa molecular weight cut-off membrane filters (Millipore, Billerica, MA). This enzyme preparation was judged to be ~60% pure and of the correct molecular weight (~50 kDa) as determined by sodium dodecyl sulfate-polyacrylamide gel electrophoresis (SDS-PAGE), Coomassie staining and Western blotting.

4-DAB and acetyl coenzyme A (both at 1 mM) were incubated in separate 1 mL assays containing the DBAT enzyme (~100 μg), as described (cf. section **2.3.4**). Each reaction was quenched after 3 h by mixing with ethyl acetate to denature the protein. The organic fraction was decanted, the aqueous fraction was extracted twice more with 5 mL ethyl acetate, the organic fractions were combined, and the solvent was evaporated under vacuum. The resulting residue was dissolved in acetonitrile (100 μL) and the total volume was loaded onto a reverse-phase HPLC column in 20 μL aliquots per load and eluted as described previously (cf. section **2.3.3**). The product eluting with identical retention time as the biosynthetic [^{3}H]-baccatin III (14.94 min) identified in the preliminary screening assays was collected and the effluent was evaporated. A small fraction of the resulting residue was dissolved in methanol (10 μL) and analyzed by electrospray ionization mass spectrometry in the positive ion mode. A solution of the remaining sample in $CDCl_3$ (100 μL) in a solvent-matched Shigemi tube was analyzed by ^{1}H-NMR.

2.4.5 Kinetic Studies

For kinetic analysis, DBAT was harvested as before except the enzyme was subjected to further purification by nickel-nitroloacetate (NI-NTA) affinity gel chromatography. The crude protein (~50 mL) was loaded onto a column containing Ni-NTA agarose resin (2 mL) that had been pre-equilibrated with phosphate buffer (pH 8). The column was washed with phosphate buffer containing 10 mM imidazole and 300 mM NaCl (6 × 10 mL, pH 8) and the protein was eluted with phosphate buffer containing 250 mM imidazole at a rate of 2 mL per min. The elutions (10 mL each) were concentrated by centrifugation using molecular weight cut-off membrane filters and the fractions were analyzed by SDS-PAGE to yield DBAT at ~70% purity (3 mg/mL) (lane 6 **Figure 2-9**).

Figure 2-9. SDS-PAGE (12%) of Ni-NTA-purified wild type DBAT; for each lane, ~20 µg total protein was loaded. Lane 1 = Cell lysate; Lane 2 = Flow through; Lane 3 = Wash 1 (sodium phosphate buffer with 10 mM imidazole); Lane 4 = Wash 5 (sodium phosphate buffer with 10 mM imidazole); Lane 5 = Protein marker; Lane 6 = Elution 1 (phosphate buffer with 100 mM imidazole); Lane 7 = Elution 2 (sodium phosphate buffer 250 mM imidazole). The asterisk (*) indicates ~50 kDa.

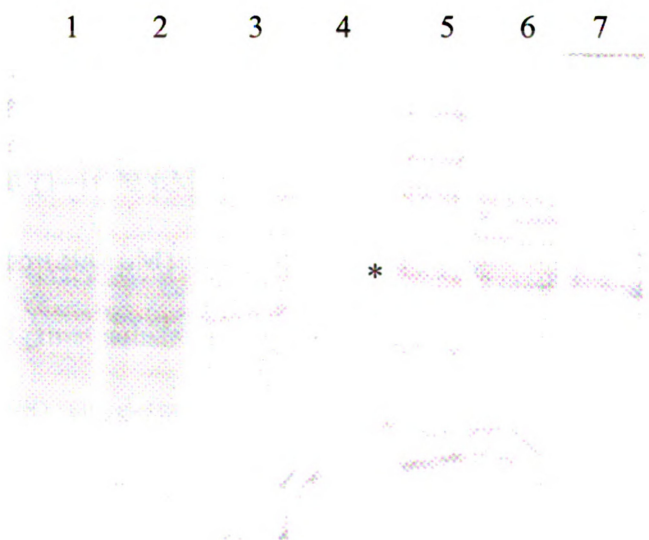

Linearity with respect to protein concentration and time was first established for DBAT (50 μg, 25 μg, and 5 μg) by varying the concentration of the natural substrate 10-DAB while maintaining the concentration of the co-substrate acetyl CoA at apparent saturation (500 μM) (**Figure 2-10**).

Figure 2-10. Analysis of DBAT catalysis (10-DAB to baccatin III) with respect to time.

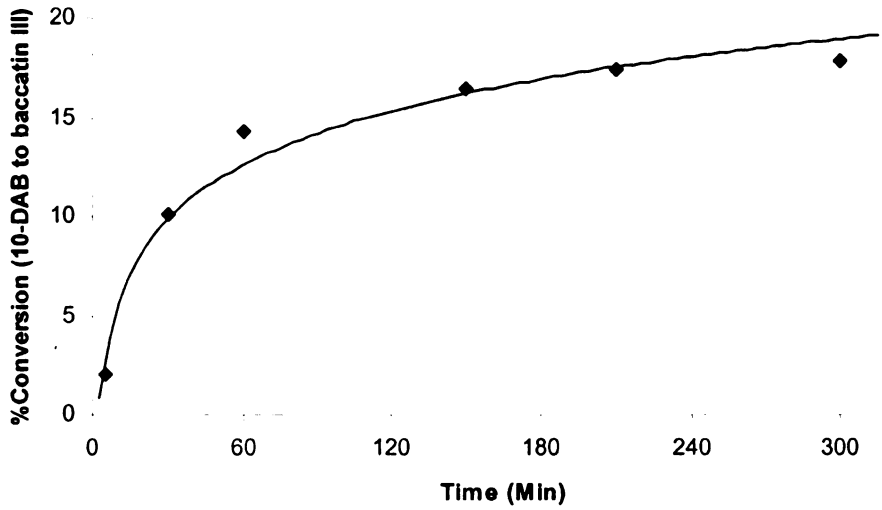

Aliquots (1 mL each) were collected and quenched at 0.5, 1, 2, 3, and 5 h. To ensure product formation was at steady-state, DBAT at 5 μg/mL was used for the kinetic evaluation of the assays, which were incubated for 20 min. For non-linear regression analysis of the reaction rate, the concentration of the taxane substrate was then independently varied (1–1000 μM) in separate assays while acetyl CoA was maintained at apparent saturation (500 μM). Michaelis-Menten plots were obtained by plotting the initial velocity (v_o) against substrate concentration (**Figure 2-11**), and the equation of the best-fit line ($R^2 > 0.98$) was determined using SigmaPlot (Systat Software, San Jose, CA) or Microsoft Excel 2003 (Microsoft Corporation, Redmond, WA).

Figure 2-11. Conversion of10-DAB to baccatin III as a function of enzyme concentration.

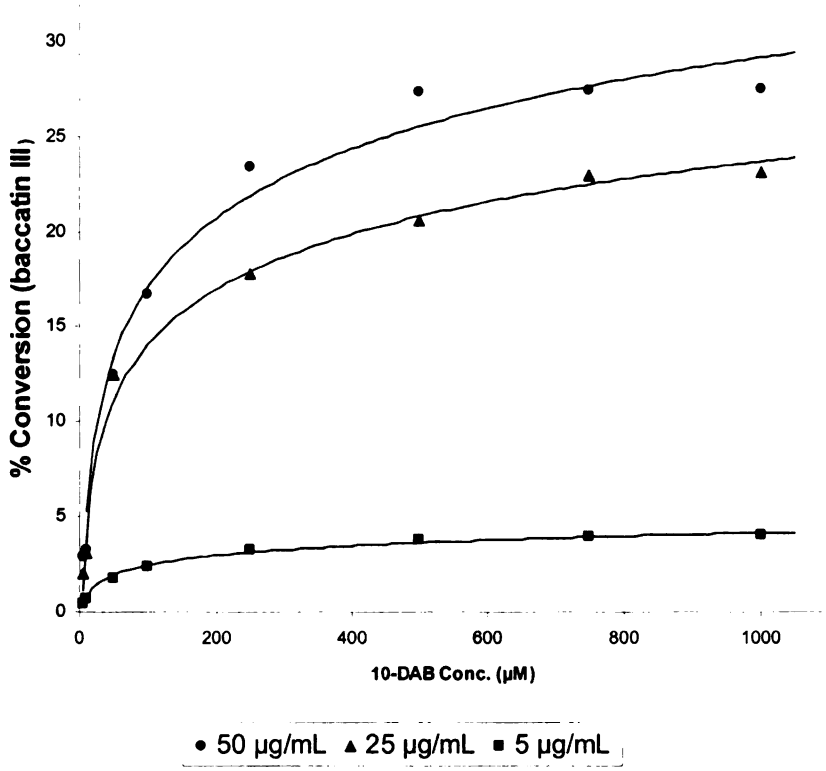

The procedure used to calculate the relative kinetic constants of DBAT for multiple diterpene substrates was adapted from a protocol used to determine the specificity constants for DBAT in a previous study.[32] The Michaelis-Menten equation (i) can be modified into expression (ii) by expressing the initial rates as a ratio of substrate concentrations. Since rates can be obtained from change of product concentration over time, these ratios correspond to their respective specificity constants for *n* substrates (iii):

$$v_o = \frac{V_{max}[S]}{K_m + [S]} \quad \text{..... (i)}$$

$$\frac{v_1}{[S]_1} : \frac{v_2}{[S]_2} : \ldots \frac{v_n}{[S]_n} = \left(\frac{k_{cat}}{K_m}\right)_1 : \left(\frac{k_{cat}}{K_m}\right)_2 : \ldots \left(\frac{k_{cat}}{K_m}\right)_n \quad \text{..... (ii)}$$

$$\frac{[P_1]}{[S]_1} : \frac{[P_2]}{[S]_1} : \ldots \frac{[P_n]}{[S]_n} = \left(\frac{k_{cat}}{K_m}\right)_1 : \left(\frac{k_{cat}}{K_m}\right)_2 : \ldots \left(\frac{k_{cat}}{K_m}\right)_n \quad \text{..... (iii)}$$

The kinetic parameters (k_{cat} and K_m) obtained from the Lineweaver-Burk regression or Hanes-Woolf plot constructed for DBAT and its natural co-substrates were used to assess the relative catalytic efficiencies of competing 4-DAB substrates in mixed-substrate assays with docetaxel and 10-DAB.

The relative substrate specificity constant of each productive 4-deacetylbacctin III substrate was assessed indirectly by comparison against the kinetic constants calculated for the natural substrate with DBAT. 10-DAB (35 μM) and docetaxel (35 μM) (a productive 10-deacetyltaxoid substrate of DBAT) were incubated for 20 min with DBAT (~5 μg) and [^{3}H]-acetyl CoA (100 μM, 1 μCi) in a single assay tube. The molar ratio of baccatin III ($Bacc_1$) and 10-acetyldocetaxel (10AcD) formed in the mixed reaction was used to convert the specificity constant $(k_{cat}/K_m)_{Bacc1}$ of DBAT, calculated for its natural substrates, to a relative specificity constant for the docetaxel substrate. In a separate mixed substrate assay, docetaxel (35 μM) was mixed with 4-DAB (35 μM) and DBAT (~5 μg, 0.1 nmol), and the ratio of 10-acetyldocetaxel and baccatin III ($Bacc_2$) was used to calculate the relative specificity constant of DBAT with 4-DAB $(k_{cat}/K_m)_{4\text{-}DAB}$) from the specificity constant of DBAT with docetaxel as follows: $[(k_{cat}/K_m)_{Bacc1} \times$

$(Bacc_1/10AcD) \times (10AcD/Bacc_2) = (k_{cat}/K_m)_{4\text{-}DAB}]$, where $Bacc_1$ refers to baccatin III obtained from incubation of 10-DAB and acetyl CoA with DBAT; $Bacc_2$ refers to baccatin III obtained from incubation of 4-DAB and acetyl CoA with DBAT, and 10AcD refers to 10-acetyldocetaxel (i.e., 10-acetyltaxotere) obtained from incubation of taxotere and acetyl CoA with 10-DAB. Analogous competitive assays were run to obtain the relative kinetic parameters of DBAT with the productive substrate 13-acetyl-4-DAB.

2.5 Results and Discussion

2.5.1 Protein Expression and Acyltransferase Screening

Six acyltransferase cDNA clones encoding for proteins on the taxol pathway and one cDNA clone encoding for a protein of unknown function were recombinantly expressed in *E. coli*. Small scale cultures of each transformed and IPTG-induced bacteria were grown and the cells were harvested by sonication. The derived soluble enzyme fractions were partially purified by anion exchange and the recombinant proteins were screened for novel transacylase activity against surrogate baccatin III substrates lacking the C-4 acetate. Assays were performed under standard conditions using tritium-labeled acetyl CoA ([^{3}H]-acetyl CoA) as an acyl donor and synthetically derived 4-DAB as an acyl acceptor.

One such assay preparation using an enzyme fraction expressed from the *dbat* cDNA clone yielded a single radioactive product peak whose retention time (14.94 ± 0.01 min) on reverse-phase radio-HPLC was exactly coincident to that of commercially obtained baccatin III (**Figure 2-12**). Control experiments with the same enzyme preparation that had either been denatured by boiling (then incubated with both substrates) or assayed in the absence of the co-substrate did not yielded products

detectable by HPLC analysis. Additionally, enzyme preparations isolated from *E. coli* BL21(DE3) host cells transformed with empty pET28 vector did not show any product formation under the same analysis conditions.

Semi-preparative *E. coli* cultures were used to demonstrate that an operationally soluble and functionally active DBAT protein was being heterologously expressed. A larger scale (6-L) bacterial culture harboring the *dbat* gene was grown and harvested using the same protocol as outlined for the semi-preparative cultures. The derived soluble enzyme preparation was partially purified by anion-exchange chromatography using diethylaminoethyl (DEAE) cellulose resin to yield DBAT in ~60% purity by SDS-PAGE. This protein extract was incubated with unlabeled acetyl CoA and 4-DAB and generated sufficient biosynthetic product for HPLC and ESI-MS analysis (**Figure 2-12**).

Figure 2-12. An overlay of HPLC chromatograms of the biosynthetic product from DBAT-catalyzed acetylation of 4-DAB with tritium-labeled CoA (red trace) and unlabeled acetyl CoA (blue trace).

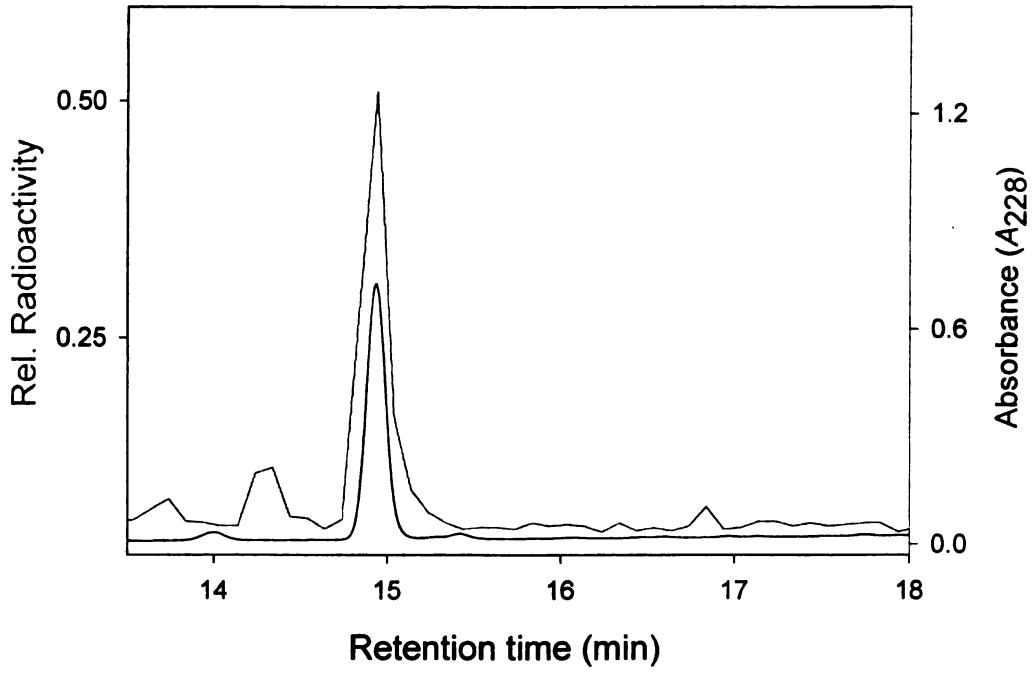

Analysis of the biosynthetic product by electrospray ionization mass spectrometry (ESI-MS) provided $[M+H]^+$ ion (*m/z* 587) characteristic of baccatin III.

2.5.2 NMR Analysis of the Biosynthetic Product

An ^{1}H-NMR spectrum was obtained from an aliquot of the HPLC-purified biosynthetic product, but due to sample limitation (~0.1 mg of product) the spectrum had poor signal-to-noise ratio. However, this spectrum provided diagnostic peaks that were identical to that of authentic baccatin III in most respects (**Figure 2-13**). Particularly distinct was the proton signal at δ = 3.86 ppm of the biosynthetic baccatin III product that coincided with the resonance of the H-3 proton of baccatin III bearing an acetyl group at the C-4 position.

Figure 2-13. NMR spectrum of authentic baccatin III (trace A) compared to that of baccatin obtained from incubation of 4-DAB, acetyl CoA, and DBAT in one reaction vessel (trace B). Due to sample limitation, the proton NMR of the biosynthetic product from incubation of DBAT, acetyl CoA and 4-DAB had a poor signal-to-noise-ratio (trace B) even after 19,000 scans. Peaks of the biosynthetic product that are coincident with authentic baccatin III peaks are marked with asterisks (*). Peaks marked with a dagger (†) are due to residual EtOAc solvent.

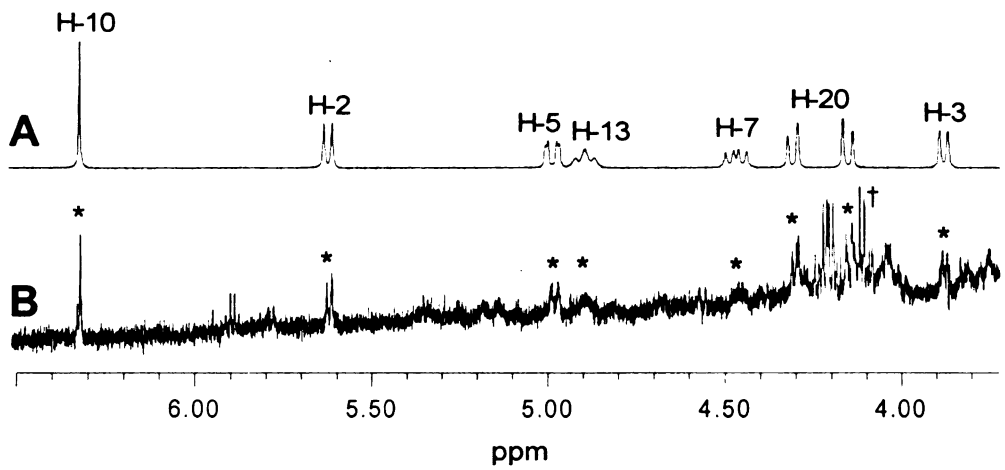

In contrast, the ^{1}H-NMR signal for H-3 of baccatin III analogs with a free hydroxyl at C-4, such as 4-DAB, is distinctly further upfield at δ = 3.58 ppm. Additionally, diagnostic proton resonances at δ 4.89 ppm and 4.49 ppm of the

biosynthetic product are coincident with C-3 and C-7 protons, respectively, in the ^{1}H-NMR of the commercially obtained baccatin III (**Figure 2-13**).

This preliminary HPLC, ESI-MS, and ^{1}H-NMR spectral data of the biosynthetic product indicated that DBAT catalyzes the conversion of 4-DAB to baccatin III in the presence of acetyl CoA. Although convincing, these data alone were insufficient to establish the regiochemistry of the enzymatic product. Moreover, sample limitations precluded the use of ^{13}C-NMR-dependent techniques for further product characterization.

2.5.3 Verification of Biosynthetic Product Using Product Standards

Further verification of the product regiochemistry was done by comparing the retention time of the biosynthetic product against synthetically derived product standards. Thus, possible regioisomeric products 7-acetyl-4-DAB and 13-acetyl-4-DAB were semi-synthesized from 4-DAB whereas the baccatin III product standard was obtained from commercial sources.

The retention time of authentic baccatin III (R_t = 14.94 ± 0.01 min) was identical to that of the biosynthetic product while authentic 7-acetyl-4-DAB and 13-acetyl-4-DAB product standards eluted at 16.90 ± 0.01 min and 14.82 ± 0.01 min, respectively (**Figure 2-14**).

Figure 2-14. Overlay of reverse-phase HPLC chromatograms of the biosynthetic product obtained from incubation of DBAT, 10-DAB and tritium-labeled acetyl CoA (red) in one assay tube, and DBAT, 10-DAB, and unlabeled acetyl CoA (blue) in a separate assay tube. Three regioisomeric product standards 13-acetyl-4-DAB (14.82 min), baccatin III (14.94 min), and 7-acetyl-4-DAB (16.9 min) were mixed in one vial and an aliquot was similarly analyzed by reverse-phase HPLC (black).

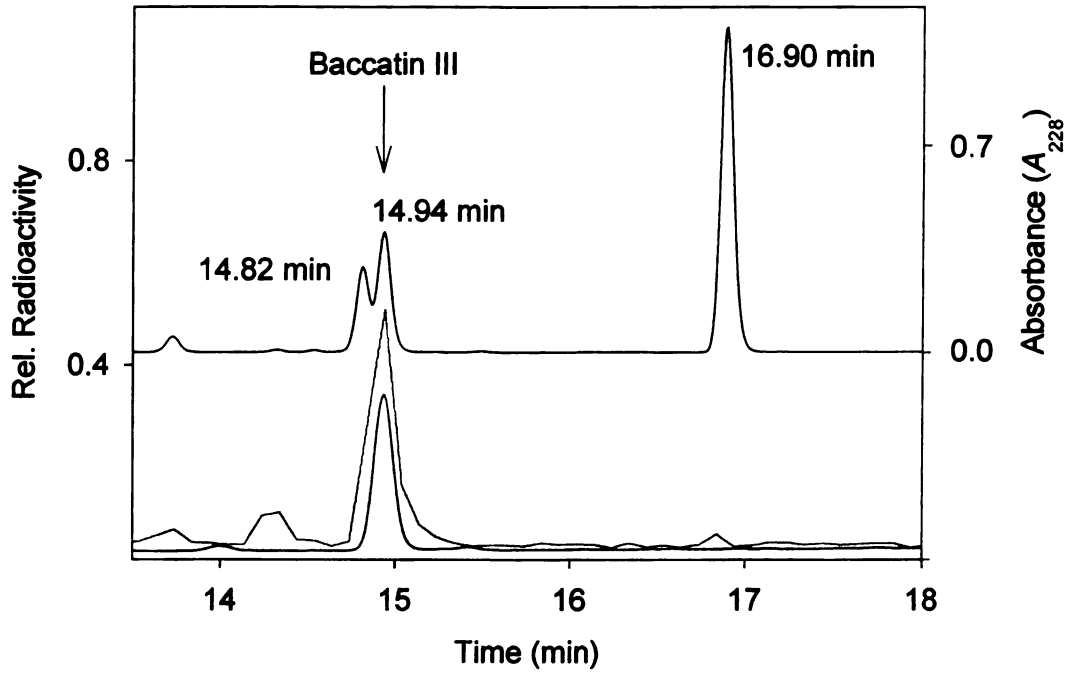

Taken together, these data show that DBAT regiospecifically transfers an acetyl group from acetyl CoA thioester to the tertiary hydroxyl of 4-DAB on the oxetane ring.[44]

2.5.4 Rationale for Turnover of Surrogate Substrates

The location and stereochemistry of the acceptor hydroxyl group (C-10β) of the natural substrate10-DAB differ from that of the surrogate substrate 4-DAB (C-4α). Therefore, it is remarkable that DBAT catalyzes transfer of acetate to both the C-4α and C-10β hydroxyl groups. Conceptually, the surrogate substrates bind to the DBAT active site in multiple orientations. Alternatively, upon binding, reorientation of the surrogate substrate takes place in the active site to place C-4α acceptor alcohol proximate to the DBAT active site for acyl delivery (**Figure 2-15**). This model proposes that acyl CoA likely docks to the DBAT active site in its native conformation while the C-4

deacetylated acceptor substrate is re-oriented in a way that places the C-4α hydroxyl group close to the acyl-donor for acyl transfer.

While substrate re-orientation or heterogeneity in binding conformations during DBAT catalysis is plausible and supports the kinetic data discussed in section **2.5.6**, it raises the question of what triggers it in the first place. This can be rationalized by invoking the concept of sequential substrate binding. The acyl donor likely binds to the active site first in a non-rate determining step, positioning the acyl group for delivery prior to the binding of the acceptor substrate. Since the surrogate substrate 4-DAB is in most respects similar to the natural substrate, it is expected to dock into the DBAT active site in a similar orientation to the natural substrate with its C-10 acetyl group projecting to the acetyl CoA that is already bound. Since this would result in an unfavorable interaction between the two acetyl groups, re-orientation of the in-coming acceptor substrate is necessary to mitigate unfavorable interactions (**Figure 2-15** cartoon B).

Figure 2-15. Proposed binding orientations of taxane substrates and catalytic triad for DBAT catalysis: When 4-DAB is flipped about its axis, its hydroxyl bears some resemblance to 10-DAB, indicating that 4-DAB turnover might be due to conformational heterogeneity (substrate has multiple binding conformations). A catalytic triad involving His, Asp, and a taxane acceptor substrate is also proposed for DBAT.

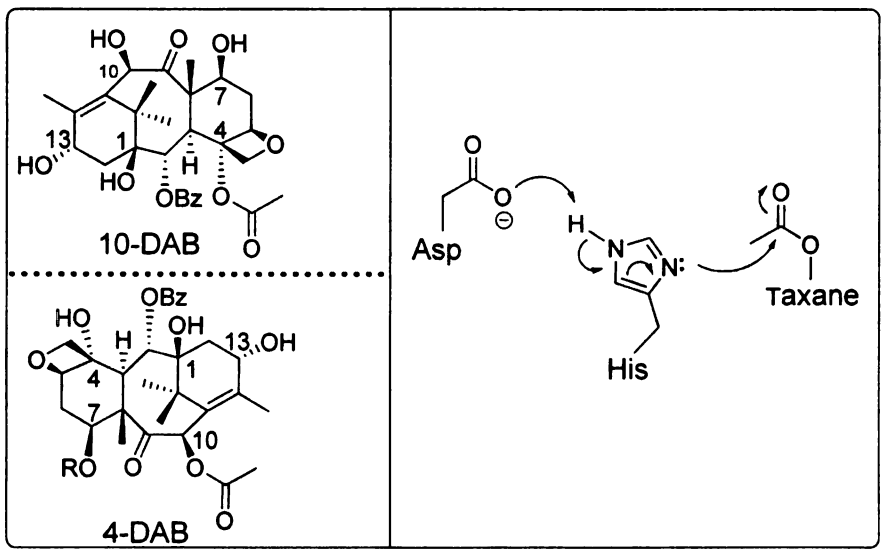

Furthermore, a 4-deacetyl substrate flipped about its axis (180-degree clockwise) bears resemblance to the 10-DAB substrate (**Figure 2-15** cartoon C), which lends further support to the concept of substrate re-orientation. Substrate re-orientation correlates to the concept of "differential ligand positioning," a strategy employed by some enzymes to fine-tune substrate promiscuity.[50]

Kinetic enzymatic resolution of the taxol side chain β-lactam using lipases from *Pseudomonas* has been achieved at near theoretical maximum yields (46-49%) with excellent (>95 %) enantiomeric purity.[51] However, preparation of 4-deacetyl taxane precursors, the β-lactam precursor of the isoserinyl side chain, and the coupling of the precursors to the tricyclic baccatin III core still involves multiple protection group manipulations,[52,53] as illustrated in **Scheme 2-2**. The foregoing discussion focused on the development of a chemo-enzymatic process for the modification of the tertiary C-4 hydroxyl of advanced taxanes. Such a process could reduce or potentially eliminate protecting groups from the semi-synthetic scheme of modified taxanes.

The results presented herein Chapter 2 reveal that *Taxus* 10-*O*-acetyltransferase (DBAT) has promiscuous activity. The recombinant DBAT enzyme transfers short-chain alkyl groups from their corresponding CoA thioesters to the secondary alcohol at C-10 of the natural substrate[7] as well as to the tertiary C-4 hydroxyl group of surrogate substrates.[44] This preliminary finding led to an assessment of DBAT as a potential catalyst for transfer of non-natural acyl groups to advanced taxane substrates of pharmaceutical interest,[49,54] which is discussed in Chapter 3.

2.5.5 DBAT-Mediated Acetylation of 13-Acylated Analogs

Several taxoids bearing acetate at the C-13 position have been isolated from *Taxus* plant species.[55] This prompted a study to establish whether DBAT-catalyzed acetylation of 4-DAB is still feasible when the C-13 hydroxyl group is blocked. Thus, DBAT was incubated with 13-acetyl-4-DAB analog and [^{3}H]-acetyl CoA under the same conditions described for the 4-DAB substrate. Analysis of the assay product by HPLC revealed a new product peak whose retention time (17.05 ± 0.01 min) was coincident with that of the semi-synthetically-derived 13-acetylbaccatin III product standard (**Figure 2-16**). To further confirm the regiochemistry of this enzymatic acetylation reaction, the other possible regioisomer 7-acetyl-4-DAB was semi-synthesized from 4-DAB as discussed in section **2.3**.

Figure 2-16. Possible regioisomers from acetylation of 13-4-DAB by DBAT, and the HPLC profiles of the biosynthetic product standards. To determine the regiochemistry of the biosynthetic product from the incubation of DBAT, 13-acetyl-4DAB, and acetyl-CoA, the possible regioisomeric product standards were semi-synthesized and their HPLC profiles compared to the radioactive HPLC profile of the biosynthetic product.

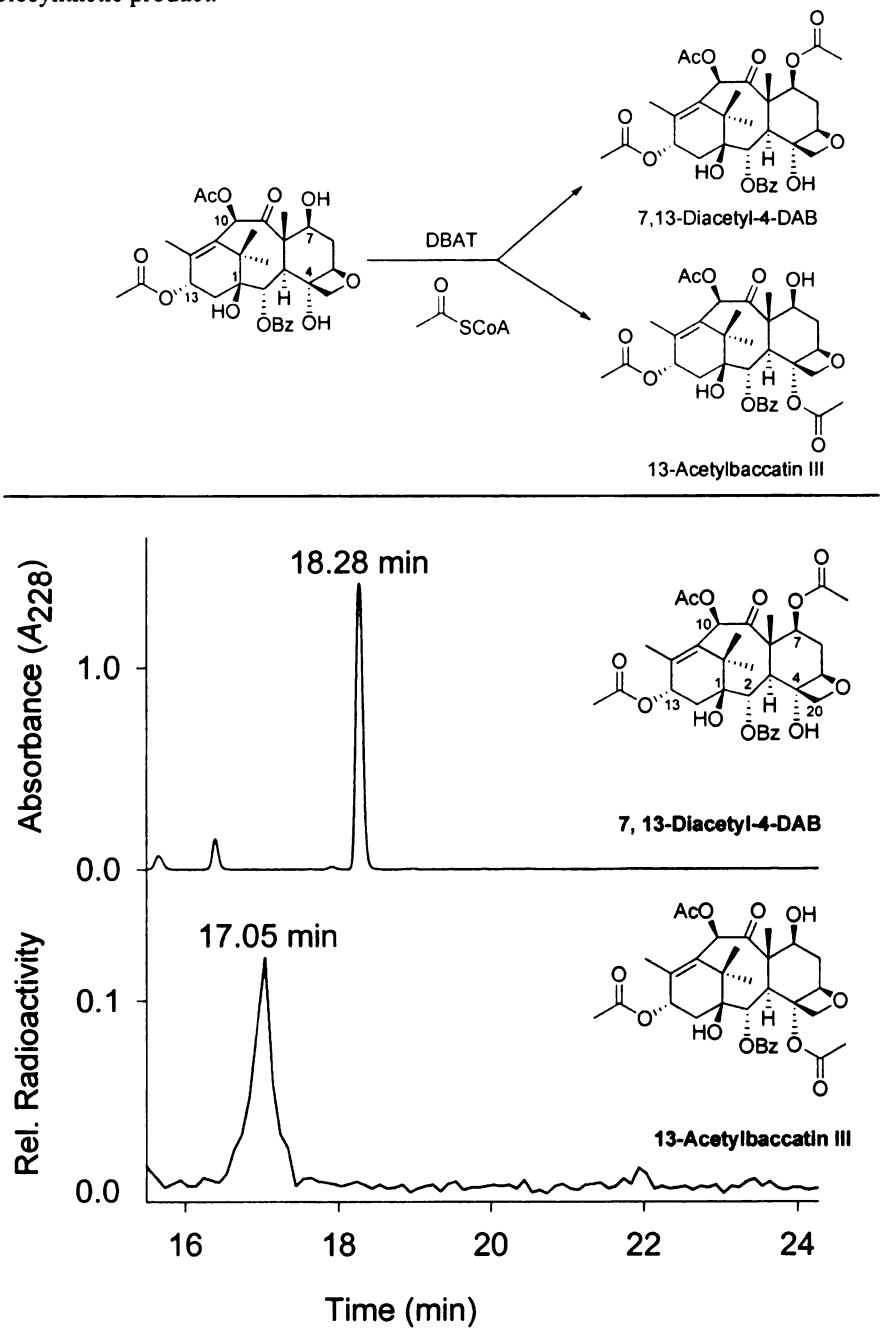

The finding that DBAT catalyzes acetylation of 13-acetyl-4-DAB implies that the enzyme might also function further downstream in the biosynthetic pathway of taxol than

initially proposed.[7] To test this hypothesis, docetaxel (taxotere), an advanced taxol analog in clinical use bearing a phenylisoserinyl side chain, 3'-*N*- *tert*-butoxycarbonyl, and a free C-10 hydroxyl group, was assessed for C-10 activity with DBAT. Enzyme preparations used for the assays described above for 4-DAB and 13-acetyl-4-DAB were used to assay for activity with taxotere.

A mixture of DBAT, taxotere, and [^{3}H]-acetyl CoA was incubated in one assay tube and the product was analyzed by reverse-phase HPLC coupled to a radioactive detector. A novel radioactive peak was observed that had a retention time (20.4 ± 0.1 min) coincident with 10-acetyltaxotere product standard. Incubation of DBAT, taxotere and unlabeled acetyl CoA under the same assay conditions yielded a biosynthetic product that co-eluted with the radio-labeled peak on reverse-phase HPLC. An aliquot of this sample was also analyzed by ESI-MS using the positive ion mode and the fragmentation pattern and the $[M+H]^+$ ion (*m/z* 807.3) matched those of 7-acetyltaxotere product standard. This data indicates that DBAT acetylates the C-10 position of taxotere.

DBAT-catalyzed acetylation of taxotere is intriguing given the relatively larger steric volume of the taxotere compared to natural substrate 10-DAB. Clearly, the DBAT active site can accommodate *N*-(*tert*-butoxycarbonyl) isoserine side chain. Conceivably, DBAT might act on more advanced substrates such as the naturally occurring-10-deacetyltaxol.[56]

Furthermore, this finding lends support to the inference made in section **2.2.2**, that the substrate specificity of BAHD acyltransferases, in general, might arise from specific spatial arrangement of polar residues in the enzyme active site rather than through the limitation of using conserved amino acids.[9] Consequently, this arrangement might require

the acceptor molecule to provide elements that define the substrate trajectory and recognition features for enzyme catalysis instead of a size-limited, pre-formed active site from conserved amino acid residues. The threshold for strict substrate recognition for some acyltransferases might be low, which would lead to substrate promiscuity. This could explain why an abundance of variously acylated taxoids exist in *Taxus* species[36] compared to taxol (cf. section **2.2.3**).

In the current study, it was noted that 4-deacetyl substrates having acetate at the C-7 and/or both C-7 and C-13 positions were not productive when incubated with DBAT and acetyl CoA. Arguably, a free hydroxyl at the C-7 position might serve as a key structural recognition element for DBAT catalysis.

2.5.6 Kinetic Analysis of DBAT with 4-DAB Substrates

Fitting the kinetic data obtained for DBAT with its natural substrate 10-DAB and unlabeled acetyl CoA into Hanes-Woolf plots yielded a K_m of 57.6 ± 3 μM for 10-DAB. Taking into consideration the amount of DBAT enzyme used in the kinetic analysis (5 μg, 0.1 nmol), the turnover number (k_{cat}) was calculated to be 0.58 ± 0.04 s^{-1}, while the specificity constant (k_{cat}/K_m) of DBAT for 10-DAB was calculated to be 10^4 ± 850 $s^{-1} \cdot M^{-1}$ (the uncertainty in the specificity constant was calculated using Gaussian error propagation). This value is only four orders of magnitude less than the diffusion limit at ~10^8 $s^{-1} \cdot M^{-1}$, indicating a proficient turnover rate of DBAT with the natural substrate 10-DAB.

The kinetic constants obtained for DBAT with 10-DAB were used to independently calculate the relative kinetic constants of DBAT for 4-DAB, taxotere, and 13-acetyl-4-DAB in mixed substrate assays.[32,57] The K_m value of DBAT with taxotere

was calculated to be 90.5 ± 8 μM and the k_{cat} was calculated to be 0.49 ± 0.04 s^{-1}; this yielded a catalytic efficiency of 5 × 10^3 ± 630 $s^{-1} \cdot M^{-1}$. The error in the specificity constant was calculated using Gaussian error propagation.

DBAT catalyzes acetylation of the C-4 position of the surrogate substrate 4-DAB to yield baccatin III; the same enzyme also transfers acetate to the C-10 alcohol of the natural substrate 10-DAB to form the same product. This precluded the use of mixed assays of 10-DAB and 4-DAB substrates to compare the relative rates for independent conversion of each substrate to baccatin III by DBAT. Therefore, the finding that taxotere is a productive substrate of DBAT proved to be advantageous and was subsequently used to indirectly determine the specificity constants for 4-DAB and 13-acetyl-4-DAB in mixed assays.

Thus, 4-DAB (35 μM) was incubated with docetaxel (35 μM) and [^{3}H]-acetyl CoA (100 μM, 1 μCi) to obtain the relative v_o of product formation catalyzed by DBAT (5 μg, 0.1 nmol) from each substrate. Analogously, docetaxel (35 μM), 10-DAB (35 μM) and [^{3}H]-acetyl CoA (100 μM, 1 μCi/μmol) were incubated with DBAT (5 μg, 0.1 nmol) in one assay tube and the ratio of their respective acetylated products was assessed. Finally, an assay mixture of 13-acetyl-4-DAB (35 μM), taxotere (35 μM), and [^{3}H]-acetyl CoA (100 μM, 1 μCi/μmol) was incubated with DBAT (5 μg, 0.1 nmol) in one assay tube and the product ratios were analyzed by radio-HPLC from where the relative catalytic efficiencies were extracted. For 4-DAB, the calculated specificity constant was found to be 190 $s^{-1} \cdot M^{-1}$, while for 13-acetylbaccatin III the k_{cat}/K_m was calculated to be 15 $s^{-1} \cdot M^{-1}$.

Taxanes with free C-4 hydroxyl group have not been isolated from *Taxus* species as yet. Therefore, it is highly unlikely that DBAT utilizes the 4-deacetyl substrates *in vivo*. Even if it does, the relatively low specificity constants calculated for 4-DAB and 13-acetyl-4-DAB implies that DBAT has an exceedingly low binding affinity for these substrates to be physiologically relevant. However, the *a priori* conclusion that low catalytic efficiency implies poor binding affinity of DBAT for 4-DAB substrates is somewhat misleading. In a parallel study, DBAT was found to catalyze transfer of acetate to the C-10 hydroxyl group of a 4-DAB analog with kinetic constants comparable to those the natural substrate 10-DAB, as discussed in section **3.4.5** of Chapter 3. Based on this finding, it is conceivable that substrate re-orientation is necessary before C-4 acylation, as proposed in section **2.5.4**. This indicates that the 4-deacetyl surrogate substrates bind to DBAT with affinity similar to the natural substrate but mostly in non-productive orientations due to the difference in the positions of the acceptor alcohols compared to the natural substrate 10-DAB. Therefore, substrate re-orientation to enable C-4 acetylation might be the rate-limiting step which erodes the overall catalytic efficiency of DBAT for these surrogate substrates.

In summary, DBAT catalyzes transfer of an acetyl group from acetyl CoA to the C-4 hydroxyl group of both 4-DAB and 13-acetyl 4-DAB with diminishing catalytic efficiencies (190 $s^{-1} \cdot M^{-1}$ and 15 $s^{-1} \cdot M^{-1}$, respectively) compared to the C-10 hydroxyl of both 10-DAB and taxotere (10^4 $s^{-1} \cdot M^{-1}$ and 5×10^3 $s^{-1} \cdot M^{-1}$, respectively). This finding sets the foundation for studies towards the improvement of the DBAT as a C-4 *O*-acetyltransferase in order to refine its substrate specificity and optimize its catalytic efficiency.

2.6 Significance

2.6.1 Implications on Taxol Biosynthesis

The finding that DBAT has promiscuous transacylase activity for the C-4α and C-10β hydroxyl groups of advanced taxanes has profound implications on the proposed acylation order of the taxol biosynthesis. Acetylation at the C-10 hydroxyl site of taxotere by DBAT is not entirely unexpected, since the C-10 hydroxyl is the native position for DBAT recognition and catalysis. However, since the taxotere substrate contains a sterically larger *N*-(*tert*-butoxycarbonyl) phenylisoserine at the C-13 hydroxyl, the proficient turnover of this substrate by DBAT is thus remarkable. Therefore, it is plausible that the position of DBAT on the biosynthetic pathway of taxol might be further downstream than initially proposed.[28] Conceivably, acetylation of an advanced intermediate such as the naturally occurring 10-deacetyltaxol[56] by DBAT could possibly be the last enzymatic step of the taxol biosynthetic pathway (cf. **Scheme 2-5**).

Additionally, the novel C-4 transacylase activity of DBAT challenges the proposed biosynthetic origin of the C-4 acetate of advanced taxanes. The current dogma proposes an intramolecular rearrangement involving oxetane ring-expansion and C-5 acetyl migration to the C-4 position[58] (cf. **Scheme 2-3**). The findings presented here suggest that an alternative acyl-independent route to oxetane ring formation and an acetyl CoA-dependent biosynthetic origin of the C-4 acetoxy group should be considered along with the current hypothesis (**Scheme 2-6**).

However, the catalytic efficiency of DBAT for 4-DAB is ~50-fold lower compared to 10-DAB. Moreover, naturally-occurring 4-deacetyl taxanes have not been

isolated from *Taxus* species yet.[59] Therefore, DBAT-catalyzed acetylation of 4-deacetyl substrates should be cautiously considered fortuitous promiscuity rather than transacylase activity of physiological relevance.

Scheme 2-6. Possible biosynthetic origins of the oxetane ring and the C-4α acetate.[44]

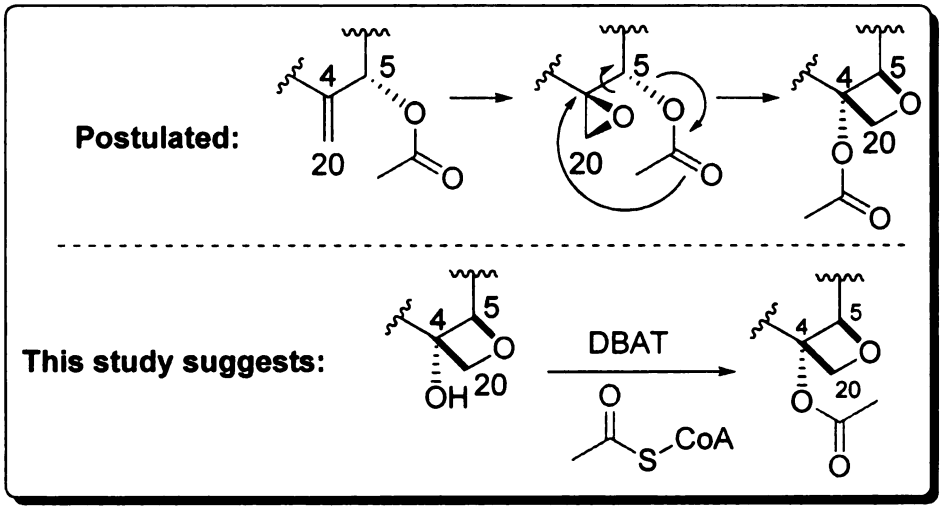

2.6.2 Significance: Potential Application in Biocatalysis

A process for the removal of the C-4 acetate of 10-DAB using culture enrichment of *Rhodococcus* species from soil has been reported.[60] This constitutes an important development for a one-step process to access the C-4 alcohol of advanced taxanes without the need for protecting groups.[61] Foreseaably, a process that incorporates this microbial process and DBAT-catalyzed C-4 acylation could potentially provide a synergistic two-step enzymatic methodology to modify the C-4 alcohol of modified taxane precursors (**Scheme 2-7**).

Scheme 2-7. Potential use of a microbial system for the deacetylation of 10-DAB coupled to DBAT catalysis. The broken arrow indicates processes yet to be demonstrated.

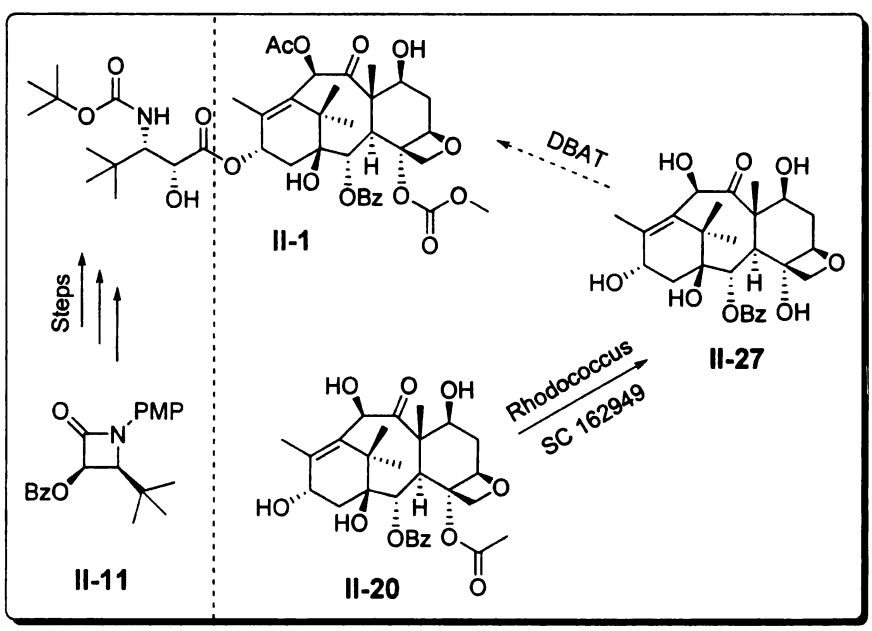

However, both enzymatic systems need necessary refinements before the envisioned process can be applied in the commercial production of C-4-modified taxanes.

2.7 References

(1) Mastalerz, H.; Cook, D.; Fairchild, C. R.; Hansel, S.; Johnson, W.; Kadow, J. F.; Long, B. H.; Rose, W. C.; Tarrant, J.; Wu, M.-J.; Xue, M. Q.; Zhang, G.; Zoeckler, M.; Vyas, D. M. *Bioorganic & Medicinal Chemistry* **2003**, *11*, 4315-4323.

(2) Galletti, E.; Magnani, M.; Renzulli, Michela L.; Botta, M. *ChemMedChem* **2007**, *2*, 920-942.

(3) Lim, S.; Tupule, A.; Espina, B.; Levine, A. *Cancer* **2005**, *103*, 417-421.

(4) Park, S.; Shim, W.; Ho, D.; Raizner, A.; Park, S.; Hong, M.; Lee, C.; Choi, D.; Jang, Y.; Lam, R. *New England Journal of Medicine* **2003**, *348*, 1537.

(5) Ganesh, T.; Norris, A.; Sharma, S.; Bane, S.; Alcaraz, A. A.; Snyder, J. P.; Kingston, D. G. I. *Bioorganic & Medicinal Chemistry* **2006**, *14*, 3447-3454.

(6) Ganesh, T.; Yang, C.; Norris, A.; Glass, T.; Bane, S.; Ravindra, R.; Banerjee, A.; Metaferia, B.; Thomas, S. L.; Giannakakou, P.; Alcaraz, A. A.; Lakdawala, A. S.; Snyder, J. P.; Kingston, D. G. *Journal of medicinal chemistry* **2007**, *50*, 713-25.

(7) Walker, K.; Croteau, R. *Proceedings of the National Academy of Sciences of the United States of America* **2000**, *97*, 583-587.

(8) Chau, M.; Walker, K.; Long, R.; Croteau, R. *Archives of Biochemistry and Biophysics* **2004**, *430*, 237-246.

(9) Unno, H.; Ichimaida, F.; Suzuki, H.; Takahashi, S.; Tanaka, Y.; Saito, A.; Nishino, T.; Kusunoki, M.; Nakayama, T. *Journal of Biological Chemistry* **2007**, *282*, 15812-15822.

(10) Renard, C. M. G. C.; Jarvis, M. C. *Carbohydrate Polymers* **1999**, *39*, 201-207.

(11) Yu, X.-H.; Gou, J.-Y.; Liu, C.-J. *Plant Molecular Biology* **2009**, *70*, 421-442.

(12) D'Auria, J. C. *Current Opinion in Plant Biology* **2006**, *9*, 331-340.

(13) Shan, L.; Thara, V. K.; Martin, G. B.; Zhou, J.-M.; Tang, X. *Plant Cell* **2000**, *12*, 2323-2338.

(14) Sirikantaramas, S.; Yamazaki, M.; Saito, K. *Phytochemistry Reviews* **2008**, *7*, 467-477.

(15) Li, A.; Steffens, J. *Proceedings of the National Academy of Sciences of the United States of America* **2000**, *97*, 6902.

(16) Steffens, J. *The Plant Cell Online* **2000**, *12*, 1253.

(17) Suzuki, H.; Shin'ya Sawada, K.; Nagae, S.; Yamaguchi, M.; Nakayama, T.; Nishino, T. *The Plant Journal* **2004**, *38*, 994-1003.

(18) Luo, J.; Nishiyama, Y.; Fuell, C.; Taguchi, G.; Elliott, K.; Hill, L.; Tanaka, Y.; Kitayama, M.; Yamazaki, M.; Bailey, P.; Parr, A.; Michael, A. J.; Saito, K.; Martin, C. *The Plant Journal* **2007**, *50*, 678-695.

(19) St-Pierre, B.; De Luca, V. *Recent Adv. Phytochem.* **2000**, *34*, 285-315.

(20) Ma, X.; Koepke, J.; Panjikar, S.; Fritzsch, G.; Stockigt, J. *Journal of Biological Chemistry* **2005**, *280*, 13576-13583.

(21) Ma, X.; Koepke, J.; Bayer, A.; Fritzsch, G.; Michel, H.; Stoeckigt, J. *Acta Crystallographica, Section D: Biological Crystallography* **2005**, *D61*, 694-696.

(22) Nakayama, T.; Suzuki, H.; Nishino, T. *Journal of Molecular Catalysis B: Enzymatic* **2003**, *23*, 117-132.

(23) Okada, T.; Hirai, M.; Suzuki, H.; Yamazaki, M.; Saito, K. *Plant and Cell Physiology* **2005**, *46*, 233.

(24) Dexter, R.; Qualley, A.; Kish, C. M.; Ma, C. J.; Koeduka, T.; Nagegowda, D. A.; Dudareva, N.; Pichersky, E.; Clark, D. *The Plant Journal* **2007**, *49*, 265-275.

(25) Grothe, T.; Lenz, R.; Kutchan, T. *Journal of Biological Chemistry* **2001**, *276*, 30717.

(26) Facchini, P.; St-Pierre, B. *Current opinion in plant biology* **2005**, *8*, 657-666.

(27) Croteau, R.; Ketchum, R.; Long, R.; Kaspera, R.; Wildung, M. *Phytochemistry Reviews* **2006**, *5*, 75-97.

(28) Walker, K.; Croteau, R. *Phytochemistry* **2001**, *58*, 1-7.

(29) Baloglu, E.; Hoch, J. M.; Chatterjee, S. K.; Ravindra, R.; Bane, S.; Kingston, D. G. I. *Bioorganic & Medicinal Chemistry* **2003**, *11*, 1557-1568.

(30) Nawarathne, I.; Walker, K. *Journal of Natural Products*, *73*, 151-159.

(31) Nevarez, D. M.; Mengistu, Y. A.; Nawarathne, I. N.; Walker, K. D. *Journal of the American Chemical Society* **2009**, *131*, 5994-6002.

(32) Loncaric, C.; Merriweather, E.; Walker, K. *Chemistry & Biology* **2006**, *13*, 1-9.

(33) D'Auria, J.; Pichersky, E.; Schaub, A.; Hansel, A.; Gershenzon, J. *The Plant Journal* **2007**, *49*, 194-207.

(34) Walker, K.; Fujisaki, S.; Long, R.; Croteau, R. *Proceedings of the National Academy of Sciences of the United States of America* **2002**, *99*, 12715-12720.

(35) Hampel, D.; Mau, C. J. D.; Croteau, R. B. *Archives of Biochemistry and Biophysics* **2009**, *487*, 91-97.

(36) Hampel, D.; Mau, C. J. D.; Croteau, R. B. *Archives of Biochemistry and Biophysics* **2009**, *487*, 91-97.

(37) Baloglu, E.; Kingston, D. G. I. *Journal of Natural Products* **1999**, *62*, 1448-1472.

(38) Green, M. R.; Manikhas, G. M.; Orlov, S.; Afanasyev, B.; Makhson, A. M.; Bhar, P.; Hawkins, M. J. *Annals of Oncology* **2006**, *17*, 1263-1268.

(39) Broker, L. E.; de Vos, F. Y. F. L.; van Groeningen, C. J.; Kuenen, B. C.; Gall, H. E.; Woo, M. H.; Voi, M.; Gietema, J. A.; de Vries, E. G. E.; Giaccone, G. *Clinical Cancer Research* **2006**, *12*, 1760-1767.

(40) Broker, L. E.; Valdivieso, M.; Pilat, M. J.; DeLuca, P.; Zhou, X.; Parker, S.; Giaccone, G.; LoRusso, P. M. *Clinical Cancer Research* **2008**, *14*, 4186-4191.

(41) Jennewein, S.; Croteau, R. *Applied Microbiology and Biotechnology* **2001**, *57*, 13-19.

(42) Kaspera, R.; Cape, J.; Faraldos, J.; Ketchum, R.; Croteau, R. *Tetrahedron Letters*.

(43) Walker, K.; Schoendorf, A.; Croteau, R. *Archives of Biochemistry and Biophysics* **2000**, *374*, 371-380.

(44) Ondari, M. E.; Walker, K. D. *Journal of the American Chemical Society* **2008**, *130*, 17187-17194.

(45) Loncaric, C.; Ward, A. F.; Walker, K. D. *Biotechnology Journal* **2007**, *2*, 266-274.

(46) Jennewein, S.; Wildung, M. R.; Chau, M.; Walker, K.; Croteau, R. *Proceedings of the National Academy of Sciences of the United States of America* **2004**, *101*, 9149-9154.

(47) Walker, K.; Croteau, R. *Proceedings of the National Academy of Sciences of the United States of America* **2000**, *97*, 13591-13596.

(48) Walker, K.; Ketchum, R. E. B.; Hezari, M.; Gatfield, D.; Goleniowski, M.; Barthol, A.; Croteau, R. *Archives of Biochemistry and Biophysics* **1999**, *364*, 273-279.

(49) Ganesh, T.; Guza, R. C.; Bane, S.; Ravindra, R.; Shanker, N.; Lakdawala, A. S.; Snyder, J. P.; Kingston, D. G. I. *Proceedings of the National Academy of Sciences* **2004**, *101*, 10006-10011.

(50) Nobeli, I.; Favia, A.; Thornton, J. *Nature biotechnology* **2009**, *27*, 157-167.

(51) Patel, R. *Coordination Chemistry Reviews* **2008**, *252*, 659-701.

(52) Kant, J.; Bristol-Myers Squibb Company.: USA, 2001.

(53) Kadow, J. F.; Mastalerz, H.; Xue, Q. M.; Hansel, S.; Zoeckler, M. E.; Rose, W. C.; Tarrant, J. G.; Bristol-Myers Squibb Company: USA, 2001.

(54) Yoo, G. H.; Tran, V. R.; Lemonnier, L. A.; Ezzat, W. H.; Subramanian, G.; Piechocki, M. P.; Ensley, J. F.; Lonardo, F.; Kim, H.; Lin, H.-S. *American Journal of Otolaryngology* **2007**, *28*, 309-315.

(55) Gunawardana, G.; Premachandran, U.; Burres, N.; Whittern, D.; Henry, R.; Spanton, S.; McAlpine, J. *Journal of Natural Products* **1992**, *55*, 1686-1689.

(56) McLaughlin, J.; Miller, R.; Powell, R.; Smith Jr, C. *Journal of Natural Products* **1981**, *44*, 312-319.

(57) Pi, N.; Leary, J. A. *Journal of the American Society for Mass Spectrometry* **2004**, *15*, 233-243.

(58) Guéritte-Voegelein, F.; Guénard, D.; Potier, P. *Journal Natural Product* **1987**, *50*, 9-18.

(59) Kingston, D. G. I.; Ganesh, T.; Snyder, J. P.; Lakdawala, A. S.; Bane, S.; Virginia Tech Intellectual Properties, Inc.: USA, 2005.

(60) Hanson, R. L.; Parker, W. L.; Patel, R. N. *Biotechnology and Applied Biochemistry* **2006**, *45*, 81-85.

(61) Mastalerz, H.; Cook, D.; Fairchild, C.; Hansel, S.; Johnson, W.; Kadow, J.; Long, B.; Rose, W.; Tarrant, J.; Wu, M. *Bioorganic & medicinal chemistry* **2003**, *11*, 4315-4323.

3 Chapter Three: Towards an Understanding of DBAT as a Catalyst

3.1 Specific Aims

Based on the observations that DBAT can utilize a non-natural substrate 4-deacetylbaccatin III (4-DAB), a potential application for this enzyme in the biocatalysis of advanced taxanes was sought. In particular, BMS 275183, a water soluble Taxol analog,, was used as a model to *assess whether DBAT could catalyze the transfer of the non-natural methoxycarbonyl functional group from coenzyme A to the C-4 position of the surrogate substrate 4-DAB*. The basis of this assessment was a previous study which demonstrated that DBAT catalyzes transfer of a propionyl group from propionyl CoA to the C-10 position of 10-DAB.[1] Even though the methoxycarbonyl moiety is isosteric to the propionyl group, the two are electronically dissimilar; thus it was anticipated that this could potentially affect DBAT catalysis.

During the course of investigating the regioselectivity of DBAT for the C-4 deacetyl substrates, a competing and equally facile "esterase" activity of DBAT against C-10 taxanes was revealed. Although this is merely an example of microscopic reversibility, it is necessary to *evaluate the physiological relevance of the enzymatic hydrolase activity of DBAT in the context of taxol biosynthesis*. As a consequence of the esterase activity, a hypothesis for the catalytic mechanism of the DBAT reaction was formulated.

Based on the rapid rates of the reverse reaction catalyzed by DBAT, a straightforward experiment was designed to *propose an alternative mechanism for the DBAT reaction* that is significantly different from the currently held mechanism.[2]

Furthermore, the fast rate of the reverse reaction implies that optimum yields in reactions employing DBAT as a catalyst could be limited by the dynamic equilibrium. Therefore, any biocatalytic process employing DBAT as a biocatalyst must address this bottleneck.

Finally, by site-directed mutagenesis, *the catalytic role of the Asp residue in the HXXXD motif of DBAT was probed.* This motif is conserved in the BAHD superfamily of enzymes and has been presumed to function as a structural component during catalysis.[2,3] However, based on preliminary studies presented herein, this residue is likely obligatorily catalytic and plays more than a perfunctory role.

3.2 Introduction: Enzyme Promiscuity

Some enzymes exhibit unparalleled chiral discrimination and accelerate reaction rates by many orders of magnitude over uncatalyzed reactions.[4] Moreover, the often strict substrate selectivity by enzymes affords efficient reactions with fewer side-products. The remarkable chemo- and regioselectivity of some enzymatic processes can minimize the need for protection and deprotection strategies that are common in organic synthesis methods.[4] Therefore, the enormous potential of enzymes as environmentally benign biocatalysts in organic transformations is an appealing prospect.

However, despite these advantages, enzymes are only slowly gaining widespread application in synthetic chemistry over conventional chemical catalysts.[5] This underutilization can be explained in part by considering that enzymes generally display a narrow range of substrate specificity.[5] However, continued demonstration of enzyme promiscuity has not only shown this generalization as an oversimplification, but it has

also become a revitalizing theme in contemporary enzyme chemistry and has spurred growth in applied biocatalysis in the last few decades.[4,6]

Even though the xenobiotic metabolizing enzymes such as cytochrome P450s are arguably the most promiscuous,[7] the inherent biocatalytic promiscuity among triacylglycerol acyl hydrolases due to their relaxed substrate specificity has found more meaningful synthetic applications. These hydrolases have been used extensively in dynamic kinetic resolution of racemic acids and alcohols.[8] Enzyme promiscuity, likely evolutionarily beneficial, has found utility in many industrial synthetic processes. However, the perceived limitation of enzymatic applications arising from narrow substrate specificity has not been fully addressed. Among feasible approaches that have been explored thus far to mitigate this bottleneck include rational protein engineering and directed evolution aimed at expanding the substrate repertoire.[4,5]

Processes such as rational design and directed evolution of biocatalysts can be employed in parallel with simpler strategies like "substrate engineering." This strategy can change the product profile of an enzyme via modification of the structure of the substrate.[5] As an example, in oligosaccharide synthesis, hydrophobic functional groups (straight-chain hydrocarbons, benzyl, benzoyl, and *p*-nitrophenol) are chemically appended to unnatural substrates of glycosyltransferases.[5] These modifications induce productive binding modes that direct the formation of distinct sugar linkages, thus facilitating stringent and yet rational control of substrate specificity and regioselectivity with wild-type enzymes.[5,9] Specifically, three distinct saccharide-polymerizing glycosyltransferases were demonstrated to utilize truncated non-natural acceptors having

hydrophobic constituents in place of saccharide extensions of the native acceptors[9] (**Scheme 3-1**). In one case, a simple exchange of an aromatic group for a straight-chain aliphatic hydrocarbon caused a change in the chemoselectivity of a glycosyltransferase enzyme LgtC. This led to glycosylation of both axial and equatorial hydroxyls at synthetically useful reaction rates, indicating that subtle substrate modifications can expand specificity of enzymes.[9]

Scheme 3-1. Galactosylation catalyzed by LgtC (top panel); Acceptors such as compound III-4 mimic the lactose binding mode[5] (bottom panel). UDP is uridine-5'-diphosphate.

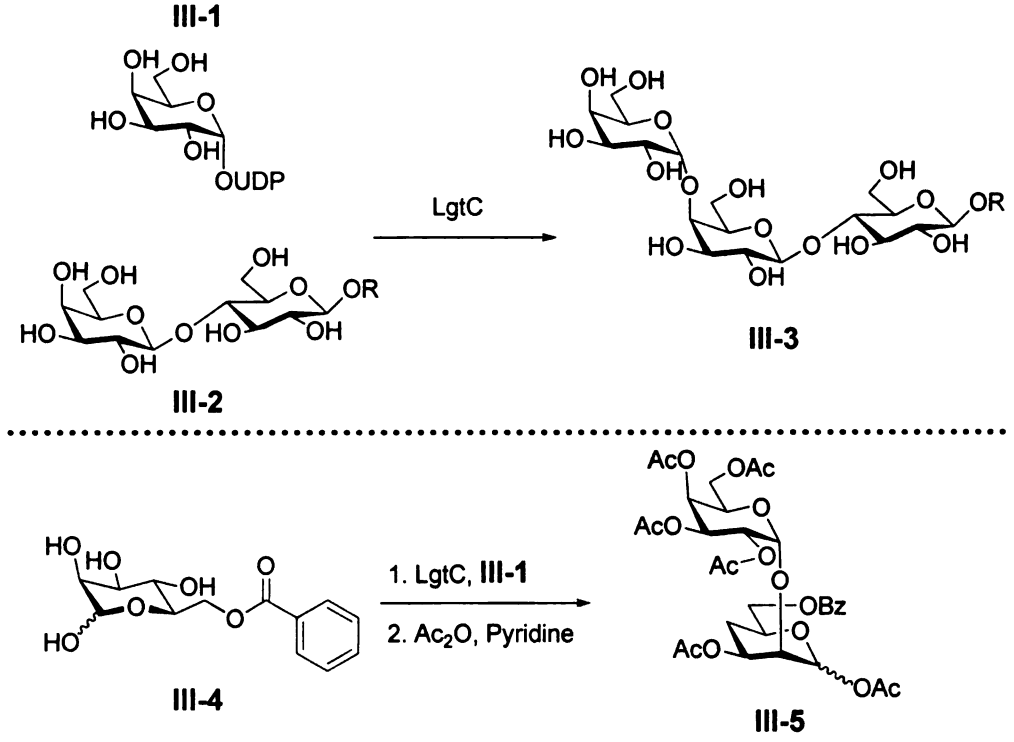

While hydrogen bonding as well as electrostatic and hydrophobic interactions within the active sites of most enzyme catalysts generally define substrate specificity, the molecular basis of enzyme promiscuity is, however, not as well established.[10] It is widely presumed that the plasticity of the enzyme correlates with active site variability, which allows for recognition of diverse structures at minimal energetic cost.[7,10] However, this

does not imply that productive binding of related substrates is a simple function of the fold or architecture of the protein. There are various manifestations of enzyme promiscuity, such as protein recognition of multiple substrates; an example of this is the recognition of multiple antigens by a single germline antibody.[6] These manifestations of promiscuity are inevitably linked to conditions that trigger them, such as differential protein expression, which may itself be dictated by the local protein environment or localization.[6]

All these factors are ultimately connected to the molecular mechanism underlying protein promiscuity, like post-translational modification of proteins. Furthermore, the ability of enzymes to exist as an ensemble of flexible conformers ensures that ligands satisfying some minimum physical and conformational properties will find matching affinities with appropriate enzyme conformers, which leads to binding or even catalytic promiscuity.[6] Additionally, oligomerization of individual protein monomers might also play a critical role of enriching the catalytic repertoire of enzymes, as might fusion of multiple protein domains within a protein family.[6] This extends the range of possible enzyme-ligand interactions and subsequent reactions.

It has also been suggested that extreme functional promiscuity could be easily achieved by distributing flexibility of an enzyme throughout an entire protein scaffold rather than limiting it to the active site.[10] For example, it has been argued that mutations responsible for drug resistance usually occur in loop regions surrounding the protein binding site and less likely in the catalytic regions, as this would be detrimental to protein function.[7] Thus, protein flexibility might itself be achieved by loop regions as a means of

partially recognizing interacting partners through imperfect complementarity or differential ligand positioning. The implication of differential ligand binding is that protein promiscuity is almost inevitably linked to ligand promiscuity.[6]

In Chapter 2, the concept of differential ligand positioning was mentioned briefly in the context of DBAT-catalyzed transfer of an acetyl group to surrogate 4-deacetyl substrates. This notion prompted a study to dissect the nature of the enzyme substrate and how segments of this substrate could be potentially modified to uncover critical structural elements within it that could be used to refine the promiscuous activity of DBAT. Described below is a brief account of one such structural feature, i.e., intramolecular hydrogen bonding in baccatin III substrate, a product of DBAT-catalyzed acetylation of 10-DAB. It was initially speculated that modulating this hydrogen bond could enhance the promiscuity of DBAT toward the 4-DAB surrogate substrate.

3.2.1 The nature of the baccatin III substrate

Baccatin III has an array of oxygen functional groups variously positioned on the taxane core which direct the chemoselectivity of the acyltransferases on the taxol pathway.[11,12] For example, when DBAT was incubated with acetyl CoA and 7-*O*-acetyl analogs of baccatin III and 4-DAB, no detectable products were observed, as discussed in section **2.4.5** This observation implies that perhaps the free hydroxyl group at the C-7β of the baccatin III scaffold is a necessary structural element for DBAT to recognize and/or bind the substrate during the regiospecific transfer of an acetyl group to the C-10 alcohol.

Even though the C-4α acetoxy appears to be distal to the C-7 site, the C-4 ester seemingly influences the stereochemistry of the C-7β alcohol in aqueous buffer. When 4-

DAB was incubated with DBAT at 31°C at pH 5.6 or higher, the C-7β hydroxyl group underwent non-enzymatic epimerization (as determined from control experiments) to give an equilibrium mixture (~1:1) of 4-DAB and 7-epi-4-DAB (compound **III-8**, **Figure 3-1**). This was an intriguing observation since baccatin III, which has an acetyl group at the C-4 hydroxyl, does not readily epimerize under similar conditions.

It has been established that the carbonyl oxygen of the C-4α acetoxy group interacts via hydrogen-bonding with the C-13α alcohol of baccatin III and related compounds[13] (**Figure 3-1**). Apparently, this hydrogen-bond contact stabilizes the baccatin III structure and, once disrupted by deacetylation of the C-4 alcohol, the molecule reverts to two thermodynamically equivalent C-7 epimers.

Figure 3-1. Putative intramolecular hydrogen bond in baccatin III (III-7); removal of the C-4 acetate results in epimerization of 4-DAB to 7-epi-4DAB (compound III-8) in aqueous media at pH 5.6 or higher.[13]

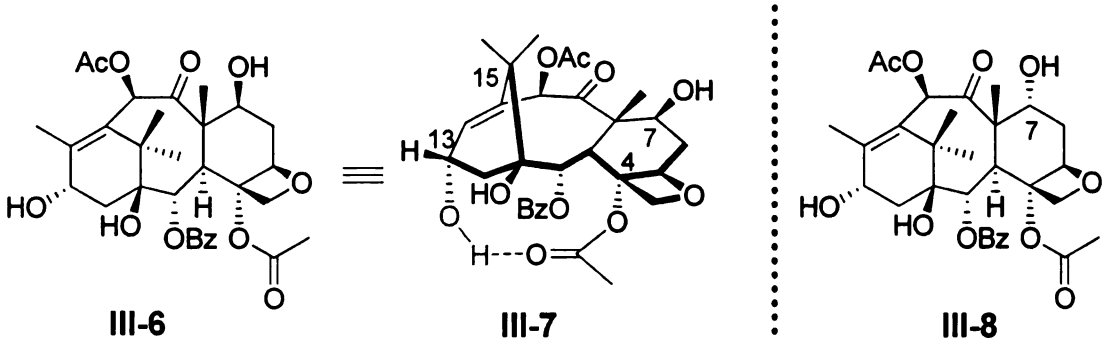

Additionally, it was also observed that the C-7 epimer of 4-DAB is a productive substrate of DBAT under conditions that promote the reverse reaction (described in section **3.4.1**). This indicates that the DBAT-catalyzed acetylation of the C-10β alcohol is not affected by the stereochemistry at C-7 hydroxyl group.

It was equally necessary to probe whether the intramolecular C-4/C-13 hydrogen-bond in baccatin III affects the regioselectivity of DBAT for the C-10 hydroxyl over the C-4 hydroxyl. To test the effect of the hydrogen bond, a series of variously acylated baccatin III analogs were synthesized and tested, and the findings are discussed in section **3.4.2**.

Substrate engineering as a design concept has been successfully used to influence the outcome of enzymatic processes in other systems, such as mentioned previously for the glycosyltransferases[5] in section **3.2**. However, it is unlikely that this concept will find appeal as a general approach in cases where the enzyme substrate lacks the necessary functional groups amenable to chemical manipulations. Ultimately, understanding the molecular properties of a biocatalyst as it relates to ligand binding and knowledge of the reaction mechanism might prove advantageous towards rational engineering of enzyme specificity.

Thus, to better understand DBAT reaction parameters, acyltransferases in the BAHD family that includes DBAT, were used as models to assess the proposed mechanism for this group of enzymes. Based on preliminary findings, it appears that DBAT proceeds along a reaction pathway that is different from that proposed in literature for members of the BAHD family.[2]

3.2.2 Proposed Catalytic Mechanism of the BAHD Acyltransferases

Even though chloramphenicol acetyltransferase and choline/carnitine acyltransferases (CAT) do not belong to the BAHD family, they share the HXXXD catalytic motif. Since a wealth of mechanistic and structural information is available for this collection of enzymes,[14] they are a good reference point for understanding the

mechanism of DBAT and the other acyltransferases in the BAHD superfamily. In the catalytic mechanism of the CAT enzymes, a substrate-enzyme ternary complex is formed and the acceptor nucleophile is activated through deprotonation by a general base.[15] Based on these observations and on evidence inferred from structural and mutational studies of vinorine synthase and anthocyanin acyltransferases (AATs),[2,3] the mechanism of the BAHD family of acyltransferases is proposed to involve *direct delivery of an acyl group from the acyl CoA donor onto the acceptor substrate* via nucleophilic attack of the substrate hydroxyl (or amine) group on the carbonyl carbon of the acyl CoA[2] (**Scheme 3-2**). For example, the mechanism of malonyl transfer to anthocyanin by SsMat1 (a member of the AAT) is a Bi-Bi system, which implies either a double-displacement or ternary-complex.[16] However, inhibition studies suggest that the reaction progresses through a ternary-complex comprised of malonyl-CoA, anthocyanin, and the acyltransferase.[16] The reactive hydroxyl group of the anthocyanin acceptor substrate is proposed to be proximate to the thioester carbonyl of the acyl donor malonyl-CoA and catalytic His residue of Ss5Mat1. This His residue (His-167) acts as a general base which abstracts a proton from the acceptor substrate triggering a transesterification reaction.[3,16]

Scheme 3-2. The proposed catalytic mechanism of vinorine synthase.[2]

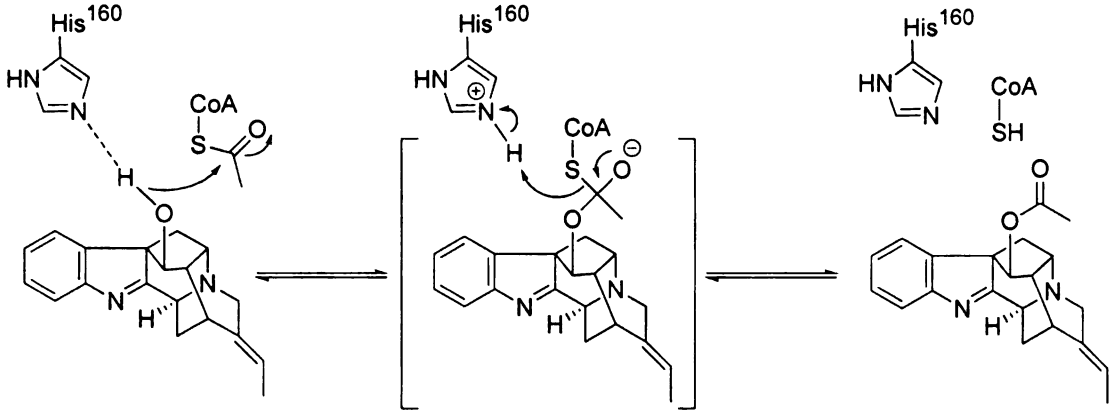

III-9 III-10 III-11

Alanine-scanning mutagenesis of the malonyltransferase revealed a 5,000-10,000-fold decrease in the k_{cat} after substitution of His-167 or Asp-390 that are conserved residues of the HXXXD and DFGWG motifs, respectively.[16] This demonstrates that these residues play a role in the catalytic competency of the malonyltransferase enzymes.[16] In a related enzyme, Dm3MaT3, a tryptophan residue (Trp-36 is conserved in all AATs) located in the malonyl CoA binding pocket is speculated to play a role in determining substrate specificity.[3] An earlier study involving Ss5Mat1 indicated a non-random order of substrate binding.[16] Malonyl CoA was proposed to bind to the active site before the anthocyanin acceptor substrate while free CoA was thought to be the last to dissociate from the enzyme-product complex. However, there was no evidence for this sequential substrate binding order in the structural studies involving a homolog anthocyanidin malonyltransferase, designated Dm3MaT2.[3]

The crystal structure of vinorine synthase (VS), a two-domain protein belonging to the BAHD superfamily, reveals that the putative catalytic His-160 of the signature HXXXD motif lies at the center of the two domains.[2] This is speculated to be an important feature

since both the acyl CoA and acyl acceptor substrates can access the active site independently. Multiple sequence alignment, site-directed mutagenesis and inhibition studies with vinorine synthase suggest that His-160 and Asp-164 are catalytically indispensable[17] (**Figure 3-2.**) When His-160 and Asp-164 were both mutated to Ala the resulting mutants were completely inactive, suggesting that a catalytic diad is involved in the vinorine synthase catalyzed reaction.[17] In the same study, chemical inhibition of Ser and Cys with *N*-tosyl-L-phenylalanine chloromethylketone (TPCK) and non-selective inhibition of histidine with diethyl pyrocarbonate (DEPC) resulted in complete loss of vinorine synthase activity, implying that these residues could be involved in catalysis.[17]

Figure 3-2. Multiple Sequence Alignment of DBAT, vinorine synthase (VS), and anthocyanin malonyltransferase (AMT).

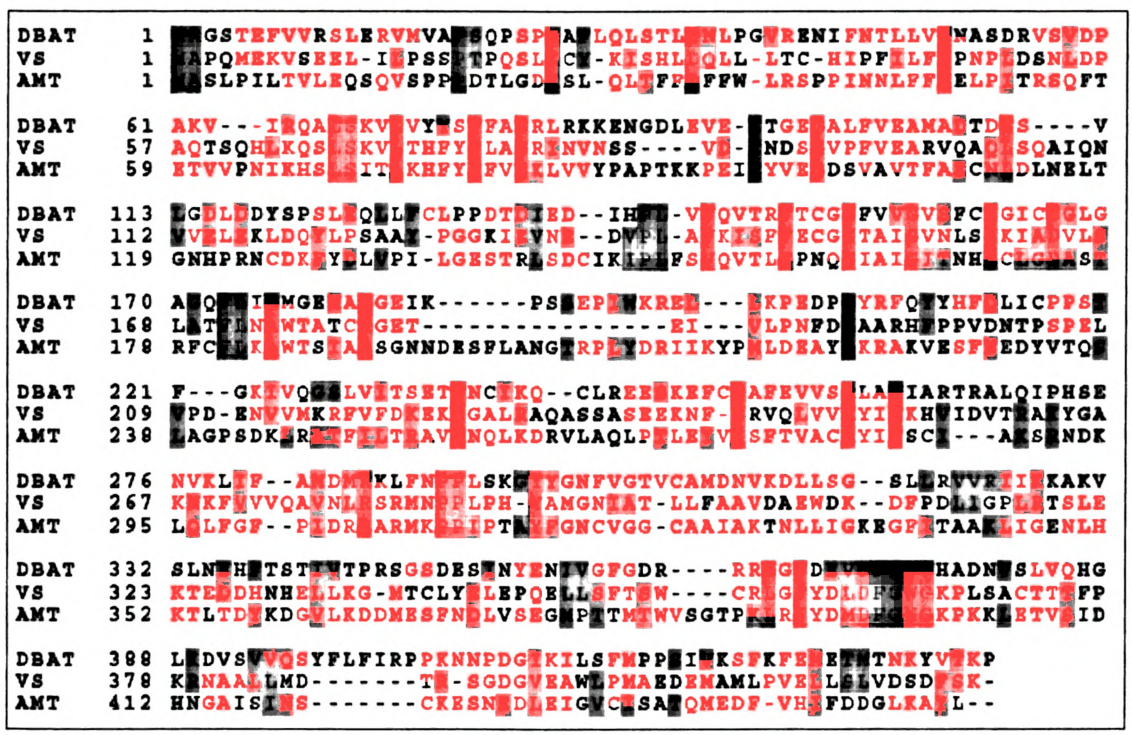

The foregoing mutational analysis suggests that vinorine synthase catalysis is independent of several nucleophilic residues (Cys, Ser, His, Asp) that could presumably

since both the acyl CoA and acyl acceptor substrates can access the active site independently. Multiple sequence alignment, site-directed mutagenesis and inhibition studies with vinorine synthase suggest that His-160 and Asp-164 are catalytically indispensable[17] (**Figure 3-2.**) When His-160 and Asp-164 were both mutated to Ala the resulting mutants were completely inactive, suggesting that a catalytic diad is involved in the vinorine synthase catalyzed reaction.[17] In the same study, chemical inhibition of Ser and Cys with *N*-tosyl-L-phenylalanine chloromethylketone (TPCK) and non-selective inhibition of histidine with diethyl pyrocarbonate (DEPC) resulted in complete loss of vinorine synthase activity, implying that these residues could be involved in catalysis.[17]

Figure 3-2. Multiple Sequence Alignment of DBAT, vinorine synthase (VS), and anthocyanin malonyltransferase (AMT).

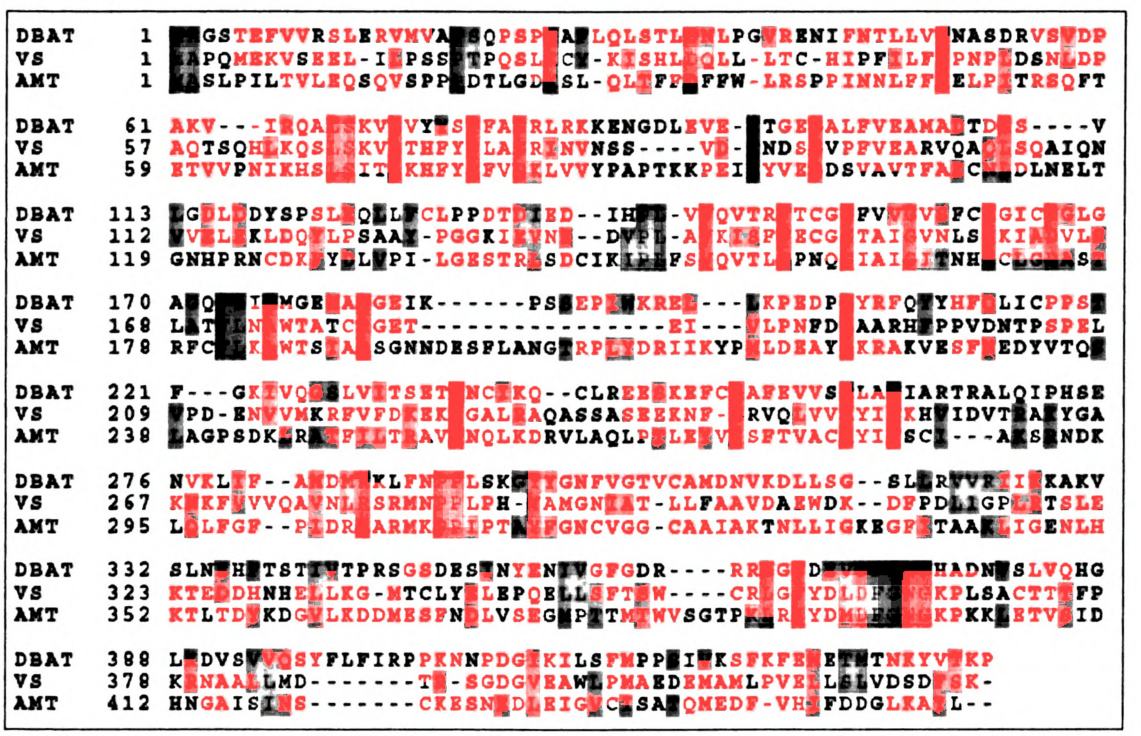

The foregoing mutational analysis suggests that vinorine synthase catalysis is independent of several nucleophilic residues (Cys, Ser, His, Asp) that could presumably

be involved in mediating or activating activity acyl group transfer. However, the proposed mechanism for the BAHD enzymes involves direct transfer of an acyl group from the acyl donor to the hydroxyl group of the acceptor substrate without the formation of a covalent acyl-enzyme intermediate.[2] This mechanism is derived in part from precedent literature for similar acyl group transfer reactions catalyzed by the CAT acyltransferase family.[14] Unfortunately, structural and mutational studies of vinorine synthase and the AATs offer little direct evidence to suggest that the acyl transfer reaction proceeds as proposed. The crystal structure of vinorine synthase apo-enzyme, on which its mechanism is based, does not provide information on the interactions between the enzyme and the bound ligand.[2] Therefore, evidence for the mode of the reaction progress remains largely speculative.

Enzyme-mediated transacylations involving *covalent acyl-enzyme intermediates* have been described in the literature.[18,19] As an example, the catalytic mechanism of glutaconate CoA-transferase (GCT) has been elucidated wherein a glutamate residue initiates nucleophilic attack on the carbonyl carbon of the acetyl CoA co-substrate.[20] The resulting acyl-enzyme intermediate is then cleaved by CoASH that attacks the glutamate carbonyl to form an enzyme-CoA thioester (**Scheme 3-3**). Reduction of the thioester by sodium [^{3}H]borohydride to the corresponding alcohol lead to identification of Glu-54 as the catalytic amino acid residue.[21] This mechanism was further elucidated by chemical hydrolysis of the enzyme-CoA thioester intermediate using [^{18}O]-acetate and tracking the ^{18}O exchange in the CoA donor, glutaryl-CoA, the acceptor substrate, and the catalytic glutamate[20] residue (**Scheme 3-3**).

Scheme 3-3. Proposed mechanism for glutaconate CoA transferase. Incorporation of [^{18}O] into glutaconate CoA transferase: ^{18}O (shown in bold) exchange between CoA, acetate (compound III-18), and the catalytic glutamate residue (^{18}O-III-20).

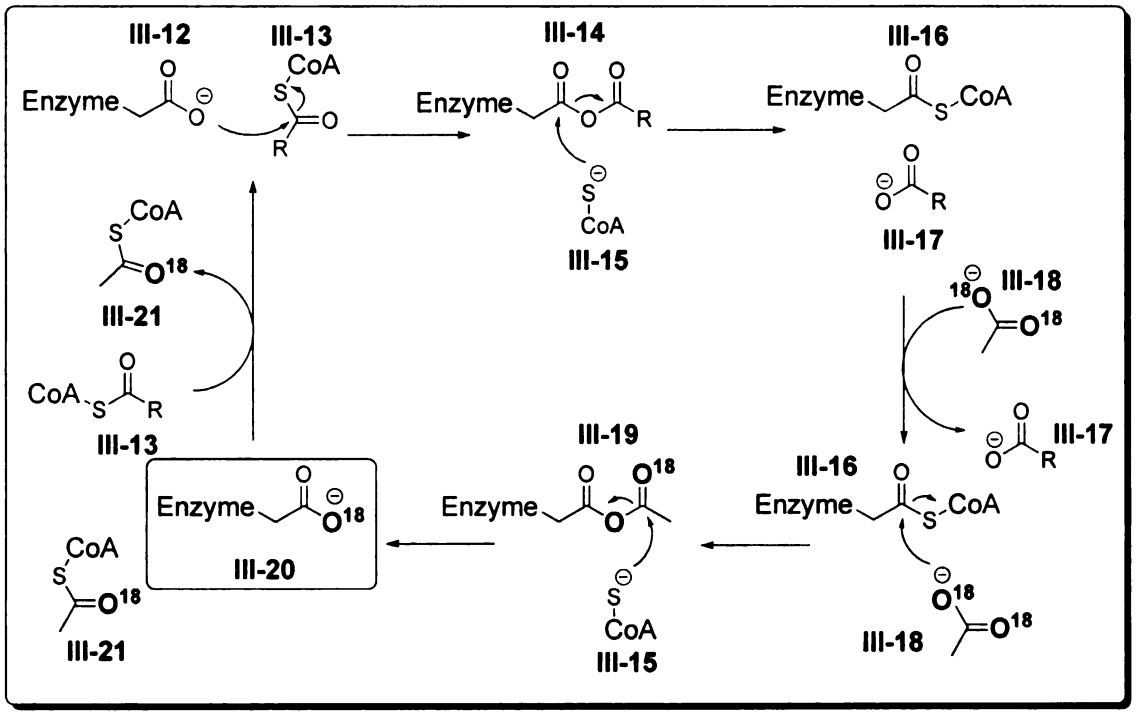

This mechanism for the GCT enzyme provides a basis for the evaluation of the catalytic mechanism proposed for the BAHD acyltransferases. Moreover, the x-ray crystallographic data for the vinorine synthase apo-enzyme do not provide sufficient evidence to support the proposed catalytic mechanism for the BAHD superfamily of enzymes. Therefore, an alternative mechanism is proposed in this study wherein DBAT catalyzes transfer of an acetyl group from CoA thioester to a nucleophilic residue in the enzyme-active site to form an *acyl-enzyme intermediate* (**Scheme 3-4**).

Scheme 3-4. Proposed mechanism for DBAT involving an acyl-enzyme intermediate.

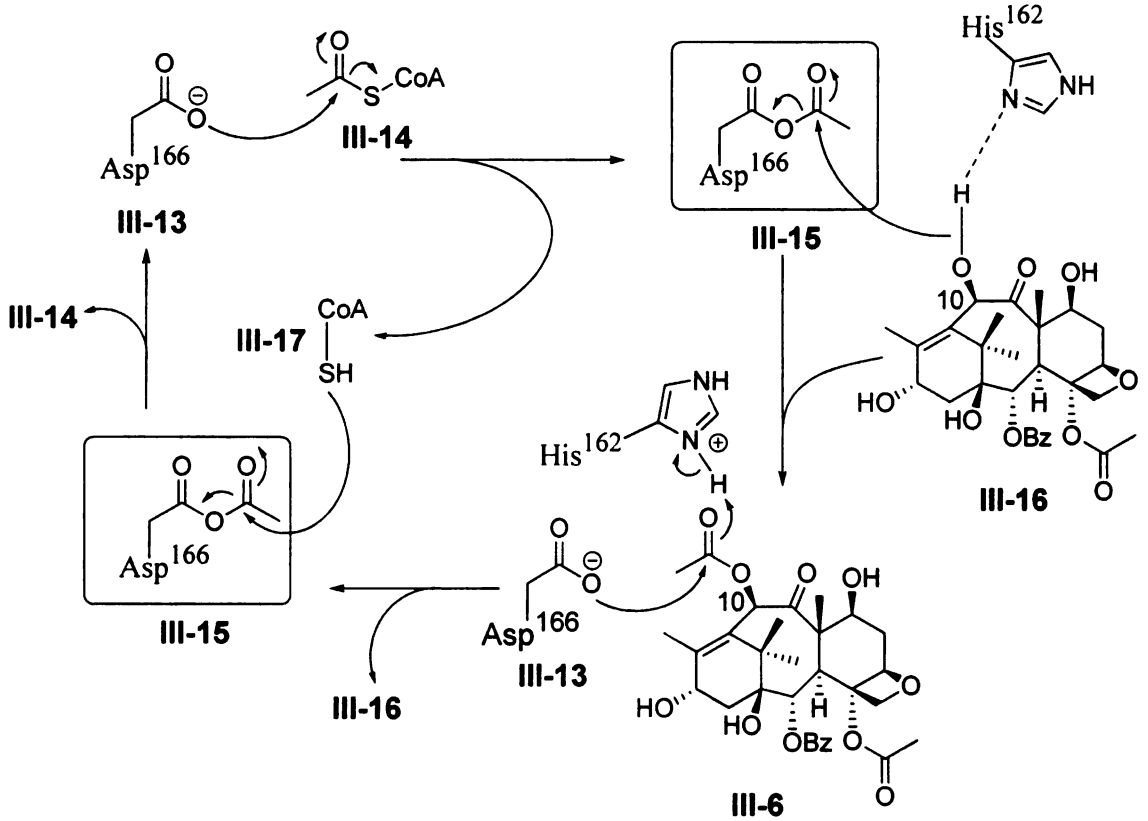

3.2.3 Using BMS-275183 as a Model Compound for Novel DBAT Catalysis

Due to their favorable physicochemical properties and low cost, alkyl carbonates have found a wide array of applications in organic synthesis and medicinal chemistry.[22,23] Alkyl carbonates have been used as synthons and protecting groups in synthetic organic chemistry and in medicinal applications as hydrolysable linkers in prodrugs or in biodegradable drug delivery systems.[22,23]

In medicinal applications, for example, development of an empirically-derived oral anti-cancer taxol derivative BMS-275183 involves attaching a methoxycarbonyl group to the C-4 position of a silyl-protected baccatin III analog.[24] This taxol derivative is 40-times more water soluble and has 50-fold higher drug plasma levels than the parent

drug in mouse models.[25] The synthesis of BMS-275183 involves *N*-acylation of a silyl-protected chiral azetidinone with $(Boc)_2O$, base-promoted coupling of the resultant *N*-Boc protected moiety to a silyl-protected C-4 carbonate taxane intermediate derived from acyl manipulation of silyl-protected 10-DAB, and finally the removal of the silyl protecting groups[24,25] (**Scheme 3-5**).

Scheme 3-5. Semi-synthesis of a second generation taxol analog BMS-275183 (**III-29**).[25,26]

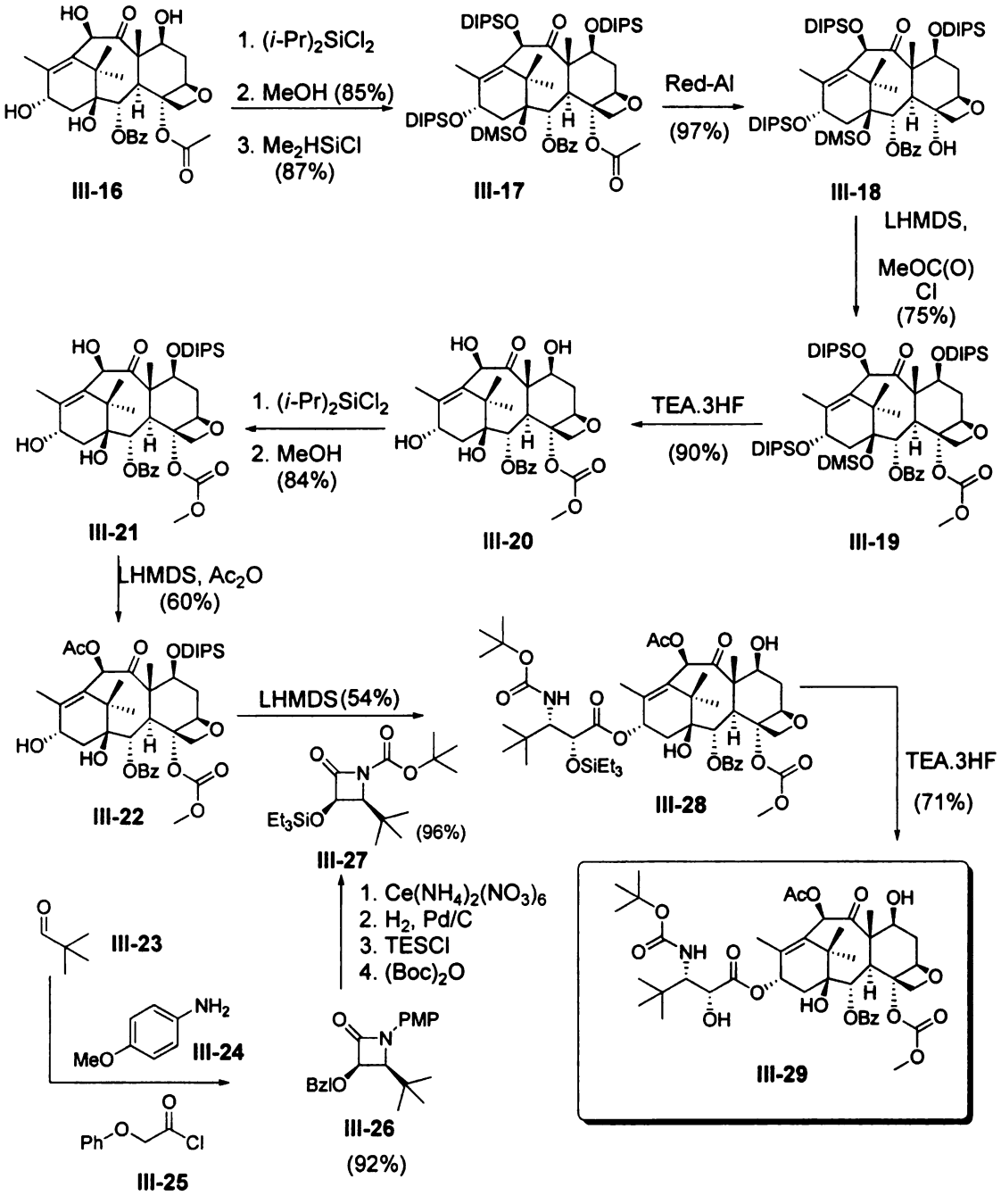

In total, there are ten protection-deprotection cycles in this scheme some of which are repetitive but necessary to direct the chemoselectivity of the reaction. Even though this synthetic achievement demonstrates the power of protecting group manipulations during synthesis of complex molecules, the final yields of elaborate synthetic schemes

such as this suffer from the technical redundancy of the iterative protection-deprotection cycles. The present investigation seeks to address this implicit drawback through the development of an enzymatic process to incorporate various kinds of acyl groups into advanced taxane substrates.

While published literature is replete with a vast array of synthetic utility of alkyl carbonates, there is only a dearth of examples reported in the literature describing enzyme catalyzed transfer of alkyl carbonates to acceptor molecules.[27-29] To my knowledge, there are no reports of naturally occurring carbonoyl transferases involved in plant secondary metabolism. Therefore, the intended use of DBAT as a methoxycarbonyltransferase is empirical due to lack of precedence in natural product biosynthesis. However, this study is important because it could provide clues as to why this functional group is rare in nature's vast inventory of acyl functionalities.

Methoxycarbonyl transesterification of a nucleoside moiety via lipase-catalyzed alkoxycarbonylation in good chemical yields has been reported previously[29] (**Scheme 3-6**).

Scheme 3-6. Lipase-catalyzed alkoxycarbonylation of a nucleoside moiety.[29]

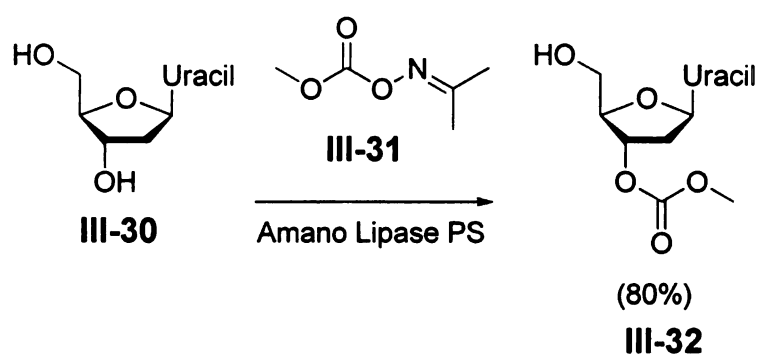

Although this is an isolated example of a promiscuous enzyme activity rather than a truly natural phenomenon, it nonetheless provides the basis to assess whether DBAT

can be developed into a robust catalyst for transfer of non-natural acyl groups. The following sections will highlight studies conducted as part of my dissertation research to understand the catalytic properties of DBAT and evaluate its potential as a methoxycarbonyltransferase.

3.3 Experimental

3.3.1 General

A Varian Inova-300, a Varian UnityPlus500, or a Varian Inova-600 instrument was used to acquire nuclear magnetic resonance (NMR) spectra; chemical shifts are reported in δ units (ppm) using the residual ^{1}H- and ^{13}C-signals of deuterated chloroform or acetone as reference. A Q-ToF Ultima API electrospray ionization tandem mass spectrometer (Waters, Milford, MA) was used for mass spectral analysis. An Agilent 1100 HPLC system (Agilent Technologies, Wilmington, DE) was employed for chromatographic separations and analyses, and was connected in series with a UV detector and, for radioactive analyses, to a Packard Radiomatic Flow-One Beta 150TR radioactivity detector (PerkinElmer, Shelton, CT), which mixed the effluent with 3a70B Complete Counting Cocktail (Research Products International, Mount Prospect, IL). Reaction products were purified by flash chromatography or by preparative thin-layer chromatography (PTLC), and were visualized by UV absorbance at 254 nm. The purity of the synthetic compounds was determined by HPLC and/or ^{1}H-NMR. Baccatin III, and 10-DAB were purchased from Natland Corporation (Research Triangle Park, NC), unlabeled and tritium-labeled acetyl coenzyme A thioesters were obtained from Sigma-

Aldrich, as were all other reagents, which were used without purification unless otherwise indicated. Taxotere was acquired from OChem Inc. (Des Plaines, IL).

The N-terminal polyhistidine-tagged *dbat* cDNA clone was a donation from the Washington State University Research Foundation (Pullman, WA) while the C-terminal *dbat* clone was generated by Danielle Nevarez –McBride in the Walker laboratory. All site-directed mutagenesis studies were done using the QuickChangeII XL kit (Agilent, Santa Clara, CA); DNA sequencing of the mutagenic clones was performed at the Michigan State University Research Technology Support Facility- Genomics Core. Protein expression was from pET28a in *E. coli* BL21(DE3) or BL21 CodonPlus (DE3)-RIPL cell lines.

3.3.2 Synthesis of substrates

Figure 3-3. Synthesis of 10-Methoxycarbonyl-10-deacetylbaccatin III.

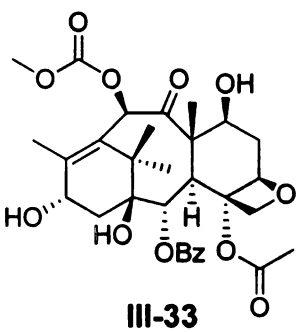

III-33

10-Deacetylbaccatin III (10-DAB) (196 mg, 0.36 mmol) in pyridine (3 mL) was stirred at room temperature for five minutes after which chlorotriethylsilane (170 μL, 1.08 mmol) was added dropwise. The reaction was stirred overnight at room temperature. After which it was quenched with water (5 mL) and diluted with 30 mL of ethyl acetate (EtOAc) and washed with saturated copper sulfate solution (3 × 20 mL). The aqueous phases were extracted twice more with 15 mL EtOAc, the organic fractions were

combined and purified by flash chromatography (50-100% step gradient of EtOAc in hexanes) to obtain 7-triethylsilyl-10-deacetylbaccatin III in 80% yield, >99% purity. ^{1}H-NMR: (300 MHz, $CDCl_3$) δ: 0.51 (m, $Si(C\underline{H_2}CH_3)_3$, 0.59 (t, *J*=9 Hz, $Si(CH_2C\underline{H_3})_3$, 1.01 (s, CH_3-16), 1.21 (s, CH_3-17), 1.65 (s, CH_3-19), 1.82 (m, 6α/β), 1.93 (m, 14α) 2.02 (s, CH_3-19), 2.23 (s, CH_3-18), 2.50 (s, $OC(O)CH_3$ at 4α), 2.57 (m, 14β), 3.90 (d, *J*=6 Hz, 3α), 4.13 (d, *J*=9 Hz, 20α), 4.28 (d, *J*=9 Hz, 20β), 4.38 (dd, *J*=9 Hz, *J*=9 Hz, 7α), 4.80 (bt, 13β), 4.93 (dd, *J*=3 Hz, *J*=3 Hz, 5α), 5.14 (d, *J*=3 Hz, 10α), 5.56 (d, *J*=6 Hz, 2β) 7.43 (m), 7.57 (m), 8.06 (m) [*m*-H , *p*-H, *o*-H of OBz, respectively].

To a solution of 7-triethylsilyl-10-DAB (51 mg, 0.08 mmol) in THF (2 mL) at -61 0°C (chloroform/dry-ice bath) was added a solution of lithium hexamethyldisilazide (LiHMDS) in THF (20 μL, 0.1 mmol) and stirred for 15 min after which methyl chloroformate (13 μL, 0.16 mmol) was added. The reaction was stirred for an additional 3 h while maintaining the reaction temperature at -61 °C. Standard work up and PTLC purification (30 % EtOAc in hexanes) yielded 7-triethylsilyl-10-methoxycarbonyl-10-DAB (20 mg, 35% yield) and was judged to be 99% pure. ^{1}H-NMR: (300 MHz, $CDCl_3$) δ: 0.63 (m, $Si(C\underline{H_2}CH_3)_3$, 0.95 (t, *J*=9 Hz, $Si(CH_2C\underline{H_3})_3$, 1.10 (s, CH_3-16), 1.21 (s, CH_3-17), 1.70 (s, CH_3-19), 1.89 (m, 6α/β), 2.23 (s, CH_3-18), 2.34 (s, $OC(O)CH_3$ at 4α), 2.57 (m, 6β), 3.86 (m, 3α and $OC(O)OCH_3$ at 10β), 4.18 (d, *J*=9 Hz, 20α), 4.34 (d, *J*=9 Hz, 20β), 4.52 (dd, *J*=6 Hz, *J*=6 Hz, 7α), 4.89 (bt, 13β), 5.00 (bd, *J*=9, 5α), 5.67 (d, *J*=6 Hz, 2β), 6.32 (s, 10α), 7.50 (m), 7.64 (m), 8.14 (m) [*m*-H , *p*-H, *o*-H of OBz, respectively].

7-triethylsilyl-10-methoxycarbonyl-10-DAB (20 mg, 0.03 mmol) in pyridine (400 μL) was stirred at 0°C for 5 min after which was added a 70% solution of HF in pyridine (400 μL) dropwise, the reaction was allowed to warm up to room temperature and stirred

overnight. Standard work up procedures, extraction with EtOAc (2 × 5 mL) and washing with saturated copper sulfate, brine and water (5 mL each) followed with PTLC purification (60% EtOAc in hexanes) yielded 10-methoxycarbonyl-10-DAB (**Figure 3-3**) in 90% yield and 95% purity. ^{1}H-NMR: (300 MHz, $CDCl_3$) δ: 1.18 (s, CH_3-16), 1.20 (s, CH_3-17), 1.68 (s, CH_3-19), 1.85 (m, 6α, β), 2.07 (s, CH_3-18), 2.26 (s, $OC(O)CH_3$ at 4α), 2.54 (m, 14α, β), 3.50 (m, 3.86, 3α and $OC(O)OCH_3$ at 10β), 4.14 (d, *J*=9 Hz, 20α), 4.43 (d, *J*=9 Hz, 20β), 4.43 (dd, *J*=9 Hz, *J*=9 Hz, 7α), 4.87 (bt, 13β), 4.98 (dd, *J*=3 Hz, *J*=3 Hz, 5α), 5.61 (d, *J*=7 Hz, 2β), 6.13 (s, 10α), 7.46 (m), 7.59 (m), 8.09 (m) [*m*-H , *p*-H, *o*-H of OBz, respectively].

Figure 3-4. Synthesis of 10-Oxo-7-epi-10-DAB.

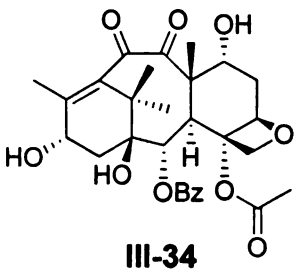

III-34

This procedure was adapted from that used in reported literature.[30] Even though 10-oxo-10-DAB was the target compound, the C-7 epimer was obtained under the reaction conditions outlined, as explained in Chapter 4 section **4.4.5**. To a solution of 10-DAB (200 mg, 0.37 mmol) in methanol (15 mL) in a 100-mL 3-necked flask was added $Cu(OAc)_2 \cdot H_2O$ (500 mg) in small portions with vigorous stirring. The reaction mixture was left to stir for 72 h with the flask unstoppered with occasional addition of methanol to prevent precipitation due to solvent evaporation. After 72 h the reaction was concentrated by evaporating methanol, and the precipitate was dissolved by adding 20 mL of water and 35 mL of EtOAc. The organic layer was washed with ammonium

sulfate, brine and water (2 × 20 mL each), dried under vacuum, and the residue was purified by flash chromatography using a step gradient (30-100% EtOAc in hexanes) to give a 1:1 mixture of 10-oxo-10-DAB and 7-epi-10-oxo-10-DAB (**Figure 3-4**). When left in EtOAc/hexanes solvent mixture this compound converted to a mixture of 10-Oxo-10-DAB and 7-epi-10-oxo-10-DAB (1:4 ratio). ^{1}H-NMR (7-epi-10-oxo-10-DAB) (300 MHz, $CDCl_3$) δ: 1.02 (s, CH_3-16), 1.03 (s, CH_3-17), 1.69 (s, CH_3-19), 1.93 (br. s, CH_3-18), 2.38 (s, $OC(O)CH_3$ at 4α), 2.11 (m, 6α/β), 2.42 (m, 14α/β), 3.82 (dt, *J*=10, 5, *J*=3 Hz, 7β), 4.16 (d, *J*=8 Hz, 3α), 4.29 (d, *J*=8 Hz, 20β), 4.41 (d, *J*=8 Hz, 20α), 4.58 (d, *J*=9 Hz, 7-OH), 4.90 (m, 5α/13β), 5.80 (d, *J*=7 Hz, 2β), 7.49 (m), 7.62 (m), 8.10 (m) [*m*-H , *p*-H, *o*-H of OBz, respectively].

Figure 3-5. Synthesis of 13-Oxo-10-DAB.

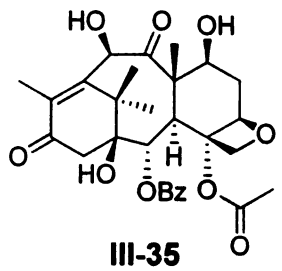

III-35

To a solution of 7-triethylsilyl-10-DAB (90 mg, 0.14 mmol) in dichloromethane (DCM) (1 mL) was added a solution of MnO_2 (120 mg, 1.38 mmol) in DCM (2 mL) dropwise. The reaction was stirred at room temperature overnight after which the residue was filtered through celite, the retentate was washed with DCM (2 × 5 mL) and the solvent evaporated under vacuum. The crude product was purified by flash chromatography (40-60% step gradient of EtOAc in hexanes) to give 84 mg of 7-triethylsily-13-oxo-10-DAB in >95 purity. The subsequent deprotection step was carried out without further purification. ^{1}H-NMR: (300 MHz, $CDCl_3$) δ: 0.52 (m, $Si(C\underline{H}_2CH_3)_3$,

0.90 (t, *J*=9 Hz, $Si(CH_2C\underline{H_3})_3$, 1.11 (s, CH_3-16), 0.18(s, CH_3-17), 1.69 (s, CH_3-19), 1.86 (m, 6β), 2.07 (s, CH_3-18), 2.16 (s, $OC(O)CH_3$ at 4α), 2.46 (ddd, *J*=7 Hz, *J*=3 Hz, *J*=2 Hz, 6α), 2. 61(d, *J*=20 Hz, 14β), 2.90 (d, *J*=20 Hz, 14α), 3.92 (d, *J*=7 Hz, 3α), 4.09 (d, *J*=9 Hz, 20α), 4.31 (m, 20β and 7α), 4.88 (d, *J*=8 Hz, 5α), 5.29 (d, *J*=7 Hz, 10α), 5.00 (bd, *J*=9, 5α), 5.61 (d, *J*=8 Hz, 2β), 7.47 (m), 7.59 (m), 8.03 (m) [*m*-H , *p*-H, *o*-H of OBz, respectively].

7-Triethylsily-13-oxo-10-DAB (50 mg, 0.08 mmol) in pyridine (500 μL) was stirred at 0 °C for five minutes after which a 70% solution v/v of HF-pyridine (500 μL) was added dropwise. The reaction was allowed to warm to room temperature and was to stir at this temperature for 12 h. Standard work up and PTLC purification (60 % EtOAc/hexanes) yielded the desired 13-oxo-10-DAB (30 mg, 99% pure) (**Figure 3-5**). ^{1}H-NMR (300 MHz, acetone) δ: 1.18 (s, CH_3-16), 1.20 (s, CH_3-17), 1.71 (s, CH_3-19), 1.81 (m, 6β), 2.04 (s, CH_3-18), 2.13 (s, $OC(O)CH_3$ at 4α), 2.46 (m, 6α), 2.66 (d, *J*=20 Hz, 14α), 2.95 (d, *J*=20 Hz, 14β), 4.02 (d, *J*=8 Hz, 3α), 4.16(dd, *J*=6 Hz, 20α/β), 4.34 (m, 7α), 4.93 (dd, *J*=2 Hz, *J*=2 Hz, 5α), 5.46 (s, 10α), 5.72 (d, *J*=7 Hz, 2β), 7.54 (m), 7.60 (m), 8.09 (m) [*m*-H , *p*-H, *o*-H of OBz, respectively].

Figure 3-6. Synthesis of 13-Oxobaccatin III.

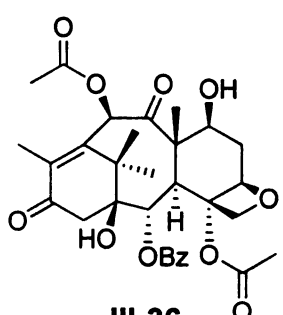

III-36

To a solution of 7-Triethylsilybaccatin III (90 mg, 0.13 mmol) (cf. Materials and Methods in Chapter 2 for preparation) in DCM (2 mL) was added a solution of MnO_2 in DCM (2 mL) dropwise. The reaction was stirred at room temperature overnight; the residue was filtered through celite, the retentate washed with DCM (3 × 5 mL), and the solvent evaporated under vacuum. The crude product was purified by flash chromatography (30-60% step gradient of EtOAc in hexanes) to give 80 mg of 7-Triethylsilyl-13-oxobaccatin III in >95 purity. ^{1}H-NMR: (300 MHz, $CDCl_3$) δ: 0.52 (m, $Si(C\underline{H}_2CH_3)_3$, 0.75 (t, *J*=20, $Si(CH_2C\underline{H}_3)_3$, 1.11 (s, CH_3-16), 1.20 (s, CH_3-17), 1.60 (s, CH_3-19), 1.58 (m, 6β), 2.11 (s, CH_3-18), 2.12 (s, $OC(O)CH_3$ at 4α), 2.16 (s, 2.25 (s, $OC(O)CH_3$ at 10β), 2.49 (m, 6α), 2.56 (d, *J*=18 Hz, 14α), 2.59 (d, *J*=18 Hz, 14β), 3.84 (d, *J*=6 Hz, 3α), 4.04 (d, *J*=6 Hz, 20α), 4.24 (d, *J*=6 Hz, 20β), 4.41 (dd, *J*=6 Hz, *J*=6 Hz, 7α), 4.86 (, *J*=9 Hz, 5α), 5.63 (d, *J*=6 Hz, 2β), 6.52 (s, 10α), 7.41 (m), 7.55 (m), 7.99 (m) [*m*-H , *p*-H, *o*-H of OBz, respectively].

To a solution of 7-Triethylsilyl-13-oxobaccatin III (80 mg, 0.12 mmol) in pyridine (1 mL) at 0 °C was added HF-pyridine (1 mL, 70% v/v). The reaction mixture was stirred at 0°C for 6 h, then quenched with water (5 mL), diluted with EtOAc (20 mL) and washed with saturated copper sulfate, brine, and water (20 mL each). The crude product was purified by silica gel flash chromatography (50-100% EtOAc/hexane gradient) to obtain 13-oxobaccatin III (**Figure 3-6**) in >99% yield and purity. ^{1}H-NMR (300 MHz, $CDCl_3$) δ: 1.16 (s, CH_3-16), 1.22 (s, CH_3-17), 1.64 (s, CH_3-19), 1.83 (m, 6β), 2.05 (s, CH_3-18), 2.15 (s, $OC(O)CH_3$ at 4α), 2.25 (s, $OC(O)CH_3$ at 10β), 2.52 (m, 6α), 2.66 (d, *J*=20 Hz, 14α), 2.95 (d, *J*=20 Hz, 14β),3.88 (d, *J*=6 Hz, 3α), 4.10 (d, *J*=6 Hz, 20α), 4.20 (d, *J*=6 Hz, 20β), 4.42 (dd, *J*=9 Hz, *J*=9 Hz, 7α), 4.91 (dd, *J*=2 Hz, *J*=2 Hz,

5α), 5.65 (d, *J*=4 Hz, 2β), 6.20 (s, 10α), 7.46 (m), 7.60 (m), 8.03 (m) [*m*-H , *p*-H, *o*-H of OBz, respectively].

Figure 3-7. Synthesis of 7,13-Dioxobaccatin III

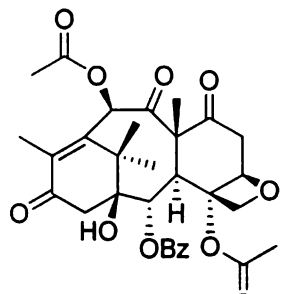

III-37

To a solution of baccatin III (50 mg, 0.09 mmol) in acetone (2 mL) was added a solution of 250 µL of CrO_3 (1 g of CrO_3 in a 3:7 mixture of H_2SO_4 and water) and the reaction was stirred in room temperature for 30 minutes. The reaction mixture was washed with water (5 × 5 mL), dried using Na_2SO4 and the solvent evaporated under vacuum to give 7,13-Dioxobaccatin III (**Figure 3-7**) in quantitative yield and >95 purity. ^{1}H-NMR (300 MHz, $CDCl_3$) δ: 1.17 (s, CH_3-16), 1.20 (s, CH_3-17), 1.95 (s, CH_3-19), 1.97 (s, CH_3-18), (m, 6β), 2.19 (s, $OC(O)CH_3$ at 4α), 2.23 (s, $OC(O)CH_3$ at 10β), 2.86 (m, 6α/β and 14α/β), 4.18 (d, *J*=6 Hz, 20α), 4.46 (m, 3α and 20β), 4.42 (dd, *J*=9 Hz, *J*=9 Hz, 7α), 4.91 (dd, *J*=2 Hz, *J*=2 Hz, 5α), 5.65 (d, *J*=4 Hz, 2β), 6.20 (s, 10α), 7.46 (m), 7.60 (m), 8.03 (m) [*m*-H , *p*-H, *o*-H of OBz, respectively].

Figure 3-8. Synthesis of Methoxycarbonyl Coenzyme A.

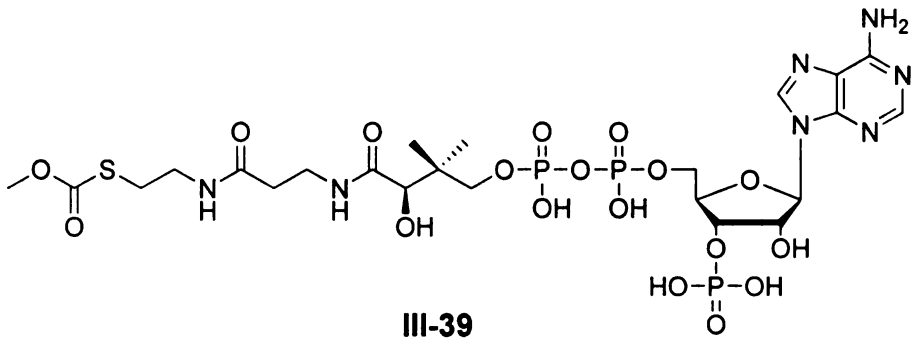

III-39

This procedures was adapted from a procedure used to synthesize benzoyl CoA from a mixed anhydride.[31] To a solution of dimethyldicarbonate (7 μL, 0.065 mmol) in *tert*-butanol (1 mL) was added a solution of coenzyme A (42 mg, 0.05 mmol) in 0.4 M $NaHCO_3$ (1 mL). The reaction mixture was stirred at room temperature for 1 h after which it was quenched with 1 M HCl (400 μL) and adjusted to pH 5 with 15 mM sodium phosphate (pH 5). The solvents were evaporated and the residue was resuspended in 10 mL of water (pH 5.6) and purified using a C-18 Sep-Pak cartridge that had been washed with methanol and pre-equilibrated with water. The product was eluted with 5-mL portions of increasing methanol in water (0-20%) and confirmed by ESI-MS (negative ion mode): m/z = 824.01 $[M-H]^{-1}$, 846.02 $[M-2H+Na]^{-1}$ (**Figure 3-8**).

3.3.3 Biochemical Methods

Bacterial cells (BL21(DE3) or BL21(DE3) CodonPlus® RIPL) were transformed with plasmids harboring the desired cDNA of wild-type *dbat* clones (both C-terminal and N-terminal His-tagged), five C-terminal His-tagged DBAT mutants, and five N-terminal His-tagged DBAT mutants. The *dbat* mutants generated were D167N, D166Q, D166E, D166L and the double mutant H161D; D166H. All *E. coli* transformants were grown overnight at 37 °C in 5 or 100 mL Luria-Bertani (LB) media supplemented with

kanamycin (50 μg/mL). The inoculum was then added to and grown in six 4-L flasks each containing 1 L LB medium with appropriate antibiotic for selection. The cells were grown at 37 °C until an OD_{600} of 0.8- 1.0 after which the cultures were induced with isopropyl-β-D-thiogalactopyranoside (IPTG, 200-500 μM final concentration) and grown at 16-18°C for 12-14 h. Subsequent steps were performed on ice or in a cold room maintained at 4°C, unless otherwise indicated. For each protein, the cultures were separately harvested and centrifuged at 6,000*g* for 15 min, and the pellet was resuspended in the lysis buffer (50 mM sodium phosphate buffer, pH 8) containing 300 mM NaCl. The cells were lysed at 4°C using a Misonix sonicator (Farmingdale, NY) with 6 × 30-s bursts at a volume-dependent power setting of 50-75%; a 2-min interval was allowed between each sonication burst for cooling purposes. The cell-lysates were centrifuged at 10,000*g* for 20 min to remove cell debris and clarified by ultracentrifugation at 100,000*g* for 2 h. For control assays, empty pET28a vector was similarly expressed from *E. coli* BL21(DE3) and the cell-free extract was obtained and assayed under the same condition as described for the cells transformed with wild-type or mutant *dbat* clones.

3.3.4 Protein Purification

Each crude protein in the lysis buffer was loaded directly onto a pre-equilibrated column packed with 2 mL bed volume of Ni-NTA agarose resin. The column was washed with 5 bed volumes using wash buffer (50 mM sodium phosphate at pH 8 containing 300 mM NaCl and 10 mM imidazole). The proteins were eluted with 5 bed volumes (10 mL) of elution buffer consisting of 50 mM sodium phosphate buffer supplemented with 300 mM NaCl and 250 mM imidazole. Alternatively, proteins were washed with 50 mM sodium phosphate buffer supplemented with 300 mM NaCl and 50

mM imidazole followed by elution with 250 mM (10 mL fractions in all cases). The fractions were concentrated using Amicon membrane filters (30,000 MWCO) to a volume between 1-3 mL and analyzed by SDS-PAGE with Coomassie staining. Fractions containing the desired protein (~52 kDa by SDS-PAGE) were pooled, buffer-exchanged and either used for enzyme assays or subjected to further purification procedures. The purity obtained from Ni-NTA purification ranged between 40-60% by SDS-PAGE analysis.

To further improve the purity of the proteins, the pooled eluents were buffer-exchanged with buffer A (50 mM Tris-HCl containing 5% v/v glycerol at pH 8) and subjected to Fast Protein Liquid Chromatography (FPLC) using 40 mL of Q-Sepharose Fast Flow resin (Amersham). The protein was loaded on to a column and eluted with 70 mL of buffer A at 5 mL/min followed by a 40-100% gradient of buffer B (50 mM Tris-HCl containing 5% v/v glycerol and 1 M NaCl at pH 8) for 33 min with UV monitoring (600 nm) of the eluents (5 mL each). The fractions were analyzed by SDS-PAGE and fractions containing protein of molecular weight corresponding to DBAT were pooled and buffer-exchange achieved using membrane filters (30,000 MWCO).

3.3.5 Activity Assays

Protein extracts from either one of the described purification protocols were buffer-exchanged with assay buffer (either 100 mM MOPSO buffer at pH 7.2 supplemented with 5% glycerol v/v with or without 3 mM DTT, or 50 mM sodium phosphate at pH 7.2 supplemented with 5% glycerol v/v).

To verify functional protein expression, baccatin III (200 μM in methanol) and CoASH (200 μM in water) were incubated with either wild-type DBAT (N- or C-

terminal His-tagged) or DBAT mutants (C-terminal His-tagged) (all at ~25-50 $\mu g \cdot mL^{-1}$) at 31°C for 3 h. Enzyme activity was determined by assessing the formation of 10-DAB in the reverse reaction catalyzed by DBAT. The reactions were stopped by adding EtOAc (4 mL), the organic phase was extracted and the dried organic extracts were dissolved in 200 μL of acetonitrile. Aliquots (10-20 μL) were analyzed by reverse-phase HPLC by UV monitoring at 228 nm at a flow rate of 1 mL/min. The products were eluted using a linear acetonitrile-water gradient starting at 30% acetonitrile with a 5 min hold and a step gradient for 10 minutes and back to initial condition with a 2 min hold. To determine whether the mutants were active in the forward reaction, a similar assay was performed except that acetyl CoA (200 μM) was used in place of CoASH.

3.3.6 Kinetic Parameters of the DBAT-Catalyzed Reverse Reaction

A time-course analysis was performed for the reverse reaction by incubating DBAT (~5 μg/mL), CoASH, and baccatin III (each at 400 μM) in 4 mL assay tubes at 31 °C. Aliquots (500 μL each) were taken after 5, 10, 20, 30 and 60 min and then hourly thereafter for a further 3 h. The product was extracted into EtOAc (3 mL), dried, and analyzed by HPLC. Having established the reaction time, the assays were performed with ~5 μg of DBAT and the concentration of baccatin was varied from 5 μM to 1 mM while keeping the CoASH concentration at apparent saturation (500 μM). The reactions were stopped after 20 min by quenching with EtOAc (3 mL); the product was extracted, dried, and analyzed by HPLC as discussed.

3.3.7 Equilibrium of the DBAT-Catalyzed Reverse Reaction

The chemical equilibrium of DBAT-mediated deacetylation of the C-10 acetylated baccatin III was established by incubating DBAT (~50 μg/mL), CoASH, and baccatin III (all at 500 μM in 6 mL) in duplicate assays at 31 °C. 500 μL-aliquots were taken at time intervals between 5 min and 48 h after incubation. Each aliquot was extracted with 4 mL EtOAc, the solvent was evaporated under vacuum and the product was dissolved in acetonitrile (200 μL) and analyzed by reverse-phase HPLC using a linear acetonitrile-water gradient as described previously (section **3.3.7**). Equilibrium concentrations were determined by first normalizing peak integrals to an internal reference standard (taxotere) and then converting the integral values to concentration using standard curves for baccatin III and 10-DAB.

3.3.8 Methoxycarbonyl CoA Assays with DBAT

Wild-type DBAT (~100 μg/mL) was incubated with methoxycarbonyl CoA and baccatin (both at 500 μM) for 5 h at 31 °C. Control experiments either lacking methoxycarbonyl CoA or DBAT in the assay were performed in parallel. To confirm that the expressed DBAT was functional, the enzyme (~10 μg/mL) was incubated with baccatin III and CoASH (200 μM each). Each assay was quenched with 4 mL EtOAc, the organic layer was extracted and evaporated under vacuum. The product was dissolved in 200 μL acetonitrile from which 10 μL was analyzed by HPLC using the protocol outlined in section **3.3.6**.

Similarly, the reverse reaction of DBAT catalysis was evaluated by incubating 10-methoxycarbonyl-10-DAB and CoASH (each at 200 μM) with DBAT (~100 μg/mL) for

5 hr at 31 °C. Control experiments were performed using denatured DBAT (boiled in a microwave) or omitting CoASH, DBAT, or both from the reaction assay.

3.3.9 Intermolecular Acetate Exchange using Wild-type DBAT

To assess the possibility of intermolecular DBAT-mediated acyl exchange between two taxane substrates, the proficiency of DBAT to catalyze the deacetylation reaction was employed. Baccatin III, taxotere, and CoASH (200 μM each) were incubated as a mixture with wild-type DBAT (~50 μg/mL) for 12 h at 31 °C and the product was analyzed by reverse-phase HPLC and ESI-MS. For control experiments, DBAT was incubated with CoASH and taxotere, but without baccatin III; taxotere, CoASH, and baccatin III were incubated together without DBAT; or taxotere and baccatin III were incubated together in the absence of DBAT and CoASH.

To determine whether the DBAT-catalyzed acetyl exchange was CoASH-dependent, an analogous set of experiments was performed without CoASH. The control experiments were quenched and extracted with EtOAc (4 mL), the organic fractions were dried under vacuum, and the product from each assay tube was dissolved in 200 μL acetonitrile and analyzed by LC-ESI-MS using a linear gradient of 70% water (with 0.5% v/v formic acid) and acetonitrile for 10 min at 0.25 $mL \cdot min^{-1}$ with concurrent monitoring of the effluent by ESI-MS in positive ion mode. To confirm the identity of the product from this set of assays, wild-type DBAT (~50 μg) was incubated in a 1 mL assay with taxotere and acetyl CoA (each at 200 μM). Concurrent control experiments included an assay containing all of the co-substrates and protein isolated from bacteria expressing empty pET28 vector (i.e., lacking the *dbat* gene). Other control experiments contained the requisite co-substrates but excluded either DBAT, acetyl CoA, or both.

3.3.10 Assessing the Formation of an Acyl-DBAT Complex

To further evaluate the mechanism of acetyl transfer catalyzed by DBAT, the formation of a proposed acyl-enzyme intermediate was assessed by determining the V_{max} of different productive acyl donors. A kinetic analysis of each baccatin III, 13-oxobaccatin III, 10-DAB, and 4-DAB substrate was separately performed with DBAT. Linearity with respect to product formation and time was established by incubating DBAT (~5 μg/mL) and CoASH (400 μM) (or acetyl-CoA in the case of 10-DAB and 4-DAB) separately with each taxane substrate (all at 400 μM) in 4 mL assay tubes at 31 °C. Aliquots (500 μL) were taken at 5, 10, 20, 30 and 60 min and then hourly thereafter for an additional 3 h. After establishing the assay duration for steady-state parameters, the concentration of each taxane substrate was independently varied from 10 μM to 1 mM while keeping the CoASH (or acetyl CoA) concentration at apparent saturation (500 μM, ~10-fold K_m). The reactions were quenched with EtOAc (3 mL), the organic fractions were extracted, and the solvent was removed under vacuum. The remaining residue was dissolved in 200 μL of acetonitrile and a 10-μL aliquot was analyzed by HPLC as described previously (section **3.3.6**). The kinetic data was calculated from the Lineweaver-Burk double reciprocal plots ($1/v_0$ vs 1/[taxane]).

3.3.11 Site-Directed Mutagenesis

The DNA template used to generate both the C- and N-terminally His-tagged *dbat* mutant clones was purified from *E. coli* BL21(DE3) cells using the QIAprep Spin Miniprep Kit (Qiagen). The concentration was determined by UV absorbance and DNA extinction coefficient at 260 nm using a Unicam Helios Gamma spectrophotometer (Thermo Scientific, Waltham, MA). Mutants were generated by mismatch oligonucleotide priming. The following DNA oligonucleotide primer set, comprising a forward primer and its reverse-compliment, generated the desired D166N *dbat* mutant (with N-terminal histidine tag) by PCR. The modified nucleotides are underlined.

D166N_Forward Primer:

5'-G GTG AGT TTC TGC CAT GGT ATA TGT AAC GGA CTA GGA GCA G-3'

D166N_Reverse Primer:

5'-C TGC TCC TAG TCC GTT ACA TAT ACC ATG GCA GAA ACT CAC C-3'

Primers for all the other mutants (D166Q, D166E, D166L, and [H162D; D166H]) follow; the mutation in each is indicated by underlined nucleotides.

D166Q_ Forward Primer:

5'- G GTG AGT TTC TGC CAT GGT ATA TGT CAG GGA CTA GGA GCA G- 3'

D166Q_ Reverse Primer:

5'- TGC TCC TAG TCC CTG ACA TAT ACC ATG GCA GAA ACT CAC C- 3'

D166E_ Forward Primer:

5'- G GTG AGT TTC TGC CAT GGT ATA TGT GAG GGA CTA GGA GCA G- 3'

D166E_ Reverse Primer:

5'- C TGC TCC TAG TCC CTC ACA TAT ACC ATG GCA GAA ACT CAC C- 3'

D166L_ Forward Primer:

5'- G GG GTG AGT TTC TGC CAT GGT ATA TGT TTG GGA CTA GGA GCA GG- 3'

D166L_ Reverse Primer:

5'- CC TGC TCC TAG TCC CAA ACA TAT ACC ATG GCA GAA ACT CAC CCC- 3'

H162D; D162H_ Forward Primer:

5'- G GTG AGT TTC TGC GAT GGT ATA TGT CAT GGA CTA GGA GCA G- 3'

H162D; D166H_ Reverse Primer:

5'- C TGC TCC TAG TCC ATG ACA TAT ACC ATC GCA GAA ACT CAC C- 3'

Each PCR reaction comprised of the *dbat* DNA template (~10 ng), the corresponding oligonucleotide primer set for each mutant (~160-180 ng, 30-35 pmol), QuickSolution, dNTP mix, and *PfuUltra* high-fidelity DNA polymerase. The total reaction volume was adjusted to 50 μL with double-distilled water, and the reaction was run using standard PCR procedure (18 cycles of 1 min at 95 °C, 50 s at 60 °C and 7 min at 68 °C). Parental *dbat* DNA was digested by incubating the PCR mixture with *Dpn* I restriction endonuclease for 1 h at 37 °C. An aliquot (2 μL) of the digested PCR mixture was used to transform either the XL10-Gold competent cells supplied with the kit or DH5α competent cells following standard heat-pulse treatment at 42 °C. The mixture was inoculated with 900 μL of NZCYM broth (Sigma Aldrich) at 37 °C for 1 h and the bacterial culture was transferred to LB agar plates that had been supplemented with kanamycin (~50 μg/mL). After overnight (~16 h) incubation at 37 °C, colonies were selected, and the plasmids were isolated by standard procedures using a QIAprep spin miniprep kit. The desired mutations were confirmed by DNA sequencing; the sequence-verified plasmids were used to transform *E. coli* BL21(DE3) cells for expression of mutant proteins.

3.4 Results and Discussion

3.4.1 Reversibility of the DBAT-Catalyzed Acetylation

During the initial screening of DBAT for C-4 activity, 4-DAB and [3H]acetyl CoA were incubated with DBAT, and the product was verified to be [^{3}H]baccatin III,[32] as shown in Chapter 2 section **2.4.3**). However, radioactive HPLC analysis of the product at various time points revealed that the relative amount of the expected [^{3}H]-baccatin III product progressively reduced by 40% with extended incubation of the assay mixture. Analysis of the radio-HPLC data also indicated the emergence of a *de novo* peak with the same retention time as the unlabeled 4-DAB substrate. Notably, the relative amount of this new product peak increased by 80% over the time period when the amount of the [^{3}H]baccatin III product decreased.

The new [^{3}H]-labeled compound was confirmed to be [^{3}H]-4-DAB by HPLC retention time and ESI-MS of non-radiolabeled baccatin III. Thus, the amount of the biosynthesized product progressively diminished due to DBAT-mediated C-10 deacetylation of the *de novo* [^{3}H]baccatin III to 10-DAB in the reverse reaction. Similarly, deacetylation of the 4-DAB substrate by DBAT likely results in the formation of 4,10-dideacetylbaccatin III, which is subsequently acetylated by DBAT using [^{3}H]acetyl CoA in the assay mixture to form [^{3}H]-4-DAB in the forward reaction of DBAT catalysis. This new [^{3}H]-labeled compound emerges as a *de novo* peak in the radio-HPLC with coincident retention time as the starting material 4-DAB.

Thus, the inverse relationship in the amount of the biosynthesized [^{3}H]baccatin III product and the [^{3}H]-4-DAB substrate can be rationalized by considering that as [^{3}H]acetyl CoA is used up by DBAT in the forward reaction, the pool of free CoASH

accumulates in the assay mixture. Free CoASH then serves as the substrate for the reverse reaction of DBAT catalysis, resulting in deacetylation of both [^{3}H]baccatin III and 4-DAB. The deacetylated compounds are acylated again by DBAT using the remaining [3H]acetyl CoA in the assay mixture and increases the amount of [^{3}H]-4-DAB and [^{3}H]baccatin III (**Scheme 3.7**). At any one given time in the course of the reaction, the concentration of 4-DAB is disproportionately higher than the concentration of the biosynthesized [^{3}H]-baccatin III. Therefore, deacetylation of 4-DAB and subsequent re-acetylation by DBAT progressively produce more [^{3}H]-4-DAB than [^{3}H]baccatin III.

Notably, due to the rapid rate of DBAT catalysis in both the forward and reverse directions (see section **3.4.2** below), [^{3}H]acetate is eventually incorporated at C-4 and C-10 of the 4-DAB substrate. Consequently, the specific activity of the biosynthetic [^{3}H]-baccatin III product is enhanced (compound **III-6b** in **Scheme 3-7**), since two [^{3}H]acetyl functional groups can incorporate onto the baccatin III scaffold. Without this signal enhancement, the detection of the biosynthetic [^{3}H]-baccatin III product would have been challenging despite of the sensitivity of the radio-HPLC detection method.

Scheme 3-7. Product distribution through deacylation-reacylation cycles catalyzed by DBAT. Compounds **III-6a** and **III-16b** are tritium-labeled at C-4; compound **III-16a** is tritium-labeled at C-10, while compound **III-6b** is tritium-labeled at both the C-4 and C-10 positions. Tritium labeled acetyl group is shown in red.

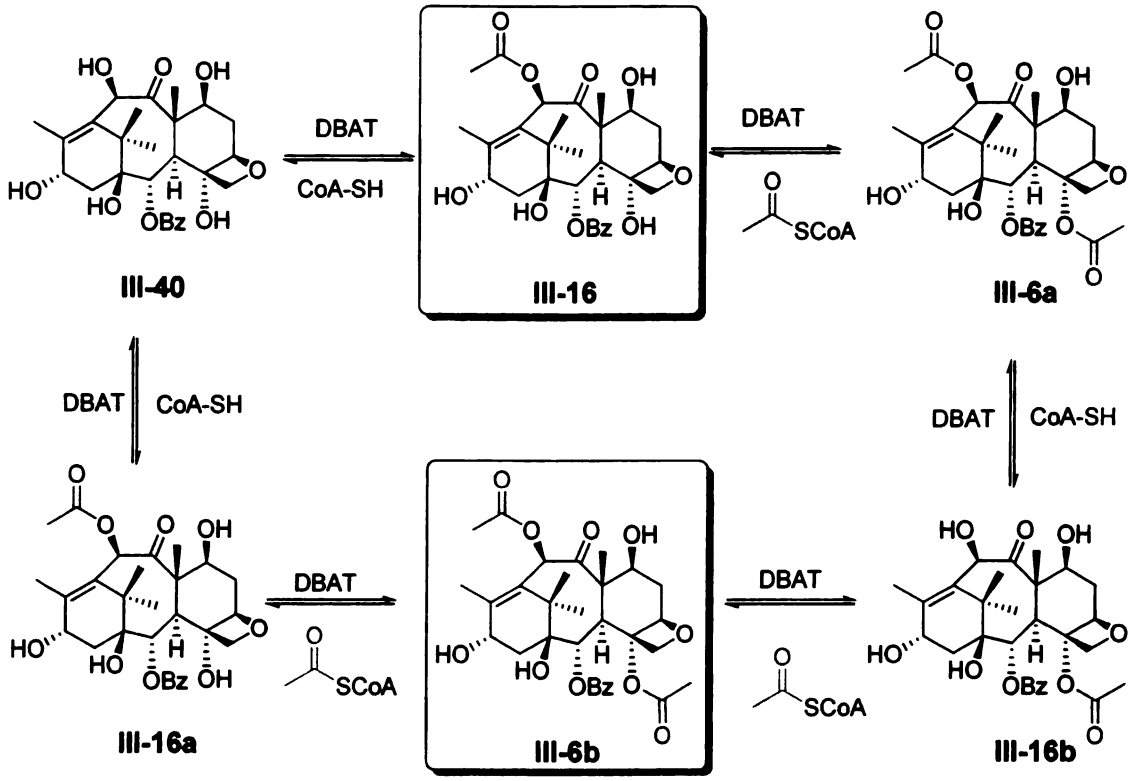

The rapid substrate-product equilibration shown in **Scheme 3-7** when the DBAT reaction is no longer operating at steady-state parameters may at first seem like a technical drawback, where product yields are limited by the equilibrium distribution between substrate and product. However, this concept presented a fortuitous opportunity to probe DBAT catalysis in greater detail.

To understand the differences in the rates of the reverse reaction and the forward reaction, baccatin III and CoASH were incubated with DBAT and the steady-state velocities for the formation of 10-DAB were obtained. From these assays, a k_{cat} of 0.83 ± 0.04 s^{-1} was calculated for the reverse reaction compared to a k_{cat} of 0.58 ± 0.06 s^{-1}

previously determined for DBAT with 10-DAB in the forward direction[32] (cf. Chapter 2, section **2.5.3**). This indicates that DBAT is slightly faster in the reverse reaction compared to the forward reaction. However, the K_m of DBAT for baccatin III in the reverse reaction (86.2 ± 4 μM) is higher than the K_m of DBAT with 10-DAB in the forward reaction (57.6 ± 2 μM).[32] Consequently, the forward reaction catalyzed by DBAT has a slightly better specificity constant (k_{cat}/K_m) of 1.0 x 10^4 $s^{-1} \cdot M^{-1}$ compared to 7.3 x 10^3 $s^{-1} \cdot M^{-1}$ for the reverse reaction, discussed in section **3.4.5**.

To determine the product distribution when a chemical equilibrium is established between baccatin III and 10-DAB in the reverse reaction, baccatin III, CoASH, and DBAT were incubated at 31°C in MOPSO buffer at pH 7.2. Using the Haldane-Briggs equation, an equilibrium constant (K_{eq}) of 1.17 was obtained for the reverse reaction (**Figure 3-9**). This reflects a small change in standard Gibbs free energy of ~ -0.093 kcal/mol ($\Delta G° = -RT\ln K_{eq}$), indicating that both the forward and the reverse reactions catalyzed by DBAT-catalyzed are equally preferred.

Figure 3-9. Determination of the equilibrium constant of the deacetylation of baccatin III (▪) to 10-DAB (•) catalyzed by DBAT at 31 °C and pH 7.2.

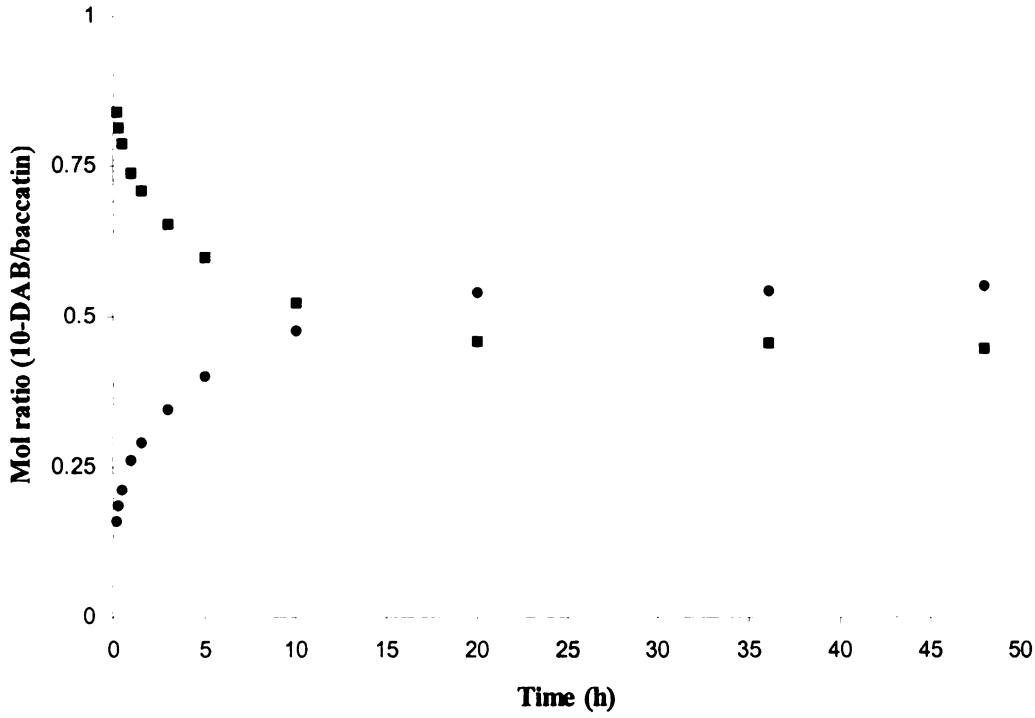

3.4.2 Assessing the Role of the Putative Hydrogen Bond in Baccatin III

As noted in section **3.2.1**, 7-*O*-acetyl analogs of 4-DAB did not yield detectable new products after incubation with DBAT and acetyl CoA. Therefore, the effects of the stereochemistry of the C-7α hydroxyl group and the putative C-13/C-4 hydrogen bond on DBAT catalysis were evaluated. Thus, the C-7, C-10, C-13 hydroxyl groups were sequentially oxidized to give 7,13-dioxobaccatin III, 13-oxobaccatin III, 13-oxo-10DAB, and 10-oxo-10-DAB (which epimerized to 10-oxo-7-epi-10-DAB as discussed in Chapter 4 section **4.4.5**). With 10-oxo-10-DAB substrate, the aim was to eliminate the C-10 hydroxyl group in order to determine whether DBAT could exclusively acylate or deacylate the C-4 position of the surrogate substrate in the absence of the C-10 hydroxyl. The 13-oxo taxane substrates were prepared primarily to disrupt the hydrogen bond

between the C-4 acetate and the C-13 alcohol in order to evaluate its effect on DBAT catalysis.

The four substrates were incubated with DBAT and CoASH for the reverse reaction; only 13-oxobaccatin III was found to be productive. The K_m of DBAT for 13-oxobaccatin III in the C-10-deacetylation reaction was found to be 185.3 ± 2 μM, while the k_{cat} value was calculated to be 0.89 ± 0.03 s^{-1} compared to the K_m and k_{cat} values of 82.8 μM and 0.83 ± 0.01 s^{-1}, respectively, of DBAT incubated separately with baccatin III and CoASH. While the K_m of DBAT for 13-oxobaccatin III nearly doubles upon disruption of the purported C-4/C-13 hydrogen in baccatin III, the turnover number remains largely unchanged. This seems to suggest that a C-13 hydroxyl is necessary for effective anchoring of the substrate to the active site and has little or no effect on the rate of DBAT catalysis.

The 7,13-dioxobaccatin III substrate had very poor solubility in the aqueous media used in these enzyme assays. Increasing portions of methanol, acetonitrile, or DMSO were used to increase the solubility of the substrate in aqueous buffer to no avail, and no detectable products were observed. This bottleneck prevented an evaluation of whether the C-7α and C-13β hydroxyl groups have an additive effect on DBAT catalysis. Consequently, this study was considered inconclusive and requires further studies before firm conclusions can be drawn.

3.4.3 Methoxycarbonyl CoA Carbonate Studies

After demonstrating that DBAT has promiscuous regioselectivity and can acetylate the C-4α hydroxyl group of 4-DAB as well as the C-10β hydroxyl group of 10-DAB (Chapter 2), studies to develop a regiospecific biocatalytic scheme for transfer of a methoxycarbonyl functional group to 4-DAB were evaluated. In the previous study, < 1% of biosynthetic baccatin III was obtained from incubation of 4-DAB and acetyl CoA with DBAT. Moreover, this assay required [^{3}H]-labeled acetyl CoA to enhance the signal for detection of the product by radio-HPLC, as discussed in Chapter 2 section **2.4.1**. Therefore, initial studies to evaluate the non-natural methoxycarbonyl as a productive substrate of DBAT employed the natural substrate 10-DAB as the acceptor substrate instead of the surrogate substrate 4-DAB, since DBAT transfers an acetyl group to the C-10 hydroxyl ~600-fold faster than it does to the C-4 hydroxyl of 4-DAB.

Since DBAT is an acyl CoA-dependent enzyme, methoxycarbonyl CoA was considered a good source of methoxycarbonyl group. This thioester was synthesized by reacting methyl chloroformate (or dimetheyl dicarbonate, DMDC) with a lithium salt of CoASH. Although TLC monitoring of the reaction progress indicated complete conversion of the starting material to product in ~45 min, purification of the product using reverse-phase column chromatography greatly affected the recovery of the methoxycarbonyl CoA thioester (<1% recovery). ESI-MS analysis of the fractions off the reverse-phase column showed that a molecular ion of correct mass was consistent with methoxycarbonyl CoA (**Figure 3-10**). This indicates that the methoxycarbonyl CoA thioester was formed but may have degraded in the aqueous solution during purification.

Methyl carbonates are reportedly susceptible to hydrolysis by water, breaking down to methanol and carbonic acid or CO_2.[33,34]

Figure 3-10. ESI-MS (negative ion mode) spectrum of methoxycarbonyl CoA.

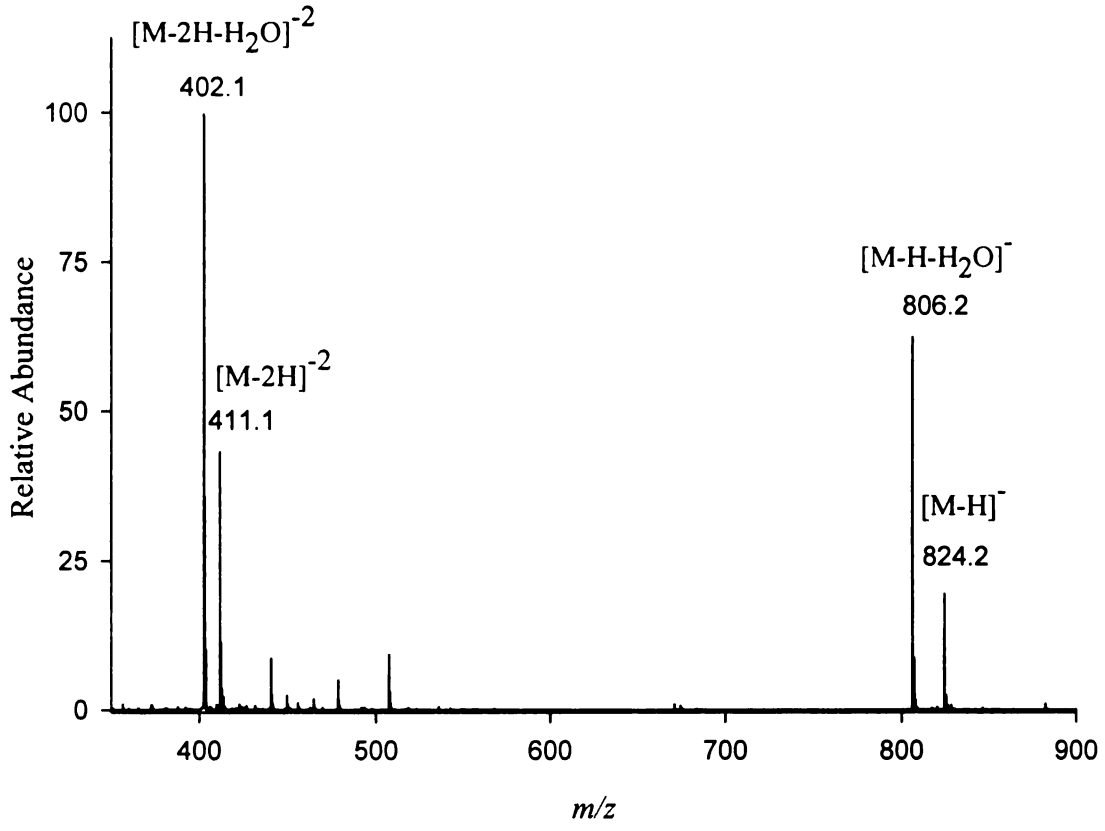

Subsequent attempts to synthesize and purify the methoxycarbonyl CoA thioester involved minimum use of aqueous solvent and yielded ~5% of the thioester, which was used in the enzymatic reaction without purification. Incubation of DBAT, 10-DAB, and the methoxycarbonyl CoA thioester thus obtained under standard assay conditions did not yield detectable product after ESI LC-MS analysis. A positive control experiment consisting of DBAT, CoASH and baccatin III was also performed to assess whether the expressed DBAT enzyme batch used in this study was functional.

An alternative strategy was developed to indirectly assess whether methoxycarbonyl is a productive substrate of DBAT. A surrogate substrate 10-

Methoxylcarbonyl-10-DAB was semi-synthesized from 10-DAB and incubated with CoASH and DBAT to evaluate the reverse reaction (**Scheme 3-8**).

Scheme 3-8. Alternative approach of evaluating DBAT enzyme for methoxycarbonyl activity. DBAT catalyzes reversible acylation of the C-10 hydroxyl group of 10-DAB. To evaluate whether DBAT can catalyze deacylation of the unnatural 10-methoxycarbonyl-10-DAB (dotted arrow), DBAT was incubated with the product standard (compound **III-33**) and the formation of 10-DAB was evaluated by reverse-phase HPLC.

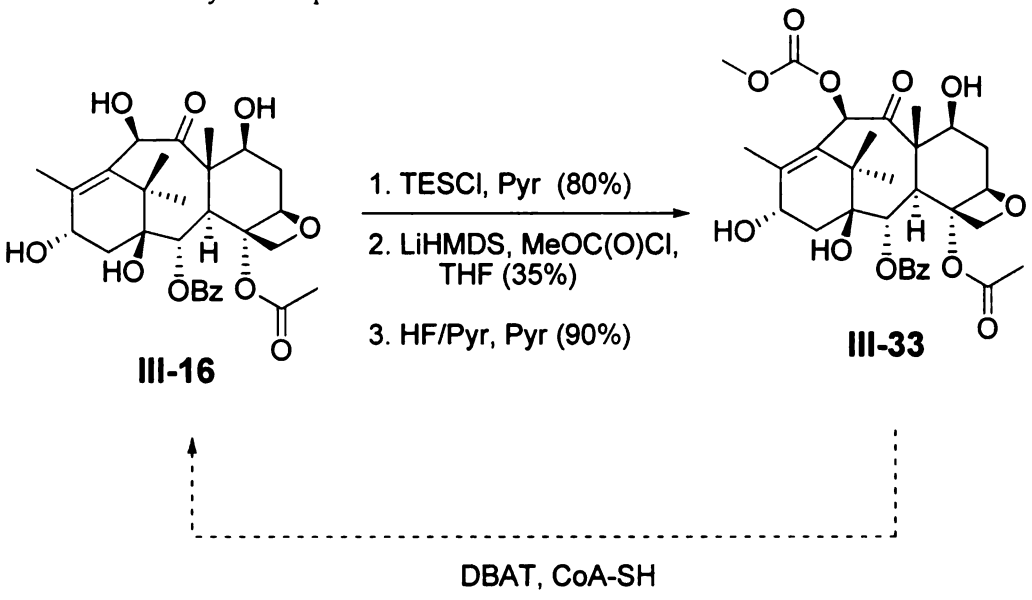

The DBAT enzyme batch used in this study was first determined to be functional by incubating the enzyme with CoASH and baccatin III to produce 10-DAB in the reverse reaction. Analysis of the assay by reverse-phase HPLC did not reveal formation of 10-DAB from the reverse reaction (**Figure 3-11**), indicating that DBAT does not catalyze deacylation of the C-10 methoxycarbonyl from 10-methoxycarbonyl-10-DAB.

Figure 3-11. Reverse-phase HPLC traces of reaction assays to evaluate the activity of DBAT with 10-methoxycarbonyl-10-DAB and CoASH. In a control experiment, 10-methoxycarbonyl-10-DAB was incubated with CoASH (panel A); an assay comprising of 10-methoxycarbonyl-10-DAB and CoASH incubated with DBAT in one reaction tube did not yield any detectable product (panel B).

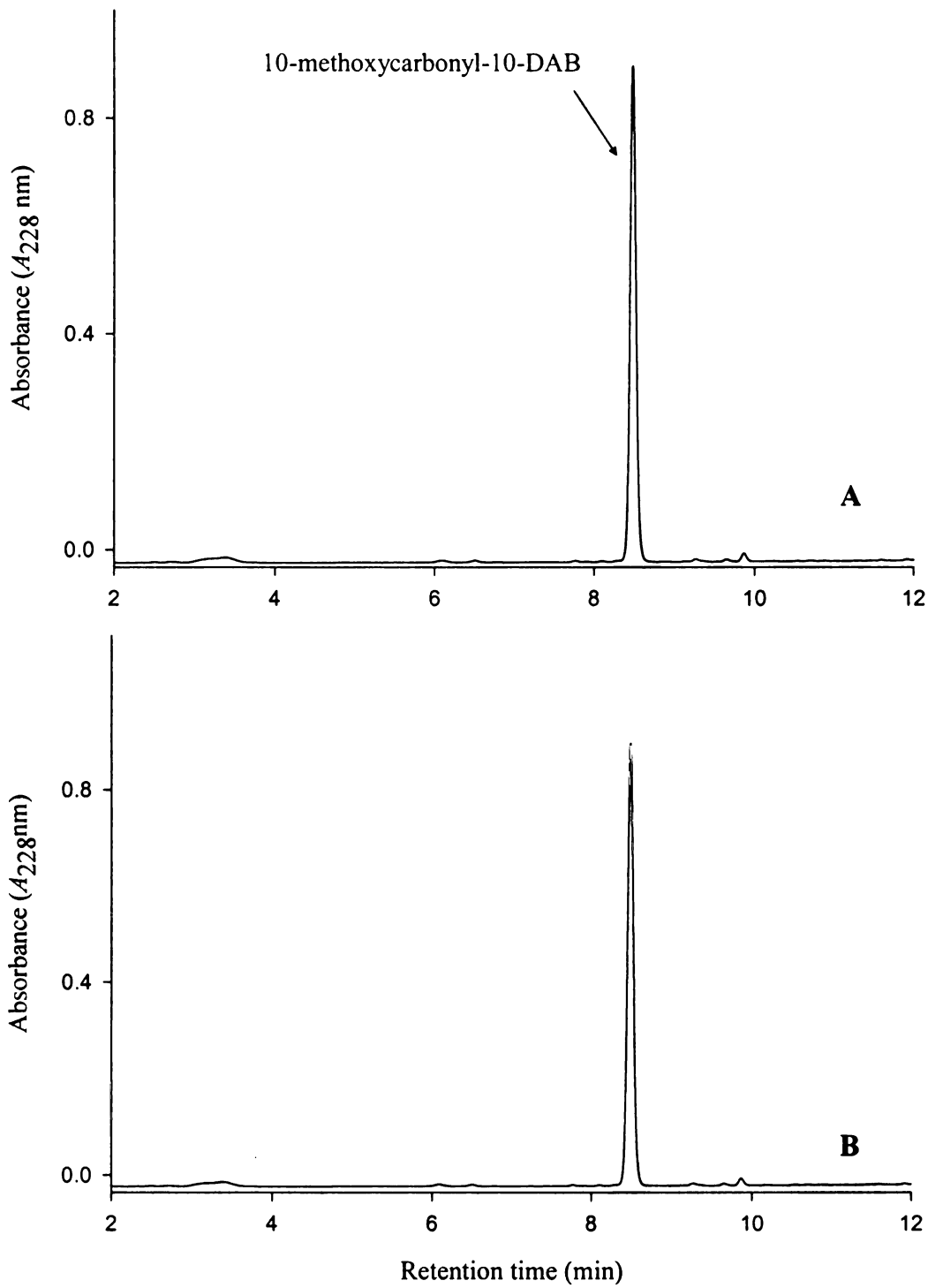

Based on these results, it was inferred that methoxycarbonyl CoA thioester is not a productive substrate of DBAT even if the thioester were to be stable in the aqueous medium used in the enzymatic reaction. Speculatively, the lack of DBAT activity against this substrate could be due to the reduced electrophilicity of the carbonyl carbon of the methoxycarbonyl since the adjacent oxygen may be involved in resonance stabilization of the carbonyl group. This finding requires an alternative strategy to synthesizing methoxycarbonyl CoA or a better methoxycarbonyl donor in order to make progress towards understanding whether DBA can catalyze transfer of the non-natural methoxycarbonyl group to 10-DAB or 4-DAB.

3.4.4 Intermolecular Acetate Exchange Using Wild-Type DBAT

Propionyl CoA has been shown to be a productive substrate of DBAT.[1] To better understand why its isostere methoxycarbonyl CoA is not, the mechanism of DBAT was evaluated using the proposed mechanism for vinorine synthase[2] and anthocyanin malonyltransferase as a model.[3] An alternative mechanism was proposed for DBAT that involves the formation of an *acyl-enzyme intermediate* from a nucleophilic attack on the acyl donor by an active site residue (cf. **Scheme 3-4** section **3.2.2**). According to **Scheme 3-4**, both the forward and reverse reactions do not involve acyl CoA or CoASH in the step leading to the formation of the acyl-enzyme intermediate. To establish the validity of this alternative mechanism, an experiment was designed where 10-deacetyl and 10-acetyl taxane substrates were incubated together with DBAT. Acetyl exchange between the two taxanes was analyzed by reverse-phase HPLC. A pilot study was conducted with baccatin III (as the acetyl group donor) and taxotere (as the acetyl group) acceptor in the presence

of CoASH. HPLC analysis of the assay product revealed transfer of acetyl group from baccatin III to taxotere. The retention time and ESI-MS fragmentation pattern of the exchange product matched that of authentic, semi-synthetically-derived 10-acetyltaxotere (**Figure 3-12**), thus confirming the regiochemistry of the acetate exchange product to be the C-10 position.

Figure 3-12: Reverse-phase HPLC profiles of the acetyl group exchange experiment. The top panel shows a chromatogram for a control experiment comprising of baccatin III (acetyl group donor), taxotere (acetyl group acceptor), and CoASH incubated in one assay tube. An assay mixture comprised of DBAT, CoASH, taxotere, and baccatin III in one reaction tube gave two products, 10-DAB and 10-acetyltaxotere (bottom trace). In the assay, baccatin III is deacetylated by DBAT to 10-DAB and the acetyl group is transferred to taxotere to form 10-acetyltaxotere.

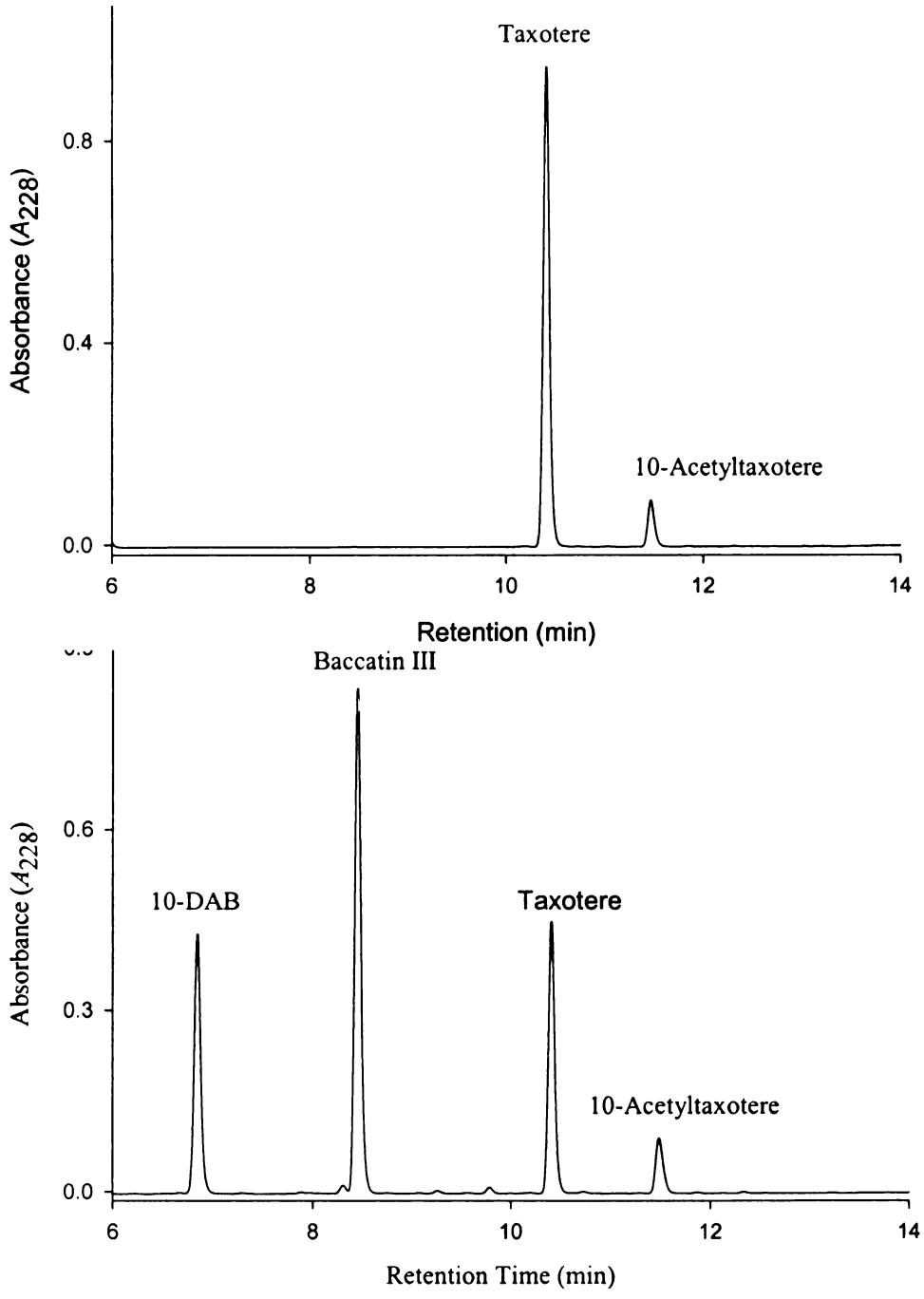

To evaluate whether the DBAT-catalyzed exchange was CoASH-dependent, DBAT was again incubated with baccatin III and taxotere in the absence of CoASH. Analysis of the assay product by ESI-MS revealed that DBAT-catalyzed acetate transfer from baccatin III to taxotere in the absence of CoASH (**Figure 3-13**). Control experiments where baccatin III and/or DBAT were omitted from the reaction mixture were similarly assayed and analyzed but did not yield 10-acetyltaxotere.

Figure 3-13. LC chromatograms and ESI-MS spectrum (positive ion mode) of the product of acetyl exchange between baccatin III and taxotere catalyzed by DBAT in the presence or absence of CoASH. Trace A is a mass-extraction of chromatogram A for 10-acetyltaxotere (MW = 849.4) while trace B is a MS chromatogram with a molecular ion pattern consistent with authentic 10-acetyltaxotere.

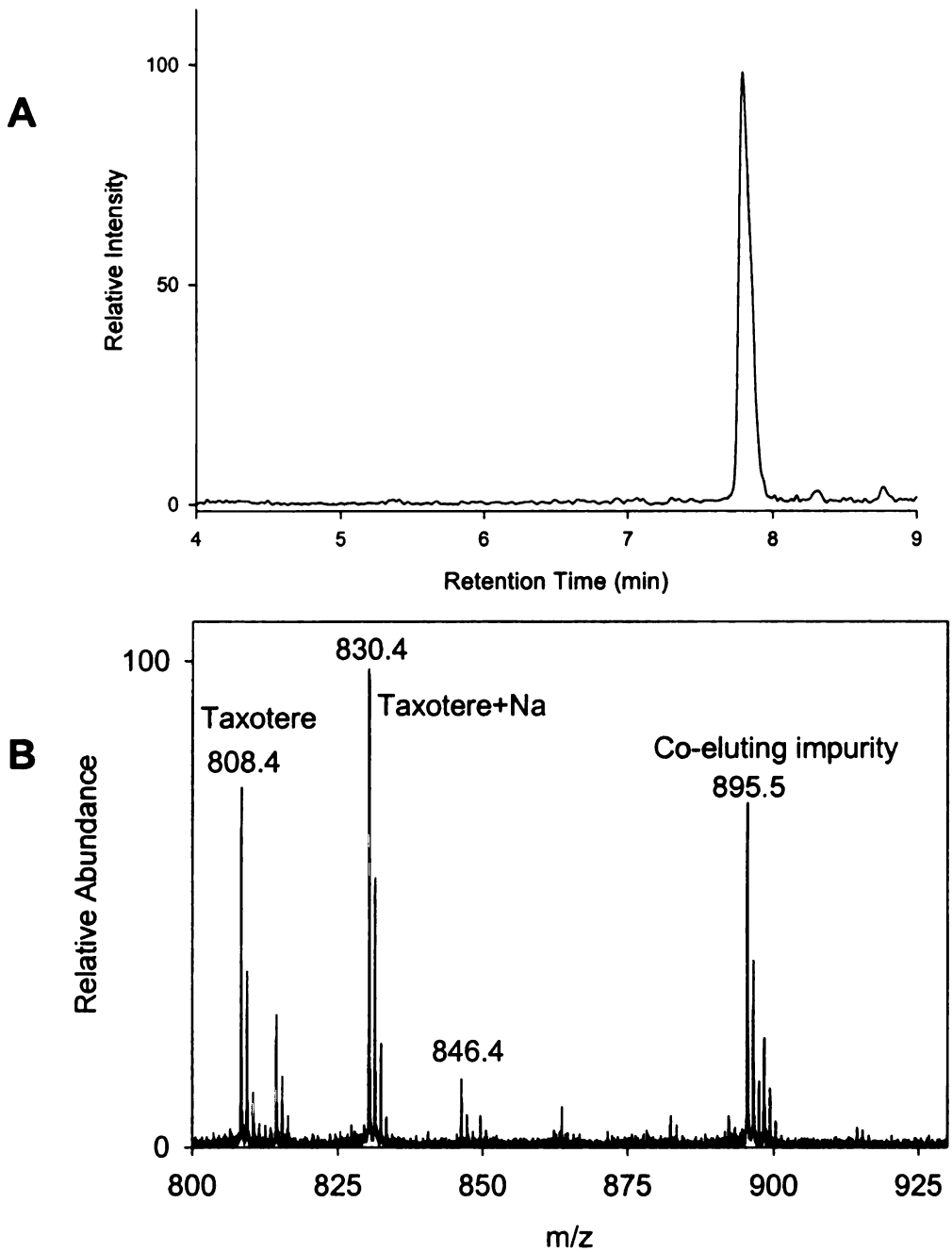

The DBAT-catalyzed transfer of acetyl group from baccatin III to taxotere in the absence of CoASH yielded 5% 10-acetyltaxotere compared to the same reaction in the presence of CoASH. Conceivably, CoASH might be involved in cyclic activation of the

acyl group, wherein the acetyl group is first transferred to an active site residue, then to CoASH, and finally to the taxane acceptor substrate, as depicted in **Scheme 3-4**.

Based on these findings, the mechanism of acetyl transfer from baccatin III and taxotere catalyzed by DBAT is proposed to involve deacetylation of baccatin III by an active site residue to form an acyl-DBAT intermediate followed by thiol-transesterification with CoASH. Finally, the acetyl group is transferred from acetyl CoA to taxotere (**Scheme 3-9**). In the absence of CoASH, taxotere likely initiates a nucleophilic attack of the acyl-enzyme intermediate.

Scheme 3-9. Proposed mechanism for DBAT-catalyzed transfer of acetate from baccatin III (**III-6**) to taxotere (**III-43**). Alternatively, Asp-166 could form a diad with His-162 to enhance the basicity of His-162 through deprotonation.

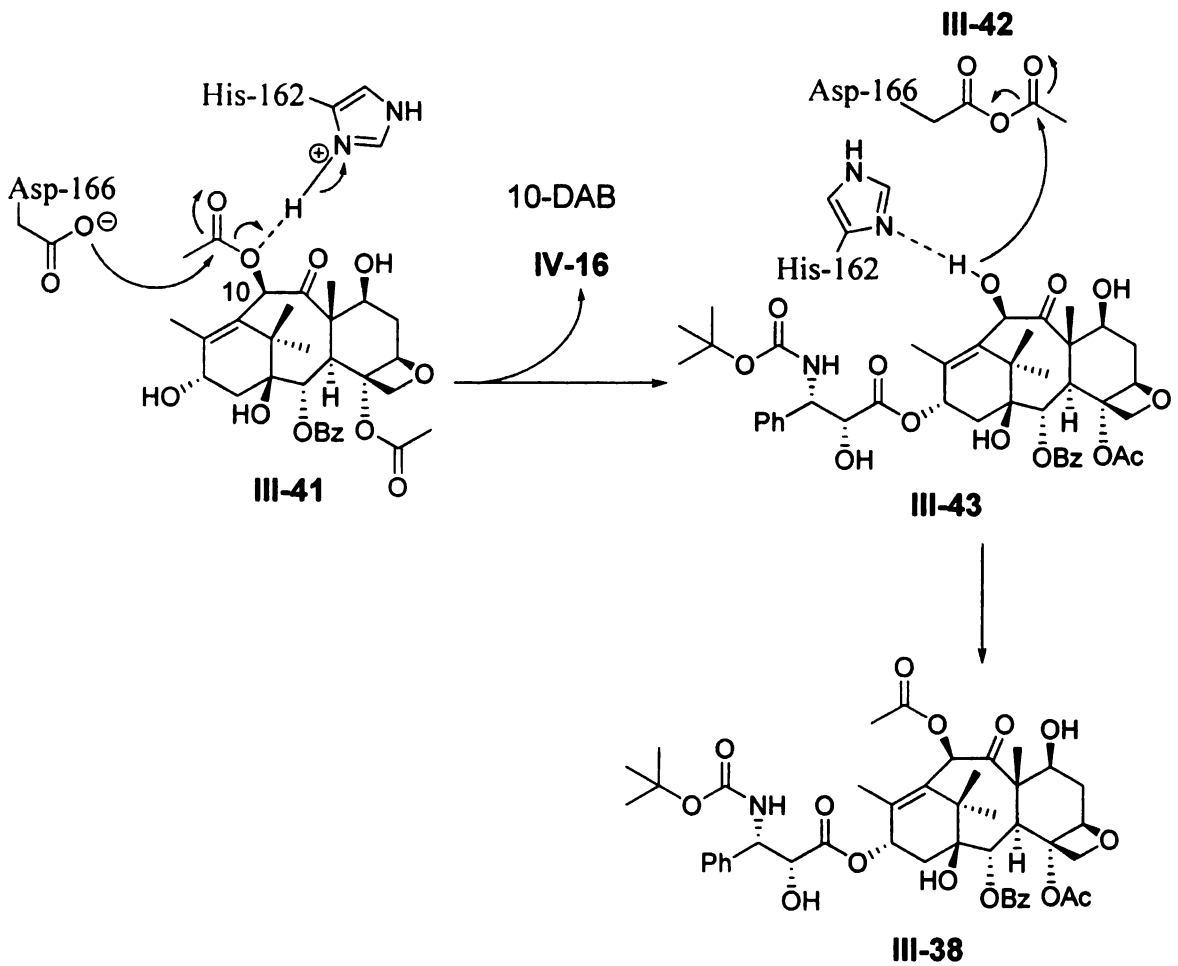

Alternatively, the mechanism of DBAT might involve a catalytic diad between His-162 and Asp-166. Asp-166 could potentially increase the basicity of His-162 through deprotonation of the His nitrogen, similar to the catalytic mechanism proposed for serine proteases.[35] However, more studies are required before firm conclusions can be drawn regarding the catalytic role of Asp-166 in the proposed mechanisms.

While the DBAT-catalyzed acetyl exchange between baccatin III and taxotere with or without CoASH does not provide direct evidence for the formation of an acyl-enzyme intermediate, this study provides a basis for re-evaluating the proposed mechanism for vinorine synthase and other acyltransferases in the BAHD family.[2,3] Even if CoASH were to act as the nucleophile in the proposed mechanism, the implicit formation of acetyl CoA is remarkable, since synthesis of acyl CoA thioesters is catalyzed by acyl CoA ligase in the presence of $MgCl_2$ and ATP cofactors *in vivo*. Neither acetyl CoA ligase nor the cofactors were supplied in this study; this seminal work could benefit from additional studies to further dissect the proposed mechanism.

From a practical standpoint, the DBAT-catalyzed acetyl exchange is a promising approach that could find potential application in one-step modification of advanced taxanes without need for protecting group chemistry. For example, synthesis of 10-acetyltaxotere (the product standard used in the acetyl exchange) involves TBDMS-protection of the C-2' alcohol, regioselective $CeCl_3$-mediated acetylation of the C-10 alcohol, and TBDMS cleavage by HF-pyridine (**Scheme 3-10**). In the model reaction, this three-step acetylation of taxotere was achieved in a single step using DBAT, baccatin III, taxotere, and CoASH. This is a cheaper alternative to direct DBAT-catalyzed acylation of taxotere with acetyl CoA since 10-DAB can be recovered and CoASH can be

potentially recycled as acetyl CoA (cf. **Scheme 3-4**). Moreover, CoASH is ~10-fold less expensive than acetyl CoA at current prices.[36]

Scheme 3-10. Comparison of the semi-synthetic and enzymatic approach to 10-acetyltaxotere (**III-38**) from Taxotere (**III-43**).

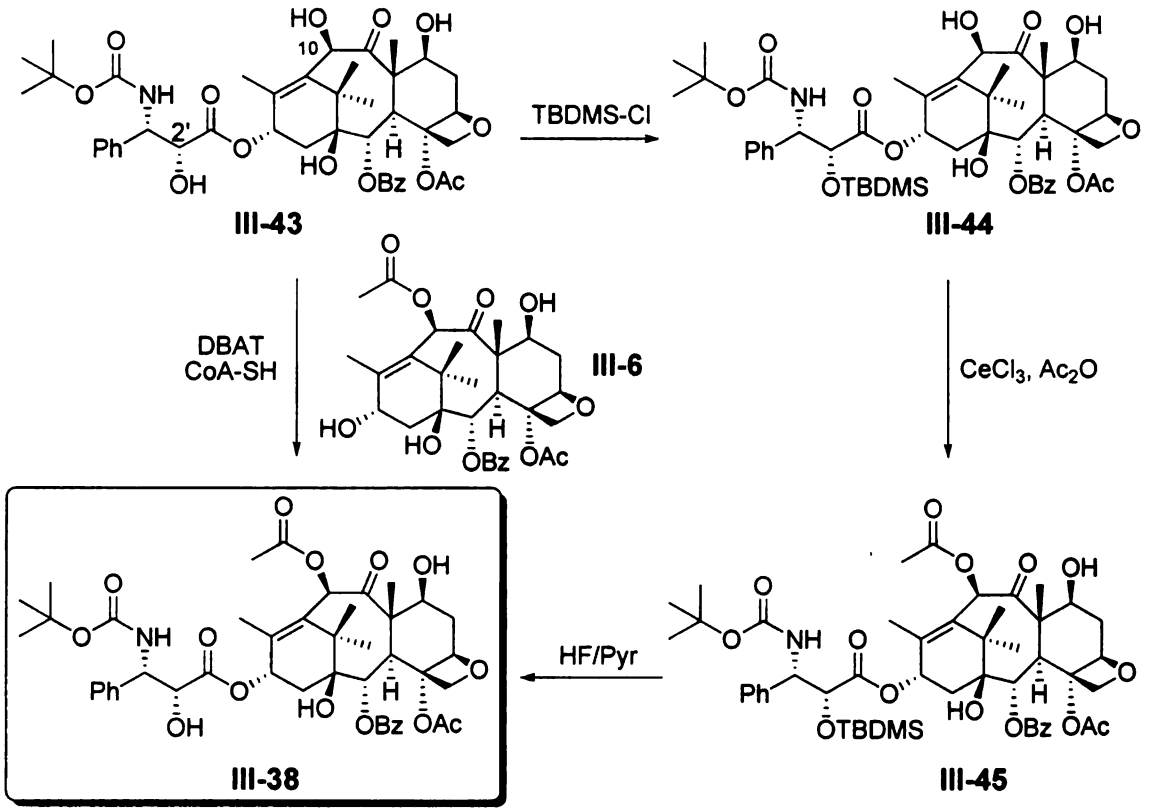

3.4.5 Kinetics of the Reverse Reaction Catalyzed by DBAT

It has been argued that the presence of an acyl-enzyme intermediate on a reaction pathway is manifested through identical V_{max} values of the enzyme for different substrates.[19] A common V_{max} for a particular enzyme with various substrate analogs implies a common rate-limiting step that is independent of the nature of the substrate.[19] To test this hypothesis with DBAT, the rates of the forward and reverse reactions were compared using two sets of taxane substrates for each direction. Maximal velocities were

evaluated for the C-10 acetylation of 10-DAB and 4-DAB in the forward reaction, and deacetylation of baccatin III and 13-oxobaccatin III in the reverse reaction. The use of 4-DAB as a substrate in the forward reaction was demonstrated previously in section **2.4.1**. As noted, 4-DAB was [^{3}H]-labeled at C-10 *in vitro* by DBAT after incubation of unlabeled 4-DAB and [3H]acetyl CoA in a deacylation-reacylation reaction cycle, presumably through the formation of 4,10-dideacetylbaccatin III. To calculate V_{max}, 4-DAB was incubated with [3H]acetyl CoA and the rate of formation of [^{3}H]-4-DAB was determined.

To determine the kinetic parameters of DBAT with the four substrates, the enzyme was incubated with increasing concentrations of each taxane substrate at saturating co-substrate concentration (500 μM) in different assay tubes and the rate of product formation was determined by reverse-phase HPLC. Analysis of the assays revealed that in both the reverse and forward reactions, DBAT had different K_m values for each substrate. The K_m of 10-DAB and 4-DAB was determined to be 57 ± 2 μM and 86 ± 5 μM, respectively (**Figure 3-14** and **Figure 3-15**). In the reverse reaction, DBAT had K_m values of 83 ± 5 μM and 185 ± 7 μM for baccatin III and 13-oxobaccatin III, respectively (**Figure 3-16** and **Figure 3-17**).

Unlike the K_m values, the calculated V_{max} values of DBAT for the four substrates were similar for each set of substrates in either direction. For 10-DAB and 4-DAB, the V_{max} values were 0.058 ± 0.002 nmol·s^{-1} and 0.063 ± 0.003 nmol·s^{-1}, respectively, while the V_{max} values of baccatin III and 13-oxobaccatin III were 0.083 ± 0.004 nmol·s^{-1} and 0.089 ± 0.002 nmol·s^{-1}, respectively.

Figure 3-14. Rate of formation of baccatin III from 10-DAB with DBAT and CoASH.

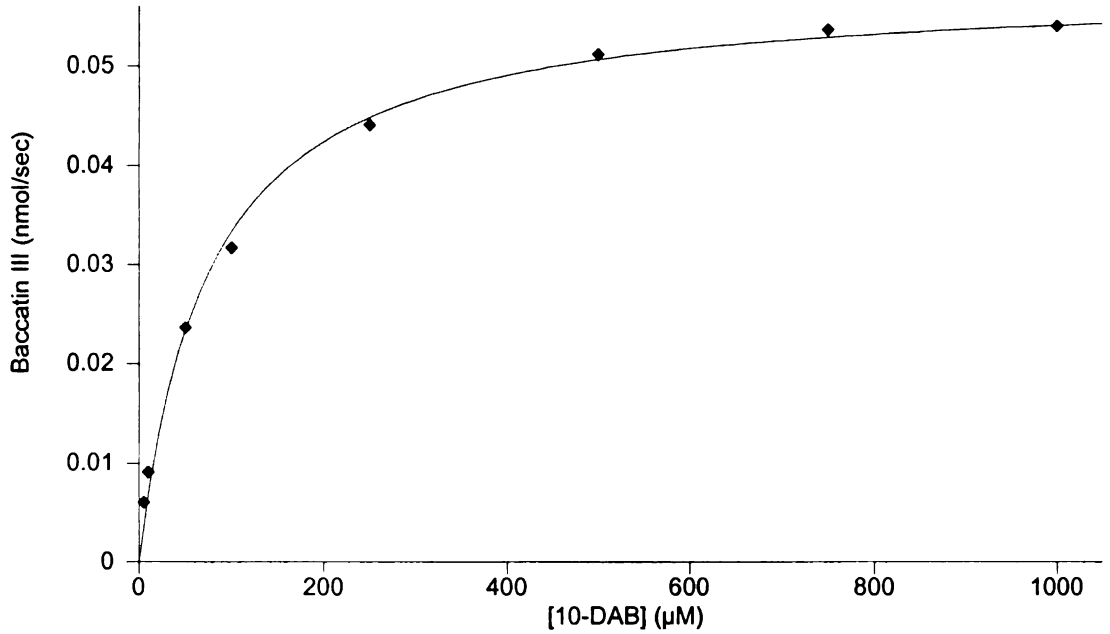

Figure 3-15. Rate of formation of radio-labeled 4-DAB from incubation of unlabeled 4-DAB with tritium-labeled acetyl CoA and DBAT

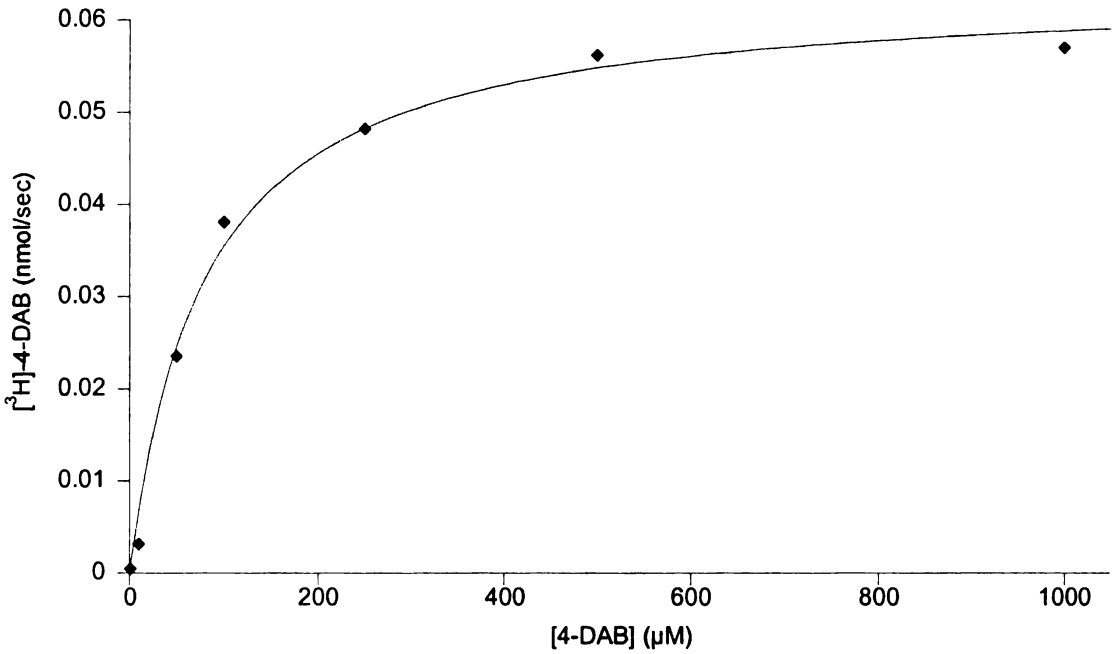

Figure 3-16. Rate of formation of 10-DAB from DBAT-catalyzed deacylation of baccatin III

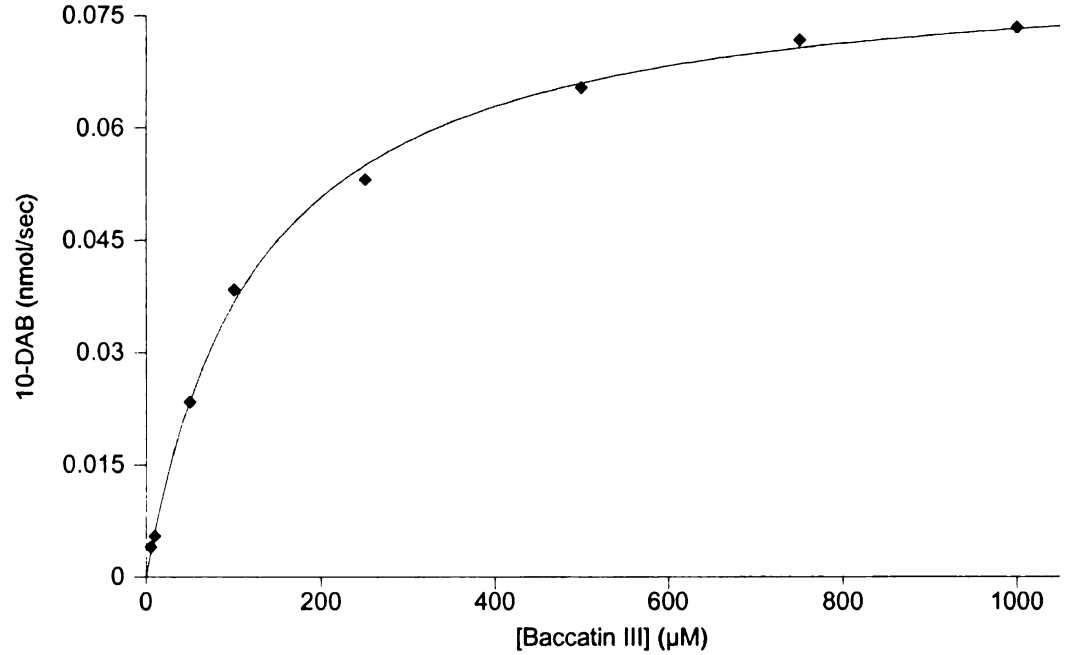

Figure 3-17. Rate of formation of 13-oxo-10-deacetylbaccatin III from the deacetylation of 13-oxobaccatin III catalyzed by DBAT using CoASH.

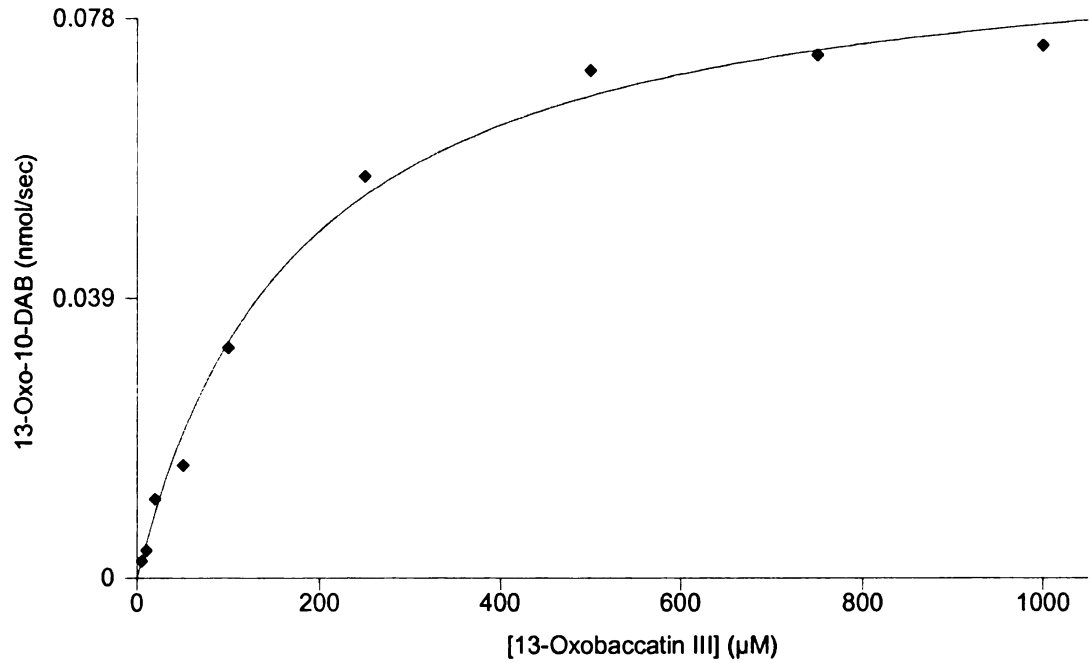

The common maximal velocities observed for each set of taxane substrate implies that the DBAT-catalyzed acetylation and deacetylation goes through a common rate-determining intermediate whose *rate of formation* is independent of the taxane substrate

used. Gibbs free energy of hydrolysis of a thioester (-8 kcal·mol^{-1}) predicts that the forward reaction will be kinetically more favored than hydrolysis of a regular ester (3-4 kcal·mol^{-1}).[37] However, the reverse reaction was found to be faster (~0.086 nmol·s^{-1}) than the forward reaction (~0.061 nmol·s^{-1}) for both sets of substrates. This could be explained by considering that, after hydrolysis, the leaving alkoxide gets effectively hydrated (has a higher proton affinity) than the thiolate. Thus, this extensive protonation may compensate for the sluggish scission of the regular ester bond in the reverse reaction.[38]

The results presented here suggest that the mechanism of DBAT involves the formation of an acyl-enzyme intermediate; however, more studies are required in order to fully elucidate this mechanism.

3.4.6 Site-Directed Mutagenesis of *dbat*

The Asp residue in the HXXXD motif, which is conserved in the BAHD family of acyltransferases, was assessed for a catalytic role during DBAT catalysis. Asp-166 of DBAT was mutated to a non-nucleophilic or more basic residue, and the activity of the resulting mutants was systematically evaluated. This study is important because in vinorine synthase and malonyltransferase, the corresponding Asp residue in the HXXXD motif is speculated to play only a structural role.[2] To determine whether this residue could play a more direct role during DBAT catalysis, Asp-166 was substituted with either an isosteric or isoelectronic residue to prevent significant alteration of the structure of the mutants.

The use of nucleophilic carboxylate residues (Asp or Glu) in enzyme mechanisms has been demonstrated. For example, Asp and Glu have been found to be second and

third to histidine, respectively, in the frequency of use as part of an enzyme active site.[39] In lysozymes from the human and chicken egg white, an Asp residue has been demonstrated to be the nucleophile.[40] Similarly, an aspartate residue is involved in the catalytic mechanism during the cleavage of a carbon-fluoride bond by a fluoroacetate dehalogenase.[41] Analogously, glutamate has been shown to be a catalytic residue in the formation of a covalent intermediate during the cleavage of glycosides by "retaining" β-glycosidases.[42]

To probe the catalytic role of Asp in the HXXXD motif of DBAT, Asp-166 was mutated to Asn-166. The goal was to introduce a similar-sized residue with somewhat similar electronics (hydrogen bonding capabilities) but basic enough to change the rate of formation of the proposed acyl-enzyme intermediate. The D166N mutant was expected to be less active than wild-type DBAT against baccatin III or 10-DAB substrates. Additionally, even if Asn-166 were to retain the nucleophilicity of Asp-166, it was hypothesized that the resultant *N*-acyl-enzyme intermediate would be relatively harder to "hydrolyze"[37] compared to an *O*-acyl intermediate proposed for wild-type DBAT (cf. **Scheme 3-4**).

Similarly, a D166E mutant of DBAT was prepared to assess the effect of introducing an intervening methylene to the proposed nucleophile. This residue was expected to retain some activity because the nucleophile, even though a little longer, is still a carboxylate. Analogously, a D166Q mutant was also generated; this mutant, like the D166N, was expected to have low to no activity because of reduced nucleophilicity of Gln-166 residue. To introduce an "isosteric" residue lacking the hydrogen bonding capabilities of Asp-166 and Asn-166, A D166L mutant was generated; since this residue

cannot act as a nucleophile, the resultant mutant (D166L) was expected to be completely inactive.

Finally, a double mutant (H162D; D166H) was prepared by switching the first and last residues in the conserved HXXXD motif. With this mutant, the aim was to break the sequence of hydrogen bonds and hydrophobic contacts of the active site residues to assess whether some reorganization could occur to rescue activity; this mutant was also expected to be inactive.

After sequence-verification of the mutants, expression from *E. coli*, and purification, the mutants were analyzed for activity using standard assays similar to those for wild-type DBAT. Mutants having N-terminal polyhistidine tags were found to be poorly expressed from *E. coli* (~52 kDa, **Figure 3-18**).

Figure 3-18. SDS-PAGE gel of wild-type N-terminal His-tagged DBAT and N-terminal His-tagged DBAT mutants before purification. (a) Three random colonies harboring *dbat* were selected from a freshly grown agar plate and grown in 100 mL LB media to evaluate the variability of DBAT expression. Total protein loaded into each well was ~120 µg. The asterisk (*) indicates the 50 kDa mark; C-terminal His-tagged DBAT and its mutants are ~52 kDa.

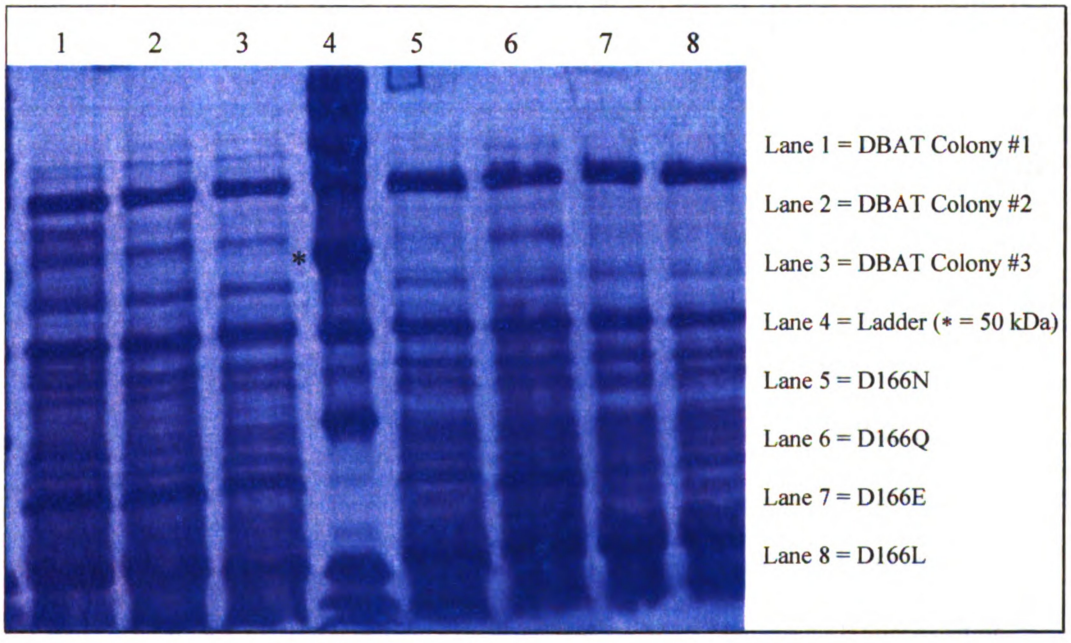

Even with Ni-NTA affinity chromatography purification (~40-50% pure by SDS-PAGE analysis) the DBAT mutants always co-purified with other endogenous bacterial proteins. When incubated with baccatin III or 10-DAB, none of the partially purified mutants showed detectable product under reverse-HPLC analysis.

To determine whether the position of the His-tag had an effect on the purity or activity of the mutants, the purification tag was changed from the N-terminal to the C-terminal. Therefore, C-terminal His-tagged mutants were generated using *dbat* DNA template having a polyhistidine tag at the C-terminal end. These mutants were expressed, purified and assayed under identical conditions as the N-terminal his-tagged mutants. After Ni-NTA and FPLC purification, SDS-PAGE analysis indicated an improvement in the purity of the C-terminal His-tagged mutants (60-80%) compared to the N-terminal His-tagged mutants (30-40%) (**Figure 3-19** and **Figure 3-20**).

Figure 3-19. SDS-PAGE gel (12% SDS) of FPLC-purified, C-terminal His-tagged DBAT mutants. Each FPLC eluent (5 mL) was concentrated into a final volume of ~500 µL from which 15 µL was loaded into each well. A Bradford assay was used to approximate the amount of total proteins in each fraction. Well 2, 3, 4, 5, 6, 7, 8, 9 contained ~15, 80, 60, 50, 50, 10, 70, and 15 µg, respectively. The asterisk (*) indicates the 50 kDa mark; C-terminal Hi-tagged DBAT and its mutants are ~52 kDa.

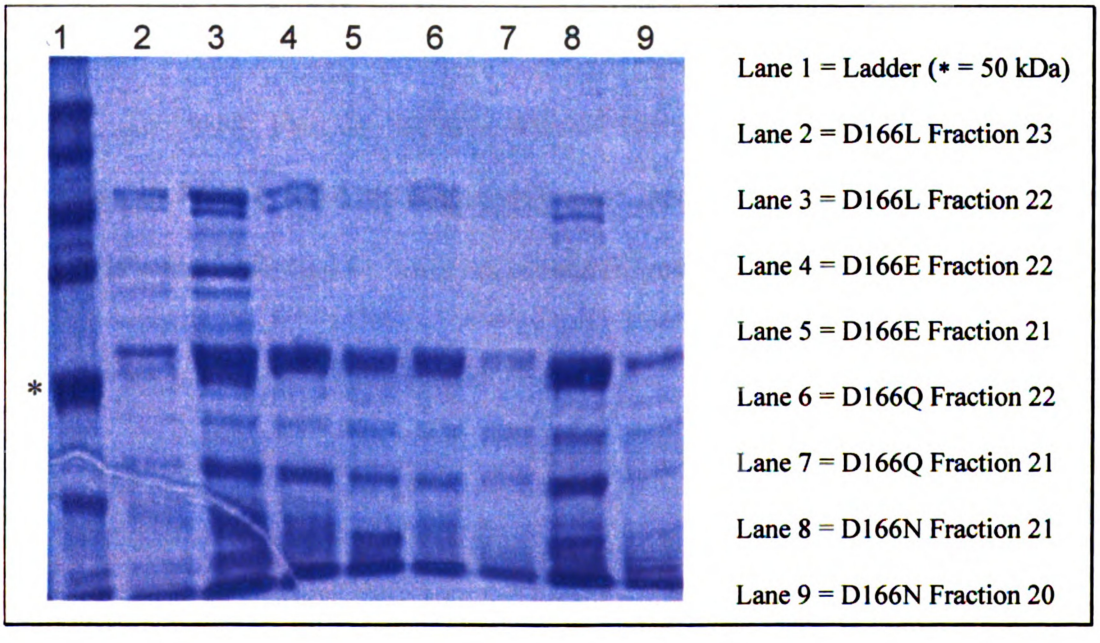

Figure 3-20. SDS-PAGE gels (10% SDS) of FPLC-purified C-terminal His-tagged (H162D; D166H) (A) and D166N (B) mutants. Each eluent (5 mL) was concentrated into a final volume of ~500 µL. A Bradford assay was used to determine protein concentration; ~20 µg (total protein) was loaded into each well. Fraction 22 of the H162H;D166H double mutant (lane 1 gel A) and fraction 21 of the D166N mutant (lane 3 gel B) gave the best protein purity and were used in assays. The asterisk (*) indicates the 50 kDa mark; the two C-terminal His-tagged DBAT mutants are ~52 kDa.

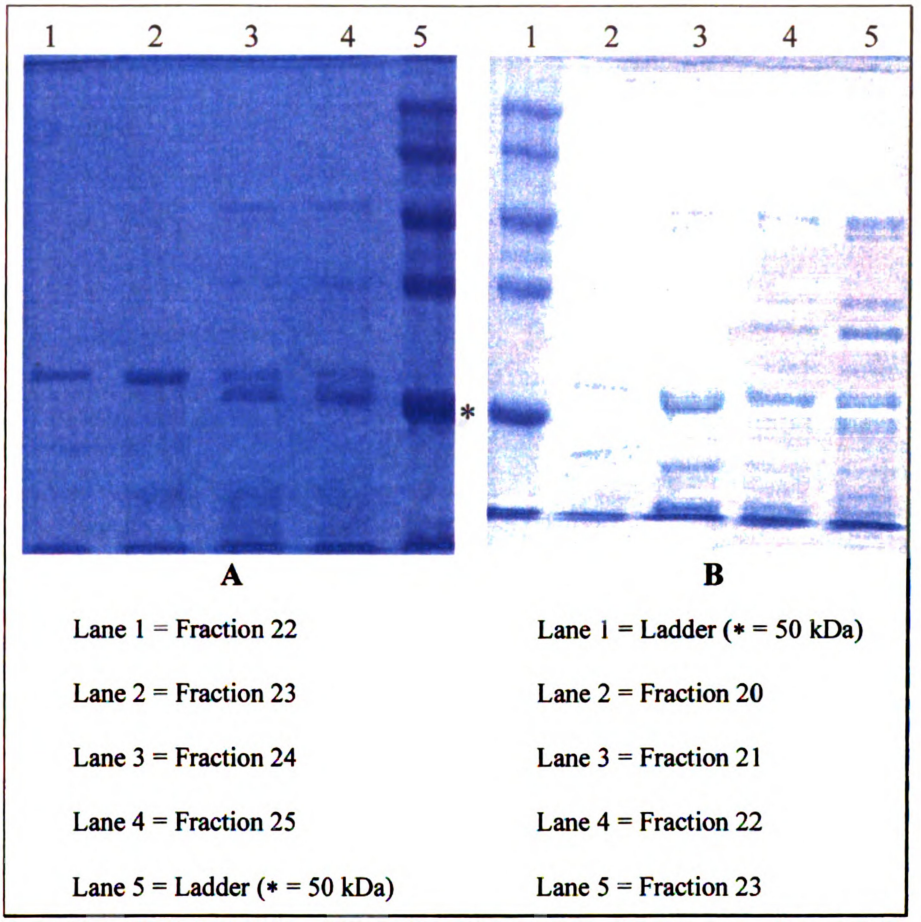

To ensure that the mutants retained the general fold of wild-type DBAT, circular dichroism (CD) measurements were performed which indicated that the mutants were unaffected by the substitutions (**Figure 3-21**).

Figure 3-21. CD spectra of wild-type DBAT and its mutants. A ~5 μM concentration of each protein in phosphate buffer (50 mM) in a 1 cm-path length cuvette was used to obtain the CD spectra. The wavelength interval was set to 0.5 nm and each sample was scanned 5 times from 300-180 nm using a JASCO J810 spectropolarimeter. The spectral data were analyzed using Dichroweb (http://dichroweb.cryst.bbk.ac.uk/html/home.shtml), an on-line server for protein Circular Dichroism spectra deconvolution, which indicated that the proteins were 78-82% α-helical, 1-4% β-sheets, and 18-22% random coiled.

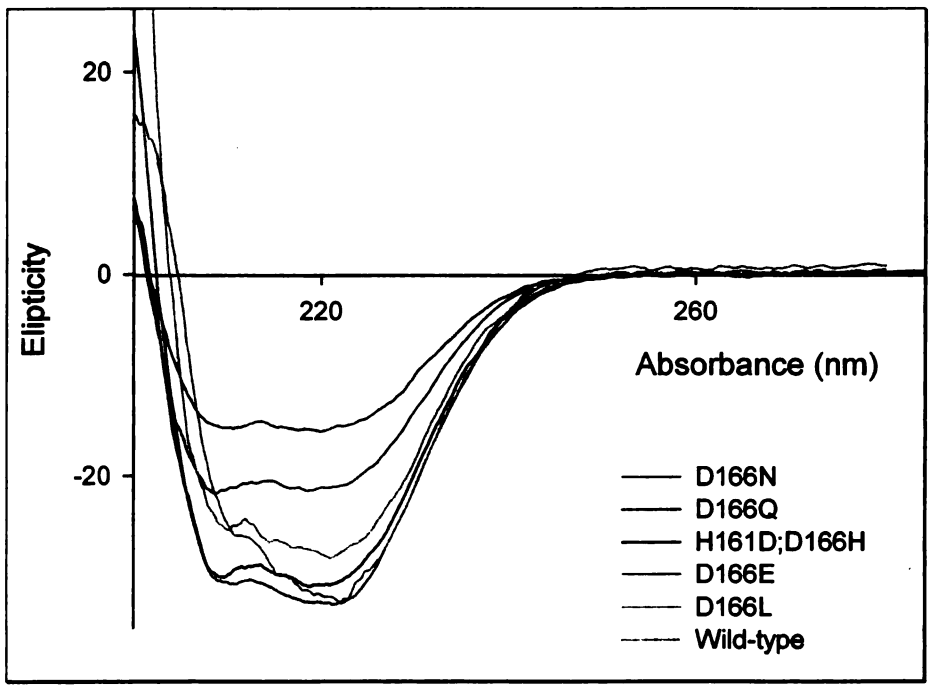

Baccatin III and CoASH were incubated in an assay mixture with each of the six mutants separately to evaluate them for the deacetylation reaction. Analysis of the products by reverse-phase HPLC revealed that the D166N mutant retained only 8% of wild-type activity in the deacetylation reverse reaction (**Figure 3-22**); the other four mutants retained 2-5% wild-type DBAT activity (**Table III-1**).

Figure 3-22. Reverse-phase HPLC chromatograms of wild-type DBAT (top trace I) and its mutant D166N mutant (bottom trace II) incubated with baccatin III and CoASH. The HPLC product peaks (6.826 ± 0.003 min) for both wild-type the D166N mutant were analyzed by ESI-MS (positive ion mode), and give a molecular ion [*m/z* 545.3] and other fragmentation patterns characteristic of authentic 10-DAB.

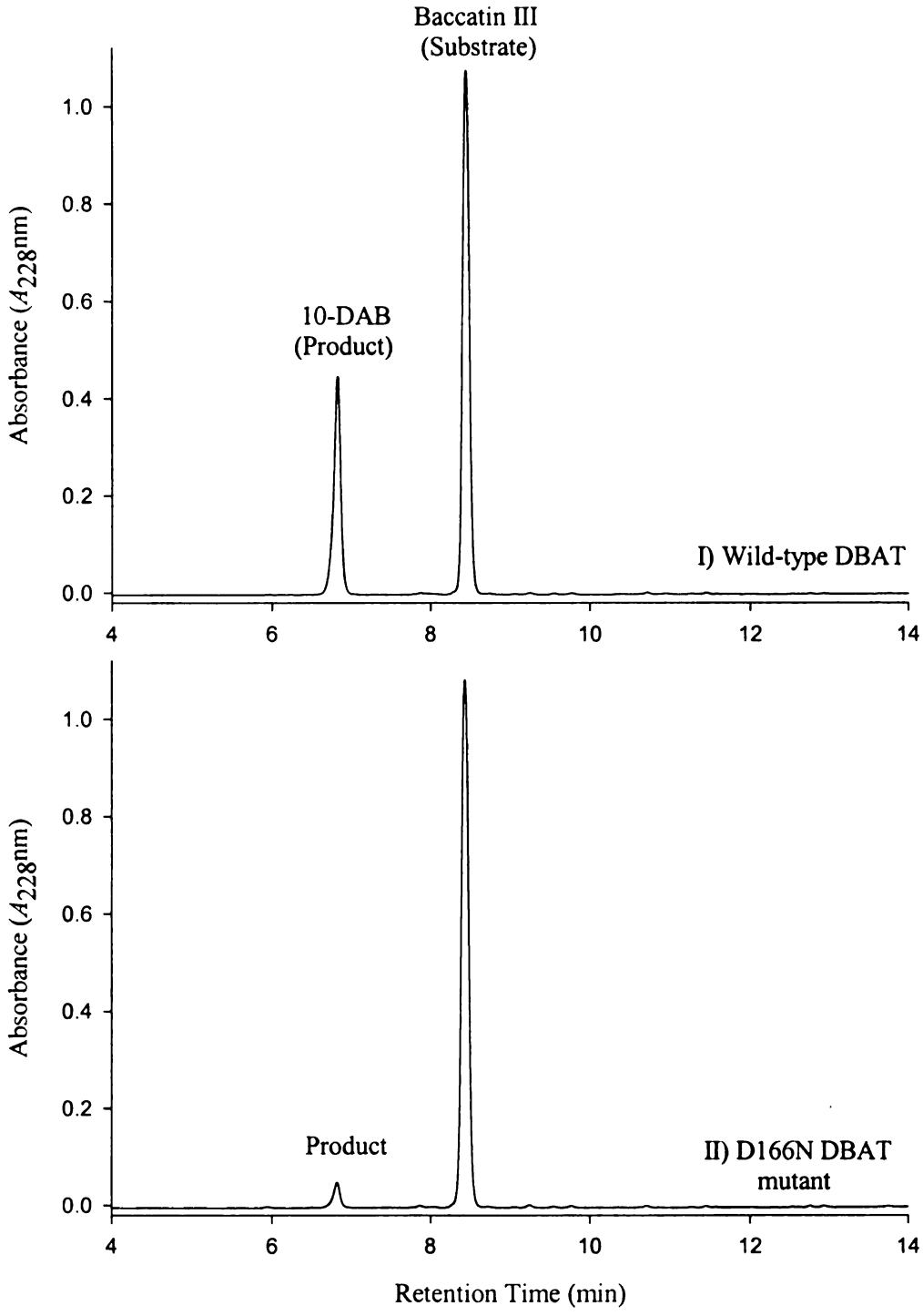

Table 3-1. Evaluation of the enzymatic activity of DBAT and DBAT mutants in the deacetylation reaction of baccatin III in the presence of CoASH. Wild-type DBAT activity was set to 100% from where the relative activity of each DBAT mutant was calculated.

Enzyme	10-DAB (nmol)	% Conversion	% Wild-type activity
Wild-type DBAT	16.6	60	100
D166N	1.4	5	8
D166Q	0.7	2	4
D166E	0.5	2	3
D166L	0.4	1	2
D161H;D166H	0.5	2	3

The D166N mutant was slightly more active against baccatin III in the reverse reaction compared to all the mutants (**Table III-I**). This could be due to the fact that Asp-166 (wild-type) and Asn-166 (mutant) residues are similar in size, implying that this mutant accommodates the substrate better than all the other mutants. For the mutants with an intervening methylene (D166E and D166Q), the proposed nucleophilic residues (Glu-166 and Gln-166) might be oriented away from the active site to avoid unfavorable contacts due to chain elongation. Furthermore, it has been argued that increasing the length of the nucleophile could create a small void in the active site which can be occupied by an active site water molecule, which could hydrolyze the acyl-enzyme intermediate.[42]

Moreover, the observed activity by D166N mutant might be due to the deamidation of Asn-166 to Asp-166 by the active site water to give, hence converting the mutant into wild-type DBAT. This phenomenon has been observed in mutants incorporating similar Asp-Asn or Asp-Gln substitutions.[42-44]

The D166L mutant was expected to be inactive because Leu-166 cannot act as a nucleophile. However, this mutant had small activity (2 % compared to wild-type DBAT) (**Table III-1**), which implies that some other residue(s) in the mutant might be responsible for this minimal activity. Extra effort was made to ensure that the observed activity of the mutants was not due to contaminating wild-type DBAT by using different Ni-NTA agarose columns for each mutant during purification. However, a possible source of residual wild-type DBAT activity would be incomplete digestion of the parental *dbat* plasmid during *Dpn* I treatment. This is unlikely since DNA sequencing of the mutant clones prior to transformation of and expression from *E. coli* did not reveal wild-type contamination. Therefore, the small activity observed for these mutants might be authentic, possibly catalyzed by a different residue and not the proposed Asp-166.

Taken together, the data from site-directed mutagenesis study suggest that Asp-166 is important for DBAT activity. While the data are admittedly insufficient for meaningful mechanistic deductions to be made, they nonetheless suggest that the Asp residue in the HXXXD motif plays a more direct role in DBAT catalysis.[2,3] Therefore, the hypothesis that the Asp residue in the HXXXD motif of vinorine synthase plays only a structural role needs to be re-evaluated since this data show >90% reduction in wild-type activity after Asp-166 in DBAT is mutated to Asn, Glu, Gln, Leu, and His residues . Equally pertinent, more elaborate studies involving these and other DBAT mutants ought to be done in order to ascertain the exact role of this residue. Ultimately, x-ray crystallographic data could help uncover the molecular basis of the DBAT-catalyzed transesterification reaction.

3.5 Significance

3.5.1 Rapid Reversibility of DBAT-Catalyzed Acylation

Baccatin III is thought to be the last diterpene intermediate in the taxol biosynthesis. This intermediate is acylated with phenylisoserinyl side chain which is further elaborated to complete the pathway. DBAT is considered to be the last acyltransferase on the biosynthetic pathway leading to baccatin III core, making it one of the key enzymes in the pathway. The initial finding that this enzyme is both promiscuous (Chapter 2) and catalyzes the reverse deacetylation reaction as efficiently as the forward reaction (Chapter 3) raises questions about the physiological relevance of these reactions. In *planta*, DBAT likely moderates the steady-state pools of endogenous acetyl-CoA, 10-DAB, or baccatin III, and plays a central role in directing the metabolic flux to taxol by diversion of precursors to pathways competing for acetyl CoA and/or 10-deacetyl taxanes.

As important, the DBAT-catalyzed reverse reaction could find practical applications in selective cleavage of the C-10 or C-4 acetates of advanced taxanes. Once optimized, such a process could be incorporated into semi-synthetic methodologies that rely on protecting group chemistry to modify taxoid compounds at these two positions. Moreover, the reverse reaction can be used to dissect the mechanism of the DBAT-catalyzed acyl transfer. Conceivably, for example, a fluorescent acyl group could be used to provide a real-time analysis of the DBAT reaction mechanism.

3.5.2 Site-Directed Mutagenesis

The results presented in section **3.4.6** on site-specific modification of the Asp-166 residue in DBAT only preliminarily address the catalytic role of this residue. Various substitutions caused significant erosion of activity (by >95%) of the mutant enzymes compared to wild-type DBAT. This indicates that Asp-166 in DBAT, and conserved Asp residues of other acyltransferases in the BAHD family,[2,3] could be catalytic. Therefore, the roles of the conserved residues in the HXXXD and DFGWF motifs need to be carefully evaluated. Once their roles are determined, these residues could be appropriately substituted to confer novel substrate specificities or to evolve catalyst for potential application in the biocatalysis of pharmaceutically useful metabolites.

3.6 References

(1) Loncaric, C.; Merriweather, E.; Walker, K. *Chemistry & Biology* **2006**, *13*, 1-9.

(2) Ma, X.; Koepke, J.; Panjikar, S.; Fritzsch, G.; Stockigt, J. *Journal of Biological Chemistry* **2005**, *280*, 13576-13583.

(3) Unno, H.; Ichimaida, F.; Suzuki, H.; Takahashi, S.; Tanaka, Y.; Saito, A.; Nishino, T.; Kusunoki, M.; Nakayama, T. *Journal of Biological Chemistry* **2007**, *282*, 15812-15822.

(4) Schmid, A.; Dordick, J.; Hauer, B.; Kiener, A.; Wubbolts, M.; Witholt, B. *Nature* **2001**, *409*, 258-268.

(5) Lairson, L.; Watts, A.; Wakarchuk, W.; Withers, S. *Nature Chemical Biology* **2006**, *2*, 724-728.

(6) Nobeli, I.; Favia, A.; Thornton, J. *Nature biotechnology* **2009**, *27*, 157-167.

(7) Hopkins, A.; Mason, J.; Overington, J. *Current opinion in structural biology* **2006**, *16*, 127-136.

(8) Ghanem, A.; Aboul-Enein, H. *Tetrahedron: Asymmetry* **2004**, *15*, 3331-3351.

(9) Griffith, B.; Thorson, J. *Nature Chemical Biology* **2006**, *2*, 659-660.

(10) Hou, L.; Honaker, M.; Shireman, L.; Balogh, L.; Roberts, A.; Ng, K.; Nath, A.; Atkins, W. *Journal of Biological Chemistry* **2007**, *282*, 23264.

(11) Chen, S.-H.; Huang, S.; Gao, Q.; Golik, J.; Farina, V. *Journal of Organic Chemistry* **1994**, *59*, 1475-84.

(12) Chen, S.; Huang, S.; Wei, J.; Farina, V. *Tetrahedron* **1993**, *49*, 2805-2828.

(13) Nicolaou, K.; Nantermet, P.; Ueno, H.; Guy, R.; Couladouros, E.; Sorensen, E. *Journal of the American Chemical Society* **1995**, *117*, 624-633.

(14) Shaw, W. *Critical Reviews in Biochemistry and Molecular Biology* **1983**, *14*, 1-46.

(15) Kleanthous, C.; Shaw, W. *Biochemical Journal* **1984**, *223*, 211.

(16) Suzuki, H.; Nakayama, T.; Nishino, T. *Biochemistry* **2003**, *42*, 1764-1771.

(17) Bayer, A.; Ma, X.; Stöckigt, J. *Bioorganic & Medicinal Chemistry* **2004**, *12*, 2787-2795.

(18) Froede, H.; Wilson, I. *Journal of Biological Chemistry* **1984**, *259*, 11010.

(19) Riddle, B.; Jencks, W. *Journal of Biological Chemistry* **1971**, *246*, 3250.

(20) Selmer, T.; Buckel, W. *Journal of Biological Chemistry* **1999**, *274*, 20772.

(21) Mack, M.; Buckel, W. *FEBS letters* **1995**, *357*, 145-148.

(22) Parrish, J.; Salvatore, R.; Jung, K. *Tetrahedron* **2000**, *56*, 8207-8237.

(23) Pacheco, M.; Marshall, C. *Energy Fuels* **1997**, *11*, 2-29.

(24) Mastalerz, H.; Cook, D.; Fairchild, C.; Hansel, S.; Johnson, W.; Kadow, J.; Long, B.; Rose, W.; Tarrant, J.; Wu, M. *Bioorganic & medicinal chemistry* **2003**, *11*, 4315-4323.

(25) Mastalerz, H.; Cook, D.; Fairchild, C. R.; Hansel, S.; Johnson, W.; Kadow, J. F.; Long, B. H.; Rose, W. C.; Tarrant, J.; Wu, M.-J.; Xue, M. Q.; Zhang, G.; Zoeckler, M.; Vyas, D. M. *Bioorganic & Medicinal Chemistry* **2003**, *11*, 4315-4323.

(26) Kant, J.; Bristol-Myers Squibb Company.: USA, 2001.

(27) Whalen, L.; Morrow, C. *Tetrahedron: Asymmetry* **2000**, *11*, 1279-1288.

(28) Matsumoto, K.; Fuwa, S.; Shimojo, M.; Kitajima, H. *Bulletin of the Chemical Society of Japan* **1996**, *69*, 2977-2987.

(29) Morís, F.; Gotor, V. *Tetrahedron* **1992**, *48*, 9869-9876.

(30) Appendino, G.; Noncovich, A.; Bettoni, P.; Dambruoso, P.; Sterner, O.; Fontana, G.; Bombardelli, E. *European Journal of Organic Chemistry* **2003**, *2003*, 4422-4431.

(31) Walker, K.; Croteau, R. *Proceedings of the National Academy of Sciences of the United States of America* **2000**, *97*, 13591-13596.

(32) Ondari, M. E.; Walker, K. D. *Journal of the American Chemical Society* **2008**, *130*, 17187-17194.

(33) Tundo, P.; Selva, M. *Accounts of Chemical Research* **2002**, *35*, 706-716.

(34) Olah, G.; White, A. *Journal of the American Chemical Society* **1968**, *90*, 1884-1889.

(35) Carter, P.; Wells, J. A. *Nature* **1988**, *332*, 564-568.

(36) Breeze, A.; Simpson, A. *Journal of Applied Microbiology* **1982**, *53*, 277-284.

(37) Lehninger, A.; Nelson, D.; Cox, M.; 5th ed.; New York: WH Freeman, 2008.

(38) http://www.orglist.net/archive/2002/0041.html, Accessed 08-19-2010; Vol. 2010.

(39) Gutteridge, A.; Thornton, J. *Trends in biochemical sciences* **2005**, *30*, 622-629.

(40) Matsumura, I.; Kirsch, J. *Biochemistry* **1996**, *35*, 1881-1889.

(41) Liu, J.; Kurihara, T.; Ichiyama, S.; Miyagi, M.; Tsunasawa, S.; Kawasaki, H.; Soda, K.; Esaki, N. *Journal of Biological Chemistry* **1998**, *273*, 30897.

(42) Withers, S.; Rupitz, K.; Trimbur, D.; Warren, R. *Biochemistry* **1992**, *31*, 9979-9985.

(43) Ichiyama, S.; Kurihara, T.; Kogure, Y.; Tsunasawa, S.; Kawasaki, H.; Esaki, N. *Biochimica et Biophysica Acta (BBA)-Proteins & Proteomics* **2004**, *1698*, 27-36.

(44) Ichiyama, S.; Kurihara, T.; Li, Y.; Kogure, Y.; Tsunasawa, S.; Esaki, N. *Journal of Biological Chemistry* **2000**, *275*, 40804.

4 Chapter Four: Towards a Truncated Semi-Synthesis of Taxol Analogs

4.1 Introduction

4.1.1 Current Methods for the Semi-Synthesis of C-4 Modified Taxoids

Due to structural complexity of the taxol molecule, production by synthetic methodologies involved several steps and was consequently low yielding.[1] Additionally, increasing resistance to the taxane class of compounds by some tumors through cellular overexpression of efflux pumps[2] is a limiting factor in the continued use of the parent drug. Therefore, modified taxol molecules have been intensely pursued, rapidly synthesized, and their biochemical profiles carefully evaluated.[3-7] Although a big collection of efficacious taxol derivatives have been prepared for the better part of the last 20 years, only a small fraction has entered into clinical trials[2] (**Figure 4-1**). However, interest in the drug has not waned and will likely persist to the foreseeable future as taxol and its analogs continue to find new applications in various disease segments such as neurodegenerative diseases.[8,9]

Figure 4-1. Second generation taxoids that entered clinical trials (their current status is unknown).[2]

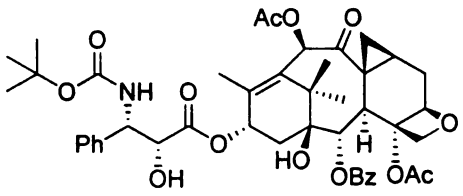

IV-1

RPR-109881A (Aventis Pharma)

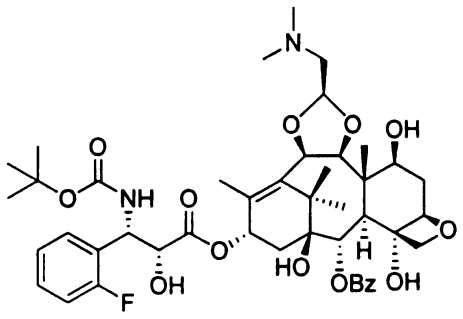

IV-2

DJ-927- (Daichi Pharmaceauticals)

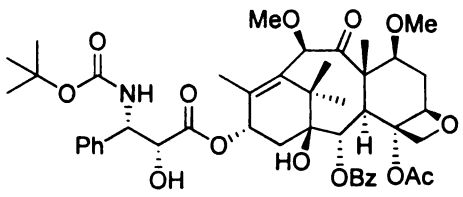

IV-3

RPR-116258A (Aventis Pharma)

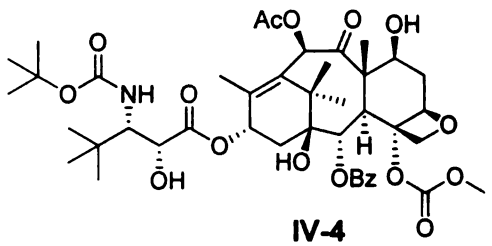

IV-4

BMS-275183 (Bristol-Myers Squibb)

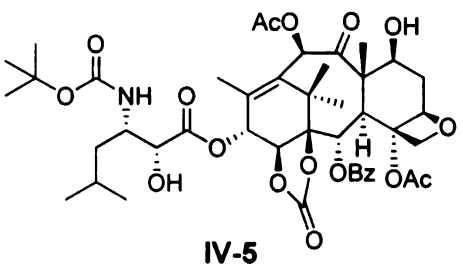

IV-5

BAY 59-8862 (Bayer/Indena)

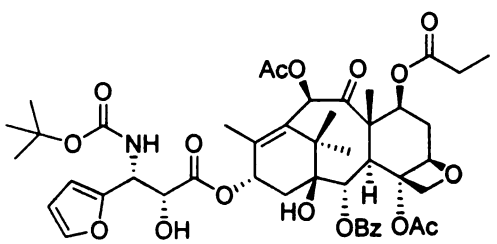

IV-6

MAC-321 (Wyeth)

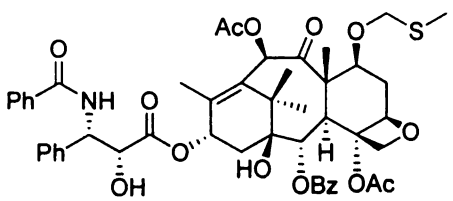

IV-7

BMS-184476 (Bristol-Myers Squibb)

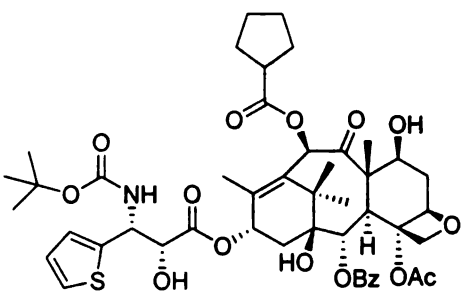

IV-8

MST-997 (Wyeth)

Rather than explore in general terms examples of strategic modifications of taxanes, this section will highlight particular features of the analogs in question, their intended clinical targets and outcome, or aspects of cancer chemotherapy that they seek to address. An example of a semi-synthetic methodology used to prepare taxol conjugates for tumor-targeted chemotherapy[10] will be presented. A second example will highlight a strategy that involves tethering the taxol molecule into a rigid macrocycle in order to increase the efficacy of the drug by reducing the number of solution-inactive conformations.[11]. By presenting the general strategy, rather than the versatility, of the protocols used in the preparation of C-4, C-10 and C-13 modified analogs, the technical redundancy inherent in some of these transformations will become apparent. The study presented herein Chapter 4 seeks to address, at least partially, some of these synthetic challenges.

4.1.2 Example 1: Development of Tumor-Specific Taxoids

Toxicity and undesirable side effects due to lack of tumor specificity by antineoplastic agents is recurring theme in cancer chemotherapy. This can be remedied in part by administration of drug conjugates that are tumor-specific.[10] As a general rule, a tumor-targeting drug delivery system (DDS) consists of a tumor recognition moiety, such as sugars, lectins, or antibodies, and a cytotoxic moiety connected directly or through a suitable linker to form a conjugate. This conjugate should be systemically nontoxic but should be readily cleaved to regenerate the active cytotoxic compound after internalization into the cancer cell.[10]

Monoclonal antibody (mAb)-taxoid immunoconjugates using disulfide linkers are currently under development.[12,13] An antibody-taxane conjugate (mAb-SB-T-12136, **IV-18**) has been synthesized and evaluated towards the development of tumor-specific cancer chemotherapy[10] (**Scheme 4-1**).

Scheme 4-1. Semi-synthesis of a taxoid-immunoconjugate (**IV-18**).[10]

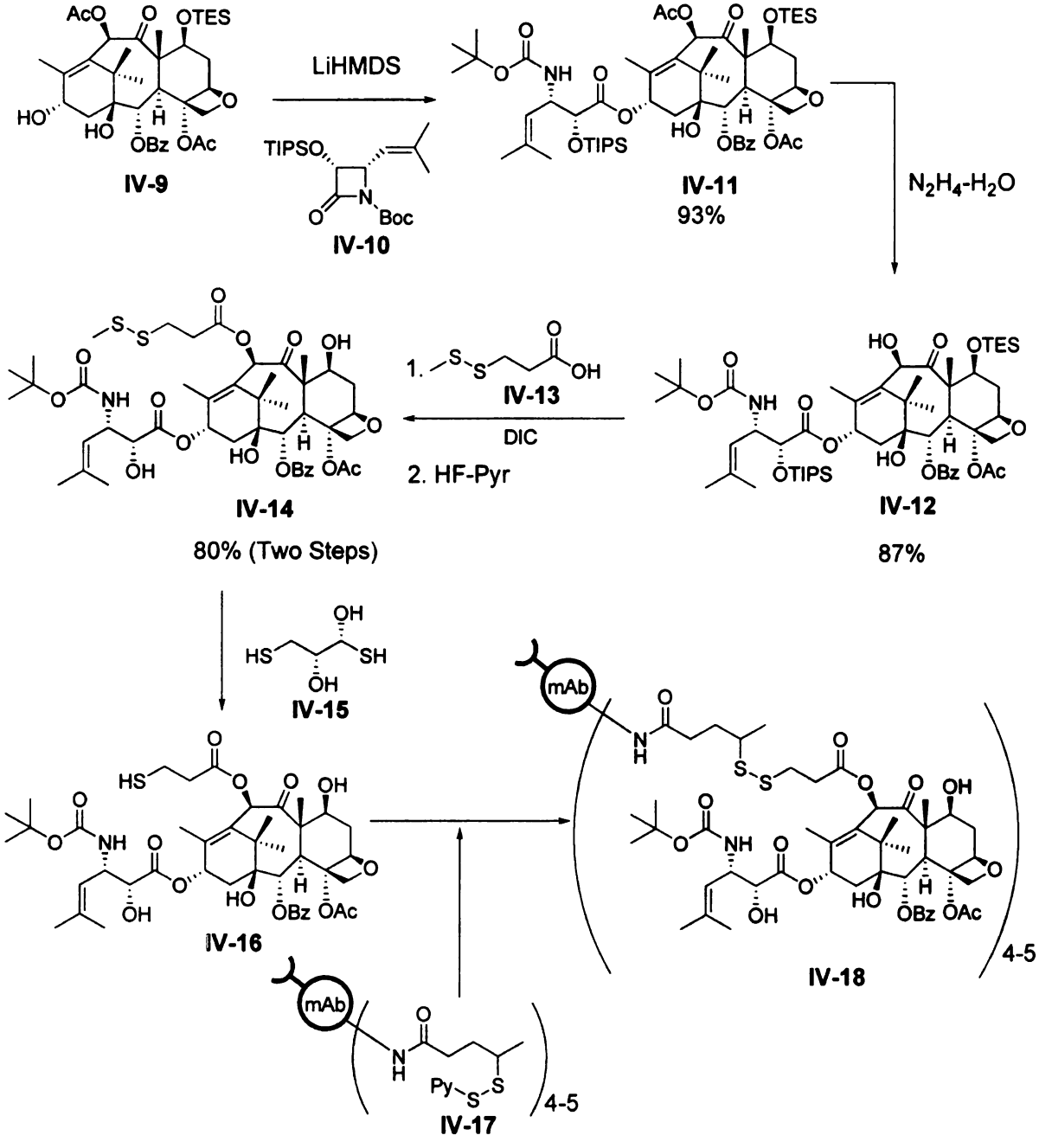

An antibody linked to a taxoid (**Scheme 4-1**) showed high potency (IC_{50} = 1.5 nM) against A431 cell line expressing the human epidermal growth factor receptor (EGFR), which is overexpressed in human squamous cancers.[10] However, since the taxoid released after glutathione reaction with immunoconjugate **IV-18** still retains part of the disulfide linker, the immunoconjugate was found to be 8 times weaker compared to the parent drug[14] (**Scheme 4-1**). Consequently, second-generation mechanism-based and self-cleaving disulfide linkers that completely cleave off the linker have been develop (**Scheme 4-2**).[14]

Scheme 4-2. A generic mechanism for self-cleavage of a disulfide linker in an mAb-taxoid conjugate.[10]

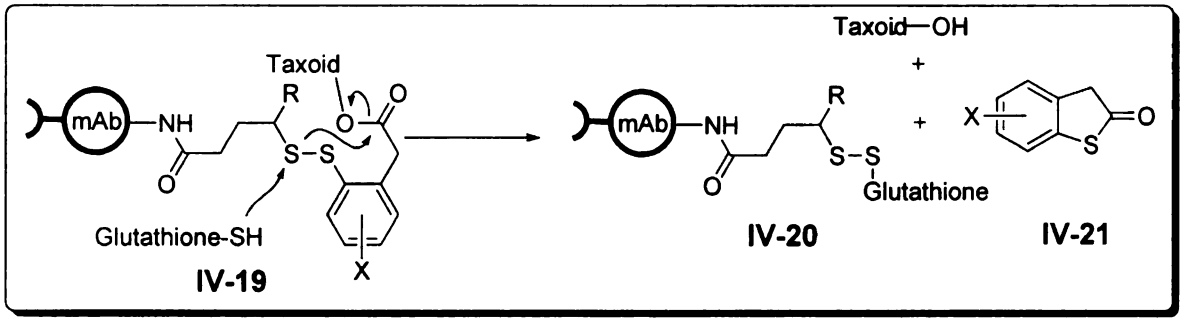

4.1.3 Example 2: Conformationally Rigid Taxol Macrocycle

Structure-activity relationship (SAR) studies and information from electron crystallography indicate that taxol has several binding conformation *in vivo*. One of these conformations is referred to as the T-taxol conformation,[11] and is arguably the closest approximation to the bioactive conformation. One of the features of this conformation is the juxtaposition of the C-3' phenyl group and the C-4 acetate within 2.5 Å of each other.[15] This model has guided synthetic efforts aimed at bridging the C-4 acetate and the

C-3' phenyl ring in order to conformationally constrain taxol and its derivatives to mimic the bioactive conformation.[16]

Semi-syntheses of macrocyclic taxol analogs involve preparation of β-lactams derivatives from *N*-(*p*-methoxy phenyl) (PMP) protected imines. These intermediate β-lactams are subsequently resolved using lipases[11] and are further modified to append necessary components for ring closing metathesis (RCM) reaction with the corresponding C-4 modified baccatin III derivatives. To prepare the C-4 deacyl substrates, 10-DAB is globally silyl-protected, deacylated at the C-4, and re-acylated at the same position with an appropriate alkenoyl group for the RCM reaction. These intermediates are then globally deprotected, selectively acetylated at the C-10 alcohol, coupled to the β-lactam through the C-13 alcohol; ring closure and deprotection steps lead to macrocyclic taxoids[11,16,17] such as **IV-33 (Scheme 4-3)**.

Scheme 4-3. Semi-synthesis of bridged taxol analogs based on the proposed T-Taxol conformation.[11]

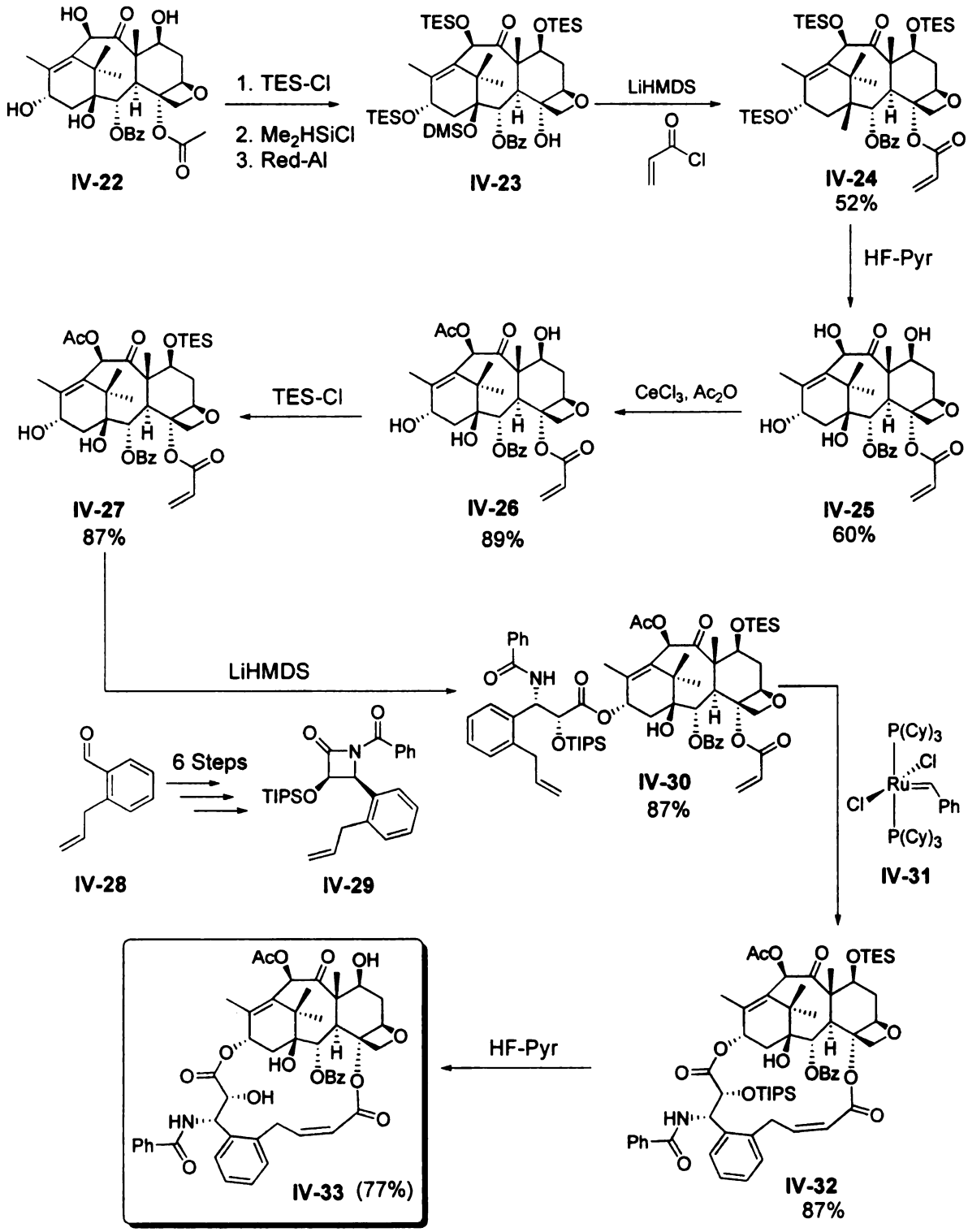

These macrocyclic taxanes, especially the *cis* conformer **IV-33**, possess up to 100-fold superior pharmacological activity against 1A9 human ovarian carcinoma cells compared to the parent drug.[11] They are also up to 1200-fold more effective towards taxol resistant cell line PTX10.

In the semi-synthesis of both the taxol-immunoconjugate and the macrocyclic taxane compound described in the foregoing discussion, redundant protecting groups are used to prevent unwanted reactions. The work presented herein Chapter 4 seeks to reduce the number of such protecting group manipulation to make the process more efficient.

4.2 Specific Aims

The studies described in the preceding chapters sought to establish the foundation for a biocatalytic process towards the production of pharmaceutically useful taxanes. However, these studies and other biochemical investigations on taxanes reported in the literature[18-20] are still under development. This implies that in the foreseeable future, production of efficacious Taxol® analogs will likely continue to rely on established semi-synthetic methodologies. Therefore, to improve chemical yields and expedite current synthetic methodologies, *the work described in this chapter primarily seeks to reduce the number of chemical transformations. The ultimate goal is to establish streamlined semi-synthetic protocols for use in tandem with the biochemical studies* described previously (cf. Chapter 2 and Chapter 3). Once optimized, these two approaches could provide an environmentally benign chemo-enzymatic process for the production of efficacious C-4 and C-13 modified taxanes.

Current methodologies for the semi-synthesis of modified taxanes use extensive protecting group manipulations on the several free hydroxyl groups of advanced taxane substrates[21,22] such as BMS-275183 (compound **IV-42** in **Scheme 4-4**).

Scheme 4-4. Synthesis of the oral Taxol analog BMS-275183 (IV-52) (i) $(i\text{-Pr})_2SiCl_2$; (ii) MeOH (85%); (iii) Me_2HSiCl (87%); (iv) Red-Al (97%); (v) LHMDS, MeOC(O)Cl (75%); (vi) TEA, HF (90%); (vii) $(i\text{-Pr})_2SiCl_2$; (viii) MeOH (84%); (ix) LHMDS, Ac_2O (60%); (x) LHMSD, β-lactam (54%); (xi) TEA, HF (71%).

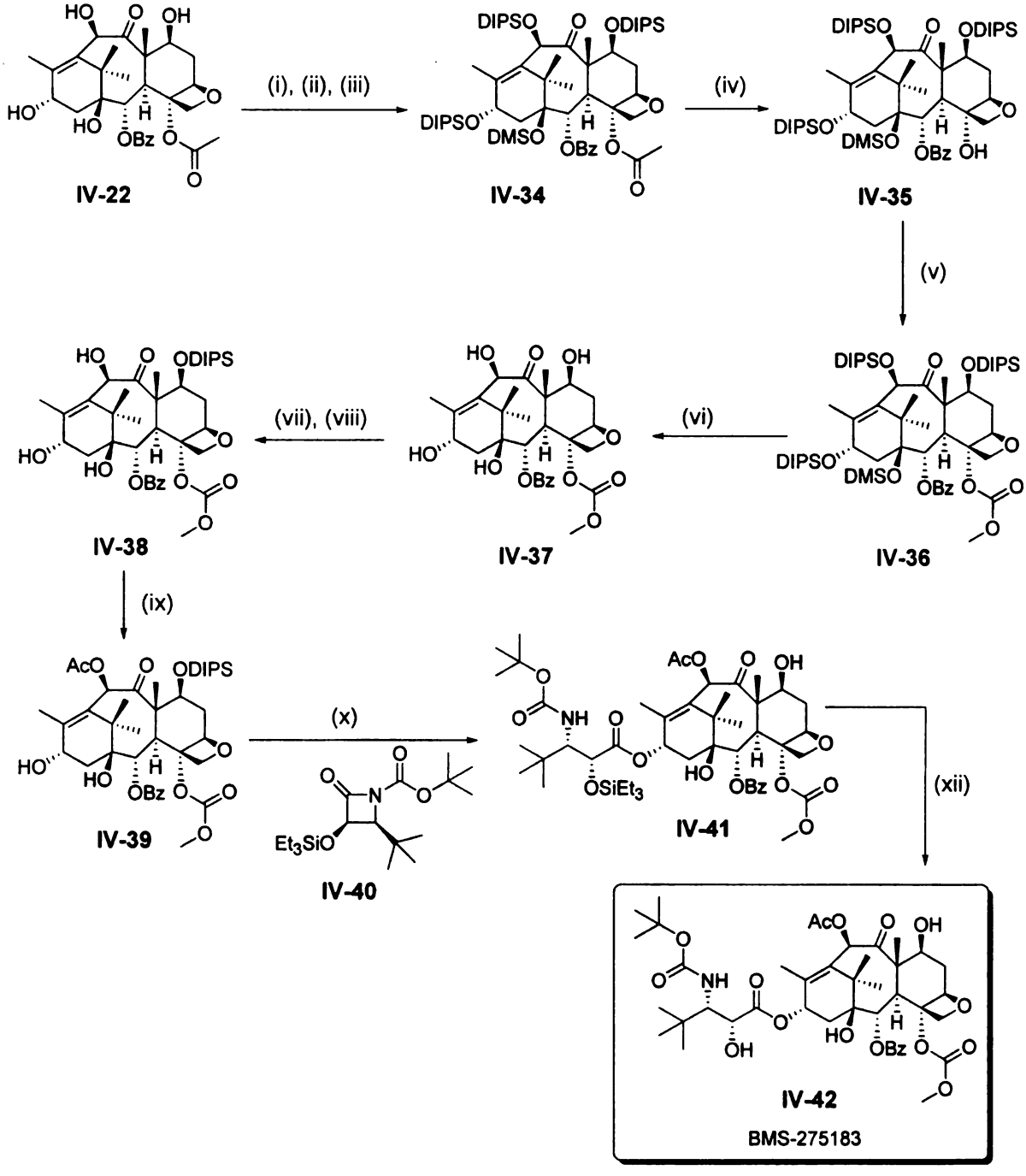

Although necessary, these transformations are often redundant and reduce the overall yield of the reactions. Thus, the aim of this study is to reduce the number of steps used in these transformations through a combination of one-pot reactions in parallel with strategies that exploit the neighboring group effects, sterics, and chemoselectivity of taxane substrates. *This investigation seeks to develop a single-step protection of the three hydroxyl groups* by taking advantage of the similar reactivity and reaction conditions of the silyl-based protecting groups. It is envisioned that the C-7 and C-13 hydroxyl groups of baccatin III or 10-deacetylbaccatin III could be protected using excess chlorotriethylsilane (TES-Cl) as commonly practiced.[11,21] The relatively inert tertiary hydroxyl group at C-1 is commonly protected with chlorodimethylsilane (DMS-Cl) under somewhat similar reaction conditions.[23] This indicates that the three hydroxyl groups could be protected consecutively but in a single reaction vessel without the need to isolate the C-7 and C-13 bis(triethylsilyl)-protected intermediate. This strategy eliminates two chemical steps from a step-wise silyl protection methodology previously reported.[24]

Due to the complexity of the taxol molecule and the inherent sensitivity of its functional groups, a number of bottlenecks are occasionally encountered during the semi-synthesis of its derivatives. Some of the challenges reported in the literature will be briefly discussed alongside unexpected reactions that were observed during the semi-synthesis of substrates used for the biochemical studies described in Chapter 2 and Chapter 3.

The differential reactivity of the hydroxyl groups on baccatin III dictates the order in which protecting groups can be introduced, which often results in redundant transformations. Therefore, finding the means to modulate this reactivity could

potentially eliminate extensive use of protecting groups. The molecular basis for the observed order of reactivity of baccatin III hydroxyl groups is will be discussed.

4.3 Experimental

A Varian Inova-300 or a Varian UnityPlus500 was used to acquire nuclear magnetic resonance (NMR) spectra. Chemical shifts are reported in δ units (ppm) using the residual ^{1}H- and ^{13}C signals of deuterated chloroform or acetone as reference. A Q-ToF Ultima API electrospray ionization tandem mass spectrometer (Waters, Milford, MA) was used for mass spectral analysis. An Agilent 1100 HPLC system (Agilent Technologies, Wilmington, DE) was employed for chromatographic separations. Reaction products were purified by flash chromatography or by preparative thin-layer chromatography (PTLC), and were visualized by UV absorbance at 254 nm. The purity of the synthetic compounds was determined by HPLC and/or ^{1}H-NMR. Baccatin III and 10-DAB were purchased from Natland Corporation (Research Triangle Park, NC). All the other reagents were obtained from Sigma-Aldrich and were used without purification unless otherwise indicated.

4.3.1 Synthesis of substrates

Figure 4-2. Synthesis of 1-Dimethylsilyl-7,13-bis(triethylsilyl)baccatin III.

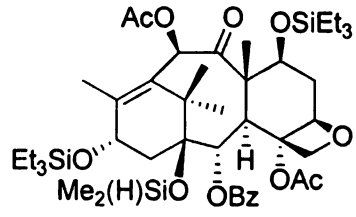

IV-43

To a solution of baccatin III (50 mg, 0.085 mmol) in DMF (3 mL) was added imidazole (70 mg, 1.02 mmol) and chlorotriethylsilane (285 μL, 1.7 mmol), and the

reaction mixture was stirred at 45 °C. After 3 h the reaction was judged to be complete by TLC monitoring. The reaction flask was cooled to 0 °C and chlorodimethylsilane (190 μL, 1.7 mmol) was added; the reaction mixture was stirred at the same temperature for 2 h. The reaction was warmed to room temperature over 2 h, quenched by adding water (20 mL), and diluted with EtOAc (50 mL). The organic fraction was washed with saturated brine and water (20 mL x 3 each), dried over Na_2SO_4, and purified by PTLC (20% EtOAc in hexanes) to give 1-dimethylsilyl-7,13-bis(triethylsilyl)baccatin III (**Figure 4-2**, compound **IV-43**) in 70% isolated yield, >99% purity by ^{1}H-NMR. The identity of the compound was verified by ESI-MS (positive ion mode), *m/z* 873.3 [M + H^+], 895.3 [M + Na^+]. ^{1}H NMR (300 MHz, $CDCl_3$) δ: −0.34 (d, *J* = 3 Hz, $CH_3Si(H)CH_3$), 0.00 (d, *J* = 3 Hz, $CH_3Si(H)CH_3$), 0.60 (m, CH_3CH_2Si–O), 0.92 (m, CH_3CH_2Si–O), 1.01 (s, CH_3–16), 1.4 (s, CH_3–17), 1.61 (s, CH_3–19), 1.80 (m, 6α), 2.00 (s, CH_3–18), 2.10 (s, $OC(O)CH_3$ at 10β), 2.20 (s, $OC(O)CH_3$ at 4α), 2.30 (m, 6β), 2.40 (m, 14α, β), 3.75 (d, *J* = 6 Hz, 3α), 4.17 (dd, *J* = 9 Hz, *J* = 9 Hz, 20α, 20β), 4.40 (dd, *J* = 6 Hz, *J* = 6 Hz, 7α), 4.50 (m, H-$Si(CH_3)_2$), 4.9 (m, 5α, 13α), 5.70 (d, *J* = 6 Hz, 2β), 6.40 (s, 10α), 7.4 (t, *J* = 6 Hz), 7.50 (t, *J* = 6 Hz), 8.00 (d, *J* = 6 Hz) [*m*-H, *p*-H, *o*-H of OBz, respectively].

Figure 4-3. Synthesis of 1-Dimethylsilyl-7-triethylsilyl-4-deacetylbaccatin III.

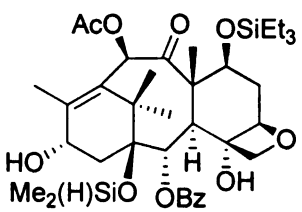

IV-44

To a solution of 1-dimethylsilyl-7,13-bis(triethylsilyl)baccatin III (48 mg, 0.082 mmol) in THF (2 mL) was added Red-Al (80 μL, 3.5 M solution in toluene) dropwise

over 5 min at 0 °C. The reaction was stirred for 40 min and quenched with 1 mL of saturated Na tartrate solution (pH 8.5), and the reaction mixture was stirred for 3 h. The solution containing crude product was diluted with EtOAc (20 mL), washed with an equal amount of water, and dried with Na_2SO_4. The organic layer was removed under vacuum, and the crude product was purified by PTLC (20:80 (v/v) EtOAc in hexane) to give 1-dimethylsilyl-7-triethylsilyl-4-deacetylbaccatin III (**Figure 4-3**, compound **IV-44**) in 70% yield and >99% purity by ^{1}H-NMR. The product was characterized by ESI-MS (positive ion mode), *m/z* 717.3 $[M + H]^+$, 739.3 $[M + Na]^+$ and by ^{1}H NMR (300 MHz, $CDCl_3$) δ: −0.40 (d, *J* = 3 Hz, $C\underline{H}_3Si(H)CH_3$), 0.00 (d, *J* = 3 Hz, $CH_3Si(H)C\underline{H}_3$), 0.50 (m, $C\underline{H}_3CH_2Si$–O), 0.90 (m, $CH_3C\underline{H}_2Si$–O), 1.00 (s, CH_3-16), 1.20 (s, CH_3-17), 1.60 (s, CH_3-19), 2.08 (s, CH_3-18), 2.13 (s, $OC(O)CH_3$ at 10β), 2.20 (s, $OC(O)CH_3$ at 4α), 2.30 (m, 6α, β), 2.6 (m, 14α, β), 3.30 (d, *J* = 6 Hz, 3α), 4.00 (dd, *J* = 6 Hz, *J* = 6 Hz, 7α), 4.20 (dd, *J* = 9 Hz, *J* = 9 Hz, 20α, 20β), 4.6 (m, $\underline{H}$-$Si(CH_3)_2$), 4.70 (dd, *J* = 3 Hz, *J* = 3 Hz, 5α), 4.9 (m, 13α), 5.60 (d, *J* = 6 Hz, 2β), 6.38 (s, 10α), 7.40 (t, *J* = 6 Hz), 7.50 (t, *J* = 6 Hz), 8.00 (d, *J* = 6 Hz) [*m*-H, *p*-H, *o*-H of OBz, respectively].

Figure 4-4. Synthesis of 1-Dimethylsilyl-7,13-bis(triethylsilyl)-4-deacetylbaccatin III.

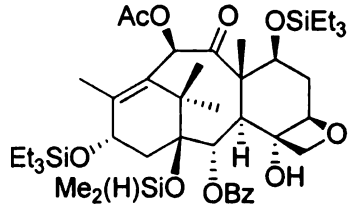

IV-45

The synthesis of 1-dimethylsilyl-7,13-bis(triethylsilyl)-4-deacetylbaccatin III was identical to that of 1-dimethylsilyl-4-deacetylbaccatin III (**Figure 4-3** compound **IV-44**) outlined above, except that during the quenching step with sodium tartrate solution (pH 8.5), the mixture was stirred for 5 min instead of 3 h. The crude product mixture was

worked up and purified by PTLC (20:80 (v/v) EtOAc in hexane) similar to the procedure described for compound **IV-44** to give 1-dimethylsilyl-7,13-bis(triethylsilyl)-4-deacetylbaccatin III (**Figure 4-4**, compound **IV-45**) in 53% yield and >97% purity by ^{1}H-NMR. The compound was characterized by ESI-MS and ^{1}H NMR. ESI-MS: *m/z* 831.3 $[M + H]^+$, 853.3 $[M + Na]^+$. ^{1}H NMR (300 MHz, $CDCl_3$) δ: −0.30 (d, *J* = 3 Hz, $C\underline{H}_3Si(H)CH_3$), 0.00 (d, *J* = 3 Hz, $CH_3Si(H)C\underline{H}_3$), 0.50 (m, $CH_3C\underline{H}_2Si$–O), 0.80 (m, $C\underline{H}_3CH_2Si$–O), 1.10 (s, CH_3–16), 1.20 (s, CH_3–17), 1.50 (s, CH_3–19), 2.00 (m, 6β), 2.1 (s, CH_3–18), 2.20 (s, $OC(O)CH_3$ at 10β), 2.30 (m, 6α), 2.4–2.8 (m, 14α, β), 3.50 (d, *J* = 6 Hz, 3α), 3.60 (bs, OH-4α), 4.1 (m, 7α), 4.20 (dd, *J* = 9 Hz, *J* = 9 Hz, 20α, 20β), 4.60 (m, $\underline{H}$-$Si(CH_3)_2$), 4.60–4.70 (m, 5α, 13α), 5.60 (d, *J* = 6 Hz, 2β), 6.40 (s, 10α), 7.40 (t, *J* = 6 Hz), 7.50 (t, *J* = 6 Hz), 8.00 (d, *J* = 6 Hz) [*m*-H, *p*-H, *o*-H of OBz, respectively].

4.3.2 Rate of Hydrolysis of Triethylsilyl Ether

To a solution of 1-dimethylsilyl-7,13-bis(triethylsilyl)baccatin III (compound **IV-43**) (160mg, 0.183 mmol) in THF (3 mL) at 0°C was added Red-Al (70% solution v/v in toluene, 250 μL, 1.26 mmol) dropwise within 1 minute. The reaction was stirred at this temperature for 2 hours after which saturated sodium tartrate (2 mL) was carefully added within 1 min and the reaction stirred at 0 °C for another 3 h; aliquots (250 μL) were then taken every 15 minutes within the first hour and every 30 min thereafter. Each aliquot was immediately quenched with saturated sodium tartrate (500 μL, pH 8.5), and the products in each aliquot were separately extracted into 500 μL of EtOAc. A fraction of this extract (50 μL) was diluted with 250 μL acetonitrile and analyzed by ESI-MS.

4.3.3 Assessment of the Conditions for Regioselective Desilylation

To determine the role of each reagent used in the work up in the selective deprotection of the C-13 triethylsilyl (TES) group, control experiments were conducted where each reagent was used separately with the appropriate silyl-protected baccatin III intermediate. For each control experiment, 250 μL aliquots were taken and immediately quenched with water (500 μL, pH 5.6) and the product was extracted into EtOAc (500 μL). A portion of the organic extract (50 μL) was diluted with acetonitrile (250 μL) and analyzed by ESI-MS (positive ion mode) as before.

To establish whether Red-Al alone was sufficient for reductive deprotection of the C-13 TES group, a time-course experiment was conducted and analyzed by ESI-MS. To a solution of 1-dimethylsilane-7,13-bis(triethylsilyl)-4-deacetylbaccatin III (compound **IV-45**) (20mg, 0.024 mmol) in THF (2 mL) at 0 °C was added Red-Al (5 μL, 0.025 mmol) and the reaction was monitored every 30 minutes for 3 hours by drawing 250-μL aliquots and analyzing by ESI-MS as described.

To determine whether Red-Al followed by work up with tap-water (as opposed to sodium tartrate) could casue the deprotection of the C-13 TES group, a solution of 1-dimethylsilane-7,13-bis(triethylsilyl)-4-deacetylbaccatin III (compound **IV-45**) (20mg, 0.024 mmol) in THF (2 mL) at 0 °C was treated with Red-Al (5 μL, 0.025 mmol) and the reaction was monitored by drawing 250-μL aliquots every 30 minutes for 3 hours and analyzed by ESI-MS as before.

To establish whether the deprotection of the C-13 TES group was due to reductive cleavage by Red-Al or base-mediated hydrolysis by sodium tartrate, a solution of 1-dimethylsilyl-7,13-bis(triethylsilyl)-4-deacetylbaccatin III (compound **IV-45**) (60mg,

0.069 mmol) in THF (2 mL) was treated with Red-Al (15 μL) at 0° C, aliquots were taken every 30 minutes for 3 hours after which sodium hydroxide (1 mL, pH 8.6) was added. After quenching with sodium hydroxide (pH 8.6), aliquots were again taken every 30 minutes for another 3 hours and similarly extracted and analyzed as described.

4.4 Results and Discussion

The goal of this study was to develop a semi-synthetic protocol that reduces the number of chemical transformations from the general scheme currently used to produce C-4 and C-13 modified taxane analogs.[11] The strategy outlined here combines two separate one-pot reactions to remove four chemical steps from the scheme (**Scheme 4-5**). This strategy diverges from current methodologies in that three hydroxyl groups were silyl-protected in one step as opposed to sequential introduction[24] commonly employed (**Scheme 4-4**). Trisilylation was achieved by using an excess (20 equivalents) of chlorotriethylsilane to protect the C-7 and C-13 alcohols. TLC monitoring indicated that the reaction had gone to completion within 6 hours. The reaction temperature was lowered to 0° C and chlorodimethylsilane was added to the same reaction vessel to protect the C-1 hydroxyl group (**Scheme 4-5**).

Scheme 4-5. One-pot trisilyl protection followed by selective reductive ester-reductive silyl cleavage. Literature protocol:[24] (i) TES-Cl, pyridine, 65%; (ii) TMS-Cl, imidazole; (iii) DMS-Cl, imidazole, 87% (2 steps); (iv) Red-Al, Sat. Na tartrate, 10 min, 85%. This study:[25] (a) TES-Cl, imidazole, then DMS-Cl, 65%; (b) Red-Al, then Na tartrate, 3 h, 70% (both steps are unoptimized).

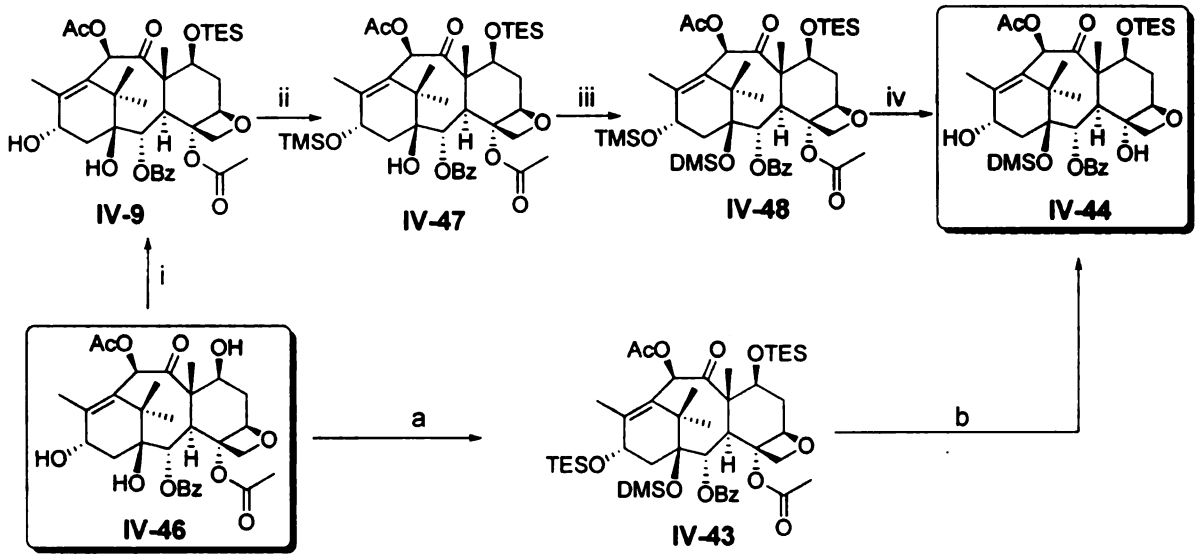

The C-4 acetate of the trisilyl-protected baccatin III substrate (compound **IV-43**) was selectively cleaved using Red-Al followed by standard quenching with sodium tartrate in less than 10 min.[24] However, when the sodium tartrate quench was extended to 3 h, the C-13 TES-group was cleanly cleaved while the more labile dimethylsilane on the C-1 alcohol and the C-7 TES group remained intact. Notably, selective deprotection of the C-13 TES group did not occur *prior* to the Red-Al mediated C-4 deacylation. Therefore, the basic sodium tartrate work up was initially thought to be responsible for the observed deprotection of the C-13 silyl group. However, the basic work up could not explain the selectivity in the cleavage of the C-13 silyl ether over the C-1 or C-7 silyl groups. Therefore, all the reagents used in the work up were sequentially evaluated to assess their role in the reaction.

4.4.1 Assessment of the Conditions for Regioselective Deprotection

To determine the conditions necessary to promote selective deprotection of the C-13 TES group, 1-dimethylsilyl-7,13-bis(triethylsilyl)-4-DAB (compound **IV-45**) was synthesized and separately treated with all the reagents used in the work-up. When reacted with Red-Al followed by aqueous work-up (water at pH 5.6) under identical reaction conditions as those that promoted C-13 TES hydrolysis, this compound did not undergo selective cleavage of the silyl ether (no reaction was observed). A similar treatment with the reductant but with basic workup (NaOH, pH 8.5) for the same time duration (3 h) did not result in the deprotection of the C-13 TES group. Moreover, no detectable products were observed when 1-dimethylsilyl-7,13-bis(triethylsilyl)-4-DAB was reacted with sodium tartrate (pH 8.5) in the absence of the reductant Red-Al, indicating that cleavage of the TES group was not base-promoted (**Scheme 4-6**). In

summary, the Red-Al reaction followed by sodium tartrate (pH 8.5) work up were the only sufficient conditions for selective deprotection of 1-dimethylsilyl-7,13-bis(triethylsilyl)baccatin III and 1-dimethylsilyl-7,13-bis(triethylsilyl)-4-DAB. This implies that both the reductant and sodium tartrate were necessary for this reaction.

Scheme 4-6. Assessing the conditions necessary for selective reductive acetyl- and silyl cleavage: (a) Red-Al 3 h, then Na tartrate (pH 8.5) 5 min, 53-80%; (b) Aqueous Na tartrate (pH 8.5) 3 h; (c) Red-Al 3 h, then Na tartrate (pH 8.5), 5 min; (d) Red-Al 3 h, then water (pH 5.6), 3 h; (e) Red-Al 3 h, then NaOH (pH 8.5), 3h; (f) Red-Al 3 h, then Na tartrate (pH 8.5), 3 h (70%).

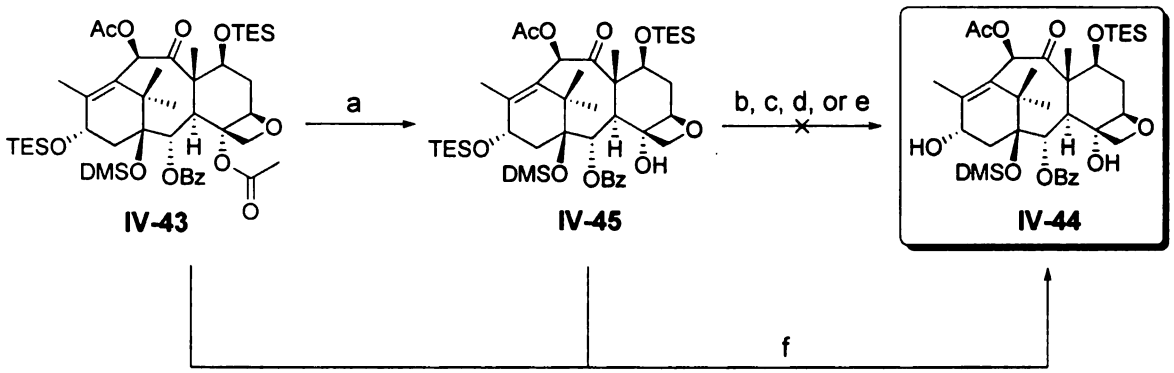

This finding prompted a search of the literature to establish whether this phenomenon has been observed with other taxane compounds. Selective cleavage of C-13 trimethylsilyl (TMS)-group has been reported under similar conditions[24]. However, in this report, the cleavage of the TMS group is proposed to occur during work up and the reaction is presumed be base-assisted hydrolysis of the labile TMS group.[24] However, systematic analysis of the reaction conditions in the study reported herein revealed that the reductant Red-Al plays a critical role in the reaction, indicating that the silyl ether undergoes reductive cleavage in sodium tartrate.

Reductive deprotection of silyl ethers on non-taxane substrates has been described previously.[26-28] In these reports, the presence of polar groups neighboring the silyl ether

(*tert*-butyldimethylsilyl, TBDMS) was presumed to be necessary for the reductive elimination of the silyl group.[26]

The mechanism for the intramolecular cleavage of TBDMS is proposed to involve direct hydride attack on the silyl group while aluminum is covalently bound to the polar group adjacent to the silyl group.[26,27] Formation of a cyclic pentavalent silicon intermediate has also been suggested but discounted due to lack of evidence for its existence[26] (**Scheme 4-7**).

Scheme 4-7. The proposed mechanism for intramolecular reductive cleavage of *tert*-butyldimethylsilyl ether, wherein a cyclic pentavalent silyl intermediate (**IV-71**) is also suggested.[26]

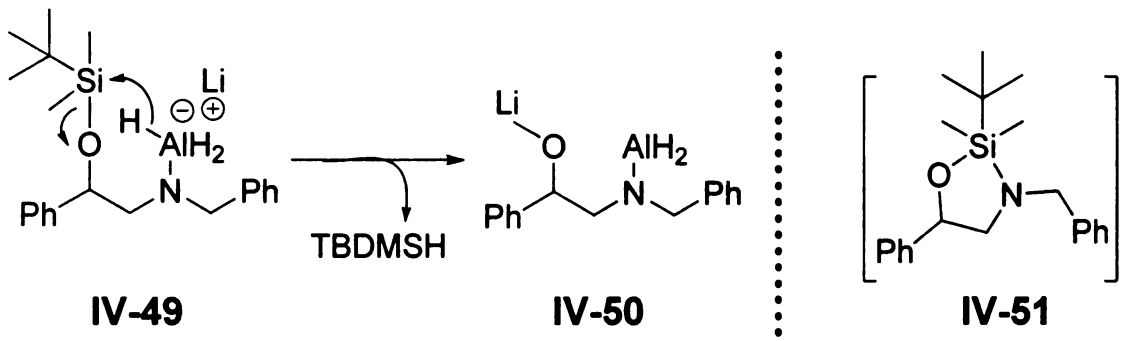

IV-49 **IV-50** **IV-51**

This argument can be extended to the current study to rationalize why selective desilylation of the C-13 TES group was not observed *prior* to the hydrolysis of the C-4 acetate. It seems plausible that after the acetate is cleaved, the free C-4 alcohol directs the reductant to the C-13 position for selective substrate-assisted cleavage of the silyl ether due to its relative proximity to the C-13 position. Unlike the mechanism proposed for the cleavage of TBDMS[26] (**Scheme 4-7**), the reduction of the TES group by Red-Al in the current study required sodium tartrate work up. Conceivably, sodium tartrate provides a better buffering effect than water and NaOH. However, it is also likely that sodium tartrate, being a good ligand for aluminum[29], might provide a coordination environment

that directs the hydride to the C-13 position (**Scheme 4-8**). This is plausible considering the loss of the C-4 acetyl group in 4-DAB that was part of a hydrogen bond in baccatin III (compound **IV-52** in **Scheme 4-8**). Therefore, in the absence of the C-4 acetate sodium tartrate could possibly play a bridging role for hydride delivery to the C-13 silyl group (**Scheme 4-8**).

Scheme 4-8. A putative hydrogen bind in baccatin III (**IV-52**), and the proposed mechanism for the reductive deprotection of C-13 TES group.

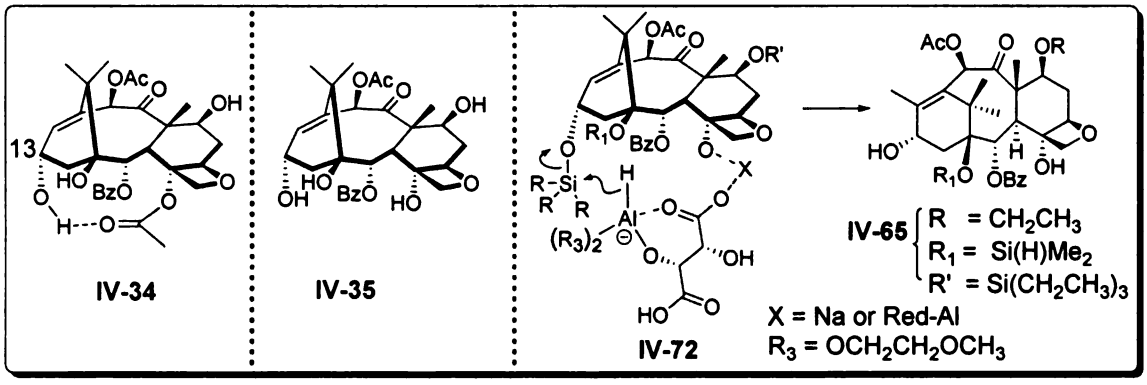

4.4.2 Rate of Selective Deprotection of Triethylsilyl Ether

After establishing the conditions responsible for the C-13 TES deprotection, it was necessary to determine the timing of the hydrolysis of the silyl ether. It is apparent that the reduction of the C-4 acetate by Red-Al is not sufficient to cause cleavage of the C-13 TES group without work up (cf. **Scheme 4-6**). Therefore, by monitoring the reaction progress before and after addition of sodium tartrate, it was determined that the cleavage of the silyl ether commenced after addition of sodium tartrate and became more pronounced with time (**Figure 4-5**). Since Red-Al is required for the deprotection of the silyl either (cf. **Scheme 4-6**), this time course indicates that sodium tartrate is also a necessary additive for the reaction to occur. Whether both reagents directly and jointly cleave the silyl group, as depicted in **Scheme 4-8**, is a matter of speculation.

Figure 4-5. Time-course for reductive cleavage of the C-13 silyl group from 1-DMS-7,13-bis(triethylsilyl)-4-DAB.

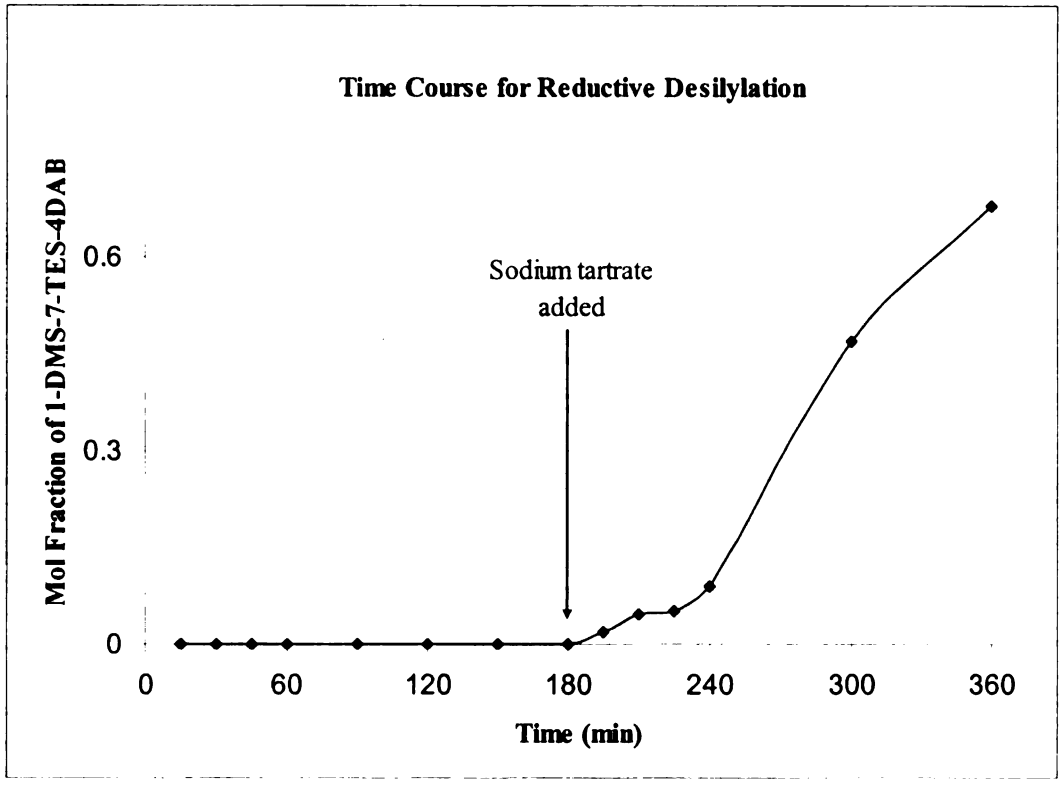

4.4.3 Potential Application in the Semi-synthesis of BMS-275183

Baccatin III structure possesses a putative intramolecular hydrogen bond between the C-13 alcohol and the C-4 acetate[30] and the proximal distance between these functional groups was envisioned to promote regioselective intramolecular cleavage of protecting groups attached to the C-13 hydroxyl (**Scheme 4-8**). Hydride reduction of the C-4 acetate has been reported[23] and the regioselectivity of this reaction is proposed to arise from coordination of the reducing reagent Red-Al to the oxetane oxygen at the C-5 position.[23,31] Thus, it was hypothesized that the free C-4 hydroxyl can serve as a coordination ligand for Red-Al and direct selective reductive cleavage of a silyl group at the C-13 position. Successful implementation of this strategy is demonstrated herein

Chapter 4; the selective cleavage of the C-13 protecting group removed two steps from currently used transformations routinely used in the semi-synthesis of BMS-275183[3] (**Scheme 4-9**). In this scheme, reductive cleavage of the C-4 ester is followed by C-4 acylation and one-pot deprotection of the C-1, C-7, and C-13 silyl-protected hydroxyl groups. The C-7 alcohol is then re-protected as a silyl ether prior to the attachment of the C-13 side chain. Conceivably, this route could be shortened by removing protecting group redundancy. Therefore, a one-pot trisilylation methodology and a process that directly couples the C-13 side chain to the silyl-protected C-4 deacyl analogs were envisioned that would remove a total of six steps from this semi-synthetic protocol[21,22] (**Scheme 4-9**).

Scheme 4-9. Comparison of a methodology for selective reductive ester-reductive silyl ether cleavage with a protocol used in the semi-synthesis of BMS-275183 (IV-42). Protocol currently used in the semi-synthesis of BMS-275183 (steps i-xi): (i) $(i\text{-Pr})_2SiCl_2$; (ii) MeOH (85%); (iii) Me_2HSiCl (87%); (iv) Red-Al (97%); (v) LHMDS, MeOC(O)Cl (75%); (vi) TEA, HF (90%); (vii) $(i\text{-Pr})_2SiCl_2$; (viii) MeOH (84%); (ix) LHMDS, Ac_2O (60%); (x) LHMSD, β-lactam (54%); (xi) TEA, HF (71%). An alternative strategy is proposed that uses five steps (steps i-v). After reversal of reactivity of hydroxyl groups, the C-13 hydroxyl is more reactive than the C-4 and C-7 hydroxyl groups. The dotted arrow indicates hypothetical transformations.

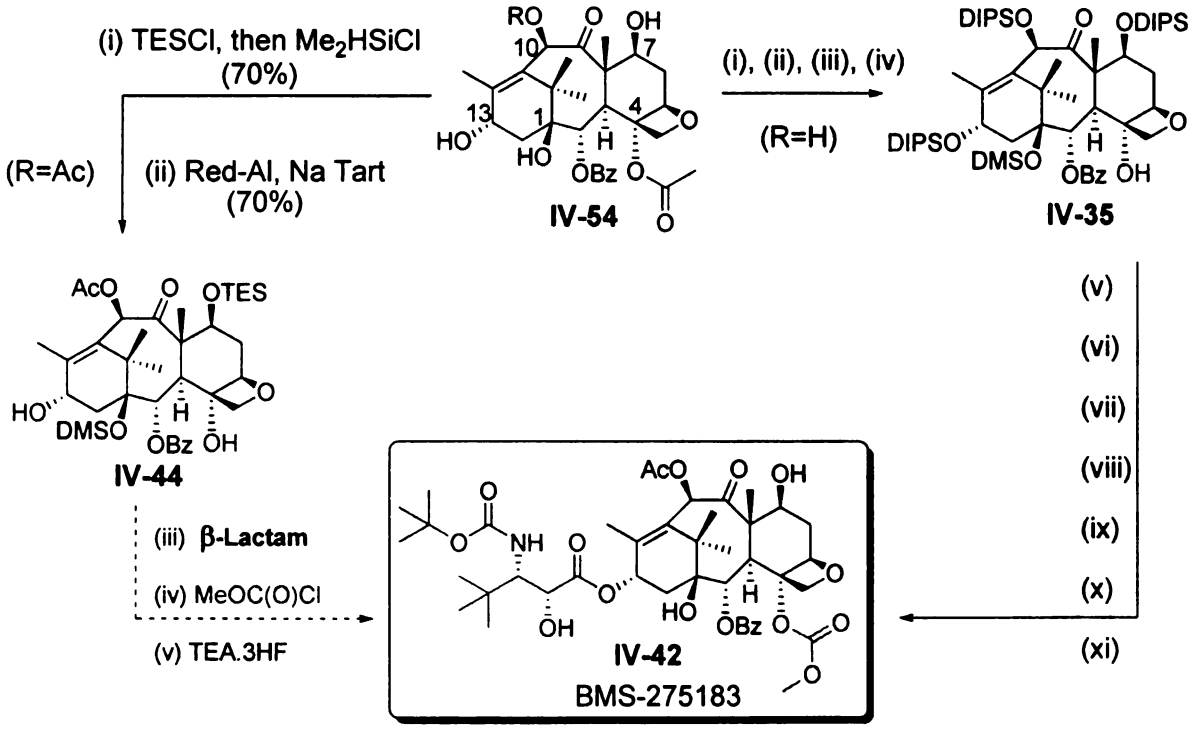

4.4.4 Molecular Basis for the Reactivity of Taxane Hydroxyl Groups

Studies for reductive cleavage of the C-4 acetate were undertaken to provide substrates and product standards for the biochemical studies described in Chapter 2 and Chapter 3. For example, the initial synthetic plan towards the semi-synthesis of 13-acetyl-4-DAB product standard involved deprotection of silyl-protected 4-DAB and subsequent conversion to 13-Acetyl-4-DAB. Surprisingly, treatment of 4-DAB with TES-Cl and imidazole resulted in facile silylation of the C-13 alcohol without the formation of the expected 7-TES-4DAB **(Scheme 4-10)**.

Scheme 4-10. Reversal of the reactivity order of the taxane hydroxyl groups after deacetylation of baccatin III, and application in the semi-synthesis of enzyme product standards.

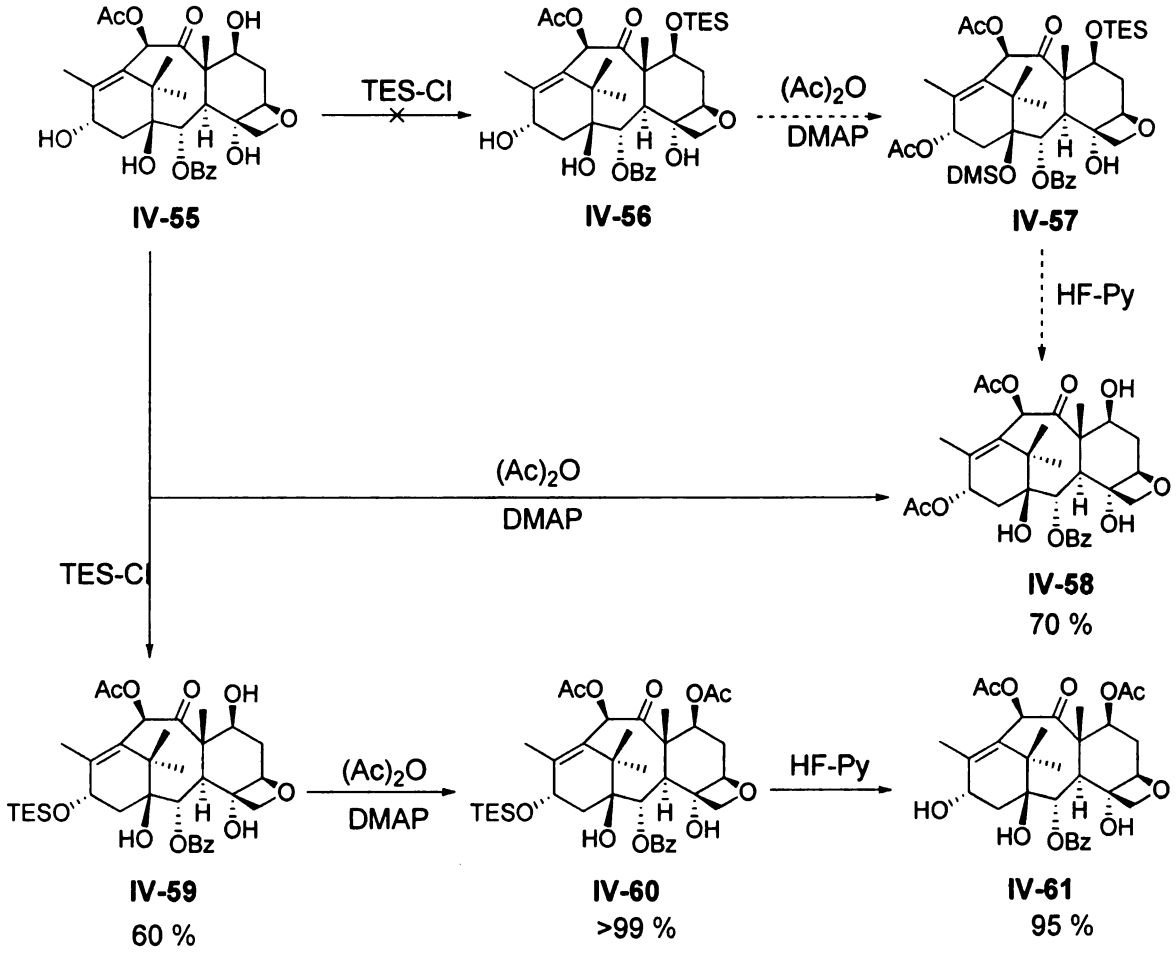

Apparently, removal of the C-4 acetate from baccatin III causes a switch in the order of reactivity of the 4-DAB hydroxyl groups where the C-13 hydroxyl is more reactive than the C-7 hydroxyl.[32]

The loss of the intra-molecular hydrogen bond between the C-4 acetate and the C-13 alcohol provides the molecular basis for the reactivity of the baccatin III hydroxyl groups. The switch in reactivity after removal of the C-4 ester of baccatin III indicates that the C-7 hydroxyl is more reactive primarily due to the inactivation of the C-13 hydroxyl group via an intramolecular hydrogen bond (cf. **Scheme 4-8**).

With this inversion of reactivity, it became evident that the C-13 sidechain of taxol or its derivatives could be attached to a substrate such as 4-DAB without the need to protect the C-7 hydroxyl group. Consequently, the 13-Acetyl-4-DAB product standard was conveniently semi-synthesized directly from 4-DAB without further silyl group manipulations. This was advantageous because others efforts to synthesize 13-Acetyl-4-DAB (**IV-76**) from 13-Acetylbaccatin III had failed to yield the desired 13-Acetyl-4-DAB product (**Scheme 4-10**).

4.4.5 Bottlenecks Encountered During Semi-synthesis of Taxol Analogs

As demonstrated in **Scheme 4-1**, **Scheme 4-3**, and **Scheme 4-9,** modification of taxol acyl groups is challenging because of the complex and poly-functional nature of taxol. To circumvent some of these challenges, semi-synthesis of taxane analogs is routinely carried out using protecting chemistry to mask reactive alcohols from participating in unwanted side reactions.[33-35] The most common examples of these side reactions include epimerization and skeletal rearrangements involving acyl migration or ring-opening.[36-38]

For example, three baccatin III analogs used in the biochemical studies described in Chapter 2 underwent epimerization at the C-7α stereogenic center (**Scheme 4-11**).

Scheme 4-11. Epimerization of the C-7 stereogenic center of baccatin III and its analogs.

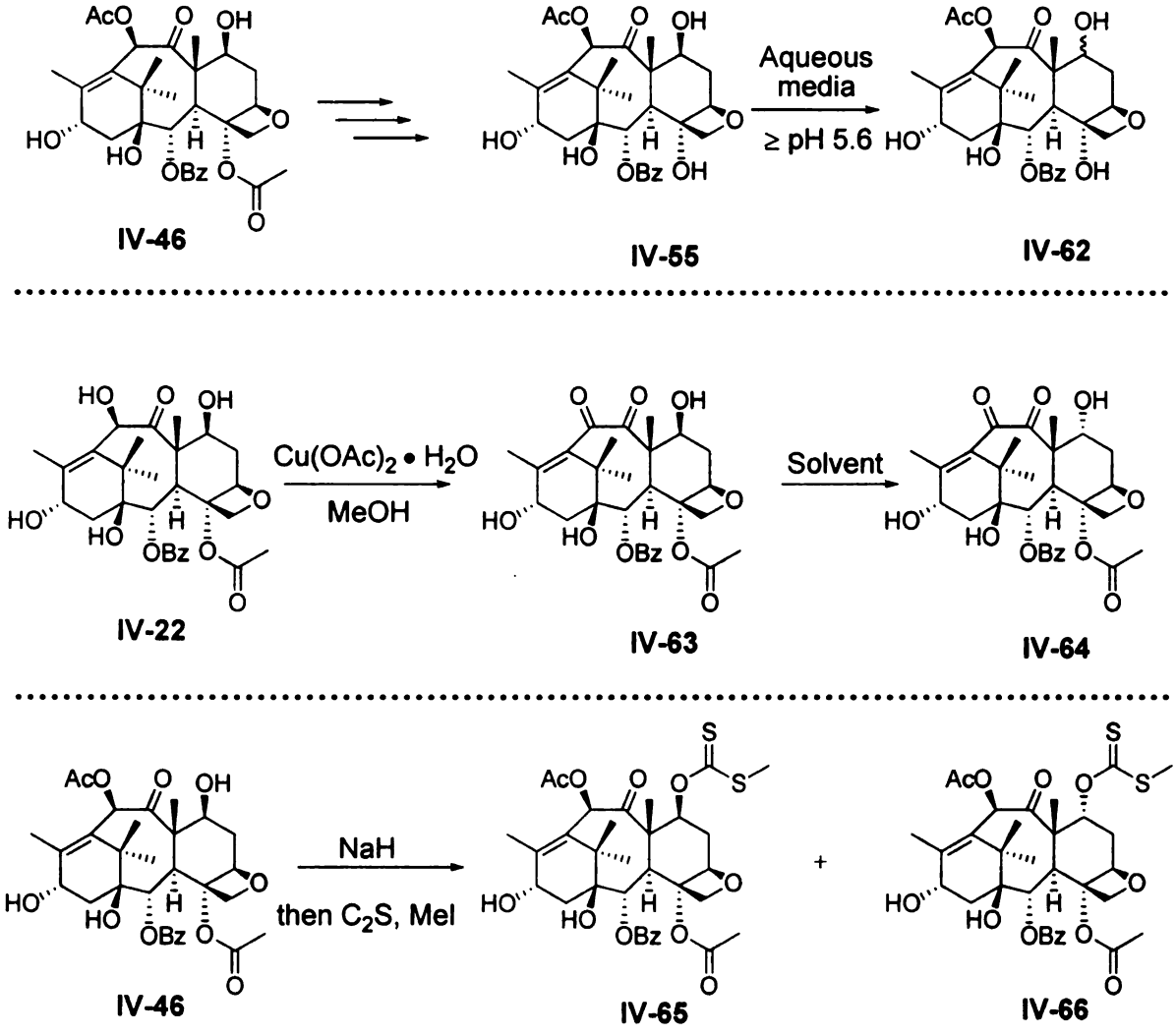

As a rationale for the epimerization reaction, it has been proposed that the C-7α hydroxyl of the epimer forms favorable hydrogen bond interaction with the C-4 acetate of baccatin III.[36,38] However, 4-DAB, a DBAT substrate which lacks the C-4 acetate, readily epimerized at the C-7α alcohol in aqueous media at pH 5.6 or higher (**Scheme 4-11**), which indicates that the proposed C-7α-OH/C-4α acetate hydrogen bond is insignificant.

The mechanism of the epimerization of the C-7 stereogenic center of baccatin III and its analogs is proposed to be due to retro-aldol-aldol chemistry involving the C-7 alcohol and the C-9 ketone[36,37] **(Scheme 4-12)**. Silyl protection of the C-7 alcohol prevents epimerization of the C-7 stereogenic center.[39]

Scheme 4-12. Proposed retro-aldol mechanism for epimerization of baccatin III under basic conditions;[36,37] B = base.

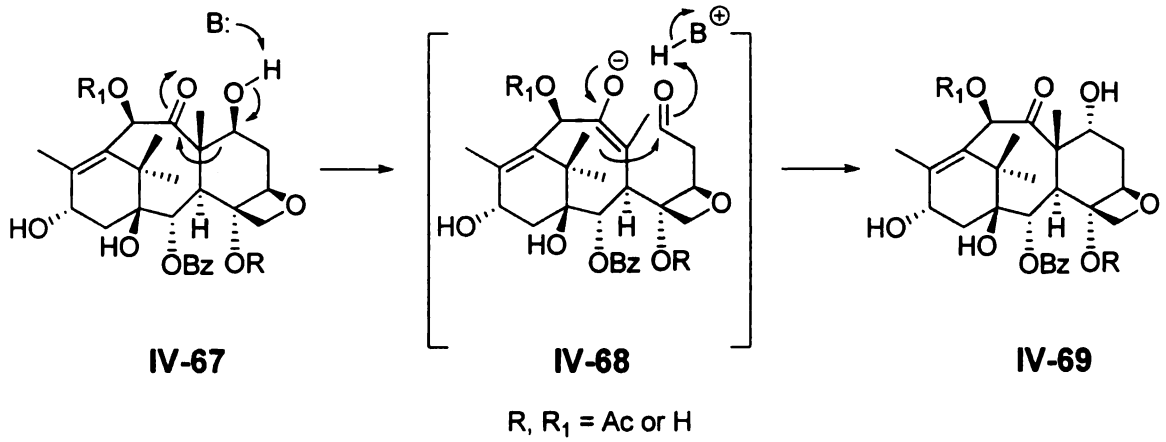

IV-67 **IV-68** **IV-69**

R, R_1 = Ac or H

In baccatin III, the C-10 acetate is the most accessible of the three acyl groups.[40] However, this accessibility makes the C-10 acetate susceptible to cleavage under strongly reducing conditions; this can become a synthetic challenge during acyl modification of taxanes.[41] For example, the semi-synthesis of BMS-275183commences with 10-DAB and the C-10 hydroxyl group is acetylated at a later stage[21] ((cf. **Scheme 4-4** and **Scheme 4.9**). This is necessary because reductive cleavage of the C-4 ester is accompanied by cleavage of the C-10 acetate when baccatin III is used as a substrate.[41] However, it is also important to note that the choice of 10-DAB over baccatin III in some synthetic schemes could be due to the higher natural abundance, and therefore ready availability, of 10-DAB over baccatin III.[42]

Cleavage of the C-2 benzoyl group also gives unexpected side products; for example, a method for selective hydrolysis using tributyltin methoxide resulted in clean debenzoylation but the resulting hydroxyl subsequently ring-opened the oxetane ring[43] (**Scheme 4-13**).

Scheme 4-13. Tributyltin methoxide-induced rearrangement of a baccatin III analog.[43]

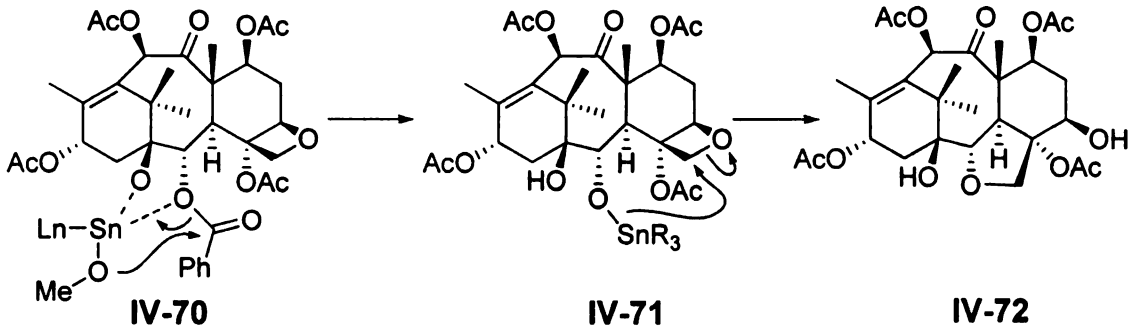

The acetate on the tertiary C-4 is not easily accessible during chemical modification of taxanes because it is relatively hindered compared to other acyl groups.[11] The presence of relatively more labile C-10 acetyl and C-2 benzoyl groups prevents selective cleavage of the C-4 ester without protecting group manipulations. Fortuitously, the adjacent oxetane ring aids in selective cleavage of the C-4 acetate by providing a coordination center for aluminum hydride, a reagent commonly used in the reductive cleavage of the C-4 acetate[31].

The oxetane ring found in advanced taxane substrates is susceptible to Lewis acids and base-catalyzed ring opening.[34] As an example, 7,13-dioxobaccatin, a substrate used in DBAT studies (discussed in Chapter III section **3.4.2**), underwent rearrangement resulting in an α-β (C-5/C-6) unsaturated system with concomitant opening of the oxetane ring and transfer of the 4-α acetate to the C-20 alcohol (**Scheme 4-14**). A similar rearrangement has been reportedly previously.[44,45]

Scheme 4-14. Proposed mechanism for the oxetane ring-opening after Jones' oxidation of baccatin III.

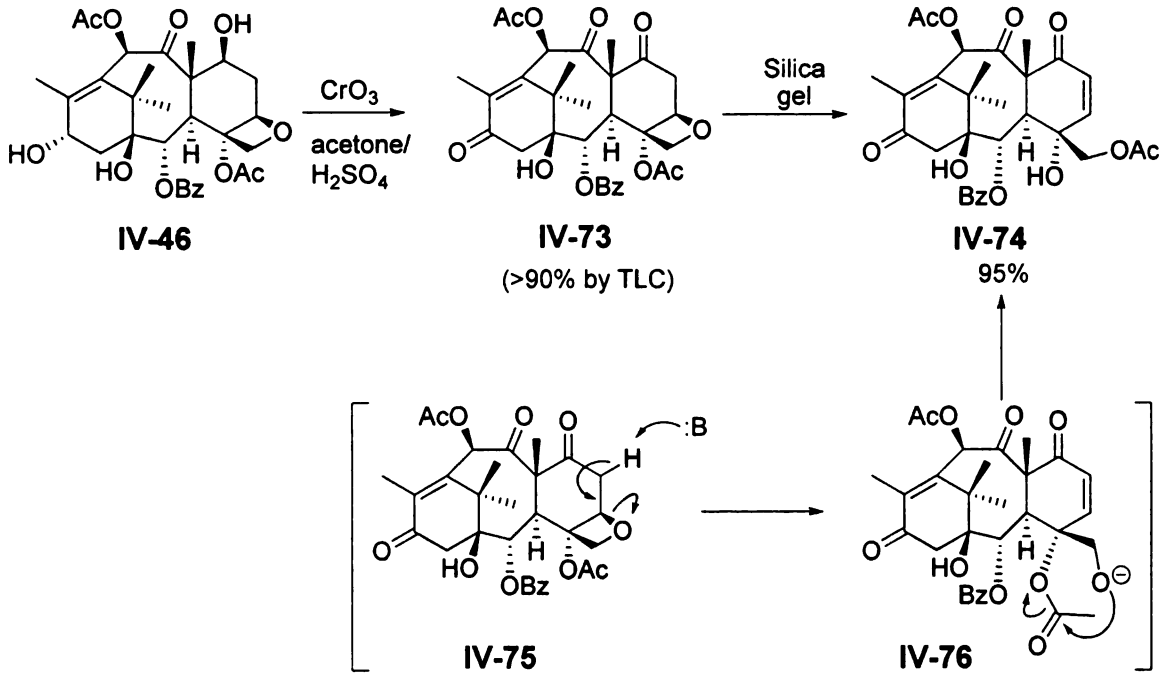

From the number of skeletal rearrangements and other side reactions reported for taxol and its analogs, it is apparent that planning a synthetic scheme involving a complex molecule requires careful evaluation of the reactivity of the functional groups already present. To mitigate some of the bottlenecks encountered during semi-synthesis of taxol analogs, the C-1, C-4, and C-10 hydroxyl groups of baccatin III or 10-DAB are commonly protected as silyl ethers.

The relative reactivity of the taxol hydroxyl groups towards acyl or silyl groups has been found be C-2'>C-7>C-10>C-13>C-1.[46] To circumvent the use of protecting groups, Lewis acids such as $ZnCl_2$ and lanthanides such as $CeCl_3$ have been used for selective acylation of the C-10 alcohol. These reagents coordinate to the proximal ketone at the C-9 position to direct acyl delivery to the C-10 hydroxyl group.[47-49] However, selective silylation of the C-10 hydroxyl in the presence of a free C-7 hydroxyl is rare.

The only report in literature, to my knowledge, for such an application involves *N-O*-bis(triethylsilyl)trifluroacetamide as a source of TES group.[50] The mechanism of this reaction is still unknown (**Scheme 4-15**).

Scheme 4-15. Selective C-10 acylation/silylation of 10-DAB (**IV-22**)[50] in the presence of a free C-7 hydroxyl group.

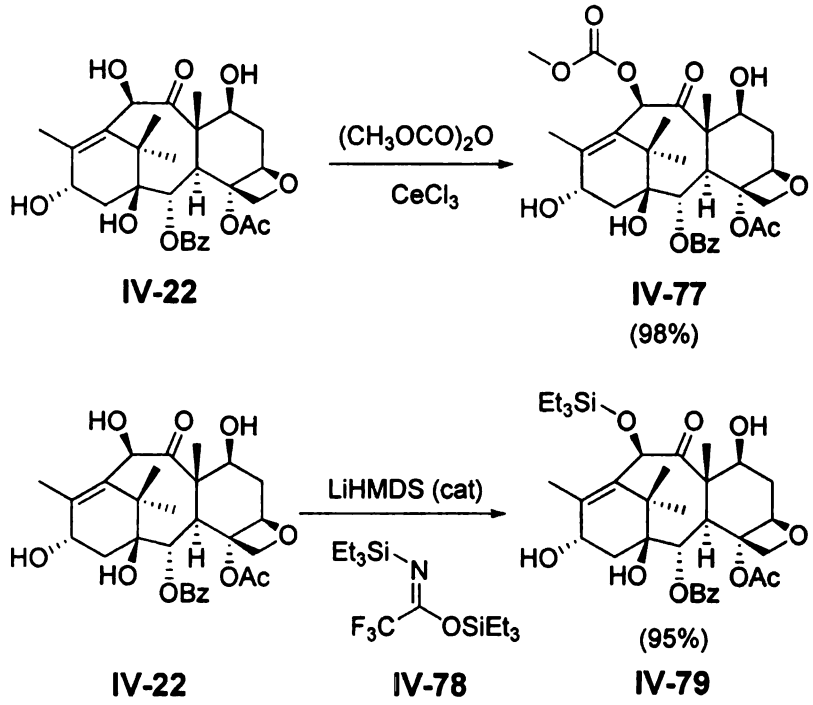

Alternative strategies that limit the number of deprotection steps include the use of different protecting groups that can be removed in one chemical step under a set of conditions where they are all labile. For example, prior to plant cell culture fermentation technology, commercial production of taxol primarily relied on coupling of a methoxypropyl (MOP)-protected azetidinone with silyl-protected protected 10-DAB[51] (**Scheme 4-16**). The two protecting groups are unmasked using trifluoroacetic acid (TFA) in aqueous acetic acid. From an industrial scale-up perspective, the use of milder deprotection conditions such as aqueous TFA mitigates the technical and safety risks associated with HF, a common reagent used in the deprotection of silyl ethers.[51]

Scheme 4-16. Trifluoroacetic acid-mediated cleavage of triethylsilyl protecting group.[51]

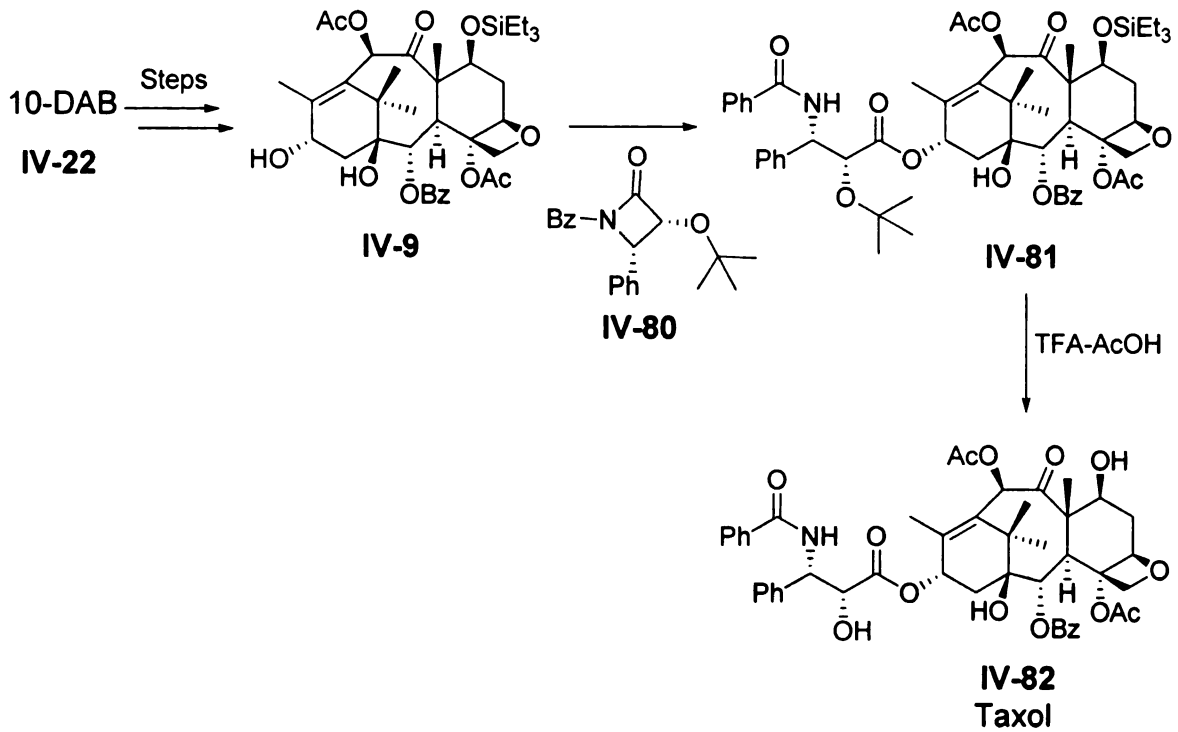

Although the strategies highlighted in the foregoing discussion indicate progress towards semi-synthetic schemes that are less dependent on protecting groups, such strategies are yet to gain routine application. Most methodologies used in the preparation of modified taxanes still rely on silyl ethers and other blocking groups to effect the desired modifications.

4.5 Significance

The aim of this study was to mitigate technical redundancy in protecting group manipulations during the semi-synthesis of C-4 and C-13-modified taxanes. Development of a methodology to introduce three silyl groups in one reaction vessel prior to the reductive cleavage of the C-4 acetate bodes well for a semi-synthetic scheme that is already burdened with multiple transformations to effect simple acyl substitutions. Once attached to baccatin III, it is difficult to routinely and selectively cleave one TES

protecting over the other. Instead, all the silyl groups are globally deprotected after the C-4 acyl substitution; the C-7 hydroxyl is then back-protected in a new round of blocking group chemistry before the attachment of the C-13 side chain.[3,11] Therefore, the discovery of a selective method for cleavage of the C-13 TES group is significant because repetitive silyl protection-deprotection of baccatin III or 10-DAB substrates can now be avoided entirely. Conceivably, semi-synthetic modifications of the C-13 hydroxyl can be achieved by direct attachment of an appropriately substituted β-lactam side chain onto a 4-deacetyl compound (**Scheme 4-9**).

Moreover, the finding that the reactivity of the hydroxyl groups in baccatin III derivatives such as 4-DAB can be reversed by cleavage of the C-4 ester (**Scheme 4-10**) is also significant. This strategy could possibly complement the selective hydrolysis of the C-13 silyl group discussed in sections **4.4.1-4.4.3**. The switch in reactivity implies that direct attachment of the taxol side-chain to silyl-protected 4-deacetylbaccatin III substrates can be achieved without the need for redundant protection-deprotection cycles. If used in combination, all the three strategies (one-pot trisilylation, one-pot selective deacylation-reductive desilylation, and inversion of reactivity) could remove a total of six chemical steps from the synthetic schemes currently used to produce C-4 and C-13-modified taxanes.[11,21,24]

More importantly, reducing the number of transformations from this semi-synthetic scheme translated into eliminating purification steps as well. This implies that the even though the alternative synthetic route presented in this study involves a modest reduction in the number of steps compared to currently used protocols, dramatic

improvement in the yield of modified taxanes can potentially be realized in large scale commercial production of the pharmaceuticals.

4.6 References

(1) Walji, A., MacMillan, D. *Synlett*, *10*, 1477-1489.

(2) Galletti, E.; Magnani, M.; Renzulli, Michela L.; Botta, M. *ChemMedChem* **2007**, *2*, 920-942.

(3) Mastalerz, H.; Cook, D.; Fairchild, C.; Hansel, S.; Johnson, W.; Kadow, J.; Long, B.; Rose, W.; Tarrant, J.; Wu, M. *Bioorganic & medicinal chemistry* **2003**, *11*, 4315-4323.

(4) Rose, W.; Fairchild, C.; Lee, F. *Cancer chemotherapy and pharmacology* **2001**, *47*, 97-105.

(5) Sampath, D.; Greenberger, L.; Beyer, C.; Hari, M.; Liu, H.; Baxter, M.; Yang, S.; Rios, C.; Discafani, C. *Clinical Cancer Research* **2006**, *12*, 3459.

(6) Galletti, E.; Magnani, M.; Renzulli, M.; Botta, M. *ChemMedChem* **2007**, *2*, 920-942.

(7) Kingston, D.; Newman, D. *Current Opinion in Drug Discovery and Development* **2007**, *10*, 130.

(8) Sgadari, C.; Toschi, E.; Palladino, C.; Barillari, G.; Carlei, D.; Cereseto, A.; Ciccolella, C.; Yarchoan, R.; Monini, P.; Sturzl, M.; Ensoli, B. *Journal of Immunology* **2000**, *165*, 509-517.

(9) Park, S.; Shim, W.; Ho, D.; Raizner, A.; Park, S.; Hong, M.; Lee, C.; Choi, D.; Jang, Y.; Lam, R. *New England Journal of Medicine* **2003**, *348*, 1537.

(10) Ojima, I. *Accounts of Chemical Research* **2008**, *41*, 108-119.

(11) Ganesh, T.; Yang, C.; Norris, A.; Glass, T.; Bane, S.; Ravindra, R.; Banerjee, A.; Metaferia, B.; Thomas, S. L.; Giannakakou, P.; Alcaraz, A. A.; Lakdawala, A. S.; Snyder, J. P.; Kingston, D. G. *Journal of medicinal chemistry* **2007**, *50*, 713-25.

(12) Ojima, I.; Geng, X.; Wu, X.; Qu, C.; Borella, C.; Xie, H.; Wilhelm, S.; Leece, B.; Bartle, L.; Goldmacher, V. *Journal of Medicinal Chemistry* **2002**, *45*, 5620-5623.

(13) Guillemard, V.; Saragovi, H. *Cancer research* **2001**, *61*, 694.

(14) Chen, S.; Zhao, X.; Chen, J.; Kuznetsova, L.; Wong, S.; Ojima, I. *Bioconjugate Chemistry*, *21*, 979-987.

(15) Kingston, D. G. I.; Bane, S.; Snyder, J. P. *Cell Cycle* **2005**, *4*, 279-289.

(16) Ganesh, T.; Guza, R. C.; Bane, S.; Ravindra, R.; Shanker, N.; Lakdawala, A. S.; Snyder, J. P.; Kingston, D. G. I. *Proceedings of the National Academy of Sciences* **2004**, *101*, 10006-10011.

(17) Ganesh, T.; Norris, A.; Sharma, S.; Bane, S.; Alcaraz, A. A.; Snyder, J. P.; Kingston, D. G. I. *Bioorganic & Medicinal Chemistry* **2006**, *14*, 3447-3454.

(18) Frense, D. *Applied Microbiology and Biotechnology* **2007**, *73*, 1233-1240.

(19) DeJong, J. M.; Liu, Y.; Bollon, A. P.; Long, R. M.; Jennewein, S.; Williams, D.; Croteau, R. B. *Biotechnology and Bioengineering* **2006**, *93*, 212-224.

(20) Tabata, H. *Biomanufacturing* **2004**, 1-23.

(21) Mastalerz, H.; Cook, D.; Fairchild, C. R.; Hansel, S.; Johnson, W.; Kadow, J. F.; Long, B. H.; Rose, W. C.; Tarrant, J.; Wu, M.-J.; Xue, M. Q.; Zhang, G.; Zoeckler, M.; Vyas, D. M. *Bioorganic & Medicinal Chemistry* **2003**, *11*, 4315-4323.

(22) Kant, J.; Bristol-Myers Squibb Company.: USA, 2001.

(23) Chen, S.; Kadow, J.; Farina, V.; Fairchild, C.; Johnston, K. *Journal of Organic Chemistry* **1994**, *59*, 6156-6158.

(24) Chen, S.; Farina, V.; Vyas, D.; DoyleP, T.; Long, B.; Fairchild, C. *Journal of Organic Chemistry* **1996**, *61*, 2065-2070.

(25) Ondari, M. E.; Walker, K. D. *Journal of Organic Chemistry* **2009**, *74*, 2186-2188.

(26) de Vries, E.; Brussee, J.; Van der Gen, A. *Journal of Organic Chemistry* **1994**, *59*, 7133-7137.

(27) Saravanan, P.; Gupta, S.; DattaGupta, A.; Singh, V. *Synthetic Communications* **1997**, *27*, 2695-2699.

(28) Patel, P.; Chang, C.; Kang, N.; Lee, G.; Powell, W.; Rokach, J. *Tetrahedron Letters* **2007**, *48*, 5289-5292.

(29) Amundsen, L.; Nelson, L. *Journal of the American Chemical Society* **1951**, *73*, 242-244.

(30) Nicolaou, K.; Nantermet, P.; Ueno, H.; Guy, R.; Couladouros, E.; Sorensen, E. *Journal of the American Chemical Society* **1995**, *117*, 624-633.

(31) Chen, S.-H.; Wei, J.-M.; Long, B. H.; Fairchild, C. A.; Carboni, J.; Mamber, S. W.; Rose, W. C.; Johnston, K.; Casazza, A. M.; et al. *Bioorganic & Medicinal Chemistry Letters* **1995**, *5*, 2741-6.

(32) Ondari, M. E.; Walker, K. D. *Journal of the American Chemical Society* **2008**, *130*, 17187-17194.

(33) Appendino, G.; Fenoglio, I.; Vander Velde, D. *Journal of Natural Products* **1997**, *60*, 464-466.

(34) Chen, S.; Huang, S.; Wei, J.; Farina, V. *Tetrahedron* **1993**, *49*, 2805-2828.

(35) Chen, S.-H.; Huang, S.; Gao, Q.; Golik, J.; Farina, V. *Journal of Organic Chemistry* **1994**, *59*, 1475-84.

(36) McLaughlin, J.; Miller, R.; Powell, R.; Smith Jr, C. *Journal of Natural Products* **1981**, *44*, 312-319.

(37) Tian, J.; Stella, V. *Journal of Pharmaceutical Sciences* **2008**, *97*, 1224-1235.

(38) Georg, G. I.; Cheruvallath, Z. S. *Journal of Organic Chemistry* **1994**, *59*, 4015-18.

(39) Samaranayake, G.; Neidigh, K.; Kingston, D. *Journal of Natural Products* **1993**, *56*, 884-898.

(40) Datta, A.; Hepperle, M.; Georg, G. *Journal of Organic Chemistry* **1995**, *60*, 761-763.

(41) Kingston, D.; Chaudhary, A.; Chordia, M.; Gharpure, M.; Gunatilaka, A.; Higgs, P.; Rimoldi, J.; Samala, L.; Jagtap, P.; Giannakakou, P. *Journal of Medicinal Chemistry* **1998**, *41*, 3715-3726.

(42) Patel, R. N. *Annual Review of Microbiology* **1998**, *52*, 361-395.

(43) Farina, V.; Huang, S. *Tetrahedron Letters* **1992**, *33*, 3979-3982.

(44) Magri, N.; Kingston, D. *Journal of Organic Chemistry* **1986**, *51*, 797-802.

(45) Barboni, L.; Datta, A.; Dutta, D.; Georg, G.; Vander Velde, D.; Himes, R.; Wang, M.; Snyder, J. *Journal of Organic Chemistry* **2001**, *66*, 3321-3329.

(46) Gueritte-Voegelein, F.; Senilh, V.; David, B.; Guenard, D.; Potier, P. *Tetrahedron* **1986**, *42*, 4451-4460.

(47) Damen, E.; Braamer, L.; Scheeren, H. *Tetrahedron Letters* **1998**, *39*, 6081-6082.

(48) Holton, R. In *United States Patent 2004/0122055 A1*, 2004.

(49) Holton, R. In *United States Patent US 2004/0072872 A1*, 2004.

(50) Holton, R.; Zhang, Z.; Clarke, P.; Nadizadeh, H.; Procter, D. *Tetrahedron Letters* **1998**, *39*, 2883-2886.

(51) Singh, A.; Weaver, R.; Powers, G.; Rosso, V.; Wei, C.; Lust, D.; Kotnis, A.; Comezoglu, F.; Liu, M.; Bembenek, K. *Organic Process Research & Development* **2002**, *7*, 25-27.

APPENDIX

Figure A1. 4-Deacetylbaccatin III

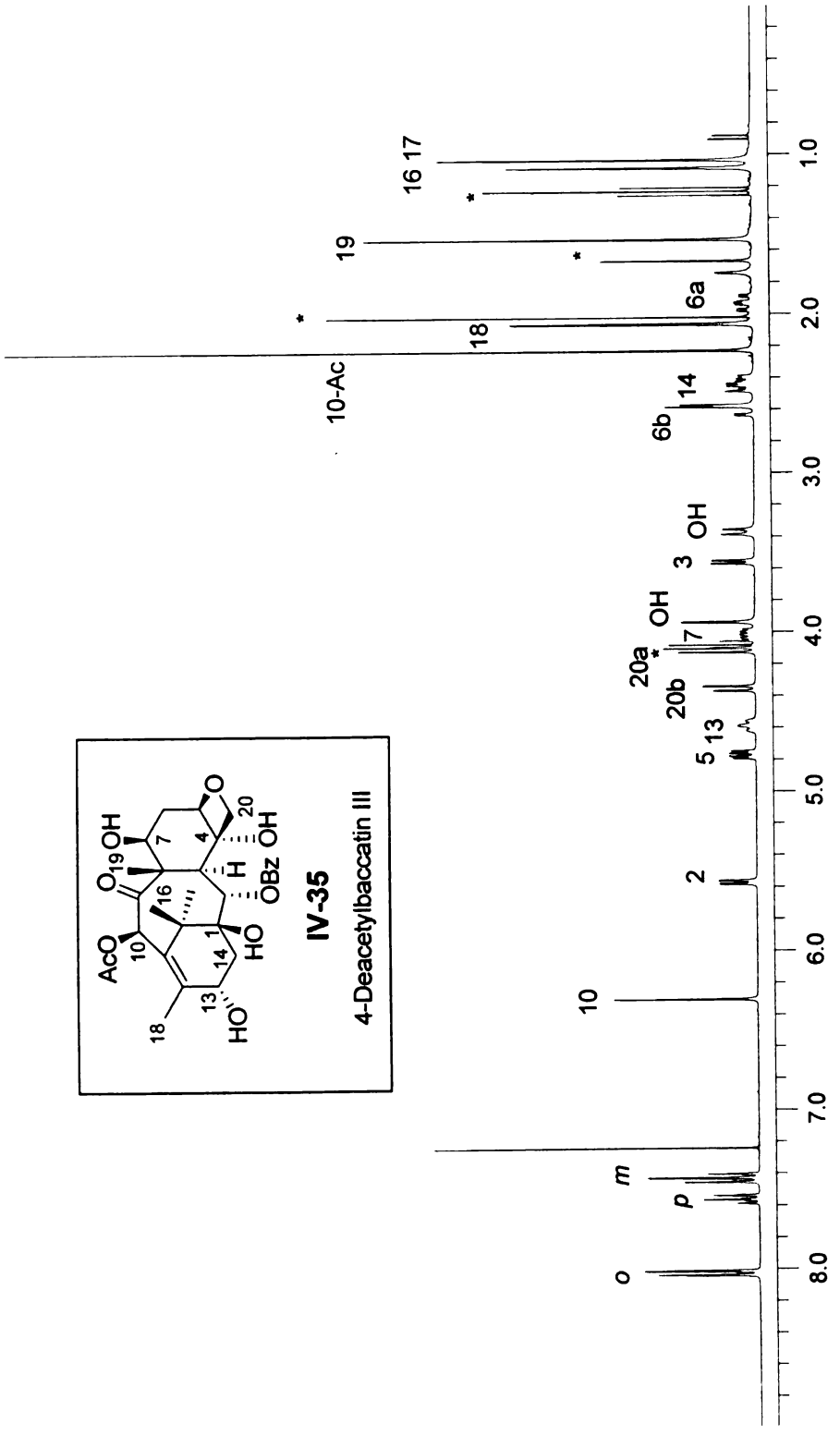

Figure A-2. 7-Acetyl-4-deacetylbaccatin III

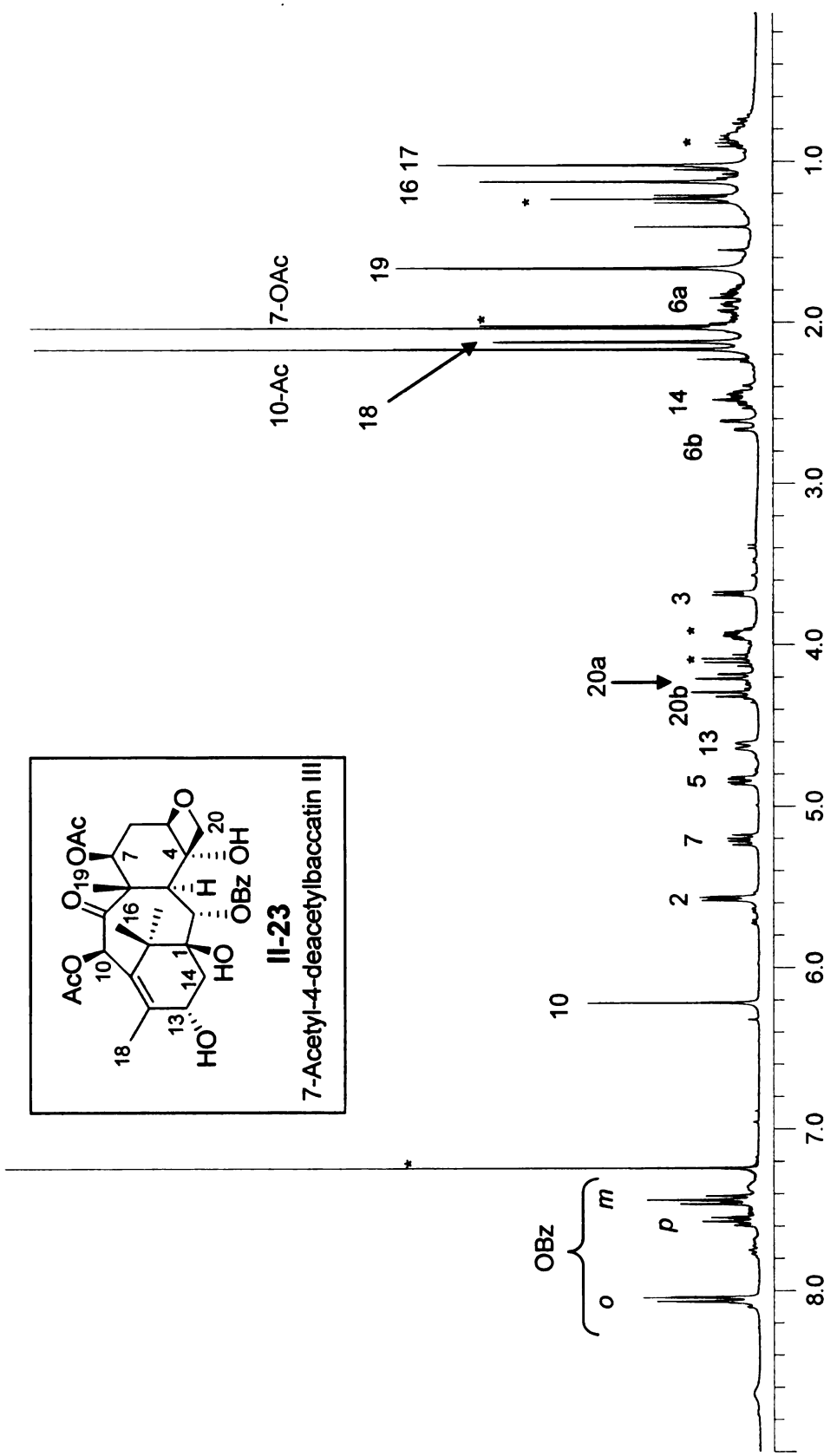

Figure A-3. 13-Acetyl-4-deacetylbaccatin III

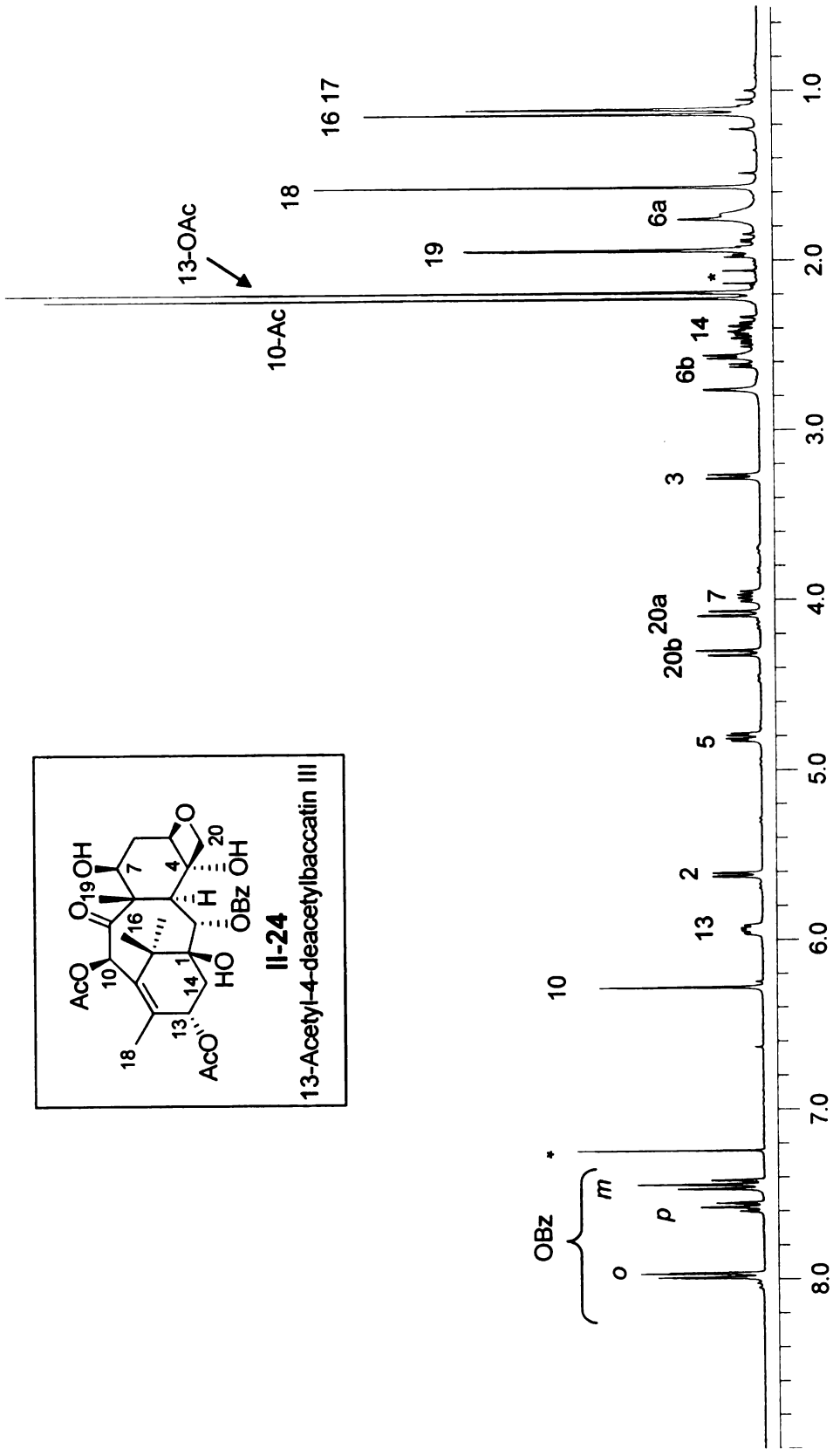

Figure A-4. 7,13-Diacetyl-4-deacetylbaccatin III

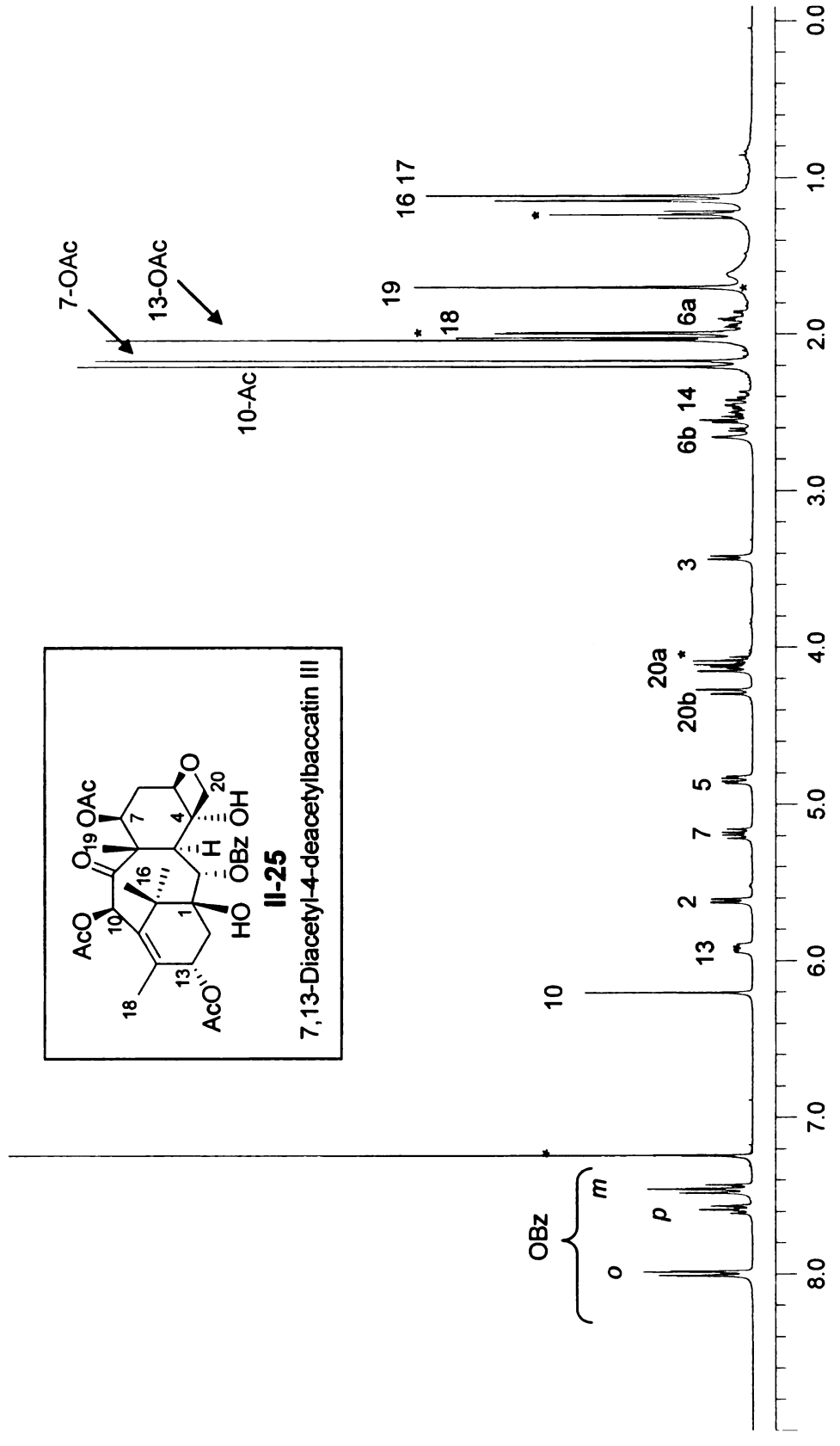

Figure A-5. 13-Acetylbaccatin III

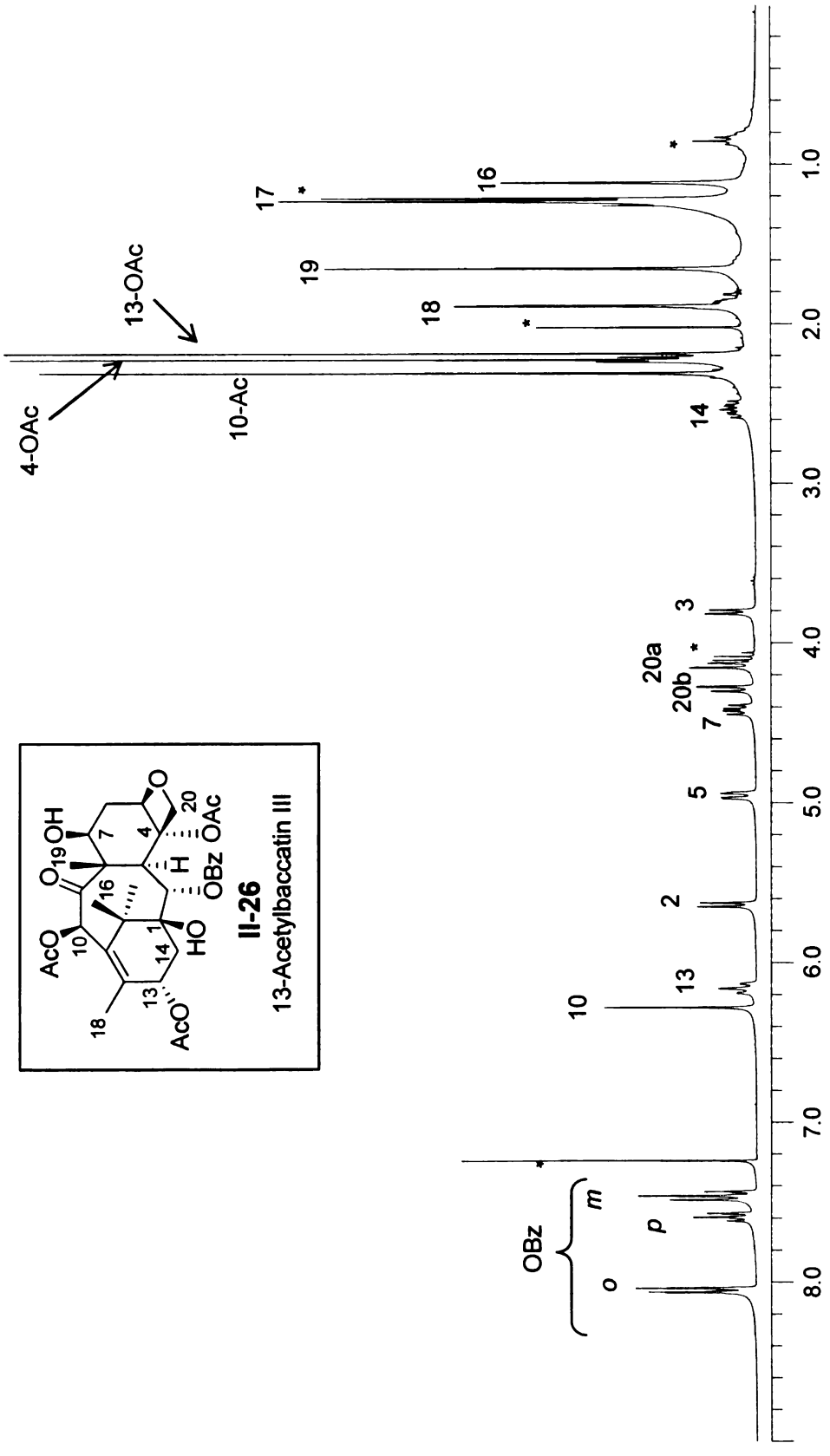

Figure A-6. 10-Methoxycarbonyl-10-deacetylbaccatin III

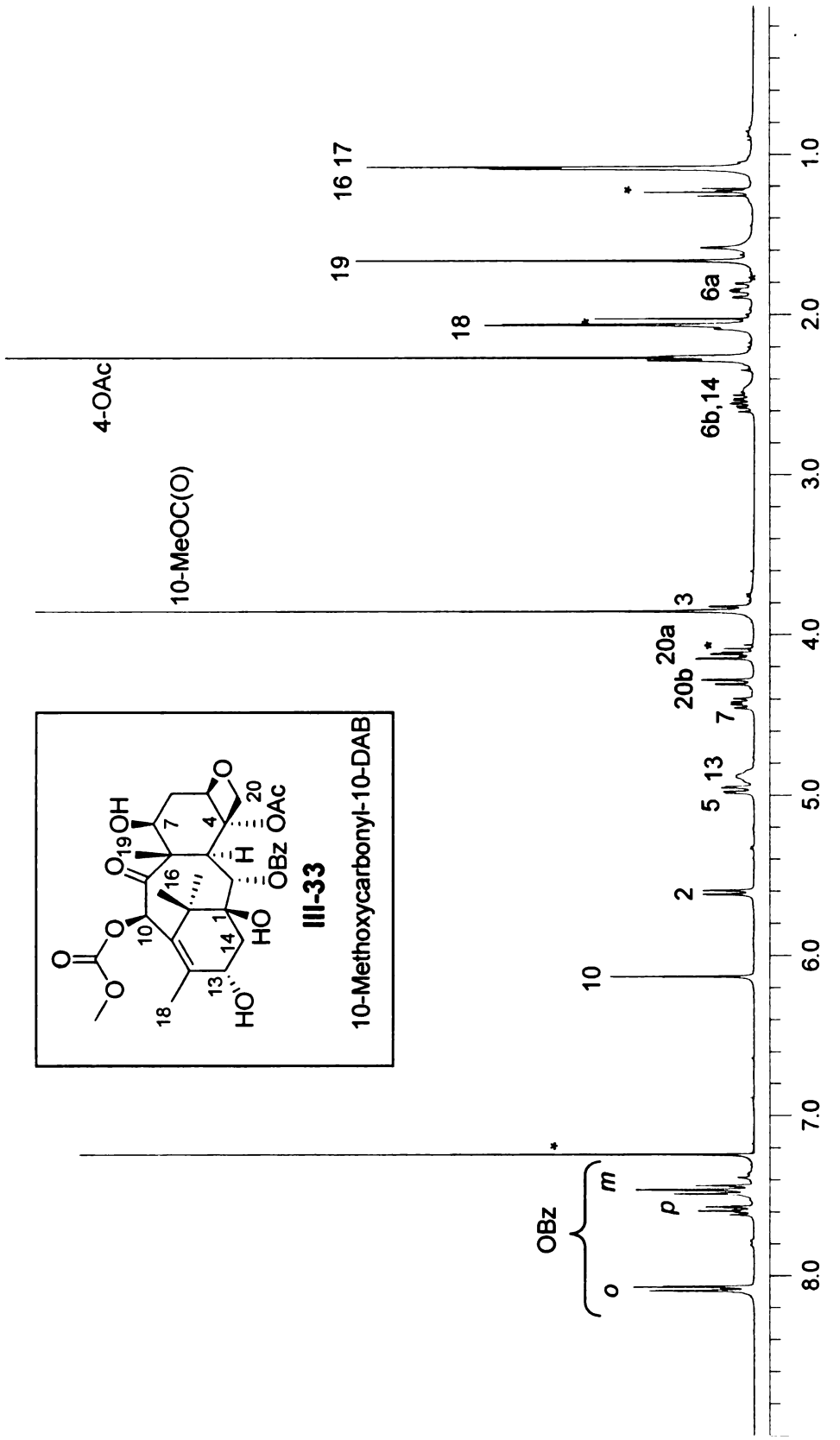

Figure A-7. 10-xo-7epi-10-deacetylbaccatin III

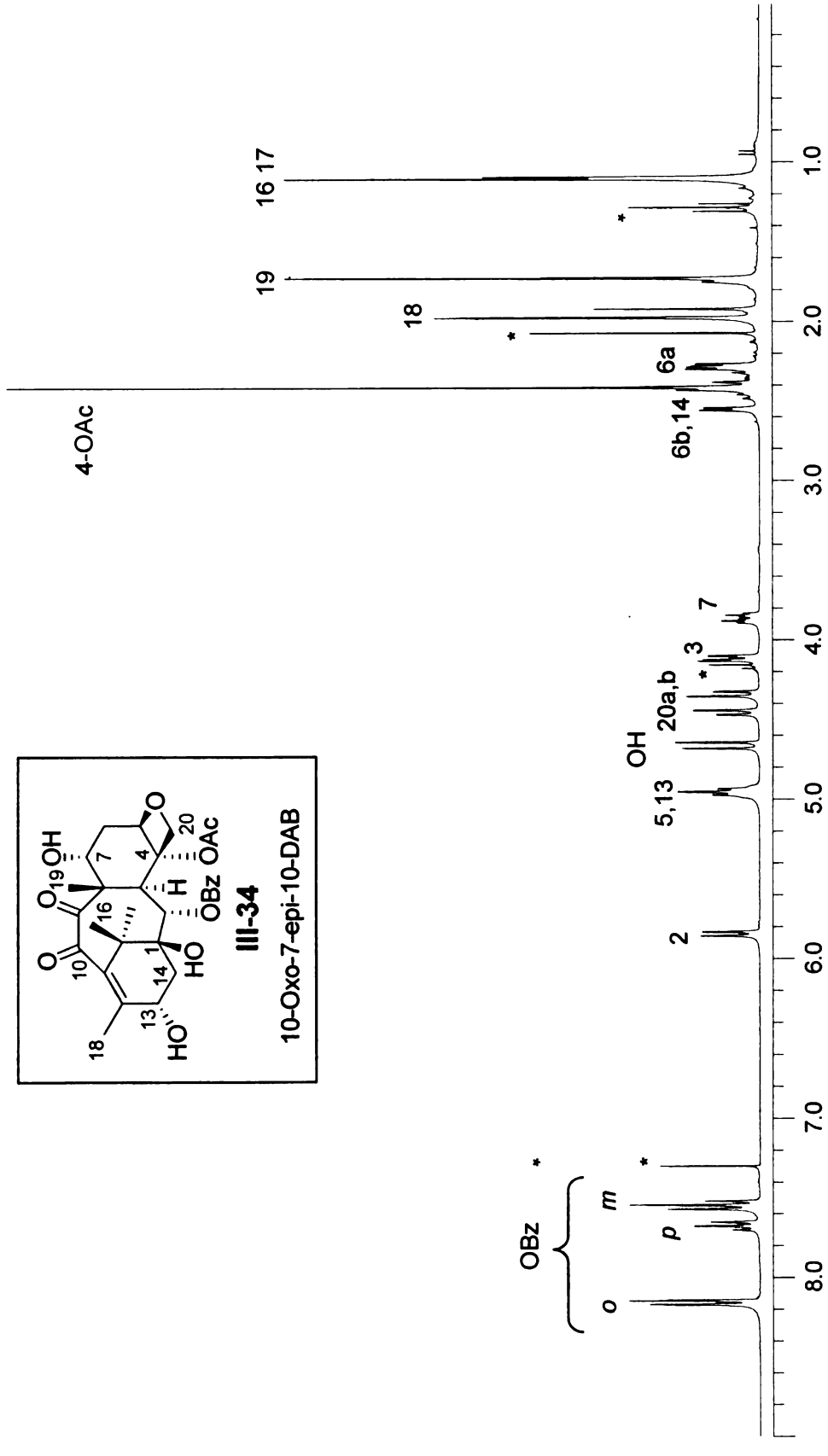

Figure A-8. 13-Oxobaccatin III

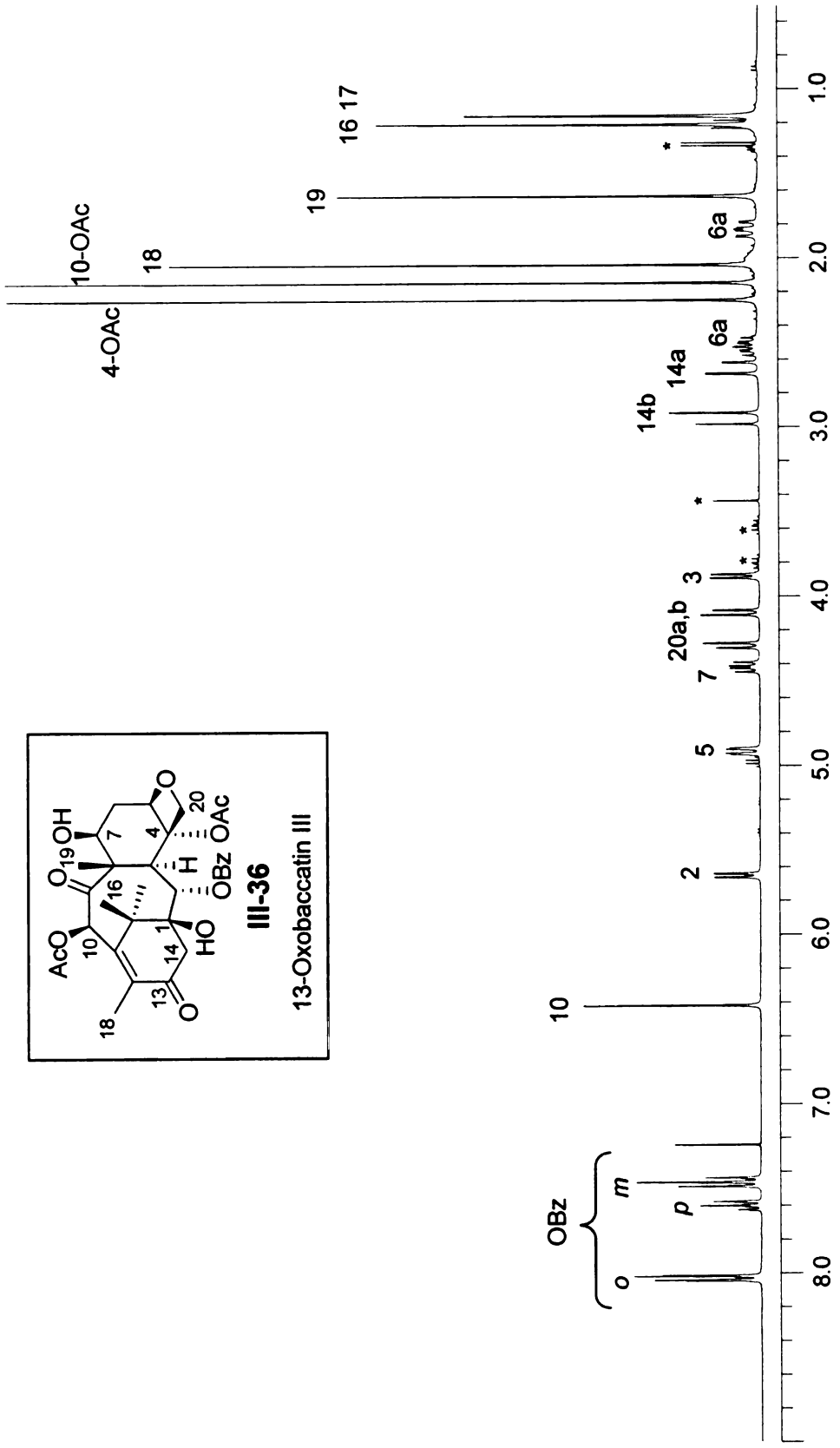

Figure A-9: 7,13-Dioxobaccatin III

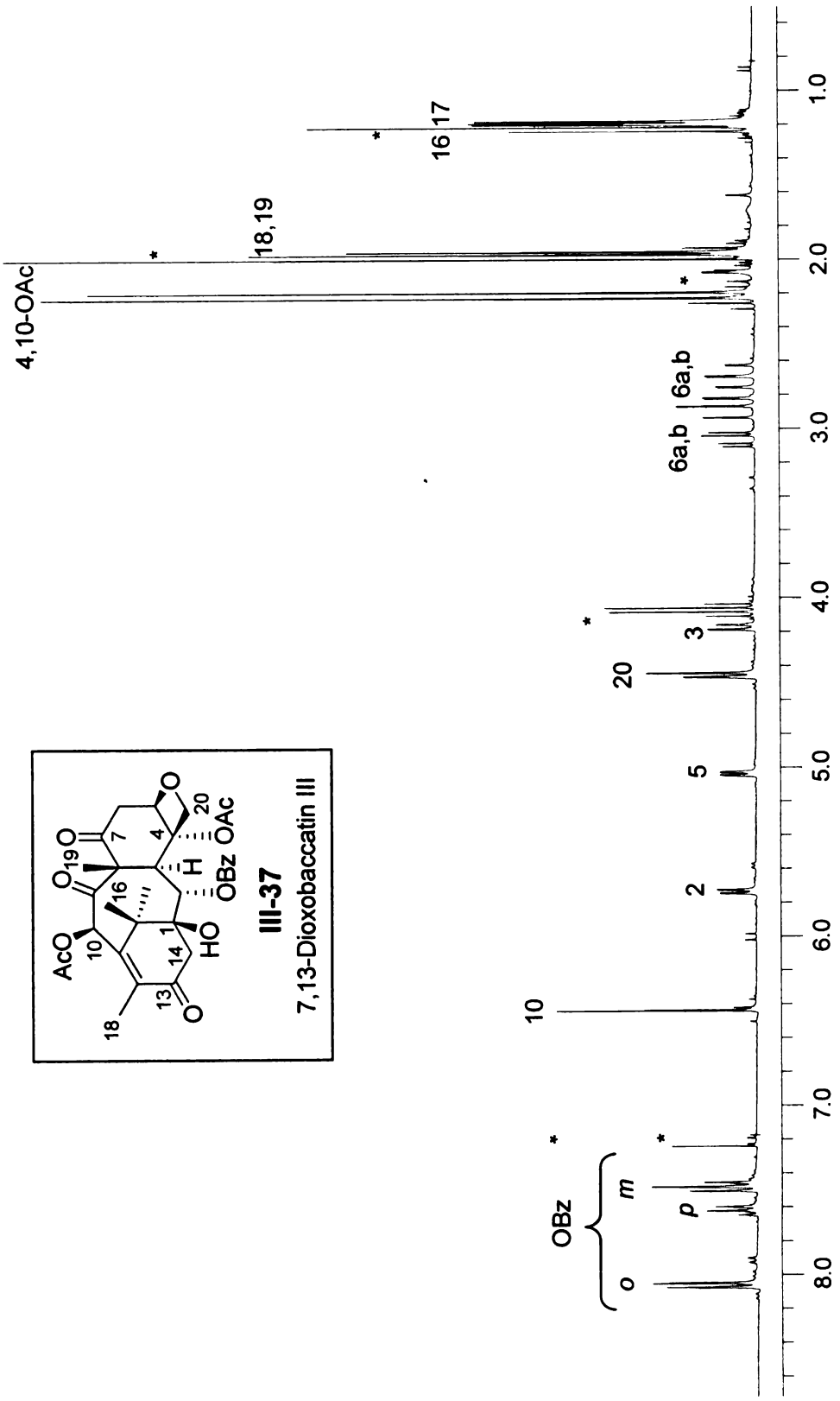

Figure A-9: 7,13-Dioxobaccatin III

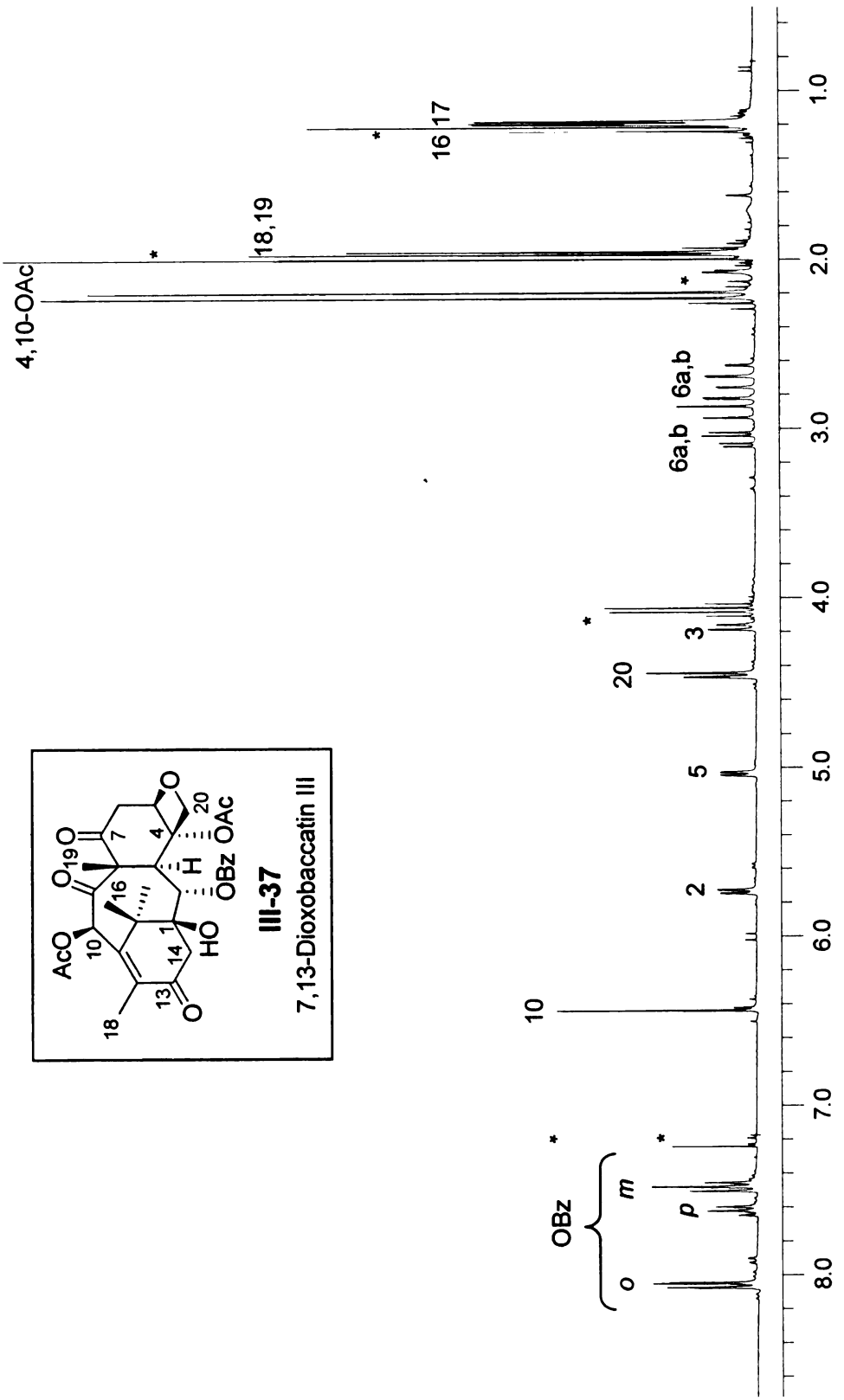

Figure A-9: 7,13-Dioxobaccatin III

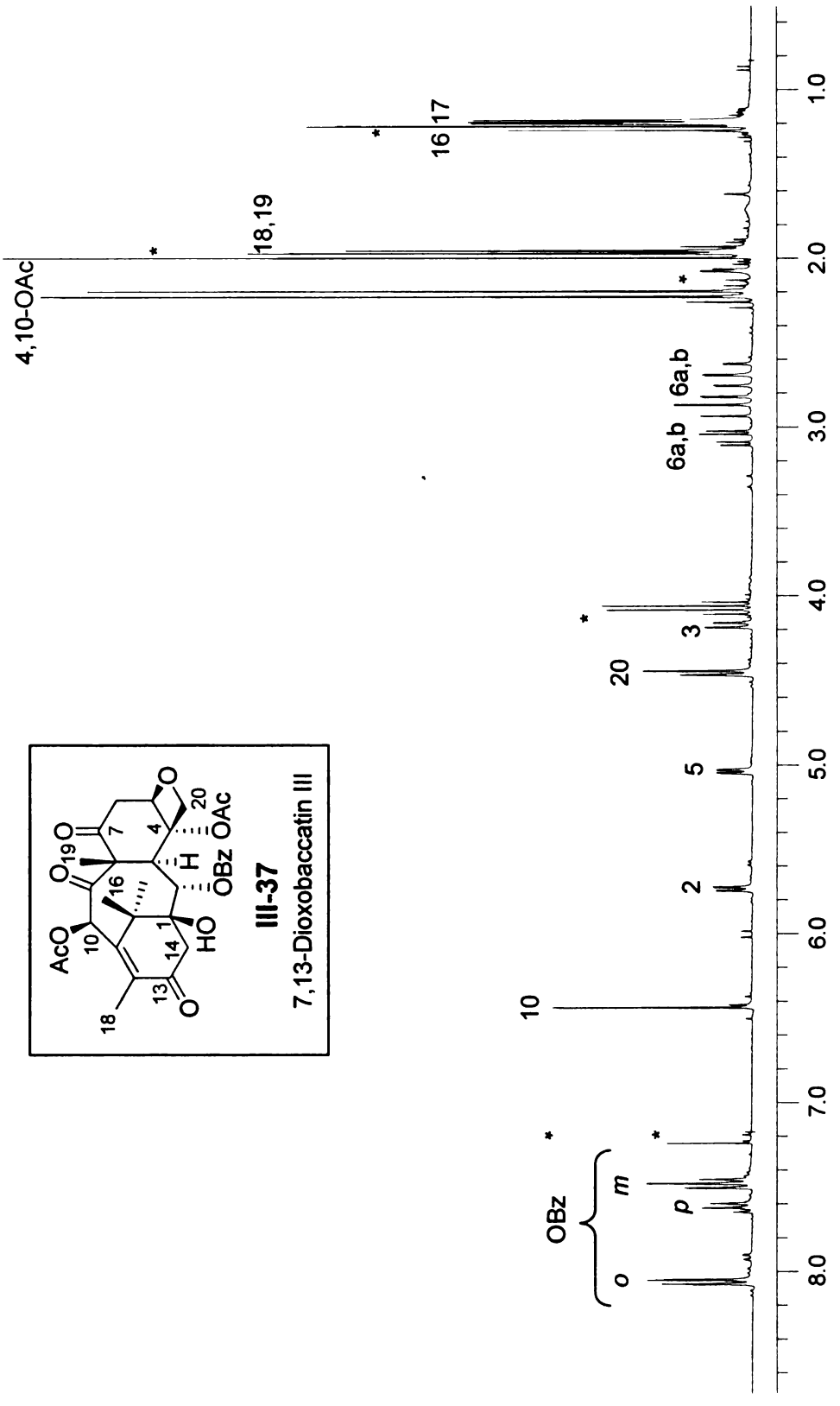

Figure A-10. I-Dimethylsilyl-7,13-bis(triethylsilyl)baccatin III

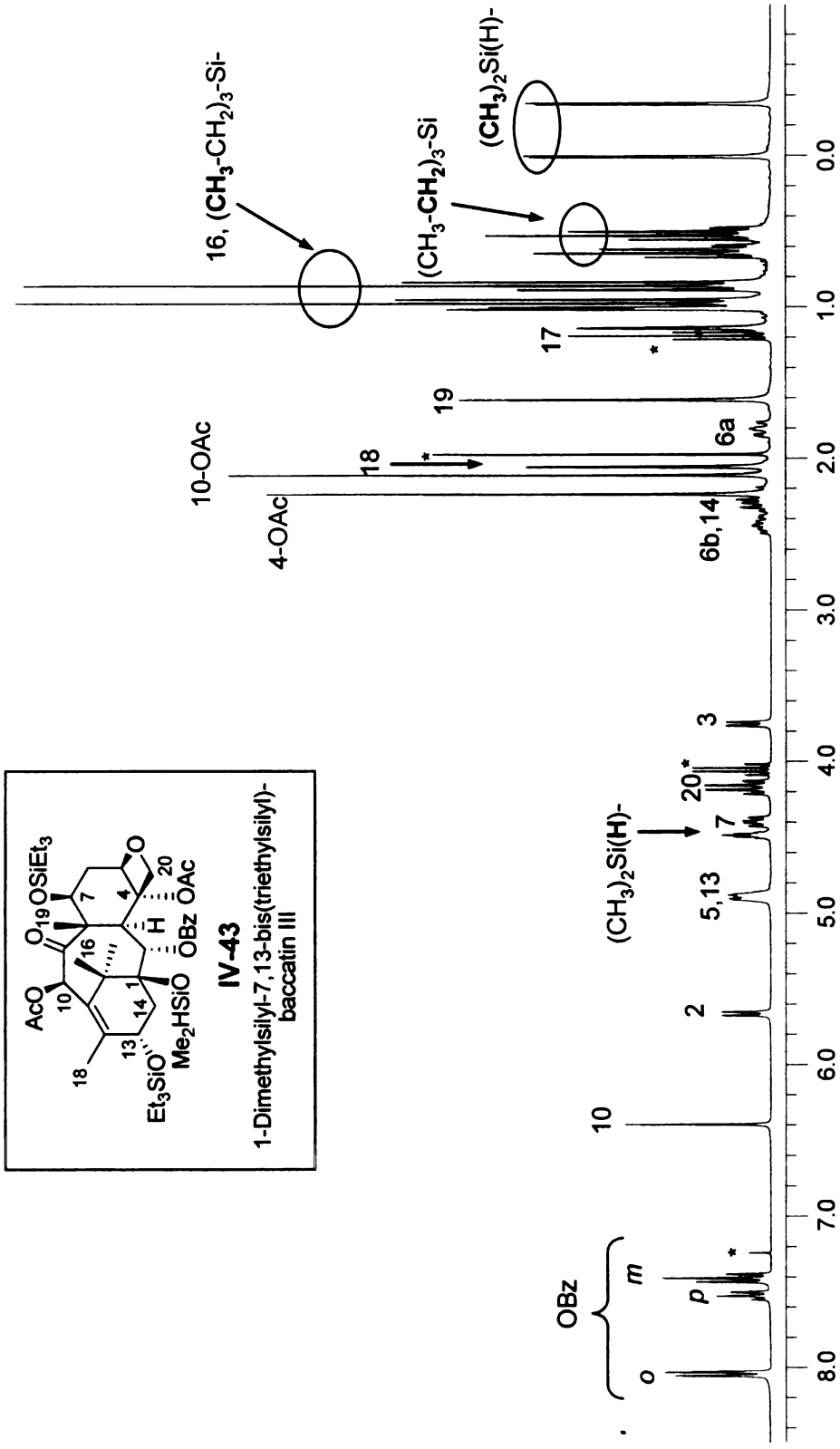

Figure A-10. I-Dimethylsilyl-7 triethylsilylbaccatin III

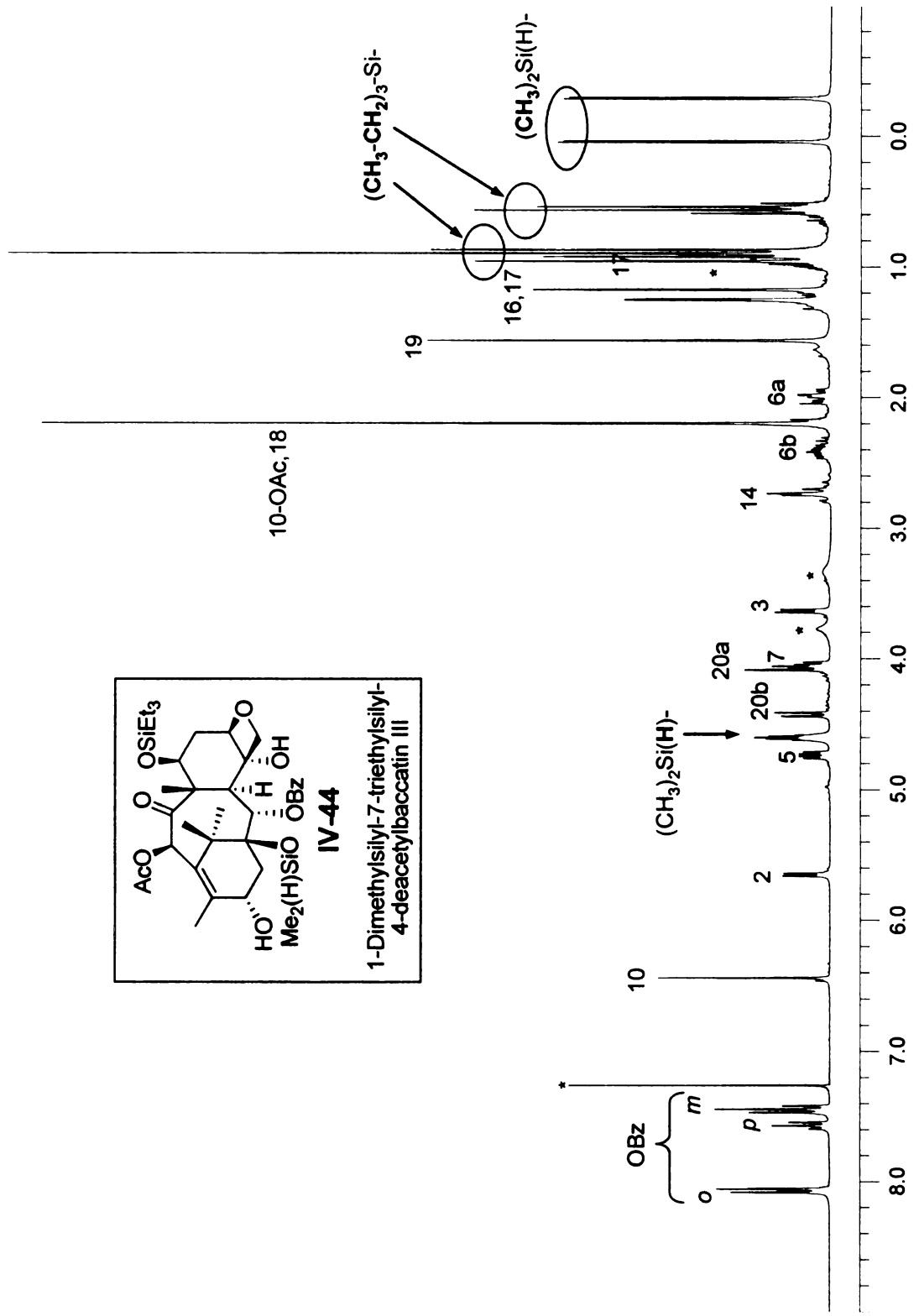

Figure A-12 -Dimethylsilyl-7,13-bis(triethylsilyl)baccatin III